Suitability of Microwave Application to Heat Reclaimed Asphalt and Crushed Aggregates as an Energy Efficient Method in the Production of Half Warm Mix

by
Riyaaz Nieftagodien

Thesis presented in partial fulfilment of the requirements for the degree Master of Science at the University of Stellenbosch

Supervisor: Professor Kim Jenkins
Faculty of Engineering
Department of Civil Engineering

March 2013

DECLARATION

By submitting this dissertation electronically, I declare that the entirety of the work contained therein is my own, original work, that I am the owner of the copyright thereof (unless to the extent explicitly otherwise stated) and that I have not previously in its entirety or in part submitted it for obtaining any qualification.

Signature:

Name: R. Nieftagodien

Date:

For Mogamat and Murreldia

SUMMARY

The pavement construction industry aims to reduce its Greenhouse Gas (GHG) emissions by investigating various energy efficient practices. The industry has focused on reducing energy consumption by producing Warm Mix Asphalt (WMA) surfacing materials that are workable at lower temperatures in relation to Hot Mix Asphalt (HMA), as a means to reduce carbon emissions. Half-Warm Foamed Bitumen Mixtures (HWF) is a relatively new material and is produced at temperatures below 100°C. This translates to large energy savings to overcome the latent heat of steam when exceeding 100°C.

The characteristics of HWF mixes are a compromise between those of Foamed Bitumen Stabilised material (BSM-foam) and HMA characteristics. These include to a limited extent the improved tensile strength, particle coating and durability of HMA; and the shear strength of BSM-foam.

The use of microwave technology as an efficient heating method to produce improved engineering properties of BSM-foam is proposed in this study. The benefits include energy saving due to its volumetric heating capability as well as rapid heating which improve productivity when using suitable materials.

The aspect of recycling material brings forth further energy saving and emissions reduction when reusing materials. The portability of the in-plant recycling machines is an ideal candidate with logistical advantages to implement microwave generators to produce HWF mixes.

This study is subdivided into four parts as it progressively investigates the potential to heat aggregates and produce HWF material. Firstly it investigates the heating potential of four aggregates, namely Hornfels, Quartzite, Eucrite, Granite and Reclaimed Asphalt (RA) at various moisture contents using a microwave apparatus. The second part discusses the thermodynamics of the preliminary investigation to provide insight into the third part, the Primary Investigation. The primary investigation evaluates the tensile strength and shear properties of two material blends by respectively implementing Indirect Tensile Strength (ITS) and monotonic triaxial tests on specimens. The two blends were a combination of RA and crushed hornfels. The fourth and final part evaluates the HWF properties in relation to those of the equivalent BSM-foam product by means of a pavement analysis.

The highest laboratory production temperature achieved was depicted by the material properties, microwave power capability and production rates. This temperature was consistently recorded at 50°C which theoretically simulates an in-field production rate of approximately 25 tons per hour.

ITS test results indicate 100% increase in tensile strengths and an increase in compaction density for the HWF mixes. Large reduction in moisture contents is also observed after curing in relation to BSM-foam.

The benefits in improving a layer within a pavement structure have an effect on the pavement's overall performance. This could assist in reducing the requirement for premium layers e.g. thickness of HMA within the structure, thereby further assisting energy conservation.

The evaluation of the microwave heated HWF mixes can be considered economical if designed with a purpose to meet the thermal dynamic requirements of a material considering the microwaves volumetric potential.

OPSOMMING

Die plaveisel konstruksie-industrie poog om hul kweekhuisgas (KHG) uitskeiding te verlaag deur verskeie energie doeltreffende metodes te ondersoek. Die industrie fokus op die vermindering van energie-verbruik deur middel van die produksie van Warm Mengsel Asfalt (WMA) oppervlak materiale wat werkbaar is in laer temperature in verhouding tot “Hete Mengsel Asfalt (HMA)” as `n metode om koolstof uitskeiding te verlaag. Half-Warm Skuim-Bitumen Mengsels (HWS) is `n relatief nuwe materiaal en word vervaardig onder 100 °C. Dit lei tot groot energie besparings en oorkom sodoende die latente hitte van stoom wanneer temperature van 100 °C oorskry word.

Die karakter-eienskappe van HWS mengsels is `n kompromie tussen Skuim-Bitumen Gestabiliseerde materiaal (BSM-S) en HMA eienskappe. Dit sluit tot `n beperkte mate in die verbeterde spankrag, partikel bestryking; en die skeer krag van BSM-S.

Die gebruik van mikrogolf-tegnologie as effektiewe verwarmingsmetode vir verbeterde ingenieurseienskappe van BSM-S word voorgestel in hierdie studie. Die voordele sluit in energie besparing as gevolg van die volumetriese verwarmingsvermoë sowel as snel verhitting wat produktiwiteit verbeter tydens die gebruik van gepaste materiale.

Die gebruik van herwinde materiaal bring verdere energiebesparing en uitskeiding-vermindering mee. Die draagbaarheid van binne-aanleg herwinningsmasjinerie is ‘n ideale kandidate met logistieke voordele vir die installering van mikrogolf-opwekkers vir die produsering van HWS mengsels.

Dié studie word onderverdeel in vier dele terwyl dit toenemend ondersoek instel na die potensiaal van hitte versameling asook die produksie van HWS stowwe. Eerstens ondersoek dit die verwarmingspotensiaal van vier versamelings naamlik horingsteen, kwartsiet, eukrite, graniet en Herwinde Asfalt (HA) teenoor verskeie vogskattings-mikrogolf aperate. Die tweede deel bespreek die termodinamika van die voorlopige ondersoek om insig te bied vir die derde deel, die primêre ondersoek. Die primêre ondersoek evalueer die rekbaarheid en skeereienskappe van twee materiaal-mengsels van ITS en monotoniese drieassige toetse onderskeidelik op verskillende monsters. Die twee mengsels was `n kombinasie van HA en gemaalde horingsteen. Die vierde en finale deel evalueer die HWS eienskappe in verhouding tot die van die ekwivalente BSM-S produk deurmiddel van `n sypad-analise.

Die hoogste laboratoriumproduksie temperature wat bereik was, was uitgebeeld deur die materiaal-eienskappe, mikrogolf krag kapasiteit en produksiekoers. Hierdie temperature was

deurlopend aangeteken teen 50 °C wat `n teoretiese voorstelling is van `n binneveld produksie tempo van ongeveer 25 ton per uur.

ITS toets resultate wys `n 100 % verhoging in spankrag asook `n toename in kompakte vir die HWS mengsels. Groot afname in voginhoud is ook waargeneem na bewerking in verhouding tot BSM-S.

Die voordeel verbonde aan die verbetering van `n lag binne `n plaveisel-struktuur, het `n impak op die plaveisel se algemene uithoubaarheid. Dit kan bydra tot `n verlaging in die vereiste binne die struktuur en verdere bydra tot energie besparing.

Die evaluering van mikrogolf verhitte HWS stowwe kan as ekonomies beskou word wanneer dit doelgerig vervaardig word om te voldoen aan die termodinamika vereistes van `n materiaal, wanneer die mikrogolf volumetriese potensiaal in ag geneem word.

ACKNOWLEDGEMENTS

I would like to thank The Almighty, who has created this Earth and everything therein; and for giving me the ability to explore it so that I may better understand Him.

I would further like to acknowledge the following persons for their time and assistance in allowing me to complete this study:

- Professor Kim Jenkins, for his time, mentorship and facilitation in financial support
- Professor Fred Hugo for his guidance and sound advice.
- Professor Steven Bradshaw for his expertise and the use of the microwave equipment
- Doctor Lucas-Jan Ebels for his insight and inspiration
- Mrs Kate Jenkins for her assistance
- Mr. Ivo Huisman for advice, guidance and support
- Institute for Transport Technology (ITT) and Wirtgen GmbH for financial support
- My fellow students and friends Alex Mbaraga, Achille Nwando, Pius Ngassa, Nathan Chilukwa, Annie Asiimwe, Johan Gerber and Matteo Dal Ben
- Laboratory technicians, Colin Isaacs and Gavin Williams
- Workshop personnel Dion Viljoen and Oom Johan van der Merwe
- Janine Myburgh, Alett Slabbert and Amanda De Wet for their kind assistance
- My wife, Zeenat for her love, patience and sacrifice
- My parents for laying a sound foundation filled with love and motivation
- My brothers and sister, Razeen, Nurudeen and Sihaam, for their love, and assistance.

TABLE OF CONTENTS

List of Figures

List of Tables

LIST OF ABBREVIATIONS AND SYMBOLS

Abbreviations:

4PB	4 Point Beam
AASHTO	American Association of Highway and Transportation Officials
BC	Binder Content
BSM	Bitumen Stabilized Materials (Emulsion and Foamed Bitumen)
BSM-emulsion	Bitumen Stabilized Materials – Emulsion
BSM-foam	Bitumen Stabilized Materials – Foamed Bitumen
CIPR	Cold In-Place Recycling
CSIR	Council of Scientific and Industrial Research; based in Pretoria, South Africa
DC	Direct Current
EM	Electromagnetic
EPDM	Ethylene Propylene Diene Monomer
ER	Expansion Ratio
Eu	Eucrite
FI	Foam Index
GHG	Greenhouse Gases
Gr	Granite
HDPE	High Density Polyethylene
HMA	Hot Mix Asphalt
Ho	Hornfels
HWF	Half-Warm Foamed mix
ITS	Indirect Tensile Strength
ITSR	Retained Indirect Tensile Strength test
ITT	Indirect Tensile Test
MC	Moisture Content
MDD	Maximum Dry Density
MW	Microwave
OMC	Optimum Moisture Content
PA	Porous Asphalt
PI	Plasticity Index
PTFE	Polytetrafluoroethylene
Qu	Quartzite
RA	Reclaimed Asphalt
SABITA	South African Bitumen Association
SAMDM	South African Mechanistic (pavement) Design Method

SBR	Styrene Butadiene Rubber
SCB	Semi-Circular Bending test
STAB	Steenslag Asfalt Beton (continuously graded asphalt)
TG2	Technical Guideline No. 2, published by the Asphalt Academy (2009)
TSR	Retained Tensile Strength
UCS	Unconfined Compressive Strength
VMA	Voids in Mineral Aggregate
WMA	Warm Mix Asphalt
ZNAC	Zuid Nederlands Asfalt Centrale

Symbols:

λ	Wavelength
f	Frequency (Hz)
c	Velocity of Propagation
ε*	Complex Permittivity
ε'	Dielectric constant
ε”	Dielectric Loss factor
j	Imaginary Unit
δ	Loss ratio
M_c	Critical Moisture Content
p	Power flux density (watts/ m^2)
$\overline{E}$	Electric field vector (volts/ meter)
$\overline{H}$	Magnetic field vector (amperes/ meter)
ε_0	Permittivity of free space (8.86 x 10-12 F/m)
E_i^2	Root mean square electric field strength (V/m)
D_p	Penetration Depth
P	Total power (watts) dissipated into the workload
M,	Material mass (kg)
T,	Temperature (°C)
s_p,	Specific heat capacity
ε_0,	Permittivity of free space, 8.854 x 10^{-12} F/m
ε”,	Material loss factor
$\mathrm{E_{int}}$,	Internal voltage stress in the dielectric material (Volts/meter)
ρ,	Material density (kg/m^3)
M_r	Resilient Modulus
R^2	Coefficient of Correlation

V	Volume
Q	Rate of heat flow
σ	Bulk Stress = $\sigma_1 + \sigma_2 + \sigma_3$
σ	Normal stress
$\sigma_1, \sigma_2, \sigma_3$	Major, intermediate and minor principal stress
σ_d	Deviator stress = $\sigma_1 - \sigma_3$
τ	Shear stress
φ	Angle of internal friction
C	Material Cohesion
A_1 and λ_1	Functions of the Biot number, obtained using Heisler charts
Bi	Biot number, Dimensionless heat coefficient, hL/k
k	Thermal conductivity, W/(m^2.K)
h	Convection heat transfer coefficient, W/(m.K)
K	Kelvin
τ	Dimensionless time value (Thermodynamics - Fourier number)

CHAPTER 1: INTRODUCTION

1.1 Background to research

The reduction of Greenhouse Gases (GHG) and the investigation of various energy efficient practices have received prominence in the Pavement Construction Industry. Scientific research has produced considerable evidence to link increasing atmospheric concentrations of GHG to the rising global temperatures, with the latter having detrimental effects on the environment and subsequently on country economies. In countries like South Africa, the main contributor of GHG is the combustion of low-cost fossil fuels, which the road building industry uses extensively. To address the abundant use of low cost fossil fuel consumption, more energy efficient practices are required. The cross-pollination of technology advancements and ideas between research fields are considered a necessity to expedite the understanding and implementation of energy efficient practices.

South Africa has voluntarily committed itself in joining the global mission to mitigate climate change by reducing its forecasted carbon footprint over the next few decades (National Treasury paper, 2010). Currently there are no carbon taxations applicable to the construction industry locally. This is in contrast with many countries associated with the Kyoto Protocol who have implemented policies in various sectors to reduce emissions. The likelihood of carbon taxation is however a reality and could adversely impact the pavement construction industry, making low-cost fossil fuel use less attractive.

The route to reduced carbon emissions can take many forms within an industry. Direct practices, which have received most consideration, include reduction in energy consumption, and more efficient or cleaner energy sources to achieve a similar quality end product if not better. The selection of energy source is however further dependant on productivity. The high caloric value of low-cost fossil fuels as well as its availability currently make it more attractive than other available energy sources. It is therefore not surprising that the asphalt industry has focused on reducing energy consumption by producing surfacing materials that are workable at lower temperatures as a means to reduce carbon emissions. This shift to consider Warm Mix Asphalt (WMA) as opposed to Hot Mix Asphalt (HMA) is still in its infancy with much research still to be conducted.

The various bituminous mixes can be categorized by its production as well as placement temperatures as shown in Figure 1.1. Foamed Bitumen Stabilized Materials (BSM-foam) are produced at ambient temperatures whereas WMA and HMA are produced at temperatures above 100°C. BSM-foam has been noted to be temperature dependent since its inception by its founder, Ladis Csanyi. Many researchers have since acknowledged improved engineering properties of BSM-foam when either applying heat to the aggregates prior to foam stabilization or applying heat to the foamed bituminous mix after mixing but prior to compaction. Apart from the temperature difference during production, BSM-foam differs from WMA and HMA due to its particle coating characteristics. This particle coating extent is amongst others, a result of temperature variation. Low temperatures results in partial particle coating, as compared to high temperatures where complete coating is possible.

Jenkins (2000) investigated the potential of mixtures higher than ambient temperature but below 100°C, and regarded this mix as a Half-Warm Foamed Mix (HWF). The observed benefits in HWF were noted as; improved tensile strength, particle coating and durability in relation to BSM-foam. These properties are those that BSM-foam fell short of in terms of HMA. The HWF benefit in relation to HMA is its shear strength; a benefit BSM-foam attained over HMA due to its non-continuous bonds of individual aggregates. HWF also provided a potential energy saving element over WMA and HMA, as the additional energy required by the latent heat of water vapour when exceeding its boiling point could be avoided.

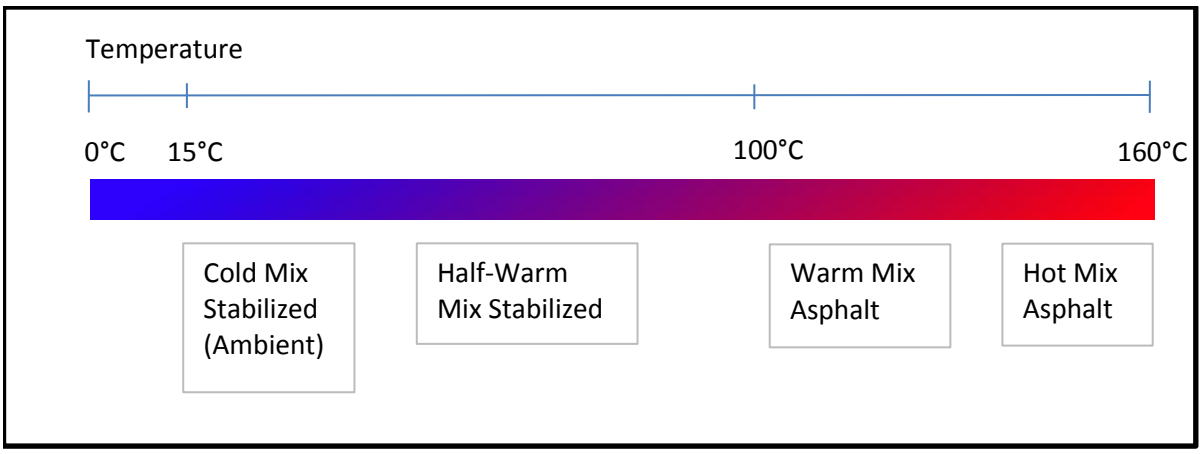

Figure 1.1: Temperature characterisation of bituminous mixes

This study proposed the use of microwave (MW) technology as an efficient heating method to produce the improved engineering properties of HWF. The benefits, when utilising this system, include energy saving as a result of its volumetric heating capability as well as rapid heating. This improves productivity when using suitable materials. Microwave heating applicators however have high set-up costs and are considered an expensive energy source

in relation to the use of low cost fossil fuels, such as propane gas. The improved properties and production costs are however benefits to be weighed up against the high set-up costs. Production costs when using a microwave source can be kept to a minimum when used in the correct environment.

The aspect of recycling material brings forth another dimension to reducing carbon emissions. Energy saving and emissions reduction are apparent when re-using materials. Underneath the asphalt surfacing within a pavement structure, cold recycling with foamed bitumen has seen favourable results in the stabilization process. There are numerous engineering and logistical advantages in cold recycling, with its environmental benefits being more apparent in recent times. The addition of the Reclaimed Asphalt (RA) in recycled material was anticipated to be beneficial in the microwave heating of the material and thus was investigated within this study.

The production of BSM-foam pavement layers are either constructed in-place or in-plant. In general in-plant facilities have more control over the material quality during production and further have the capacity to house a microwave applicator. The use of microwave technology is therefore best suited for in-plant practices.

The introduction of WMA is a fairly new product to compete if not replace HMA. WMA meets the recent requirements such as resource conservation and environmental stewardship which holds the additional benefits of improved construction efficiency with adequate pavement performance.

The evaluation of a half warm foam mix can be considered economical if designed with a purpose to meet certain partial benefits provided by BSM-foam and /or WMA at a reduction in working time and energy requirements. The benefits in improving a layer within a pavement structure has an effect on the pavement's overall performance. This could assist in reducing the requirement for premium layers within the structure and thereby further assisting energy conservation.

1.2 Objectives

The primary objective of the research is to investigate the potential use of microwave volumetric heating applications to produce quality HWF at suitable production rates. This objective can be divided into several secondary objectives namely:

- The applicability of various road construction materials suitable for microwave heating, and ascertain at which stage during production is the heating applicable, i.e. pre-heating aggregates or post-heating BSM-foam.
- Secondly, the efficacy of the microwave heating needs to be ascertained with representative virgin and recycled aggregates, in order to determine what temperature increase can be achieved using this technology.
- To quantify the benefits of the HWF produced, its improved material characteristics will be evaluated by means of linear elastic analysis of various pavement structures incorporating the HWF layer in relation to a BSM-foam layer.

1.3 Scope of study

The scope of this research is limited to the microwave technology used and the materials considered for testing. The range of possible heating temperatures is limited by the microwave unit to simulate in-field production. It is noted that when scaling down for emulation of in-field scenarios, heat dissipation is greatly affected by the reduced volume of the material. The influence of mass as well as volume is evident in heat and mass transfer equations.

The microwave frequency used operates at 2450MHz, and no other microwave heating frequencies were investigated for this study. The investigation into the use of microwaves was preliminary and included only foam bitumen stabilised material, with manufactured specimens to be tested by means of the Indirect Tensile Strength (ITS) tests and monotonic triaxial tests. These results were evaluated by means of a multilayer linear elastic analysis within a pavement structure.

Various G1 and G2 specification aggregates were tested to deduce its heating potential under microwave application. For final mixture consideration, the best performing aggregate was blended with RA. Two variations were considered, namely high RA fraction and high virgin aggregate fraction.

The procedures implemented during this investigation phase were focused on simulating in-plant manufacture of BSM-foam. Where the decision was taken to fore-go laboratory best practice techniques, justification will be provided in this paper, to substantiate this decision in line with simulating the in-plant production.

1.4 Layout of study

This study branches out into various fields of interest, i.e. microwave heating, BSM-foam production and material thermodynamics. The use of microwaves, in the heating application, is better discussed in relation with the thermodynamic aspects of materials. It is the dielectric thermodynamic properties of the road building materials that quantify the benefits of the microwave application. This is most notable when considering that BSM-foam characteristics vary, not only depending on the materials used in mixes but also particle fraction variations and the temperature dependency of bitumen viscosity. It therefore becomes apparent that the material interaction between the bitumen and particles plays an increasing role as the temperature rises.

In accordance to the above factors mentioned, the layout of this study progresses as is illustrated in Figure 1.2 and can be described as follows:

- Microwave heating fundamentals. This section investigates the properties and complex nature of microwaves. Understanding the microwave heating philosophy as well as the materials interaction thereof provides cognisance of its benefits and limitations.
- The BSM-Foam. Investigations of previous literature on the production of BSM-foam have been perused to determine the factors affecting its engineering properties. The importance to investigate mix properties became evident, to ascertain the type of impact the electromagnetic heating process could have. In this section, the mixing material, material interactions and sample preparation procedures together with engineering properties were investigated.
- Half-Warm Mix (HWF). The section introduces the benefits achievable by adding heat to bitumen stabilized materials as investigated by previous researchers.
- Testing methodology. This section serves as an overview to the procedures and equipment utilised during this study. The path followed identified the numerous modifications to be considered, to overcome the obstacles that became apparent within this study.
- Results. This section firstly discusses the Preliminary investigation of the virgin aggregates and utilises thermodynamics to provide insight into the relation between the microwave heating technology and BSM-foam production potential. The thermodynamic properties of the various cold mix ingredients will be investigated. Thereafter inferences are made and implemented in the Primary investigation

- Theoretical pavement analysis. The obtained results of the HWF material will be evaluated within a pavement structure in relation to using BSM-foam. This will provide further understanding of the benefits resulting from the current investigation.
- Conclusions and recommendations will thereafter follow so as to provide a summary of the current investigation. Recommendations will be provided for future research on the use of microwaves within the field of producing HWF mixes.

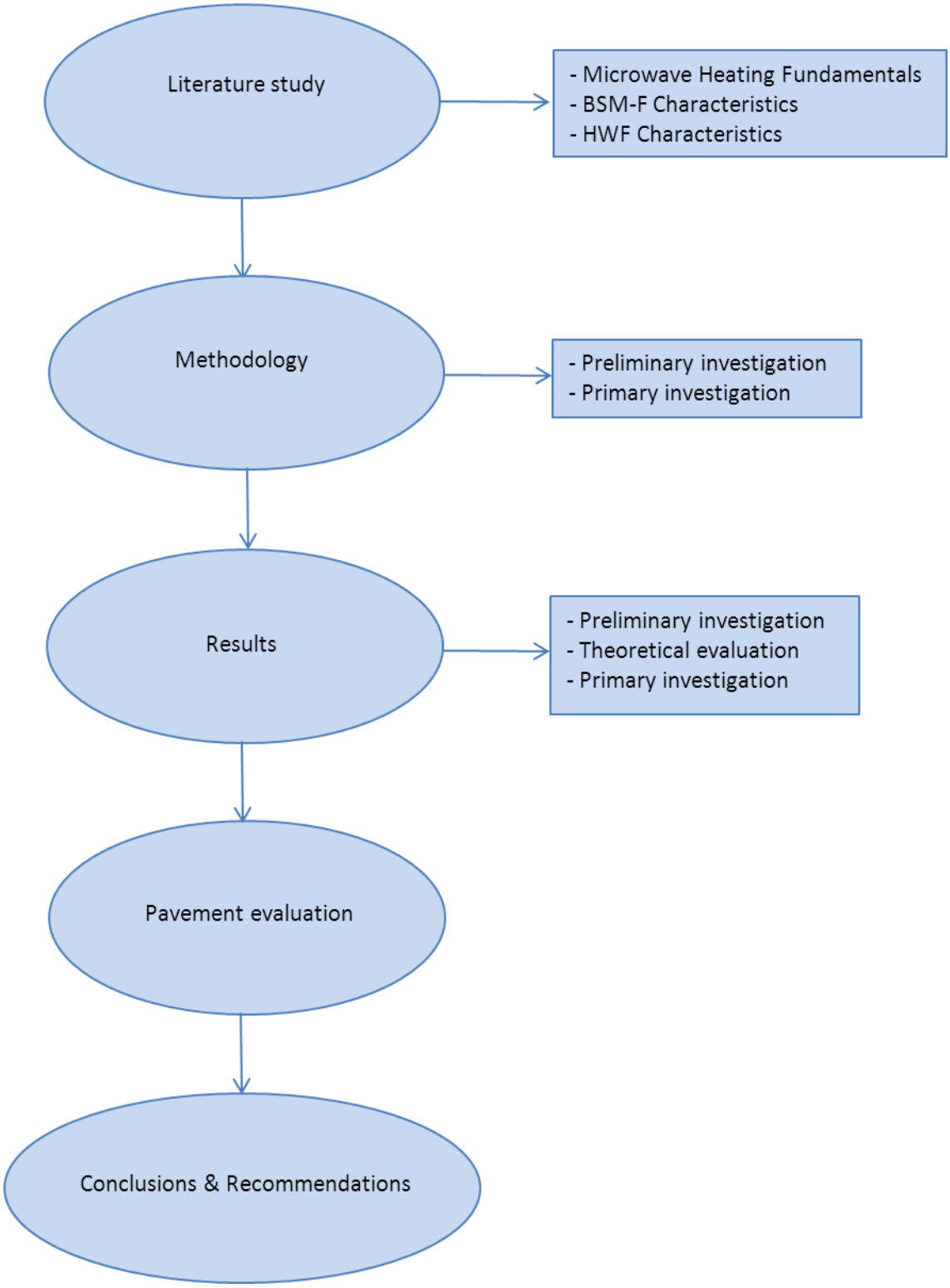

Figure 1.2: Study layout

CHAPTER 2: LITERATURE STUDY ON MICROWAVE HEATING

2.1 Introduction

The development of microwave heating applications took form during the post-World War II era. Microwave technology was initially studied whilst developing high definition radar during the war. Through random experimentation using a microwave generator (the magnetron valve), its potential to heat objects was accidentally discovered. Microwave heating has since progressed in both industrial applications as well as the consumer market. The counter-top microwave ovens frequently used in most household kitchens have created widespread familiarity to this technology. The technology's rapid growth in the 1970's has been considered to be more a result of its versatility over conventional heating (convection) than its affordability. The growth however has been marred by socio-technical events questioning the safety of exposure to microwaves, (Osepchuk, 1984).

This chapter subsequently discusses the theory behind microwave heating process. The following section focuses on the microwave heating in relation to conventional heating to create an understanding to the inherent differences between the two methods.

2.2 Advantages of microwave heating

Conventional heating requires all heat energy to be dissipated into the workload through its surface. The rate of heating is limited by temperature and energy gradient within the material. Increasing the outside temperature to expedite the process could cause surface damage to a workload. Non-uniform edges or sides usually tend to be hotter and thus reduces heating uniformity. The larger and denser the work piece, the longer the heating process is required. The maximum heating rate is therefore depicted by the maximum allowable temperature a material can withstand and its inherent thermal diffusivity to transfer the heat energy throughout. These factors have a considerable impact on production rates.

Production rates can be increased by using larger ovens; however, larger ovens are slower in response to temperature changes. They further take a longer time to heat up and have higher energy consumptions rates, due to heat loss through its oven walls. Microwave heating has the potential to heat a workload volumetrically where all elements of a uniform workload are heated individually, (Meredith, 1998). Volumetric heating therefore allows for all minute elements contained in the volume of the workload of a homogenous material to be ideally heated individually at the same rate.

In contrast to convection heating techniques, microwave heating also allows for selective heating and therefore energy savings are possible. The energy injected into the material is transferred electromagnetically and not as a heat flux as in conventional heating. Thus, the rate of heating is no longer limited by thermal diffusivity and surface temperature considerations. Heating times can often be reduced to 1%, with energy variation in the workload being less than 10% as discussed by Meredith (1998). A summary of the differences between microwave heating and conventional heating are tabulated in Table 2.1.

Table 2.1: Summary of the differences between microwave heating and conventional heating (adapted from Kobusheshe, 2010)

	Microwave	Conventional
Source	Energy transfer	Heat transfer via conduction
Start up	Immediate	Dependant on heating chamber
Rate	Rapid heating possible	Dependant on thermal diffusivity
Uniformity	Volumetric and selective heating	Temperature gradient from surface
Energy loss	Waveguide to reduce loss	Loss due to radiation externally

The exceptional efficiency of high-power magnetrons makes the overall efficiency of well-designed microwave heating systems very high, 85% at 900MHz and 80% at 2450MHz, (Meredith, 1998). The efficiency is measured by the energy put into a workload in relation to the power supplied. Conventional heating techniques operate at around 30% efficiency. Microwaves also allow space saving of up to 80% compared to conventional heating units, (TechnoCommentry, 1987). Cognisance should be observed in the high electric power cost in relation to less expensive gas or oil cost. The industrial microwave system had installation costs of around $4000 to $7000 per kilowatt (in 1995) which includes the cost of the microwave generator, applicator, conveyor and control systems, (Clark et. al., 1995).

2.3 Electromagnetic spectrum

Electro-heating techniques apply electrical energy to heat a workload. There are four techniques in practice, each containing their own operating frequency band in the electromagnetic frequency spectrum. These techniques are induction, ohmic, radio frequency and microwave heating. No singular electrical technique is effective in all applications. Microwave heating however in relation to induction, ohmic or radio frequency heating does not have to be in or near contact to the workload to take effect (Meredith, 1998). Figure 2.1 shows the frequency band of microwaves in relation to other electromagnetic waves.

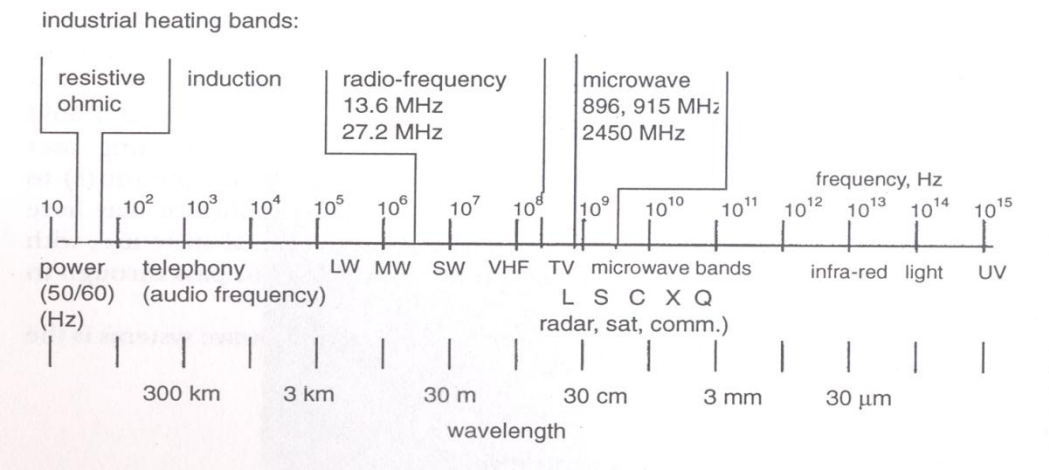

Figure 2.1: Frequency band of microwaves in relation to other electromagnetic waves (Meredith, 1998)

The electromagnetic (EM) waves generated during electro-heating are self-propagating and comprise of combined electric (E, volts/meter) and magnetic fields (H, amperes/meter) which vary sinusoidal in time and space. EM waves can be illustrated as plane waves and obey the basic wave formula. These two fields are the fundamental components which exist orthogonally to each other, with the electric field being the prime energy source to heat the workload (Meredith, 1998). Figure 2.2 depicts the electromagnetic plane wave.

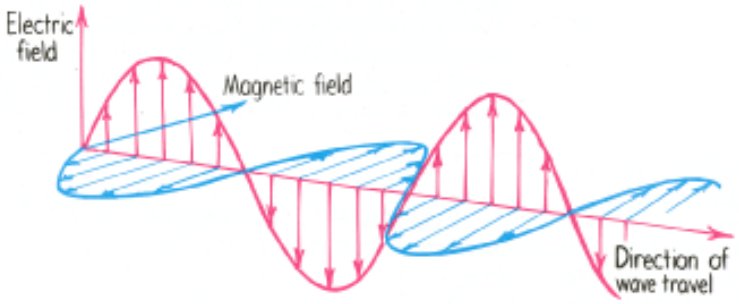

Figure 2.2: Illustration of electromagnetic plane wave, (Randomthink, 2012)

The simplest way in which electromagnetic energy propagates is as plane waves. They can propagate through free unbound space at the speed of 3 x 10^8 m/s irrespective of frequency, (Meredith and Metaxas, 1983). The sinusoidal wave propagation can be illustrated in Equation 1 below, where frequency and wavelength are bound by the propagating speed.

$$c = f.\lambda \qquad \text{(Equation 1)}$$

Where: f = frequency of oscillation
c = velocity of propagation
λ = wavelength

Microwave heating is performed at frequencies either close to 900MHz or at 2450MHz. These frequencies are chosen by international agreement with the principal aim to minimize interference with communication services, (Meredith, 1998).

2.4 Microwave heating theory

The origin of microwave (high frequency) heating lies in the interaction between an electric field and a dielectric material. Heating results from either the ability of an electric field to polarize the charges in a dielectric material and the inability of the polarization to follow the extremely rapid reversals of the oscillating electric field or via direct conduction effects. Most materials can be heated directly using microwave energy provided they are neither a perfect electrically conductor, nor a perfect insulator. Thus the material range extends from metals to dielectric materials considered as good insulators. Materials suitable for microwave heating can be classified as those which absorb microwaves, whilst the remainder of the materials are divided between those which are transparent to microwaves or those which reflect microwaves. Three primary mechanisms at which microwave heating is induced are dielectric polarization, interfacial polarization and conduction mechanisms, (Metaxas and Meredith, 1983).

Dielectric polarization is the process whereby heat is generated in polar molecules by means of rapid oscillations. This oscillation increases the kinetic energy and collision of molecules and since temperature is the measure of the average kinetic energy, microwaves essentially increases the temperature. The frequency range of the oscillating electric field is vital for the promotion of adequate intermolecular interaction. Frequencies that are too high will stop the motions of a polar particle before it follows a field resulting in inadequate interaction. Very low frequencies, on the other hand, allow sufficient time for polar molecules to align themselves in phase with the applied electric field, (Metaxas and Meredith, 1983).

Dielectric polarization can further be subdivided into three parts. These subdivisions are dependent on the atomic or molecular nature of the material:

- Electronic polarization: Displacement of electrons around the nuclei;
- Atomic polarization: Relative displacement of the atomic nuclei due to unequal charge distribution in molecule formation; and

- Orientation polarization: permanent dipoles in polar dielectrics re-orientate under the influence of changing electric field.

Loss mechanisms due to atomic and electronic polarization are referred to as distortion polarization and play no part in high frequency heating as they occur in the visible and infrared part of the electromagnetic spectrum, (Metaxas and Meredith, 1983).

Conduction mechanisms generate heat through the resistance of an electric current. The externally applied electric field is responsible for conducting paths due to the redistribution of charged particles. The dielectric material behaves like a poor electrical conductor having a finite resistivity, thus resulting in heat. At low temperatures and high frequencies, heating is primarily achieved by dielectric polarization. Figure 2.3 illustrates the dielectric polarization mechanisms.

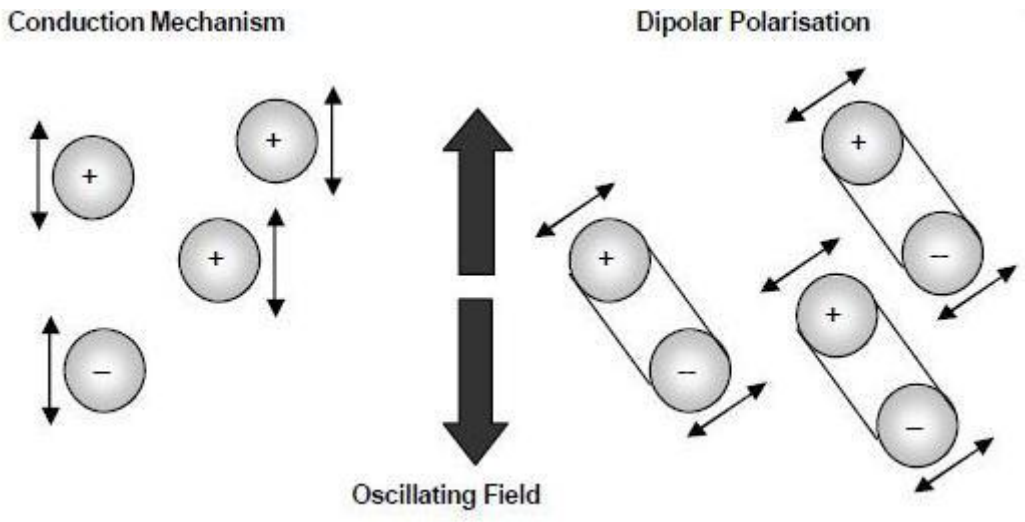

Figure 2.3: Dielectric polarization mechanisms (Puesherner, 1999)

Interfacial polarization is the charge build up at interfaces between components in heterogeneous systems. It can be considered as the combination of dielectric polarization and conduction mechanisms. It is important for interfacial polarization that a material comprises of a conducting material dispersed in a non-conducting medium, (Metaxas and Meredith, 1983).

Essentially, dielectric material particles couple electrostatically to the microwave electric field by aligning themselves mechanically. The constant rates of mechanical oscillation of molecules in an attempt to realign during field reversals induce frictional forces causing heat

development, (Meredith, 1998). It should be noted that mechanical resonance within molecules in the microwave frequency region results in peaks of power absorption, often referred to as thermal runaway.

2.5 Dielectrics

By definition, a dielectric material is a very poor conductor of electricity, but can support an electrostatic field. The molecule's dipolar components of many dielectric materials tend to couple electrostatically to the microwave electric field and align themselves mechanically, thus absorbing energy. Dielectric properties of a material are not constant and can vary with temperature, moisture content, density, molecular structure, frequency and material orientation, (Metaxas and Meredith, 1983). For microwave processing, the knowledge of a material's dielectric properties and their variation under certain environments are essential for successful design of microwave applicators. Dielectric data of a material is used to evaluate and quantify power dissipation and penetration depth of a material.

Many dielectric materials display polar characteristics, with water being the most commonly understood to absorb microwave energy effectively even in its near pure state. There are also non polar dielectric materials with high Direct Current (DC) resistivity which do not heat significantly in microwave fields. These materials are very important, as without it, microwave insulators and transparent windows would not have been possible. The most common insulators are quartz, alumina, PTFE, polycarbonate, polyethylene and polypropylene, (Meredith, 1998).

2.5.1 Permittivity

A dielectric material's ability to absorb and dissipate microwaves lies in its complex permittivity, ε (F/m). This value exists mathematically in a complex number form to account for losses experienced within the dielectric. The real component is called the dielectric constant and relates the materials ability to be polarized and store energy. The imaginary component is called the dielectric loss factor and measures the materials ability to dissipate the stored energy into heat (Meredith, 1998). The relationship is illustrated in Equation 2 below.

$$\varepsilon^* = \varepsilon' - j\varepsilon'' \qquad \text{(Equation 2)}$$

Where: ε^* = Permittivity

ε' = Dielectric constant

ε'' = Loss factor

$$j = \sqrt{-1}$$, (Imaginary unit)

In practice it is difficult to separate the contribution of loss due to the various heating mechanisms. The effective loss factor used above therefore considers all possible mechanisms such as conductivity and dipolar polarization. The loss factors are frequency dependent and for a given frequency band, one or two mechanisms may dominate over the others, (Metaxas and Meredith, 1983).

The effective loss tangent is the ratio of the effective loss factor to the dielectric constant as illustrated in Equation 3. It essentially provides an indication of the material's ability to absorb the electromagnetic wave in relation to its ability to dissipate the energy into heat.

$$tan\delta = \frac{\varepsilon''_{eff}}{\varepsilon'}$$ (Equation 3)

Where: δ = Loss ratio
ε'' = Effective dielectric loss factor
ε' = Dielectric constant

Many materials in their natural state are transparent to high frequency energy due to their low loss factor. These materials can be made suitable for microwave heating applications by introducing "lossy" impurities or additives. Materials used for many years include, carbon black, SBR, butyl or EPDM rubbers to enhance pre-treatment with microwave energy, (Metaxas and Meredith, 1983). The bulky constituents such as –(CH2)2CF3 or –(CH2)C in these additives are reported to increase speed and uniformity of curing of these materials with microwave heating, according to Lee (1979), as stated by (Metaxas and Meredith, 1983).

2.5.2 Dielectric property variation

Both the dielectric constant as well as the dielectric loss factor are frequency and temperature dependant and are further affected by density and moisture content, (Meredith, 1998).

Dielectric constant and loss factor increases with increasing frequency in materials where dipolar heating mechanisms dominate. A point exists where the dipoles rotation cannot cope with the frequency change, thus bringing about a phase lag which reduces the heating effect, (von Hippel, 1954). This effect is referred to as the relaxation time of a material and is

the time taken for the dipoles to return to equilibrium, when the external electric field is removed.

The frequency bands allocated, for industrial microwave heating, have been set to approximately 900MHz and 2450MHz as not to interfere with other frequency use in telecommunication, defence and maritime applications. The variation in dielectric properties is therefore not significantly crucial since this frequency will remain constant during processing (Meredith, 1998).

Noticeable in Table 2.2 are the variability in dielectric constants of materials as a result of frequency variation.

Table 2.2: Dielectric constants of various materials (Meredith, 1998)

Material	Temp (°C)	30 MHz		1 GHz		2.5 GHz	
		ε'	ε''	ε'	ε''	ε'	ε''
Water, ice	-12	3.8	0.7	3	0.004	3.2	0.003
Water, distilled	25	78	0.4	77	5.2	77	13
Water, distilled	85	58	0.3	56	1	56	3
Fused quartz	25	3.78	<0.001	3.78	<0.001	3.78	<0.001
feldspar	24	-	-	2.61	0.024	2.61	0.02
Sandy soil 0%MC	25	2.55	0.033	2.55	0.012	2.55	0.007
Sandy soil 17%MC	25	20	30	20	0.3	17	0.3
NaCl (0.1 molal sol.)	25	76	480	76	30	76	20

Water which is heated by dipolar re-orientation shows an increase in dielectric constants with increasing frequencies. In comparison, aqueous sodium chloride (NaCl) which is heated predominantly by ionic conduction illustrates a decrease in dielectric constants with increasing frequency (Meredith, 1998).

2.5.2.1 Moisture

Industrial high frequency operates in the frequency range $1 \times 10^7 < f < 3 \times 10^9$ Hz, at which the mechanisms of heating of concern, should be dipolar heating and DC conductivity. This depends on the state of water absorbed in the material, (Metaxas and Meredith, 1983).

Water is extremely polar in its chemical structure and readily absorbs microwave energy which converts it to heat. The dielectric properties of absorbed water are further significantly different to that of liquid water. Absorbed water, in this context, refers to when the water

molecules are in contact with another material. Hasted (1972) as cited by (Metaxas and Meredith, 1983), observed that the maximum loss factor for water occurred at a frequency of 18GHz, whereas the maximum loss factor for absorbed water occurred at a much lower frequency. The nature of the absorbed water therefore has a marked effect on the dielectric properties and subsequently on the materials interaction with the high frequency field. Absorbed water in wet materials exists in two defined states. These are free water which resides in cavities, and bound water which exists either as chemically or physically absorbed within the material. Figure 2.4 illustrates two distinct regions as a result of the different nature of the water states within the original material.

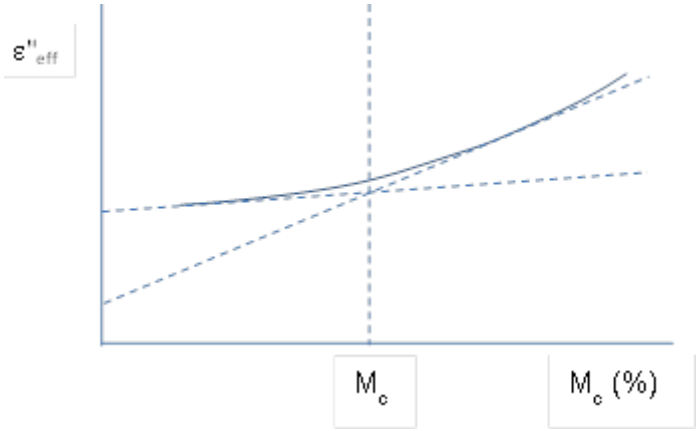

Figure 2.4: Loss factor dependency on moisture content, (Metaxas and Meredith, 1983)

The flatter slope on the lower end of the moisture scale indicates bound water, whereas the steeper slope at higher moistures is largely due to the presence of free water. The “bound” water molecules at the surface of a material are less rotationally free than water residing in capillaries and cavities. The change of slope occurs at the critical moisture content (M_c) although in many cases the change is gradual making the identification of the M_c very difficult, (Metaxas and Meredith, 1983). The M_c value for non-hygroscopic materials such as sand occurs at about 1% moisture, (Stuchly, 1970) as cited by (Metaxas and Meredith, 1983).

The presence of water in any material is bound to increase its effective loss factor and thus rendering it a better candidate for microwave heating, (Metaxas and Meredith, 1983).

2.5.2.2 Temperature

The variation of the dielectric properties of a material with temperature change is of great significance in industrial microwave heating. The variation with heat might spur chemical and

physical changes to the material which in turn alters the interaction of the microwaves, (Meredith, 1998). These variations make the calculation of proposed temperature changes complex.

Researched by Tingas (1969) as cited by (Metaxas and Meredith, 1983) on Douglas fir has shown that with low moisture content, the loss factor increases with increasing temperature and at higher moisture content, the loss factor decreases with increasing moisture content. The increase in loss factor at low moisture contents, is believed to be as a result of the reduction in physical binding as temperature increases, and the dipoles are freer to re-orientate.

Bengtsson and Risman (1971) as cited by (Metaxas and Meredith, 1983), showed large variation in both the dielectric constant and loss factor between ice and liquid water. The dielectric properties of ice are observed to be significantly lower than that of water. Atwater and Wheeler (2004), suggests that the variation in the dielectric constant and the loss factor of a material subject to microwave heating are related to the heating mechanism of the material.

2.6 Microwave interaction

Microwaves in themselves do not carry heat energy. It is the interaction between the incident microwaves and the dielectric material which causes the material to be able to create heat volumetrically. There are numerous physical parameters which play an important role during this interaction of the microwaves and the dielectric material. The theoretical equations introducing the physical properties will be discussed briefly.

2.6.1 Power dissipation

Microwave heating is the result of the conversion of electromagnetic energy into heat. The energy transfer occurs through space or any medium in the form of electromagnetic waves, (Metaxas and Meredith, 1983). The resultant power flows in the same direction of propagation to which the electric and magnetic field lies normal to. This represented by the Poynting equation, a vector product of the electric and magnetic fields. Dimensionally this vector product is regarded as the power flux density p (watts/m^2), (Meredith, 1998). The relationship between power flux density and the electric and magnetic fields are presented in Equation 4.

$$p = \bar{E} \times \bar{H} \qquad \text{(Equation 4)}$$

Where: p = Power flux density (watts/ m^2)

$\overline{E}$ = Electric field vector (volts/ meter)

$\overline{H}$ = Magnetic field vector (amperes/ meter)

The power flow through a closed surface can be calculated by means of the integration of the Poynting vector over the workload surface. The power flux density is not the actual power dissipated into the medium of the workload, but rather the power incident on the workload. It is the power dissipation density dependence on the electrical properties of the workload that defines the power absorbed. The power dissipation density is thus the power absorbed per unit volume of the workload and therefore has the dimension of watts per cubic metre and is expressed in Equation 5 below, (Meredith, 1998).

$$p = 2\pi f \varepsilon_0 \varepsilon" E_i^2 \qquad \text{(Equation 5)}$$

Where:

p	=	power density (Watts/m^3)
ε_0	=	permittivity of free space (8.86 x 10-12 F/m)
$\varepsilon"$	=	dielectric loss factor
E_i^2	=	root mean square electric field strength (V/m)

Propagation and power of an electromagnetic wave to a workload is affected by material properties and the electromagnetic wave properties such as the field intensity and power flux density, (Metaxas and Meredith, 1983). As previously discussed, there exists in many cases, variation of the electric field (E) due to temperature, moisture, etc. To account for these variations, the electric field is left in an integral form, however should no variation exist; the electric field can be assumed constant.

From Equation 5, it is evident that microwave frequency and the material loss factor have an effect on the workload. Thus, high frequencies or large loss factors reduces the heating time and improves the production output. The electric field stress variation has the greatest impact on the energy output due to the exponential influence of its square in the equation. It is important to note the existence of the external electric field stress and that its relation to the internal electric field stress is dependent on the electric field vector at the surface of the dielectric, (Meredith, 1998). There are numerous factors that bear reason to the non-uniform nature of the electric fields present in microwave applicators. Therefore, the difficulty in the estimation of external electric field is compounded and numerical methods are required.

When electromagnetic waves passes from one medium into another of different characteristic impedances, reflected waves occur on the surface of the interface, (Meredith 1998). The magnitude of the reflected wave increases with increasing impedance mismatch. The reflected wave is undesirable as it represents power wasted and can adversely affect the performance of the generator. Hence “impedance matching” is an important procedure during microwave applicator design.

According to Meredith (1998), non-uniform heating may be induced by large particle workloads which experience a concentration of displacement current around and between the particle points of contact. The concentration can be intense depending on the size, shape and dielectric constant of the particle. The magnitude of the effect to the material is dependent on the materials thermal diffusivity and results in localised overheating. Equilibrium can be achieved if the rate of heat flow equals the rate of heat dissipation. This effect can place a maximum limit on power dissipation density allowable in the workload.

Personal safety during exposure to electromagnetic waves has been a debateable topic since the beginning of the technology. Although the waves are regarded as non-ionising, the limit to safe exposure has been set to 10mW/cm^2 for which the electric field stress is 2.0 V/cm. The basis for this decision is that this concentration of energy is of the same order of magnitude as the heat flux from a human body in a sedentary state, (Grant, 1981). Hence the body should be able to dissipate the heat easily for long periods without adverse effects. There have been publications on damaging effects of prolonged exposure to levels below 1mW/cm^2, although this has been difficult to confirm without a prolonged systematic research programme. It is however difficult to reduce leakage of high power microwave devices to below 1mW/cm^2 unless sophisticated choking systems are introduced, (Meredith, 1998).

2.6.2 Penetration depth

As microwaves penetrate a dielectric workload its amplitude decreases as the power flux density falls. This reduction is due to power dissipation within the material caused by the dielectric loss factor. Should no reflective waves be generated, the rate of field intensity decay is exponential with increasing distance from the materials surface, (Meredith, 1998). Literature defines penetration depth, as the depth to which the power flux is reduced to 1/e (0.368) of its surface value. The penetration depth is given by Equation 6 below.

$$D_p = \frac{\lambda_0}{2\pi(2\varepsilon')^{0.5}} \frac{1}{\left[\left\{1+\left(\frac{\varepsilon''}{\varepsilon'}\right)^2\right\}^{0.5}-1\right]^{0.5}} \qquad \text{(Equation 6)}$$

Where: D_p = Penetration depth

λ = Wavelength of incident radiation

ε' = dielectric constant

ε'' = dielectric loss factor

Where error of up to 10% is not significant and $\varepsilon''<\varepsilon'$, the Equation 6 can be reduced to:

$$D_p \approx \frac{\lambda_0(\varepsilon')^{0.5}}{2\pi\varepsilon''} \quad \text{(Equation 7)}$$

Equation 7 indicates the adverse effect frequency has an on penetration and thus heat uniformity of large workloads. The heat dissipated in a layer between the surface to a plain at depth D_p is 63.2% of the total, with the remainder being dissipated at depths greater than D_p, (Meredith, 1998). The importance of the dielectric constant ε' is evident in the penetration depth. With increased ε', the rate of decay of the power flux density falls correspondingly to the increasing penetration depth. Likewise, larger loss factor values for good microwave energy absorbing materials reduce the penetration depth and results in non-uniform temperature distribution from the surface to the centre of the workload, (Metaxas and Meredith, 1983). Surface heating is therefore most likely to occur with materials of high ε' and ε'', (Clark et. al., 2000).

With penetration depth referring to a materials power dissipation, skin depth is another term referring to surface skin of a conducting wall in which the majority of the microwave power flows. The microwave energy is however nearly fully reflected with only a very small portion being absorbed within the wall, (Meredith, 1998).

2.6.3 Microwave thermodynamics

Rate of heat flow is predetermined by the materials physical properties. These include: specific heat, thermal conductivity and material density which are combined in one parameter called the thermal diffusivity. Thermal diffusivity is the temperature rise within a material as a function of time and depth from the surface and is dependent on external surface conditions, (Carslaw and Jaeger, 1959) as cited by (Meredith, 1998).

To achieve an ideal volumetric heating system, the temperature increase rate of a dry and constant workload is related to the power dissipation in the workload, mass of the work load

and the workloads specific heat capacity. This can be illustrated by Equation 8 for any heating process, irrespective of the nature of the power source.

$$P = M \frac{dT}{dt} s_p \quad \text{(Equation 8)}$$

Where,

P is the total power (watts) dissipated into the workload

M, material mass (kg)

T, Temperature (°C)

s_p, specific heat capacity of the material

The specific heat capacity (s_p) for various individual materials is readily available. For a mixture however, a weighted average can be used to estimate its total specific heat capacity. Although the equations are for dry workloads, they may be adapted by including the latent energy required for evaporation of liquids.

Ignoring the latent heat requirement, the microwave heating equation can be written as per Equation 9 to incorporate material densities for dry materials and give the rate of temperature rise:

$$\frac{dT}{dt} = \frac{2\pi f \varepsilon_0 \varepsilon'' E_{in}^2}{s_p \rho} \quad \text{(Equation 9)}$$

Where,

T, Temperature (°C)

ƒ, frequency of the microwave generator (Hz)

ε_0, permittivity of free space, 8.854 x 10^{-12} F/m

ε", material loss factor

E_{int}, internal voltage stress in the dielectric material (Volts/meter)

ρ, material density (kg/m^3)

s_p, specific heat capacity of the material

From Equation 9, it can be observed that frequency and loss factor plays an important role in the energy absorption. This equation further puts into perspective how density and specific heat reduces the heating rate. Hence, even though water has a high loss factor making it a good candidate for dielectric absorption, its high specific heat value moderately reduces its

heating rate. The equation is based on the assumption that the loss factor or electric field strengths remain constant and that the material is homogenous with no heat loss on the surface during microwave irradiation.

In the mining industry, microwave heating is considered to be able to reduce grinding costs through the thermal assisted communition of ore. The process uses the combination of thermal gradients between materials and the selective heating potential of microwave heating. Walkiewicz et. al. (1988) investigated the heating potential of various aggregates (25g sample mass) using a 1kW, 2.45 GHz microwave oven. A summary of the results are provided in Table 2.3 below. The specific heat capacities were sourced from (Knacke and Hesselmann, 1991).

Table 2.3: Summary of various aggregates heating potential. (Walkiewicz et. al., 1988)

Mineral	Chemical composition	Specific heat capacity @298K (J/kg.K)	Maximum temp (°C)	Time (min)
Chalcopyrite	$CuFeS_2$	516.5	920	1
Galena	PbS	208.95	956	7
Magnetite	Fe_3O_4	654.2	1258	2.75
Orthoclase	$KAlSiO_3O_8$	-	67	7
Pyrite	FeS_2	517.1	1019	6.75
Quartz	SiO_2	740.5	79	7
Sphalerite	ZnS	467.6	88	7

The silicate, carbonate and sulphate minerals are commonly referred to as gangue or unwanted materials in the mineral processing field are not readily heated by microwave irradiation, Chen et. al. (1984) as cited by Kobusheshe (2010). These include minerals such as dolomite, quartz which are common to road building aggregates.

Metal oxides and metal sulphides such as magnetite and pyrite for example are easily heated by microwave irradiation, Chen et. al. (1984) as cited by Kobusheshe (2010). These ore rich materials such as magnetite can have a high specific gravity depending on the quantity of ore they possess and are usually located in areas of mining activity. Weinert (1980) suggests that ore rich rocks such as magnetite are one and a half times denser than other natural road building materials and thus pose high haulage expenses. Chalcopyrite

heats readily with microwave irradiation, however, this sulphide material is suggested by Weinert (1980) to decompose rapidly when exposed to the atmosphere.

In terms of Equation 9, the factors to be considered in evaluating the suitability of microwave heating should include the following:

- Appropriate material loss factor (0.01 to 1);
- Material sensitive to excessive heat exposure;
- Conventional heating is inefficient, time consuming; and
- Selective volumetric heating is required for energy saving.

Impurities such as salts in water can increase the effective loss factor due to their polar nature. The occurrence of impurities in water might, however, be counterproductive to the natural stone aggregate strength properties.

2.6.4 Thermal runaway

A rise in dielectric loss factor initiated by temperature increase of a material can induce a thermal “runaway” effect. This phenomenon is started with the initial absorption of the microwave energy causing an initial rise in temperature which in turn causes an increase in the initial loss factor. This subsequently results in a further rate of temperature increase in the material. Some materials show a positive increase in loss factor with temperature rise such as, styrene butadiene rubber (SBR), glass bonded mica steatite ceramic, (Metaxas and Meredith, 1983). Microwave design techniques are aimed at avoiding thermal runaway such that the energy input is in equilibrium with the thermal diffusivity resulting in adequately fast processing time. Thermal runaway is more likely at the lower frequency as loss factors are generally higher there, (Meredith, 1998).

2.7 Microwave sources and application method

As previously mentioned, microwave heating is the result of the interaction between a dielectric material and the electromagnetic field. The electromagnetic field is created by manipulating the movement of electrons generated by electron tube devices in a controlled manner, (Meredith, 1998).

The range of microwave generators varies from magnetrons and klystrons to solid state power sources. The magnetron, see Figure 2.5, is overwhelmingly superior in satisfying industrial needs in relation to other devices, (Meredith 1998). This is evident as, Meredith (1998), indicates that magnetron’s make up 98% of the industrial and domestic usage

market. It is the technical and economic considerations that make many of the microwave generating sources unsuitable for industrial purposes. Industrial applications require high power outputs and this aspect makes solid state sources such as diodes and transistors furthermore unsuitable. Microwave applications have a high capital cost and operating cost in relation to conventional heating sources. Sutton (1989) states that microwave usage is difficult to justify on energy costs alone, as fossil fuels are less expensive. For technical considerations, the power output, frequency and efficiency are important.

Figure 2.5: Typical magnetron: 75kW at 915MHz.

Meredith (1998) explains that for over 20 years, a klystron of 50kW at a frequency of 2450MHz has been available in relation to the 30kW supplied by the magnetron. Higher power magnetron generators (200kW) are available at the 900MHz frequency range. The klystron has better frequency stability than the magnetron but its high capital and operating costs make it only viable where stiff frequency restrictions are to be imposed. The development of the magnetron has had a major impact on the microwave heating industry due to its efficiency and lower operating costs. High power magnetrons can be rebuilt at the end of its life at a cost of less than 10% of the energy that they require, (Meredith, 1998).

Microwaves also obey the laws of optics and therefore can be reflected, absorbed or transmitted, depending on the material type, (Sutton, 1989). Metals are good reflectors for microwaves. The reflective properties are utilised to guide microwaves from the magnetron to the applicator. Rectangular hollow waveguides with reflective surfaces are used for this purpose. The material choice for wave guide construction is important; although power loss might be small, it may raise the temperature in the wave guide significantly. Most industrial

purposes use aluminium in wave guide construction. In these instances, the electromagnetic field descriptions are more complicated than a plane wave, (Metaxas and Meredith, 1983).

Applicators are classified depending on the field pattern within them. The three common types of applicators are; multimode, single mode and travelling wave. Multimode ovens are the most common applicators used due to its simplistic mechanics and its diversity to process workloads, (Meredith, 1998). A drawback of multimode applicators is its non-uniform electric field distribution, (Sutton, 1989).

During industrial microwave applications, the reflective power is a result of reflected waves not absorbed by a workload. Excessive reflected power can cause damage to the microwave source, i.e. the magnetron. It is common therefore to provide a terminating load to absorb the unused residual power. A water bath is usually used due to its high loss factor and waters high specific heat value. The knowledge of reflective power and its relation to incident power is vital for determining the microwave applicators efficiency and evaluating impedance matching, (Meredith, 1998).

Numerous authors have outlined criteria for successful adoption of microwave processing systems. Criteria quoted by Clark (1995) are as follows:

- Energy transfer, high speeds, short line lengths, less wastage, energy conservation.
- Deep penetrating heat: uniform heating, greater yields.
- Selective heating, unique solutions to problems, Ability to heat within a package.
- Electronic mechanism: automation, control and data logging, environmentally clean and quiet, quick setup and fast change over to new products.

According to Clark et. al. (1995), speed by itself is considered rarely the single reason for microwave use. Careful analysis of factors is required and the commercial viability should be considered.

The stored energy for various materials is quantified by their energy density values. There are several types of reactions that release these energies, such as chemical, electrical, etc. Table 2.4 provides a summary of the energy density of a few materials It is useful to note that 1MJ (mega-joule) is equivalent to approximately 0.28 kWh (kilowatt hours).

Table 2.4: Energy density of various materials (Wikipedia, 2012)

Material	Specific energy (MJ/kg)	Energy density (MJ/litre)
Crude oil	46	37
LPG propane	49	25
Petrol	46	34
Coal, bituminous	24	20
Natural gas	54	0.036

2.8 Microwave interaction with crude oils

Asphaltene molecules are polar by nature and its concentration in crude oil affects the temperature rise under microwave irradiation, (Mutyala et. al., 2010)

It is commonly known that microwave interaction with materials is physical in nature and heating is a result of frictional forces generated. It is interesting to note in this study that work by Gunal and Islam (2000) as cited by Mutyala et. al., (2010) suggests that asphaltic crude properties experience irreversible alterations under electromagnetic irradiation. It is suggested that the microwave irradiation produced changes in the colloidal orientation of the asphaltene molecules.

Bjorndalen and Islam (2004) as cited by Mutyala et. al., (2010) explain that at high concentrations of asphaltene reduces crude oil viscosity under microwave irradiation. It was further noted that a non-linear dependency exists between crude oil viscosity and both the electromagnetic power and asphaltene concentration.

The information on microwave irradiation effects on asphaltene molecules as stated above have been studied for crude oils and although bitumen contains asphaltenes, it is unknown if the same effects apply. If so, the bitumen viscosity would well be affected by the microwave irradiation.

CHAPTER 3: LITERATURE STUDY ON BSM-FOAM

3.1 Introduction

Foam bitumen stabilised mix (BSM-foam) was conceived through progression whilst attempting to find a means of applying thin films of bituminous binder to ungraded fine minerals. In HMA production, well graded aggregates are required, as a low fines content results in bleeding of paved surfaces and a high fines content resulted in balling during mixing, (Csanyi, 1957). After having initially focused on bituminous binder in an atomized form, Csanyi later turned his attention to the potential of foamed bitumen. At the time, foamed bitumen was considered an undesirable phenomenon occasionally occurring at HMA plants. The foamed bitumen process when used in a controlled environment however provided the means to reduce viscosity of the bitumen binder allowing improved coating of the fine ambient temperature mineral particles, (Csanyi, 1959).

The use of bitumen emulsions was already prevalent at the time Csanyi (1959) discovered foamed bitumen's potential. Despite emulsions energy saving nature, it has its own inherent draw backs. Bitumen emulsion was required to break at the correct time and the moisture removed so that the required strength gains could be achieved. This process of curing required additional equipment and operations which created time delays. BSM-foam did not suffer these draw backs, (Csanyi, 1959).

It has been shown that emulsion and foamed bitumen produced similar mixes when bitumen content was below 1.5%, with the exception of permeability. Thereafter, BSM-foam mixes displayed improved structural properties, (Bowering and Martin, 1976).

There are guidelines available such as the TG2 (2009), Bitumen Stabilized Materials produced by the Asphalt Academy of Southern Africa, as well as Wirtgen's Cold Recycling Technology handbook (2010) providing sound recommendations for successful construction of BSM-foam layers.

Numerous advantages have been acknowledged in the use of BSM-foam. These include cost savings of up to 75% on conventional repair and reduction in normal energy needs by 60%. The added benefit of reduced construction time during recycling with BSM-foam in relation to conventional reconstruction methods not only benefit the client and contractor, but extends to road user cost saving, (Ackeroyd, 1989).

This chapter introduces the characteristics of the material to be utilized as the “workload” to which the microwave applicator will impart electromagnetic waves. The physical constituents of foamed mixes are optimized to improve the engineering properties of the mixture during its placement and service life in a pavement structure. These basic constituents are therefore reviewed in light of understanding the benefits of optimization and possible impact electromagnetic waves could have on it.

3.2 Material and mix considerations

The interactions of the various materials forming a cold mix are paramount to the BSM-foam pavement layer’s performance. In an attempt to obtain a broader understanding of these interactions, the properties and performance of the individual materials will be considered first.

3.2.1 Aggregate properties

3.2.1.1 Suitability and grading

BSM-foam can be produced with a wide range of materials such as weathered gravels, crushed rock and sands obtained from both virgin and recycled sources. The foamed bitumen process is further independent on particle charges in acidic or basic rocks, unlike bitumen stabilization by emulsion.

Bowering and Martin (1976) and Ruckel et. al. (1983) provided a list, Table 3.1, of various materials acceptable for use in BSM-foam. The list provided has been categorized by the Unified Soils Classification System and hence only takes account of the particle size, particle size fraction and clay content with no indication of chemical composition differences. The TG2 (2009), Technical Guideline: Bitumen Stabilized Materials, does however indicate that calcrete gravels are less suitable for foamed bitumen treatment based on past in field experiences.

Table 3.1: Material suitability for BSM-foam production (Ruckel et. al., 1983)

Soil type	Suitability for foamed mix	Optimum Bitumen Content (% m/m)	Comments
Well graded gravel, little or no fines	Good	2.0 – 2.5	Permeable (improve with crushed fraction)
Well graded gravel + some clayey silt	Good	2.0 – 4.0	Permeable (improve with crushed fraction)
Well graded gravel + sandy silt	Good	2.0 – 4.0	Permeable (improve with crushed fraction)
Poorly graded gravel + sandy clay	Good	2.5 – 3.0	Low permeability. Improve with crushed fraction)
Clayey gravel	Poor	4.0 – 6.0	Improve with lime
Well graded sand	Fair	4.0 – 5.0	Needs filler
Well graded silty sand	Good	2.5 – 4.0	
Poorly graded silty sand	Poor	3.0 – 4.5	Use lower pen bitumen, add filler
Poorly graded sand	Fair	2.5 – 5.0	Needs filler
Silty sand	Good	2.5 – 4.5	
Slightly clayey, silty sand	Good	4.0	
Clayey sand	Poor	4.0 – 6.0	Needs small % lime
Clayey sand (After lime modification)	Good	3.0 – 4.0	

The majority of aggregates are classified as hydrophilic (water loving) or oleo-phobic (oil hating). HMA research indicates that aggregates also differ in their degree of affinity for bitumen. Therefore aggregates with high silicone content (e.g. granite, an acidic rock) are easily susceptible to stripping and more difficult to coat than basic rocks, such as limestone. Jenkins (2000) suggested that aggregate prone to stripping in HMA mixes will have a lesser likelihood to be suitable for BSM-foam production.

Castedo et. al. (1984) tested the Modified Marshall Stability for various aggregates in a water sensitivity analysis. His research concluded that the crushed limestone was inherently

stronger relative to the other aggregates tested and therefore outperformed them as foam bitumen treated materials, (Castedo et. al., 1984).

It is apparent from previous studies, that chemical composition of the aggregates is not as significant as the material grading to produce good quality BSM-foam. The grading envelopes to be used for the production of foam stabilization, as illustrated in Figure 3.1, have been developed by Mobil Oil based on their experiences with numerous material types (Ackeroyd & Hicks, 1988). The grading curve is still used presently.

The purpose of the inception of BSM-foam was to produce a functional pavement layer from inadequate loess material, it is therefore expected that BSM-foam should perform satisfactory with fine grained mixes. Majority of research has confirmed foamed bitumen's affinity for finer fractions of a grading curve. As a result it produces good quality mixes when utilizing a sand skeleton aggregate structure due to its nature. Due to its importance, the finer fraction would subsequently be used in mixes so as to optimize in both the optimum bitumen and water content.

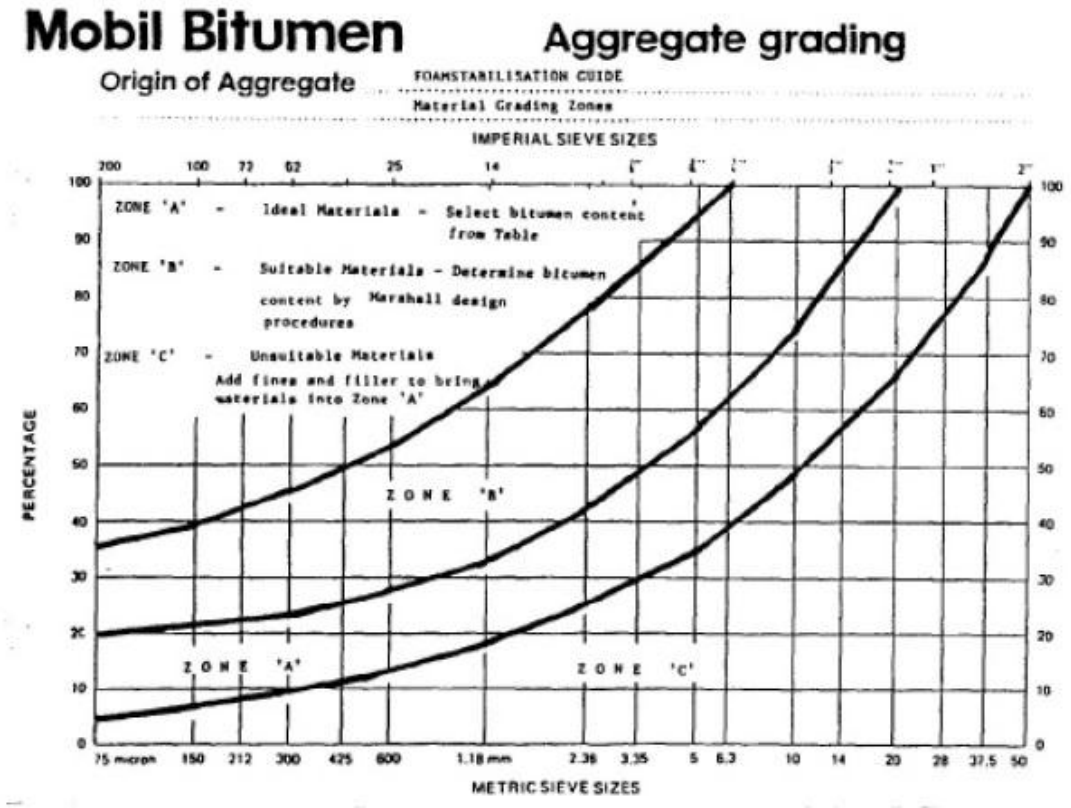

Figure 3.1: Grading curves ranking aggregate suitability, (Ackeroyd & Hicks, 1988)

The spacial composition of sand skeleton mixes produces the densest and most suitable grading for BSM-foam. Grading's close to the stone skeleton, i.e. too little fines content, will result in mixes characterized by balling of the bitumen as conglomerates cling together.
Sakr and Manke (1985) illustrated the stability of foamed mixes to be most affected by aggregate interlock than the viscosity of the binder. Although the viscosity grade of bitumen is not critical for BSM-foam mixes, Jenkins (2000) suggested that softer grade bitumen (80 to 250 penetration) are preferred in foamed bitumen production as blockages in the expansion chambers and spray nozzles can be eliminated. Wirtgen (2010) indicate that low penetration grade (hard bitumen) could result in poor quality foam and dispersion of bitumen. Sakr & Manke (1985) also indicated aggregate angularity of the finer aggregates is a good indication of stabilization suitability using foamed bitumen.

Although grading curves provide a good indication of material suitability to produce a good quality mix, it is not comprehensive enough on its own. Therefore additional material properties such as Voids in the Mineral Aggregate (VMA) are required to further improve the mixtures performance. Jenkins (2000) indicated that a reduction in VMA results in a more desirable BSM-foam product. With the assistance of mechanical forces during compaction, the reduction in VMA of the sand fraction results in improved tensile strength and subsequently a reduction in permeability reducing BSM-foam's moisture susceptibility shortfall.

Myre (1997) indicates filler fractions required for BSM-foam can range from 2% to 20% and with the fractions passing 2mm not less than 30%. Saleh (2004) indicated a maximum aggregate size for foam bitumen of up to 19mm and no more than 12.5% for the filler fraction. TG2 (2009) recommends a maximum stone size of 19mm with the filler fraction ranging from 5% to 15%. The addition of virgin aggregates can vary from 15 to 20% of the coarse fraction and materials should not be colder than 15°C when mixing with foam.

Bowering and Martin (1976) tested three types of crushed rock namely; basalt breccia and quartzite. When compared to basalt and breccia, the quartzite did not perform as well during the Marshall Stability and cohesion tests. The quartzite fines (0.075mm) did however range from 2% - 7%, with 2% being well below the recommended minimum filler content.

Bowering (1970) noted that hard crushed aggregates generally required less bitumen 1.5% to 3.5% by dry aggregate weight when compared to the weaker materials which required 4% to 6% bitumen. The hard materials consisted of coarse particles (19mm) whereas the weak

loess material contained maximum particle sizes of 2.36mm. These values appear to be related to the surface areas of the aggregates and its influence on binder quantity selection.

3.2.1.2 Fines and filler

The fines content in an aggregate holds a great significance in the production of good BSM-foam. The TG2 (2009) provides a minimum acceptable requirement for this fraction within a mix, which is set at 5%.

Filler fractions influence the foamed bitumen's dispersion due to surface area and subsequently heat transfer during BSM-foam production. BSM-foam has an affinity for the fines, (Jenkins, 2000). The ability of foamed bitumen to selectively coat the fines creates a higher viscosity. This mastic of bitumen and fines increases the tensile strength in the mix. An upper limit binder content exists at which the binder starts acting as a lubricant in the mix. When this limit is exceeded, there is a loss in strength and stability of a mix. Sakr & Manke (1985) showed that higher fines content had higher stability. A similar trend was indicated for tensile strength by Bissanda (1987).

3.2.1.3 Active filler and plasticity

Mixing of foamed bitumen is affected by the plasticity of aggregates, Bowering and Martin (1976). High plasticity gravels respond poorly to foam bitumen unless modified with cement or lime before the addition of the binder. Lee (1981) indicated that a minor fraction of plastic fines are acceptable, however lime stabilization is recommended and economically viable when the Plasticity Index (PI) exceeds 8%. Lancaster et. al. (1994) later indicates a maximum PI limit of 12% is allowable before any lime modification is required. The TG2 (2009) recommends stabilization prior to foaming for natural and weathered gravels having PI greater than 10%.

The addition of cement is recommended to improve the dispersion of the bitumen and assists in stiffness of BSM-foam. The TG2 (2009) specifies a limit of 1% cement addition, exceeding this limit results in the material losing its flexibility and performing similar to a cement stabilized layer. Wirtgen (2010) advises care when adding cement to foam bitumen as the cement hydration occurs immediately when in contact with water. The cement then binds with the fines and effectively reduces the fine fractions required for foamed bitumen dispersion. Jenkins (2000) observed that the addition of active filler generally increased cohesion in excess of 800kPa and reduced the materials friction angle close to 0°.

3.2.1.4 Reclaimed Asphalt

The typical percentage of RA used in recycling within South Africa is approximately 25% or less. This is as a result of a typical surfaced pavement containing an asphalt surfacing layer of 40mm being combined with the base during recycling at a depth of 200mm.

In the cold mix context, the use of RA can be classified as a “black rock” due to the low equilibrium temperatures at mixing and hence not significantly affecting the residual bitumen. During Hot-mix recycling the aged and residual bitumen becomes a one phase system. An increase in heat addition to a BSM-foam mix with RA might increase the amount of blending between the two bitumen phases. It is known that with WMA at temperatures of 120°C, blending of phases does occur.

Increase in the use of RA in BSM-foam may reduce the design binder content due to:

- Reduced binder absorption of the coated RA particles
- Increase in cohesion due to the higher affinity of the fresh bitumen to RA over virgin aggregates
- Durability and moisture susceptibility is improved due to the already coated RA particles

Ebels (2008) noted that increasing use of RA in BSM resulted in the reduction of shear strength.

3.2.2 Bitumen

3.2.2.1 Bitumen properties

The rheological properties of bitumen have been extensively studied by many due to its high dependency on time and temperature. The bitumen‘s chemical composition and physical arrangement of molecules in the material defines the characteristics at a given temperature, as indicated by the Shell Bitumen Handbook (2003). It is therefore essential to understand these physiochemical changes and interactions and their influences on rheology. Due to microwave energy dissipation theory, this section further reflects on bitumen chemistry so as to better ascertain the potential influence microwaves could have.

Crude oils in general differ in their physical and chemical properties and even though approximately 1500 crudes are produced globally, only a select few are considered suitable for bitumen manufacture. According to the Shell Bitumen Handbook (2003), the precise

composition of bitumen varies according to source of the crude oil, the refining process used and in service binder ageing. The internal structure configuration is further determined by the chemical composition of the molecular species present. Along with certain trace metals in the form of organic salts and oxides, an elementary analysis of a typical crude oil would consist of:

- Carbon 82 - 88%
- Hydrogen 8 - 11%
- Sulphur 0 - 6%
- Oxygen 0 - 1.5%
- Nitrogen 0 - 1%

Chemical composition of bitumen is extremely complex and a complete analysis is unlikely to be possible. Bitumen is made up of complex hydrocarbons and can be divided into two broader chemical groups called maltenes and asphaltenes. The maltenes can further be subdivided into saturates, aromatics and resins.

Shell bitumen handbook (2003), defines the general composition of a 100 penetration bitumen sample as follows:

- Asphaltenes are insoluble amorphous solids, complex aromatic materials and are considered to be highly polar, possessing a fairly high molecular weight. Depending on the method and separation techniques used, these molecular weights can vary widely, with the majority of results ranging from 1000 to 100 000. Particle sizes vary from 5 to 30 nm and a hydrocarbon atomic ratio of 1. Asphaltenes has large effects on the rheology characteristics and constitutes 5 to 25% of bitumen.
- Resins are similar to asphaltenes and predominantly composed of hydrogen and carbon with small amounts of sulphur, oxygen and nitrogen. They are polar in nature and are strongly adhesive. The proportion of resins to asphaltenes governs the solution gelatinous nature of bitumen to a certain extent. Molecular weights range from 500 to 50 000, particle size of 1 to 5nm with an H/C ratio of around 1:3.
- Aromatics make up approximately 50% of bitumen and are viscous in nature. They consist of non-polar carbon chains in which unsaturated ring systems (aromatics) dominate. Average molecular weight range from 300 to 2000.

- Saturates are non-polar viscous oils consisting of straight and branch chain aliphatic hydrocarbons. Their molecular weight is similar of that to aromatics. They form 5% to 20% of bitumen composition.

Bitumen is traditionally thought of as a colloidal system in which the heavier asphaltene micelles are dispersed in suspension of lower molecular weight maltenes. The micelles are considered to be surrounded by an absorbed sheath of high molecular weight aromatic resins which act as a stabilizing solvent layer. Moving further away from the center of the micelles, there is a gradual transition to less polar aromatic resins which are suspended in a less aromatic oily dispersion medium.

The two types of bitumen can be characterized as follows; the solution or gelatinous types, depending on the aromatic/ resin fraction. In the presence of sufficient resins and aromatics, the good mobility of the micelles results in solution type bitumen. Lower fractions of aromatics and resins resulting in insufficient solvating power of asphaltenes lead to an irregular open packed structure of linked micelles consisting of internal voids filled with intermicellar fluid. These are regarded as gelatinous type bitumen. Most bitumen are of intermediate character.

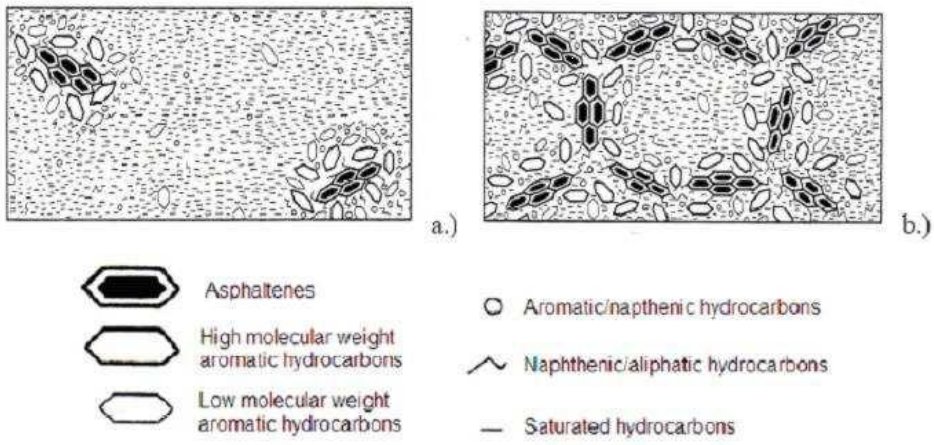

Figure 3.2: Schematic representation of sol and gel type bitumen (Hagos, 2008)

The solvation and colloidal behaviour has an influence on the viscosity of the system. The effect decreases with increasing temperature and the gelatinous character of certain bitumen may be lost when heated at high temperatures. The presence of maltenes, the continuous phase, imparts an inherent viscosity to bitumen. Increase in the dispersed phase, asphaltenes, increases the viscosity. Increased saturates decreases the maltenes ability to saturate the asphaltenes leading to agglomerations. The asphaltene and saturate content

therefore has an influence on the bitumen's gel type characteristic as well as its temperature dependence.

The following maltene relationships influence bitumen rheology:

- Aromatics have little effect on rheology;
- Increased saturates softens bitumen; and
- Increasing resins hardens bitumen, reduces Penetration Index and increases viscosity.

There is a correlation between the chemical composition and physical properties of bitumen; however it has also been found that bitumen with different chemical compositions could have similar physical properties when derived from different crude oils. It is therefore not possible to define physical properties based on chemical composition in the broader sense, (Shell bitumen handbook, 2003). Possibilities of the polar nature of bitumen could however assist the heating process using microwaves.

Jenkins (2000) indicated the following bitumen properties that contribute to foam behaviour characteristics:

- Viscosity verses temperature relationships
- Ratio of Maltenes to Asphaltenes
- Bitumen composition- Maltenes (Saturates- paraffin and naftenes, Aromatics, Resins) and Asphaltenes

The origin, refining and manufacturing process determines the above properties. There are instances of silicone anti-foamants used in the refining process that are very difficult to monitor or identify. Silicone anti-foamants are synonymous with BSM-foam as they reduce bitumen foamability during production, (Jenkins, 2000)

In field bitumen hardening are amongst other caused by photo-oxidation and nuclear energy changes perpetuated by beta and gamma rays. The photo-oxidation results in the formation of a skin on the surface of the bitumen of approximately 5 micrometers thick. This is cause by the ultra-violet radiation which penetrates to about 10 micrometers within the bitumen. The skin can however retard oxidation although it is soluble in water which results in further bitumen exposure, (Shell bitumen handbook, 2003). This type of radiation differs from microwaves due to their wavelengths and might not have the same effect.

3.2.2.2 Foamed bitumen

The introduction of foamed bitumen to aggregate is the basics of producing foamed mixes. BSM-foam is produced by the injection of cold moleculised water, typically 2% by mass, into hot bitumen. The process occurs in an expansion chamber with the foam collapsing soon thereafter. The foamant water droplets undergo a phase change as it makes contact with the hot bitumen. The process is essentially depicted within the laws of energy conservation where the hot bitumen supplies the heat energy to the water droplet sufficient for the water to exceed the latent heat of steam and enter a vapour phase. Trapped within the bitumen, this volume change intrinsic to water vapour (steam) results in the rapid expansion observed during the foaming process. The physical properties of the bitumen, importantly the viscosity, are temporarily altered during the foaming process. The temporary state of low viscosity experienced allows for improved mixing with moist mineral aggregates at ambient temperatures. Figure 3.3 illustrates the foam production in the expansion chamber.

The application of this unstable foamed bitumen to aggregate in a mixing chamber causes the bitumen bubbles to erupt during collision, with the airborne aggregate resulting in bitumen speckles uniformly spread across the volume of aggregate. These bitumen speckles are later forced into contact between the aggregate particles during compaction thus creating spot-welds which improve the materials resistance to fatigue.

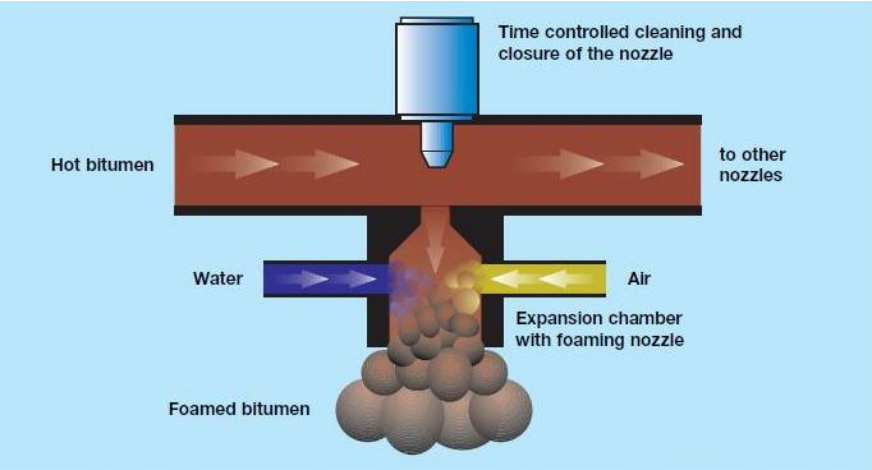

Figure 3.3: Illustration of foam production in the expansion chamber, (Wirtgen, 2010)

Foamed bitumen is characterized in terms of its half-life and expansion ratio (ER). The expansion ratio is the maximum volume achieved in the foamed state in relation to the bitumen's volume in its original state, TG2 (2009) or Wirtgen (2010). Half-life is the time in seconds taken for the foam to be reduced to half its maximum foamed volume.

Brennen et. al. (1983) found that the expansion ratio and half-life characteristics were affected by the water quantity and bitumen temperature during the foam production. Increase in bitumen temperature or water flow rate results in an increase in ER, but a decrease in half-life.

Varying water application rates of the foamant water, a plot can be constructed to illustrate its influence on the expansion ratio and half-life as shown in Figure 3.4. Such a plot indicates that no optimization point exists, yet a trade-off between the expansion ratio and half-life is evident which may be used as a basis for the selection of foamant water percentage.

Bowering & Martin (1976) illustrated the advantages of average expansion foam ER= 15 on mix characteristics in comparison with low expansion foam ER= 3. Although a noteworthy insight, the comparison would seem one dimensional as no half-life value was provided. Jenkins (2000) further illustrated in comparison with HMA that an ER= 4 is the lowest value possible to achieve adequate mixing of all BSM-foam.

Bowering & Martin (1976) indicate higher expansion ratio created mixes with greater cohesion strength and compactive strength. Macarrone (1994) suggested high expansion resulted in better foamed mixtures. It can be expected that improved ER and half-life will promote bitumen dispersion during mixing.

There is currently no standard specification on ER or half-life as research has yet to definitively prove their influence on mix performance. There are however, recommended minimum values for ER and half-life. As indicated on Figure 3.4, Wirtgen (2010) suggests values of ER> 8 and half-life> 6 to produce acceptable results, adding that non-compliant foamed bitumen be rejected. The specified optimum percentage foamant water is taken as the average of the two contents required to meet the minimum criteria.

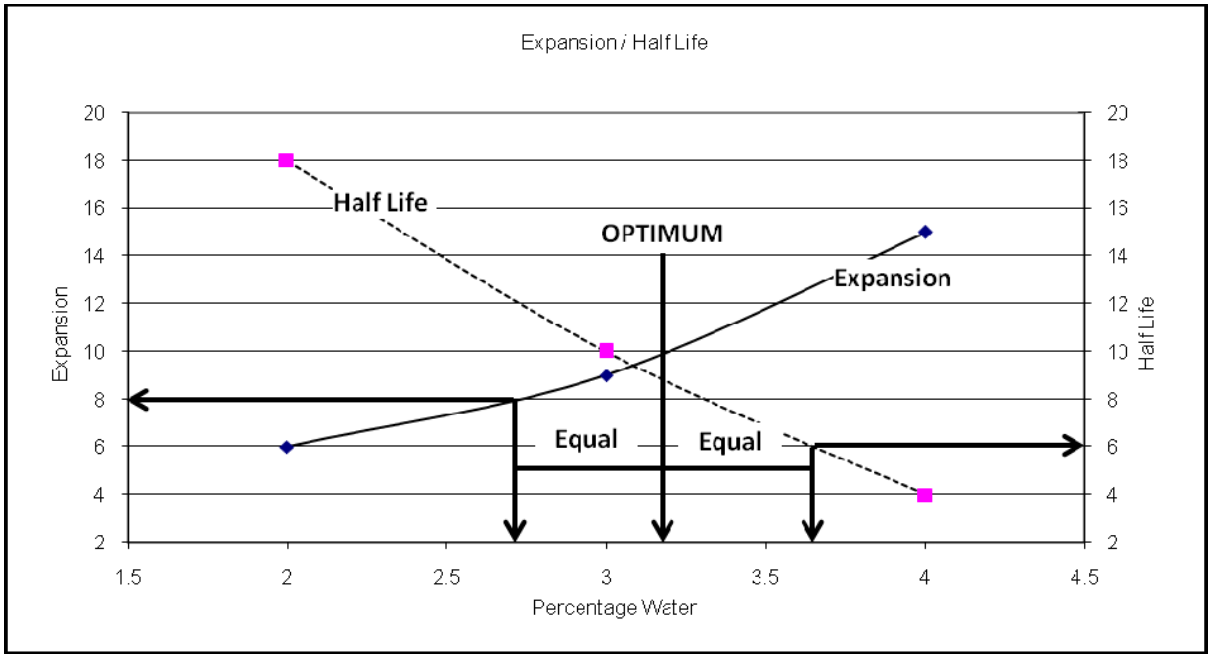

Figure 3.4: Determination of the optimum foamant water content, (TG2, 2009)

Jenkins (2000) discovered that factors such as temperature reduction, gravity drainage and elongation limits of the bitumen film influence the stability of the foam and are responsible for its decay.

Jenkins (2000) suggests after extensive research on foaming characteristics that half-life and ER are insufficient when evaluated as two independent points during foam dissipation. The two variables are dependent on each other and this resulted in the formulation of the Foam Index (FI) value being developed. The FI value is defined as the area under the ER curve and is an indication of the energy stored by the foam with respect to time, see Figure 3.5. FI uses a minimum ER in its area calculation to account for a minimum acceptable mixing viscosity. The use of the FI is cumbersome in relation and although not designed to replace ER and half-life value functions, it can be used to optimize the application rate of both foamant water and additives. Jenkins (2000) concluded that a greater FI could indicate improved foaming properties and result in better foam mixes even though the foam bitumen would have been unacceptable if considering ER or half-life alone. The research also indicated that although certain additives are perceived to increase the ER, instead they extend the half-life values creating the same effect.

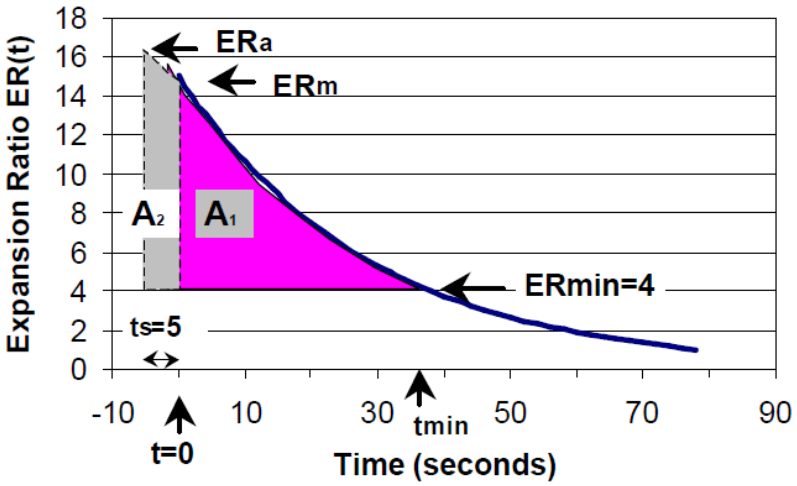

Figure 3.5: Example of the Foam Index concept as developed by Jenkins (2000)

Abel and Hines (1978) as cited by Castedo and Wood (1982) observed acceptable foamed mixes when the bitumen temperature was above 149°C. Bissada (1987) found that higher viscosity bitumen produced BSM-foam with the lowest stability values. Abel and Hines (1978) found that lower viscosity bitumen created foam more readily with higher expansion ratios and half-life than higher viscosity bitumen. The higher viscosity bitumen did however create superior aggregate coating. Wirtgen (2010) suggests that although hard bitumen can be used successfully, hard bitumen generally produce poor quality foam and dispersion of the bitumen.

The reduction in viscosity is cited as the benefit of foamed bitumen, although Brennen et. al. (1983) relates that viscosity alone does not affect formability. Castedo and Wood (1982) found that any bitumen can be used to create foam provided the nozzle type, water, air and bitumen pressures were correct. Surface active additives can also assist in either increasing the ER or extending the foams half-life according to research done by Maccarone (1994). In its collapsed state, foamed bitumen remains soft even at temperatures where the parent material stiffens, Csanyi (1959). Voskuilen et. al. (2004) discovered increased ageing of bitumen binder when recovering bitumen used to make porous asphalt (PA) with foamed bitumen at HWF temperatures. It was suggested that the increased ageing could also be a result of either the increase in exposure to oxidation of the foamed bitumen or long circulation times of the binder in the Wirtgen WLB-10 foaming apparatus during mix production (2 hours). Twagira (2010) investigated the effects of binder ageing of 80/100 penetration binder over circulation times of 1, 4 and 8 hours in the Wirtgen WLB 10 foaming apparatus. The two binders evaluated had displayed an increase in viscosity (age hardening) with increasing circulation time.

3.2.2.3 Binder interaction and particle coating

Previous studies have focused more on material grading to produce good quality BSM-foam than chemical composition of the aggregates. The importance of the particle distribution of the aggregate is therefore evident. Numerous researchers have further shown that the filler component of aggregates in a foam bitumen mix is extremely important during its metastable state. Csanyi (1959) discovered that the chemical constituents of bitumen after foaming still remained the same as before even though the viscosity was lowered.

Jenkins (2000) has discussed this physics of particle coating probability briefly. Comparing two different sphere sizes of the same unit weight and equal mass per volume, it was indicated that the combined surface area of the smaller spheres are greater. This would encourage a greater probability of the smaller particles being coated than the larger ones and hence the importance of filler fraction to prevent bitumen droplet from cohering to each other during mixing. Csanyi (1959) discovered that softer penetration binder and higher binder content improved particle coating of coarse fractions.

Ruckel et. al., (1983) provides a guide to determining the optimum binder content by using the natural filler as a guideline, see Table 3.2. Ruckel et. al. (1983) consequently recommended that the filler/binder ratios should range from 1% to 2.5% for gravels and from 1.2% to 2.2% for sands.

Table 3.2: Optimum bitumen content selection using natural filler as a variable. (Ruckel et. al., 1983)

Passing 4,75mm sieve (%)	Passing 0,075mm sieve (%)	Foamed bitumen content (% m/m dry aggregate)
< 50	3.0 – 5.0	3.0
	5.0 – 7.5	3.5
	7.5 – 10.0	4.0
	>10.0	4.5
> 50	3.0 – 5.0	3.5
	5.0 – 7.5	4.0
	7.5 – 10.0	4.5
	>10.0	5.0

The TG2 (2009), suggests that BSM-foam only require low amounts of bitumen to be added to stabilize materials successfully, typically between 1.7% and 2.5%. Jenkins (2000) proposed that above 3.5% foamed bitumen the mix loses its aggregate interlock

characteristics due to excessive bitumen content and behaves similar to HMA. Jenkins (2000) continues by explaining that exceeding 3.5% binder contents results in a mix being defined by a fatigue life. Collings and Jenkins (2011) suggest that excessive amounts of bitumen and/or cement in BSM production can introduce the concept of continuous binding thereby making the material prone to fatigue cracking. This material subsequently does not comply with the BSM definition.

3.2.3 Moisture

Moisture content during the mixing process is considered to be of the utmost importance by numerous researchers within the mix design criteria.

Csanyi (1960) stated that moisture is required to soften and breakdown agglomerations in the aggregate. It also aids in bitumen dispersion during mixing and compaction and further extends shelf life.

Jenkins (2000) states that the role of the moisture in the filler is integral in the stiffening process of the mix. The water provides lubrication during compaction at ambient temperature and is released during consolidation during compaction. Water also extends the shelf life of foam bitumen mixes and can therefore be stockpiled.

Insufficient water reduces workability of the mix, resulting in poor binder dispersion. Excess water on the other hand extends the curing time, reduces the strength and density achievable as well as a reduction in particle coating. Brennen et. al. (1983) illustrated that the Optimum Moisture Content (OMC) varied depending on the mix property to be optimized; such as strength, density, water absorption and swelling. Moisture is however critical for mixing and compaction and subsequently these should get preference.

The TG2 (2009) suggests the mixing OMC value occurs at the material “fluff point”. The material fluff point is defined as the condition where the aggregate is at its maximum loose bulk density, typically between 70 – 80% of its Mod AASHTO density OMC. This fluff point OMC for mixing was confirmed by Bissada (1987) and Jenkins (2000). TG2 (2009) recommends 70% of OMC and Wirtgen (2010) suggest a fluff point ranging from 65% - 90%. The TG2 (2009) and Wirtgen (2010) further suggests determining the optimum compaction moisture content to achieve the optimum densities required. Lee (1981), however, concluded that the addition of water to reach OMC for compaction resulted in lower stability values and also below those equivalent mixes produced at 100% OMC.

Castedo and Wood (1982) indicate that the best moisture content for BSM-foam occurred when the total fluid content (water and bitumen) was approximately equal to the OMC.

Bowering (1970) indicated that where moisture contents were low, poor foam dispersion occurred. These also showed low compaction densities and no benefits were gained by adding water after the foam bitumen treatment.

Csanyi (1959) determined that without sufficient moisture, satisfactory mixtures were not possible. He further added that excess water was as detrimental to the mix as insufficient water. The TG2 (2009) suggests a maximum moisture content equalt to the OMC of the virgin aggregate.

3.2.4 Mixing

Mixing foamed bitumen with aggregate occurs whilst the aggregates are flung into suspension. The foamed bitumen is then sprayed directly onto the suspended aggregates. This allows the foamed bitumen to be distributed evenly amongst small particles thus producing good quality mixtures.

Eggers et. al. (1990) stated the necessity to use lab mixers that would emulate field mixing techniques. The rotary mixing motion of blenders is not ideal for preventing particle separation or simulating on site manufacturing. Mixers that ensured the particles were airborne, such as the twin shaft pugmill, drum mixers, free fall mixers and milling drum mixers were better suited at providing sufficient volume in the mixing chamber and agitation energy.

The TG2 (2009) discusses the use of proper mixers in laboratories that would simulate in field conditions. It was found that the blender mixers such as the Hobart mixer creates segregation in a mix which affects foamability and did not replicate in field mixing adequately. Discrepancies in material strength properties of up to 25% were noted between different mixers.

Castedo and Wood (1982) observed increasing bitumen reduced workability although good quality mixes were generated and no lumping occurred. Resilient modulus test results however indicate that optimum binder content is apparent irrespective if mixes passed the visual assessment test during mixing.

Laboratory techniques attempt to mimic the actual process in the construction field. Wirtgen (2010) recommends 30 seconds of mixing to emulate the loss of energy occurring in laboratory mixes.

3.2.5 Compaction

Compaction level is important in the mix design and is paramount in producing samples of good strength, durability and performance. Compaction improves contact, reduces voids and improves binder adhesion to stone aggregates.

Saleh (2004) produced a comparative study on compaction methods using the gyratory compactor (80 cycles at 240kpa with 2% angle), Marshall compaction and the vibratory compactor to determine OMC of a mix. He observed that the gyratory gave the highest density and the lowest water content compared to other compaction techniques. Jenkins (2000) identified that although extensive research had been done on the various lab compaction techniques, no method has been defined as ideal in simulating field compaction in the lab.

Castedo and Wood (1982) relate the air voids content to be essential for drainage of moisture in mixes as these aid the curing process. Too high air voids content is however not desirable as compaction under traffic can lead to rutting of the pavement. Castedo and Wood (1982) also noted compaction was best achieved when optimum fluids content approached the (percentage moisture plus percentage bitumen) soils OMC value.

Lee (1981) observed that VMA values of BSM-foam after compaction were higher than those computed the aggregate bulk volumes. The air voids encountered were also higher than those for dense graded hot mixes. The moisture content during mixing and compaction was however recorded at 70% OMC.

Kelfkens (2008) investigated the use of the vibratory hammer to determine laboratory compaction methods for BSM materials. The Mod AASTO compaction method was evaluated, indicating the optimum compaction moisture content to be at 80% of the virgin aggregate OMC for the G2 material used. Moisture contents for BSM-foam at 90% OMC, however, resulted in similar densities using the same surcharge weight, but at a fraction of the compaction time. The test also revealed that excess pore water seeped out at the foot of the mould during compaction at 90% OMC. Compaction at elevated temperatures was cited to improve the achievable density at the same compaction effort.

Kelkens (2008) further indicated that time cannot be taken as the singular variable to achieve comparative in-field compaction density. The material in-field layer thickness plays an important role as well. The research concluded that compaction at 80% OMC for BSM-foam resulted in sufficient particle orientation at adequate compaction duration.

Wirtgen (2010) suggests that the optimum compaction moisture content (OCMC) needs to be determined to achieve the required level of compaction for samples in the laboratory. It further suggests that the OCMC normally approximates the OMC of the parent material.

3.2.6 Curing

Csanyi (1959) observed improved stability of mixtures as the specimens were allowed to dry. Subsequent researchers have validated this observation by finding that cold mixes do not develop full strength after compaction until large percentages of its moisture is lost. Curing is therefore the process of gradual strength gain in cold mixes and is accompanied by a reduction in moisture content through evaporation, particle charge repulsion and pore pressure inducing flow paths.

Ruckel et. al. (1983) concludes that the moisture content of BSM-foam during curing had a profound effect on the ultimate mix strength. Lee (1981) summarized similar findings that curing improved particle coating and strength gain, however, suggested via experimental evidence that moisture loss is not a prerequisite for strength gain in foam mixes during moisture susceptibility tests. It would therefore suggest that strength gains only suffice whilst the moisture remains absent.

The hydrophobic nature of bitumen assists in foam mixes rapid strength gain. The rapid strength gain allows the newly compacted foam mix to be open to traffic immediately without detrimental effects provided the traffic volumes are not too high.

In-situ curing takes several months and a need for an accelerated curing procedure was apparent to simulate early, intermediate and ultimate strength gains. This characterisation became exceptionally important for structural capacity analysis using laboratory measured strengths.

Maccarrone (1995), indicates that curing using Bowring's method is representative of the in service mix state of a year after construction. Concerns have been cited over the ageing of bitumen when exposed to temperatures of 60°C over the curing period. At 60°C, the temperature exceeds that of the bitumen softening point for most bitumen used in road

works and could lead to possible changes in bitumen dispersion within the mix. Bowering and Martin (1976) had determined that a variation in curing temperature between ambient and 60°C had little or no effect on test results.

Bissada (1987) observed the fastest gain in Marshall Stability occurred when oven curing at 40°C (highest of three curing temperatures) with no significant further increase thereafter. The moisture content of the sample was measured at 0.5%, the same result achieved after 21 days in air at a constant temperature of 21°C. Wirtgen (2010) recommends accelerated curing at 40°C for the preparation of 150mm briquettes for testing sample characteristics.

Jenkins (2000) suggested that laboratory curing methods should relate to the actual pavement layer conditions such as the position of the layer as well as the climate and environment the pavement finds itself in.

3.2.7 Temperature considerations

Bowering and Martin (1976) first documented the effects of aggregate temperature on BSM-foam characteristics. During their investigation, it was observed that depending on aggregate type, the minimum suitable temperatures required for adequate BSM-foam ranged from 13°C to 23°C. The use of a higher foaming temperature or lower viscosity binder was found to reduce the minimum temperature; however it was noted not to be a complete solution.

Castedo and Wood (1982) conducted experiments using three different ambient mixing temperatures (10°C, 22°C and 38°C) to evaluate temperature influence on BSM-foam characteristics. It was found that increasing the mixing temperature improved coating of aggregate particles and hence obtaining stronger mixes based on the Modified Hveem Stability, as illustrated in Figure 3.6. The plateau would seem to indicate no further improvement could be obtained from raising the temperature.

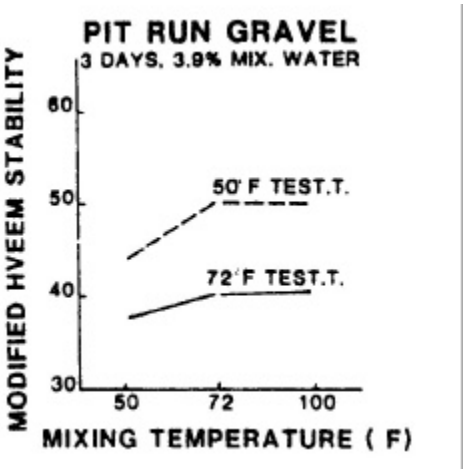

Figure 3.6: Influence of aggregate mixing temperature on Modified Hveem Stability, (Castedo & Wood, 1982)

Buschkuhl et. al., (1990) investigated the heating of foam stabilized incinerator slag. The mix temperature was increased to 60°C before compaction which resulted in stability values increasing by up 158%. Eggers et. al. (1990) investigated the same material with the inclusion of tensides as an additive to improve compatibility and Marshall Stability. Post mix heating was applied to raise temperatures to 115°C prior to compaction which resulted in stability values being doubled.

3.3 Engineering properties

The physical interaction of foamed bitumen and aggregates defines the characteristics of BSM-foam. Aggregate strength and angularity are able to assist in the stabilized materials resistance to shear due to the bitumen's non-continuous dispersion. BSM-foam with binder contents greater than 3.0% however are considered to encourage deformation due to the lubricating effect of the excess bitumen, (Wirtgen, 2010). Addition of cement or lime at quantities larger than 1.0% and 1.5% respectively negates the benefits of bitumen in BSM-foam. To quantify the influence of these constituents, numerous tests have been used and are summarized in Table 3.3.

Table 3.3: Historical tests performed on BSM-foam and their functions (Jenkins, 2000)

Performance property	Mix (engineering) property	test
Workability	Cohesion	Vane shear
Fracture resistance	Tensile strength and fracture energy	Indirect tensile strength (ITS)
	Cohesion	Hveem Cohesiometer
Fatigue resistance	Tensile strain and strength	Long term pavement performance
Permanent deformation	Plastic deformation Shear strength stability	Static Creep, Dynamic Creep Triaxial Hveem Cohesiometer Vane Shear Marshall Stability Hveem Resistance
Load spreading and stress distribution	Resilient modulus or stiffness	Indirect Tensile Test ITT (Dynamic) Dynamic or Static triaxial
Moisture susceptibility	Retained strength, stability or stiffness after moisture exposure	Marshall Stability Indirect Tensile Strength ITS Indirect Tensile Test ITT (Dynamic) Triaxial
Crushing resistance	Compressive strength	Unconfined Compressive Strength UCS

3.3.1 Moisture susceptibility

BSM strength characteristics are more moisture dependent when compared to HMA. This is due to lower binder contents, aggregate moisture requirements during mixing and high air voids content.

Little et. al. (1983) found samples of silicious gravels and sands were very moisture susceptible when stabilized with foam. van Wijk and Wood (1983) found similar behavior (moisture susceptibility) for RA and virgin aggregate mixtures using the marshal stability test.

Roberts et. al., (1984) implemented a wet curing cycle of 3 days at 24°C and found a strength reduction of 50% compared to the dry cured specimens. Castedo et. al. (1984)

found that the introduction of active filler such as lime and cement reduced the moisture susceptibility.

3.3.2 Temperature susceptibility

Bissada (1987) found that after 21 days of curing, BSM-foam had a higher stiffness than HMA when tested at temperatures above 30°C. In BSM-foam, the lack of large aggregate particle coating allows the friction between aggregate particles to be maintained at high temperatures whereas with HMA, the bitumen viscosity decreases therefore reducing strength. He concluded that the discontinuous nature of BSM-foam made it less temperature susceptible.

The use of temperature susceptibility for a mix criterion in selection of potential materials was suggested by Little et. al. (1983). Testing was performed under temperature sensitive analysis at 0°C, 23°C, 50°C by using the repeated load Indirect Tensile Test (ITT). The frequency was set to 10Hz to simulate the duration of a moving load. There has been a marked decline in Resilient Modulus (M_r) as increased compacted specimen temperatures are used during testing. This is typical for visco-elastic materials to experience a reduction in Resilient Modulus as binder content and temperature increases.

3.3.3 Compressive strength

The CSIR (1998) considered BSM-foam to be more “brittle, bound” materials than HMA and therefore viewed crushing as being a representative failure method.

Semmelink (1991) noticed that the Unconfined Compressive Strength (UCS) test results of a sand and calcrete dust mix treated with foamed bitumen was dependent on the filler when tested at 25°C. Increasing in percentages passing the 0.075mm sieve between 10% and 20% had the greatest influence in UCS results.

Bowering (1970) recommended UCS strength guidelines for BSM-foam below thin surfacing layers at 700kPa and 500kPa for cured and soaked specimens respectively. Bowering and Martin (1976) extended the work and discovered UCS results predominantly range between 1.8MPa and 5.4MPa when tested at ambient temperatures.

3.3.4 Stiffness modulus

The visco-elastic nature of bitumen affects the nature of BSM-foam in such a way that it is dependent on temperature and frequency. BSM-foam further observes a non-linear stiffness relationship dependent on its stress state, and material characteristics such as the cement

and foamed bitumen content. Shackel et. al. (1974), observed the optimum M_r results for BSM-foam using breccia, was a function of saturation, binder content and binder penetration. Low penetration binders or high binder contents increased stiffness of mixes within limits.

Franco and Wood (1982) found that the maximum M_r was dependent on curing time. Tia and Wood (1982) indicated rapid increase in M_r for RA materials over the first week of curing at ambient temperature, followed by leveling off. The initial week coincides with observations where most of the moisture loss was experienced.

Macarrone et. al. (1994) indicated a relationship between filler content and mix stiffness. These filler quantities tend to be similar to those Semelink (1991) noticed whilst observing strength increases.

3.3.5 Fatigue resistance and tensile strength

Tensile strength is considered to be a primary influence on material fatigue performance. Maccarone (1994) recommends, for good performance, cured BSM-foam mix specimens should have a minimum indirect tensile strength of 100kpa when tested soaked, and 200kpa when tested dry at 25°C and 0.87 mm/sec. Tensile strength is not a deterministic value and varies with moisture content. Engelbrecht et. al. (1985) found that the higher curing temperatures resulted in lower moisture contents together with higher tensile strengths.

Jenkins (2000) noted that unlike granular materials, multi-stage monotonic triaxial testing of cold foamed mixes was not possible due to the disturbance of the bonds within the specimen. It was therefore required to conduct testing on BSM-foam samples using at least three different specimens, at different confining stresses. The general trend noted by stabilizing granular material was an increase in cohesion in excess of 100 kPa after moderate curing and an associated reduction in friction angle.

Twagira (2006) indicated that high RA content displayed a reduction in strain at break properties. Through the study, it was concluded that the reduced “fresh” bitumen might play a role in this. However, it was noted that various anomalies, in strain at break properties, had presented themselves.

Research studies have confirmed the link between shear and tensile strength parameters to the long term performance of BSM-foam. Mixes with relatively low binder contents exhibit a stress dependent behaviour where permanent deformation is a predominant mode of failure.

Colling and Jenkins (2011) cited the principals of crack propagation and stiffness gains with time of heavily trafficked pavements to suggest deformation as the primary mode of failure for BSM-foam materials. The current focus on permanent deformation as the primary mode of failure differs from those of past researchers who viewed BSM-foam as defined by fatigue.

3.3.6 Shear strength

Permanent deformation is a result of the accumulation of repeated plastic strain. It is caused by the combined efforts of consolidation and shear movement. Proper compaction and mix design are important to alleviate consolidation and shear deformation respectively. Acott and Myburgh (1982) observed that small amounts of foamed bitumen to sand increased the shear strength significantly. Using a vane shear and triaxial test, they recorded cohesion increases from 31kPa to 110kPa when 3% foamed bitumen was added. Ebels (2008) observed that variation in cohesion of BSM-foam was related to the binder types used.

Shackel et. al. (1974) established using triaxial tests that permanent deformation was a function of binder content and degree of saturation in foam mixes. It was recorded that the ratio of axial strain to peak strain decreased with increasing binder and degree of saturation. Good correlation was observed between static and dynamic testing mode in terms of pavement deformation.

Bissada (1987) found that BSM-foam had higher stability values at lower binder contents than in relation to HMA. The stability values were found to be similar at binder contents of 1.5% to 2% less than in the control HMA mixes.

When granular materials come under load, a maximum deviator stress experienced by the material relative to the material strength will determine the rate of permanent deformation. It is recommended in Southern Africa that the stress ratio should be limited to 0.7 for granular materials after which accelerated deformation occurs. Jenkins (2000) indicated that limiting the stress ratio from 0.5 to 0.55 is applicable to BSM-foam to ensure satisfactory performance depending on the active filler added and binder content. Once the deviator stress exceeds the critical stress as defined by the critical stress ratio, accelerated deformation occurs. The accelerated deformation curve takes a hyperbolic shape form.

3.3.7 BSM Classification

The TG2 (2009) suggests a material classification for bituminous stabilised materials. This classification system sub-divides the stabilized materials into 3 categories as follows:

- BSM1: high shear strength, suitable for traffic application of greater than 6 million standard axles.
- BSM2: Moderate to high shear strength, suitable for traffic application of between 1 and 6 million standard axles.
- BSM3: stabilized soil or gravel, suitable for traffic application of less than 1 million standard axles.

The classification is determined by the BSM's engineering properties. The predominant engineering properties affecting the classification are:

- Grading;
- CBR;
- Plasticity Index (PI);
- Shear parameters, Cohesion and friction angle; and
- Retained cohesion.

The relevant test indicators and their limits are provided in Appendix A.

CHAPTER 4: LITERATURE STUDY ON HALF WARM MIXTURES

4.1 Background

Foamed bitumen has been used to stabilize pavement materials at ambient temperature for over 50 years. Since its inception, the effect that aggregate temperature had on the mix properties was only initially documented many years later by Bowering and Martin (1976). In their research, a minimum temperature requirement per aggregate type was noted to produce acceptable BSM-foam. No mention was made of aggregate mixing temperatures above 23°C. The research did however investigate BSM-foam mixed at ambient temperatures thereafter heated to 110°C before compaction.

Humberto and Wood (1982) investigated BSM-foam mixes, using pit run gravel, manufactured at mixing temperatures of 10°C, 22°C and 38°C and found an improvement in the Hveem stability values as the mixing temperature increased. Improved particle coating was also visually noted but not tangibly quantified. The increase in stability value in the results appeared to plateau between 22°C and 32°C. No indication was provided on the compaction temperature during the production of samples.

Initial research on Half Warm Foam bitumen mixes (HWF) as it is now known was produced and evaluated by Jenkins (2000). The study consisted of heating aggregates just below 100°C prior to mixing. The general description of HWF therefore is the production of a BSM-foam at temperatures above ambient, but below 100°C. Within the bituminous mix frame of reference, it fills the zone between BSM-foam and WMA. The broad definition of Half Warm bituminous mixes along with the current asphalt mixing technologies available allows for the production process to be facilitated in numerous ways. The methods available can be divided between single phase and double phase systems. The phase system defines the process of bituminous binder addition to the mix. Double systems employ two different grades of binder with one binder being foamed such as the SHELL WAM process. The single phase system may be further differentiated as Pre-aggregate heating or post mix heating, where the addition of heat is defined by its position in the HWF mix process.

This study primarily focuses on the single phase system using foamed bitumen. The production of BSM-foam has to date been acknowledged as being primarily mechanical in its facilitation to improving engineering properties. The addition of pre- or post-heat application has not been studied in comparison although improvements of mix quality have been recognised using both methods. Bowering and Martin (1976) heated foamed surfacing mixes

for compaction and curing of specimens in their study. When compared to a similar mix compacted at 23°C, the former resulted in improved densities and cohesion although variable Marshall Stability values were recorded.

Following this trend, it was generally speculated that any additional heat input above ambient temperature had beneficial effects on the mixes. The addition of heat to cold recycling has however been considered economically unviable in most construction cases due to double handling of the material. The current in-plant or in-place recyclers have not been designed to accommodate heating equipment. During cold in-place recycling (CIPR) infrared heating equipment to preheat road surfaces before recycling is available, but the heat penetration depth is usually limited to the upper 50mm of a pavement.

van de Ven et. al. (2007) noted the production of HWF resulted in a reduction in productivity in relation to that of HMA in a batch plant. The in-plant production peak is limited by the extra time required for the substantial application of the bituminous binder to be foamed. The addition of RA reduced the quantity of fresh binder required in mix, therefore increasing production rate. Mixes suitable for addition of high percentage RA are bituminous base layers where the capacity during production was recorded as almost similar to that of HMA. Bituminous surfacing materials have limits to the amount of RA that may be added and production rates using foam bitumen remain low. Lower production rates will likely increase energy consumption.

The last decade has seen limited progress into the HWF technology. To the author's knowledge, most of the existing published data on HWF is represented by Jenkins (2000) and van de Ven et. al. (2007), and thus the majority of the HWF salient characteristics discussed under this chapter has been sourced from the work produced by these researchers. It is noted that HWF mix is currently a registered trademark product in the Benelux region.

4.2 Energy considerations

The first law of open system thermodynamics states that the increase in the internal energy of a system equals to the amount of energy added to the system (heat or mass flow) less the mass outflow by work done of the system. The production of HMA requires a large energy supply to heat aggregates prior to mixing with the bituminous binder. The purpose for heating aggregate is to expel moisture and improve binder film thickness during mixing. To expel moisture however, the water requires enough energy to exceed the latent heat of steam before evaporation takes place. This is the enthalpy of a molecule to overcome the

intermolecular forces at the surface of the liquid. This energy demand for water is more than 500 times the demand than the water's specific heat requirement to increase its temperature by 1°C.

Figure 4.1 as shown by Jenkins (2000) provided a simplified illustration of the energy requirements for the production of various bituminous mixes and energy savings achievable by remaining below 100°C. Depending on the moisture content of the aggregate, it is suggested that in excess of 40% of energy savings for HWF can be realized when compared to HMA. The illustration does not account for additional heat requirements due to energy loss through radiation which could account for a further 10% – 20% of energy losses.

On the temperature axis at 100°C, Stage 2 as shown in Figure 4.1, represents the boiling point of water where the latent heat requirement is to be satisfied. During boiling, water undergoes a phase change at which sufficient energy has been attained by the water molecules to overcome the surrounding intermolecular forces. Boiling however, is a special form of vaporization. Another type of vaporization to be considered is evaporation. Although the rate of evaporation increases substantially at boiling point, in reality the loss of energy to overcome latent heat in the system occurs gradually before this. The process of evaporation is initiated by the transfer of energy between particles at the surface of a liquid and once the energy accumulated is sufficient to exceed the intermolecular forces holding a particle, evaporation occurs. The rate of evaporation increases with increasing temperature and thus releasing energy and mass from the system prior to the boiling point. Figure 4.1 ignores the effects of evaporation and its accompanied energy losses within Stage 1.

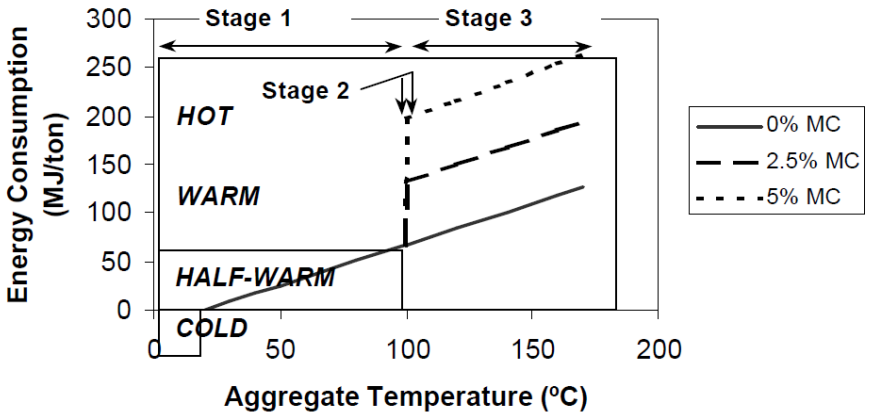

Figure 4.1: The classification of bituminous mixes in terms of energy consumption, (Jenkins, 2000)

Venturing into stage 3, temperature range exceeding 100°C, has not been included in research of HW mixes for the following reasons:

- Energy consumption benefits become redundant;
- Aggregate moisture losses become significant and reduces compactibility;
- Total moisture loss of the mix in addition to the high mixing temperature would result in WMA and therefore losing the BSM-foam benefits such as rut resistance.

van de Ven et. al. (2007) reported a 33% reduction in CO_2 emissions in relation to HMA whilst conducting in-plant trials at the Zuid Nederlands Asfalt Centrale (ZNAC) batch plant near Breda, Netherlands. These benefits confirm the environmentally friendly nature of the HWF low energy production technique. The in-plant trials further reported good particle coating of up to 22mm, with no additional moisture whilst producing HWF material. The aggregates did however contain residual moisture which was sufficient to achieve compaction during the infield construction of the pavement layer. This resulted in further savings not envisaged during laboratory trials.

4.3 Particle coating

Particle coating characteristics has a profound effect on HMA mixtures with certain specifications requiring a minimum film thickness around aggregates. The improved distribution of a binder within the bituminous mix can increase the mixes consistency, durability and resistance to water damage. This is similar to BSM-foam, although on a lesser extent, due to the spot welds and lower binder contents in relation to HMA.

The temperature gradient between the hot foamed binder and ambient aggregates during mixing has a significant influence on the foamed bitumen collapse rate during BSM-foam production. Bitumen inherently has poor thermal conductivity properties (γ = 0.17 Joule/m.s.Kelvin) and generally maintains its heat well. The coefficient of thermal conductivity for road building aggregates such as limestone or granite are 10 to 20 times higher than that of bitumen. The variation in mass between the binder and aggregates is however vast (usually 20 times) and the eventual equilibrium temperature of the final BSM-foam mix is usually not more than 10°C higher than the initial cold aggregate temperature.

Jenkins (2000) calculated the heat transfer rate between the bitumen and ambient aggregates to be approximately 1 second during mixing, based on thermal conductivity constants. The foaming process increases the binders exposed surface area by creating thin

filmed bubbles. The large thermodynamic variation therefore suggested rapid energy loss from the foamed binder to the aggregates resulting in low binder viscosities.

The resultant equilibrium temperature of the ambient BSM-foam is below the softening point of the binder. The cold mix requires adequate mixing energy to facilitate sufficient binder dispersion. The aggregate temperature therefore has a dominant effect on mixing.

In the case of HWF, the equilibrium temperature after mixing remains moderately elevated due to a reduced temperature gradient between the BSM-foam and half warm aggregates. This provides a slightly longer duration of moderately low binder viscosity which assists in improved binder dispersion and aggregate coating. Jenkins (2000) identified three probable scenarios for describing the interaction between the foamed bitumen and aggregate during mixing:

- If the particle penetrates the foam bubble, it may be burst mechanically leaving bitumen droplets either attached to or separate from the particle.
- If a large particle makes contact with a foam bubble, high energy transfer will occur, reducing the steam pressure in the bubble causing it to collapse and reducing the temperature and hence increasing the viscosity of the bitumen, causing less coating of the particle surface as mixing continues.
- If a small particle makes contact with the foam bubble, less heat is transferred, leaving the bubble either intact or deflated, but allowing the bitumen to retain more heat and hence remain at a lower viscosity. This allows the bitumen to displace the water around the particle and encourage coating on the relatively smaller surface area as mixing continues, before equilibrium temperature of the entire mix is reached.

These three probabilities indicate a critical particle size at which complete coating of particles is no longer possible. Ruckel et. al. (1983) observed little or no coating of particles larger than 9.5mm and suggested a critical aggregate particle diameter for fine sand mixed at ambient temperature to which complete particle coating was no longer possible. No explanation was provided for this phenomenon. The CSIR (1998) speculated that heating of aggregates will improve binder dispersion and aid in coating of larger particles.

Jenkins (2000) suggested this critical particle size is related to aggregate type and temperature, amongst other factors. Using spherical volume and surface area equations, he

was able to relate the mass to surface area of various stone sizes in a simplified manner. This provided the basis of his theory for foamed bitumen's affinity for smaller particles at ambient temperatures. The theory suggested the probability of mixing with smaller aggregates was inversely proportional to the third power of the particles radius. Therefore increasing the sand component of the aggregate skeleton would improve BSM-foam tensile strength, which is widely published. It also suggested that a raised temperature increases the foamed bitumen's ability to completely coat moderately sized aggregate, provided the temperature gradient is kept low between the aggregate and binder.

Jenkins et. al. (1999) discovered the plausible temperatures for half warm mix above ambient to be in the region between 30°C and 90°C. During the research, three categories of binder coating abilities were observed whilst assessing a continuously graded hornfels aggregate material. The maximum stone size during the investigation was 26.5mm and the aggregate temperature varied between 35°C and 85°C. The results were assessed visually and classified according to the coating characteristic as follows:

- Practically uncoated (less than 20% binder coverage);
- Partially coated (21% to 99% coverage); and
- Completely coated (100% coverage).

In additional to the improved quantity of increased binder coating, darkening of the aggregate was also apparent as the temperature increased. Figure 4.2 provides the graphical representation of binder coating distribution.

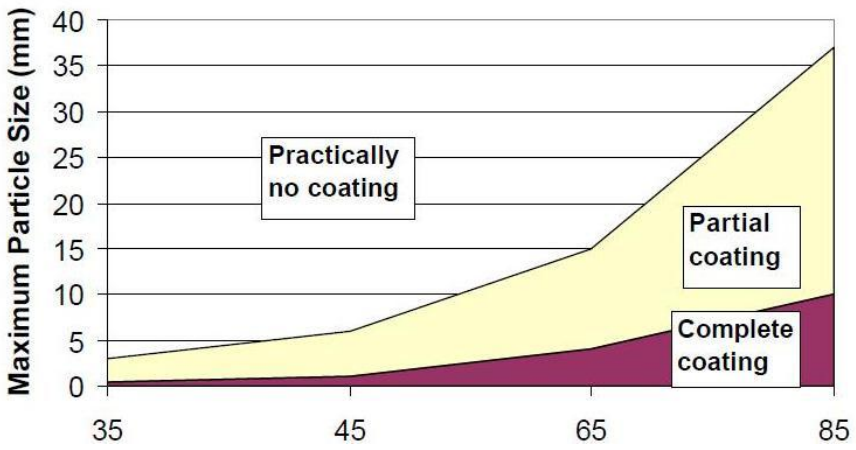

Figure 4.2: Effect of aggregate temperature during mixing on particle coating (Jenkins et. al., 1999)

Figure 4.2 indicates an exponential increase in complete particle coating rising as the temperature increases from 35°C to 85°C. Partial coating of particles improved more significantly than the complete coating and can be beneficial in achieving improved binder distribution and minimizing the aggregate interlock familiar with BSM-foam stabilization. The upper most temperature range for HWF mixes appears to contain the best potential. Aggregates containing maximum particle sizes below 19mm on the other hand might only require temperatures no more than 70°C to appreciate the benefits. Jenkins (2000) suggested that this influence of aggregate temperature on particle coating was applicable to continuously graded, semi-gap graded natural gravels and sand materials.

van de Ven et. al. (2007) conducted in-plant trials of HWF using a HMA batch plant mixer modified to include foamed bitumen spray bars. The production process managed to obtain good particle coating of aggregate sizes up to 22mm. No indication of the binder penetration type used was provided. The production was reported to initially start with moderate moisture contents as determined by preliminary laboratory trials, but this was gradually reduced. The particle coating and compaction for the in-plant production seemed adequate although discrepancies between laboratory and in-plant results arose in the form of adhesion inconsistencies. This prompted initial moisture added to be reduced to zero eventually. The result was total coating of aggregates at residual aggregate moisture contents. Voskuilen et. al. (2004) during production of HWF Porous Asphalt (HWF PA) also noted that whilst no moisture was required for production of HWF PA, the hydroscopic moisture content of the materials were sufficient to ensure good binder dispersion and adhesion.

Jenkins (2000) considered the composite binder penetrations when incorporating RA into his HWF mixes. It was contemplated that when using 50% RA, it could be beneficial to incorporate 200 penetration bitumen to achieve a final composite blend consisting of 80 penetration. Cognisance was given to the likely scenario that complete blending of the new and old binder would not be achievable and that the approach would therefore not be viable.

4.4 Material selection

The suitability of aggregate types for HWF has not been investigated substantially to date. This is not surprising considering the mechanical nature of the BSM-foam production process. The addition of heat might however open limitations that WMA or HMA experience for basic rock types such as limestone that have a hydrophobic nature. Castedo et. al. (1984) had previously observed improved engineering properties using limestone for BSM-foam in comparison to other aggregate types.

In a feasibility study conducted by Jenkins (2000), the primary factors that could influence HWF are:

- Aggregate type and gradation;
- Aggregate temperature (at mixing and compaction); and
- Associated factors, e.g. moisture factor at various stages of mixing process.

The aggregate type defined by Jenkins (2000) study refers more to grading classification, which define materials such as sand in comparison to silt. The grading envelope noted by Jenkins (2000) to best suit the HWF process was a continuously graded aggregate. The gradation curve was based on a power curve (n = 0.45) which provides the least voids in the mineral aggregate (VMA) skeleton. The low voids facilitate the potential for spot weld probability between aggregate particles and therefore benefits cohesion.

The use of RA in the production of HWF mixes has been noted to improve durability and mechanical properties. The use of RA in HWF relies on the potential for its old residual binder to assist in adhesion between particles and a reduction in moisture susceptibility of the new mix. To promote these attributes, the mix requires sufficient heat to promote blending of the new and the old residual binder. A fundamental factor to the blending potential is the softening point of the residual binder.

Jenkins (2000) tested the use of RA within the HWF mix region. The test compared heated RA mixed with filler and water, as opposed to RA without filler or water during the HWF production. HWF-RA mixes containing filler and water resembled conventional BSM-foam, whilst the HWF-RA without filler resembled HMA at mixing temperatures 85°C and above.

The results of the RA mix without water or filler was comparable to that of HMA. Complete coating was achieved for the dry mix. However, the results indicated that the lack of moisture prevented any shelf life. The lack of water also required high compaction temperature, 65°C minimum, to achieve adequate densities. A low viscosity, 200 penetration grade, bitumen was used at a high binder quantity similar to HMA. The particle coating and shelf life results are summarized in Table 4.1.

Table 4.1: Characteristics of HWF mixes produced using RA. (Jenkins, 2000)

RA supplements	Filler and water	None
Particle coating	Partial	Complete
Shelf-life	Good	Very poor

The HMA log-pen rule was used by Jenkins (2000) to determine the required high penetration (lower viscosity) bitumen in order to obtain a composite blend for the binder when incorporating RA into a HWF mix. The log-pen rule is only valid if complete blending between new and aged binder occurs and become a one phase system. The scenario of complete blending was indicated as being unlikely.

Csanyi (1957) investigated the addition of heat to dry aggregates prior to mixing with foamed bitumen in an attempt to investigate the effects of temperature on mix production. The investigation contained virgin aggregates but without any moisture. Although complete coating was achieved using high binder contents, the results indicated lower engineering properties in relation to HMA and mixes produced using atomized foam. The maximum particle size used in the mix was 9.5mm. The results are summarised in Figure 4.3.

TABLE 11

TYPE A ASPHALTIC CONCRETE CONSTRUCTION SAMPLE

% asphalt cement	6.5
Marshall stability, lb	1260
Flow	12
Unit weight, pcf	142
Percent voids	7.1

TABLE 12

Aggregate temperature	180 F	200 F
% asphalt cement content	6%	7%
Marshall stability	610	700
Flow	8	10
% voids in compacted specimen	8	5
Unit weight, pcf	138	138

Figure 4.3: Summary of HWF/BSM-foam construction sample test results (Csanyi, 1959)

Voskuilen et. al. (2004) discovered that binder softening point of recovered bitumen of Porous Asphalt (PA) was high, such that no visual change to binder viscosity was evident up to 150°C. They therefore concluded very little blending between the fresh and aged binder would result and that the RA would interact as “black rock”. The residual binder of reclaimed

PA is noted to have a high softening point in relation to the HMA residual binder. The severely aged residual binder of reclaimed PA was attributed to the thin films and high voids content characteristics of PA.

Voskuilen et. al. (2004) observed during the investigation of HWF PA that inclusion of 55% PA RA did not improve Semi-circular Bending test results. The Semi-circular Bending properties provide an indication of material bending tensile strength and fracture energy toughness. The HWF PA with RA did however perform better under the Retained Indirect Tensile Strength (ITSR) test which could be a result of the pre-coating characteristic of the residual binder.

The use of a soft binder whilst producing HWF mixes with RA follows a similar trend as WMA where the aggregates are pre-coated with a hard binder before exposing the mix to the soft binder foamed bitumen. No studies to date have been reported on the influence of using different penetration grades of binder to the HWF mix. Considering the method of post heating BSM-foam to procure a HWF mix, the binder penetration grade and its subsequent softening point might be vital in determining the regions where mixing temperature will have adequate influence on improved engineering properties.

4.5 Moisture

Moisture assists BSM-foam production by assisting binder dispersion, facilitating shelf life, providing lubrication during compaction. HWF in contrast requires raised temperatures which not only increases the foams viscosity, but initiates additional moisture evaporation which requires monitoring. The addition of heat excites the water molecules and aids rapid evaporation.

Jenkins et. al. (1999) noted that although moisture improved binder distribution of mixes, the moisture had a counter effect on the tensile strength improvement. The results indicated that although the additional heat improved tensile strength, the results were still in the same order as for BSM-foam. The study was a preliminary investigation where the aggregates where heated, although compaction was carried out at ambient temperature. It was recommended that moisture content selection was to be based on the relation between maximizing binder dispersion whilst minimizing loss of adhesion. Moisture susceptibility was not investigated in the study.

Jenkins (2000) acknowledged the importance of water in HWF to assist compaction at the low temperatures. The moisture also aided the ability to stockpile the mix. It is considered

that even though the material was cooled during stockpiling, the improvement in particle coating still assisted in improving engineering properties once compacted.

There exists a relationship compromise between temperature and water content in HWF mixes. The aggregate temperature is vital in maintaining the viscosity of the foamed bitumen during mixing. The lack of aggregate heat can however be supplemented by the addition of water to facilitate mixing. The two mechanisms differ and provide variation in the particle coating characteristics of the final product. The relationship between moisture and temperature are not mutually exclusive. The heat energy stimulates moisture evaporation, and it therefore becomes uneconomical to simultaneously achieve acceptable moisture contents and a high aggregate temperature.

Jenkins (2000) monitored several different mixes at an average of four different moisture contents each to determine moisture loss during HWF production. This resulted in formulation of Equation 10.

$$MC_f = 0.640MC_i - 0.0232T_a - 0.093BC + 2.978 \qquad \text{(Equation 10)}$$

Where: MC_f = Final moisture content immediately after mixing (%)
MC_i = initial moisture content immediately before mixing (%)
T_a = Temperature of aggregate (°C)
BC = Binder content of foamed bitumen (%m/m of aggregate)

Equation 10 has a low coefficient of correlation due to its simplified relation to different physical and thermodynamic variables. It ignores factors such as aggregate type, humidity and mixing technique. Limitations provided included maximum bitumen temperature value of 190°C, aggregate temperature range between 45°C and 98°C and a mixing time no more than 20 seconds.

Jenkins (2000) determined that up to 2.5% of moisture is lost during mixing aggregates at 90°C. This would make the “fluff point” mixing moisture content invalid. It was proposed that Equation 10 be used to determine the initial adjustment to the mixing moisture content. Inadequate moisture has a detrimental effect on BSM-foam in terms of reduced coating, low densities after compaction and balling within the mix.

Voskuilen et. al. (2004) observed that during laboratory research on HWF PA that although it was possible to produce PA at HW temperatures, the mechanical properties and durability of

the mix was poorer than HMA. The inclusion of water was suggested to be the primary cause of this shortfall. The inclusion of RA did provide some benefit to the durability and mechanical properties in relation to HWF PA with only virgin aggregate.

The results of van de Ven et. al. (2007) observed during in-plant production, that no moisture was required for the mix production in relation to preliminary laboratory HWF samples. There seemed to be a significant difference between the laboratory and in plant production conditions.

4.6 Workability

A preliminary investigation on the variation of workability for HWF with temperature increase was conducted by Jenkins (2000). Workability is a measure of the cohesion encountered in a material. Increased cohesion would therefore indicate improved binder continuity. The two aggregates compared were continuously graded hornfels and a gravelly sand. A definite increase in the cohesion is observed as the temperature increase; however, the increase of the gravelly sand was more profound. This signifies that increase in partial coating as previously recorded by Jenkins (2000) is not as beneficial on tensile strength as complete coating would be. It was suggested that this was due to improved continuity of the binder and the foamed bitumen's affinity for smaller aggregate sizes. The continuously graded aggregate in comparison relies more on its aggregate interlock which is not affected by temperature increases, but the increase in cohesion is a result of improved binder coating at a higher temperature as indicated in Figure 4.4. The increase in cohesion is related to shear strength, but increased cohesion could also implicate improved tensile properties of a mix.

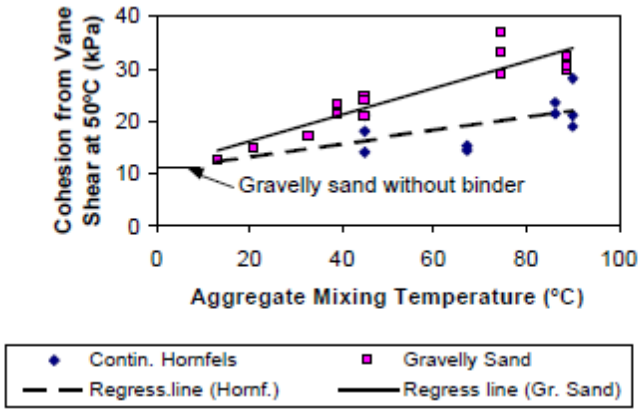

Figure 4.4: Influence of mixing temperature on cohesion for HWF, (Jenkins, 2000)

Jenkins (2000) suggested improved particle coating and binder distribution would create a more continuous network or web of binder, increasing fatigue resistance of a mix. Bissada

(1987) on the other hand perceived that the discontinuous nature of BSM-foam made it less temperature susceptible, therefore requiring a certain degree of aggregate interlock. Bowering and Martin (1976), observed during laboratory tests using surface active agents and increase compaction temperature that poorer mixes resulted due to thinner films of bitumen being distributed over a broader particle size range.

4.7 Compaction

The addition of water may improve binder dispersion; however it affects the surface energy condition between the binder and the aggregate. The stabilization process does not adequately promote complete particle coating due to the low binder content used in BSM-foam. The use of mechanical forces during compaction is required to promote adhesion between binder and aggregate as well as water repulsion to facilitate curing.

Jenkins et. al. (1999) conducted an initial study into the HWF process and observed that compactibility was mostly influenced by the mix temperature and fluid content than initial aggregates temperatures at the time of mixing. The test entailed mixing moderately warm aggregates whilst compacting samples at ambient temperatures.

Mix densities have a direct relation to engineering properties of pavement materials. Eggers et. al. (1990) discovered that when producing HWF at approximately 90°C, an increase in compaction temperature of 42°C resulted in a 2% reduction of air voids in mixes. Jenkins (2000) similarly recorded reduced air voids whilst compacting below 90°C. The compaction at raised temperatures soon after mixing, results in reduction of air voids by up to 30% when the half warm temperature is still in the region of 45 to 90°C. Eggers et. al. (1990) further noted that even though compaction temperatures remained constant at 28°C for continuous graded and semi-gap graded mixes, the densities of compacted specimens reduced slightly with increasing mixing temperatures.

van de Ven et. al. (2007) had achieved similar compaction success in the laboratory with the incorporation of 3% moisture to promote shelf life. In-field compaction of HWF was achieved at comparable or lower compaction energy than HMA with only residual moisture. This occurred provided the temperature remains sufficiently high in the HWF range. Figure 4.5 provides an illustration of the compaction achievement during in-field trials for HWF.

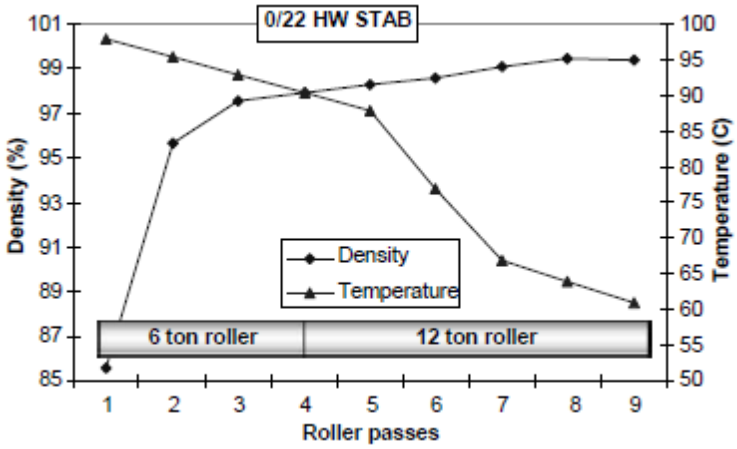

Figure 4.5: Compaction of HWF during in-field trials, (van de Ven, 2007)

Figure 4.5 illustrates a reduced cooling rate for the surfacing mat during infield compaction of HWF to that recorded for the HMA control section. Further results indicated that the rapid initial rate of compaction for HWF using less compaction effort. The total compaction effort was however higher to achieve similar results to HMA. After 85°C the rate of compaction begins to level off and by 60°C the achievable maximum density plateaus. This phenomenon resembles the minimum compaction temperature requirement noted by Jenkins (2000) whilst producing HWF containing RA and no additional moisture or filler.

4.8 HWF production

Jenkins (2000) highlighted the importance of moisture and temperature control of aggregates prior to mixing. Relevant factors observed for improved properties included moisture content before mixing, mixing temperature, duration of mixing, compaction temperature and compaction effort.

The mixing technique for BSM-foam was previously highlighted by Jenkins (2000) to be an important factor in attaining good engineering properties. The same trend would appear reasonable for HWF. Voskuilen et. al. (2004) discovered HWF PA mixes experienced binder stripping of larger aggregate particles during prolonged mixing with a Hobart mixer.

The introduction of water in BSM-foam and HWF mixtures results in larger variability of samples after production when compared to HMA. The variability of results for BSM-foam, HWF and HMA was compared by Jenkins (2000). The lack in reliability of HWF indicates the necessity of adequate research to provide better understanding of the materials characteristics and attributes.

van de Ven et. al., (2007) discovered variable results when mass producing HWF in a modified batch plant mixer. The laboratory mixes required moisture whereas the in-plant mixes did not require moisture for good consistent results.

4.9 Engineering properties

Investigations into the engineering properties of the HWF mixes assess the benefits gained from its improved particle coating in relation to the other bituminous mixes. The HWF temperature range provides a spacial reference although various factors such as binder percentage or moisture contents have not been included. The variation in binder contents and temperature facilitates complete particle coating albeit at sub boiling temperatures of critical particle sizes. This then makes it possible to achieve both asphaltic mixes and bitumen stabilized mixes within the HWF range. The two are visually defined by the binders coating of aggregate particles. It is noted that the binder percentage across research practices on current HWF products has varied, resulting in complete coating of particles in instances of high binder contents rendering them as asphaltic mixes rather than stabilized mixes. This review considered all research performed in the Half-Warm temperature range however all binder percentages noted were above 3.5%.

4.9.1 Tensile strength

Jenkins et. al. (1999) noted improved tensile strength for HWF mixes tested using the Indirect Tensile Strength (ITS) test. The warming of aggregates resulted in improved binder dispersion and particle coating. The improved binder distribution increased the tensile strength and in similar manner the improved aggregate coating increased the material's durability. The ITS test is however infamous for low repeatability problems, but general trends can be investigated with ease in relation to more sophisticated repeated loading tests. The relation to the improved tensile strength was not correlated to any fatigue benefits at the time. The investigation further realized the necessity of maintaining the half-warm temperatures between mixing and compacting as the engineering properties compacted at ambient temperatures remained low.

Jenkins et. al. (1999) conducted an evaluation of HWF mixes by measuring their tensile strength using the ITS and Semi-Circular Bending (SCB) tests to determine the effects of heating various aggregates. The tensile strength and particle coating of continuously graded mixes, incorporating both virgin aggregate and RA, responded the best and was used for further detailed investigations. Other aggregate types used were sand, gravels, stone mastic asphalt and semi-gap graded. These aggregates initially illustrated good potential for the HWF process, however, additional action was required to assists coating of particles. Figure

4.6 indicates improvements to ITS results as mixing aggregate temperature increased using binder contents of approximately 4.5%.

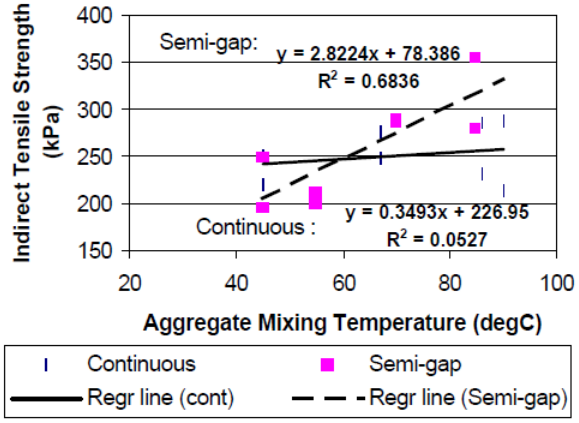

Figure 4.6: ITS results for various aggregates in relation to mixing temperature, (Jenkins et. al., 1999)

van de Ven et. al., (2007) discovered that in contradiction to his preliminary laboratory mixing technique, the required moisture contents during in-plant mixing was to be reduced to zero, thus resulting in only residual moisture of aggregates during mixing. The in-plant mix consisted of a 50% RA blend, containing 4.5% total binder of which 2.3% fresh binder was added, using 70/100 pen bitumen. In-field test results as recorded, indicated ITSR results of 93% with the addition of RA. The ITS tests were conducted at 25°C and 0.85mm/s. Jenkins et. al., (1999) performed HWF trials on 100% RA with either using moisture with filler or no moisture without filler. The results were not promising as indicated in Figure 4.7. Although the residual and fresh binder percentages were similar, the influence of the amount of RA or the softening point of the residual binder might be responsible for the difference.

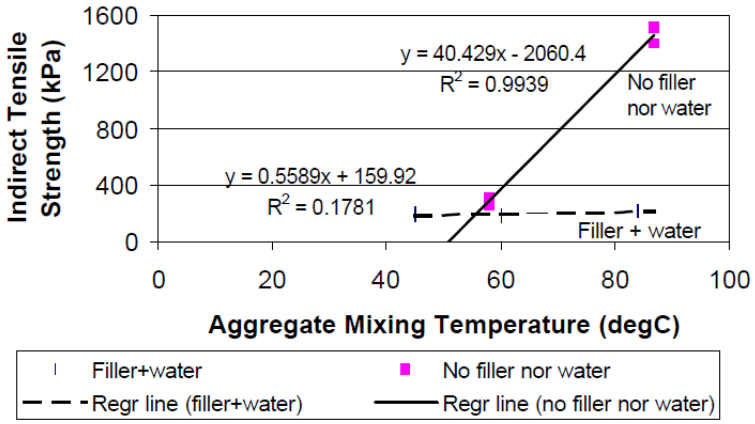

Figure 4.7: Indirect tensile strength results for RA, with and without, water and filler, (Jenkins et. al., 1999).

Voskuilen et. al. (2004) discovered improvement in ITSR when incorporating RA during the production of HWF PA. A total of 55% RA was added which resulted in approximately 10% increase in the ITSR ratio. The HWF PA ITSR values were still lower than HMA PA. It is suggested that the coating of the residual binder in the RA improves the water resistance. Further investigation into the raveling of HWF PA in relation to HMA PA was conducted. The results varied and although no tangible relation could be sought, it was concluded that some HWF PA could have the same resistance to raveling as HMA PA.

4.9.2 Compressive strength

Jenkins (2000) conducted monotonic compression tests on HMA, HWF and BSM-foam. The loading rates varied between 0.85mm/s and 0.425mm/s over testing temperature ranges between 8°C and 40°C. Figure 4.8 illustrates the results of the investigation for the HMA STAB (Hot Mix Asphalt– Steenslagasfaltbeton); HWF STAB (Half Warm Foam – Steenslagasfaltbeton) and CM STAB (Half Warm Foam – Steenslagasfaltbeton). Steenslagasfaltbeton (STAB) refers to an asphalt concrete.

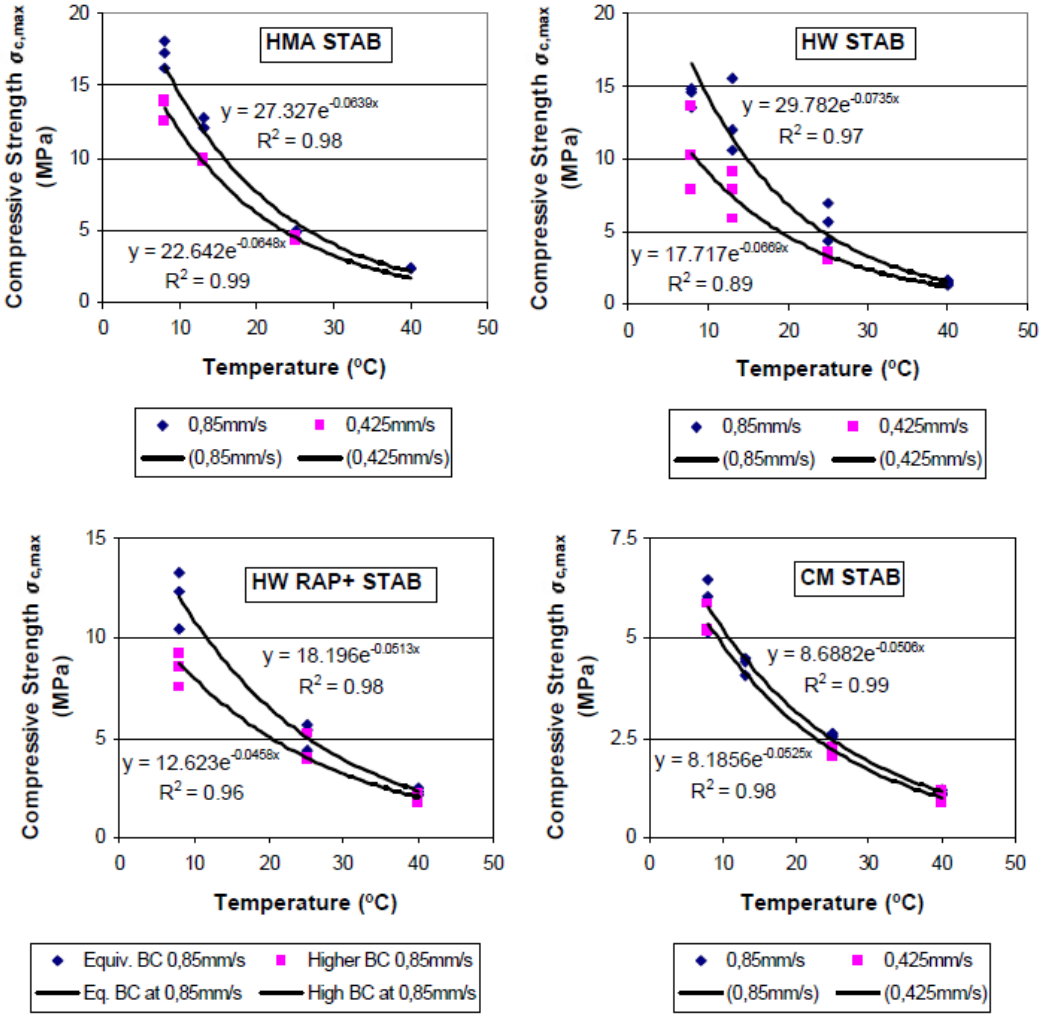

Figure 4.8: Compression strength comparison for four equivalent asphaltic mixes relative to test temperature and displacement rate. (Jenkins, 2000)

The improvements due to increased temperature of aggregates are evident in terms of the UCS results recorded. The sensitivity to the displacement rates increased with increasing aggregate temperature of the mixes. Noting this variation in compressive strength at the low test temperature, the ratio of compressive strength variation between the mixes remained the same as illustrated in Figure 4.9. HWF achieved similar results to HMA and more than double when compared to that of BSM-foam.

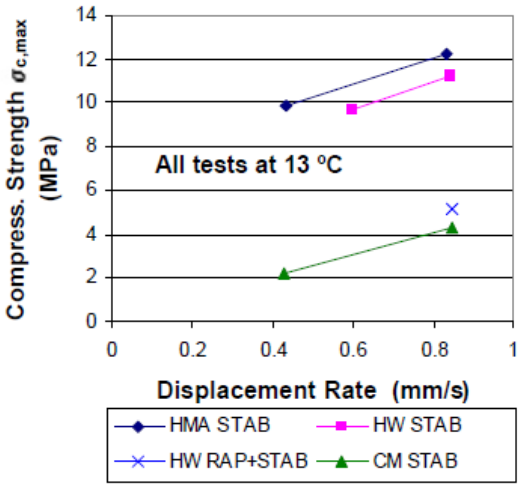

Figure 4.9: Maximum compressive strength as a function of displacement rate of four asphaltic materials, (Jenkins, 2000)

4.9.3 Cohesion and Shear strength

Bowering and Martin (1976) relate improved abrasion resistance of foamed mixes was achievable when incorporating a heating and drying cycle followed by hot compaction. The heating temperatures did however exceed 100°C. In their study, four BSM-foam mixes and one HMA control mix were compared. A BSM-foam mix was produced at ambient temperature (23°C), and then put through a heating and drying cycle prior to compaction at 110°C. In general, the heated mix showed improved densities and cohesion but low Marshall Stabilities in comparison to BSM-foam mix compacted at 23°C, See Figure 4.10. Samples were further evaluated and compared with aggregates pre-treated with imidazoline surface active agents and compacted at ambient and 110°C (Foam mix 3 and 4). The variability of the results for mixes using the additives were attributed to particle redistribution under compaction.

Table 7. Potential Surface Course Mixes—Foamed Bitumen

	Foam Mix 1	Foam Mix 2	Foam Mix 3	Foam Mix 4	Hot Mix Control
90 Penetration Bitumen, % wt	5.0	5.8	5.0	5.0	5.8
Additive, % of aggregate wt	Nil	Nil	0.05	0.05	Nil
Compaction Temperature, F (C)	73 (23)	230 (110)	73 (23)	230 (110)	230 (110)
Compaction Moisture, %	6.0	0.5	6.0	0.4	Nil
Curing Period at 140 F (60 C), days	3	Nil	3	Nil	Nil
Moisture content after curing, %	0.7	--	0.4	--	—
Dry Density, lb/cu ft	136	147	140	146	151
Estimated Air Voids, %	10.6	7.5	9.3	8.5	4.5
Relative Stability	47	27	22	30	34
Relative Stability after M.V.S.	28	—	21	28	20
Cohesion	74	200	36	343	290
Cohesion after M.V.S.	161	—	209	328	340
Marshall Stability, lb	2150	2175	1450	2278	2870
Flow Value, in. $\times 10^{-2}$ (mm)	8 (2.0)	—	16 (4.1)	16 (4.1)	14 (3.6)

Aggregate Characteristics: High quality crushed rock suitable for conventional mixes

Grading:

Sieve No.	3/4 in.	3/8 in.	1/4 in.	7	14	25	36	52	100	200
(mm)	(19.1)	(9.5)	(6.4)	(2.41)	(1.41)	(0.71)	(0.425)	(0.280)	(0.149)	(0.074)
% Passing	99	79	59	49	34	24	19	12	6	3

Figure 4.10: Comparative results of HWF, BSM-foam and HMA, (Bowering & Martin, 1974)

Jenkins (2000) analysed and compared the shear strength of HMA, HW and BSM-foam using the Leutner shear apparatus. The variation in the failure envelopes for the four equivalent mixes is depicted by increased cohesion value and only limited change in friction angle as illustrated in Figure 4.11. At low test temperatures, HMA out-performed HWF and BSM, but at 25°C, the HMA and HWF performed equally and noticeably better than BSM. HWF illustrates a reduced influence of test temperature on shear strength in relation to HMA at low temperatures. This trend is similar to the BSM-foam mix.

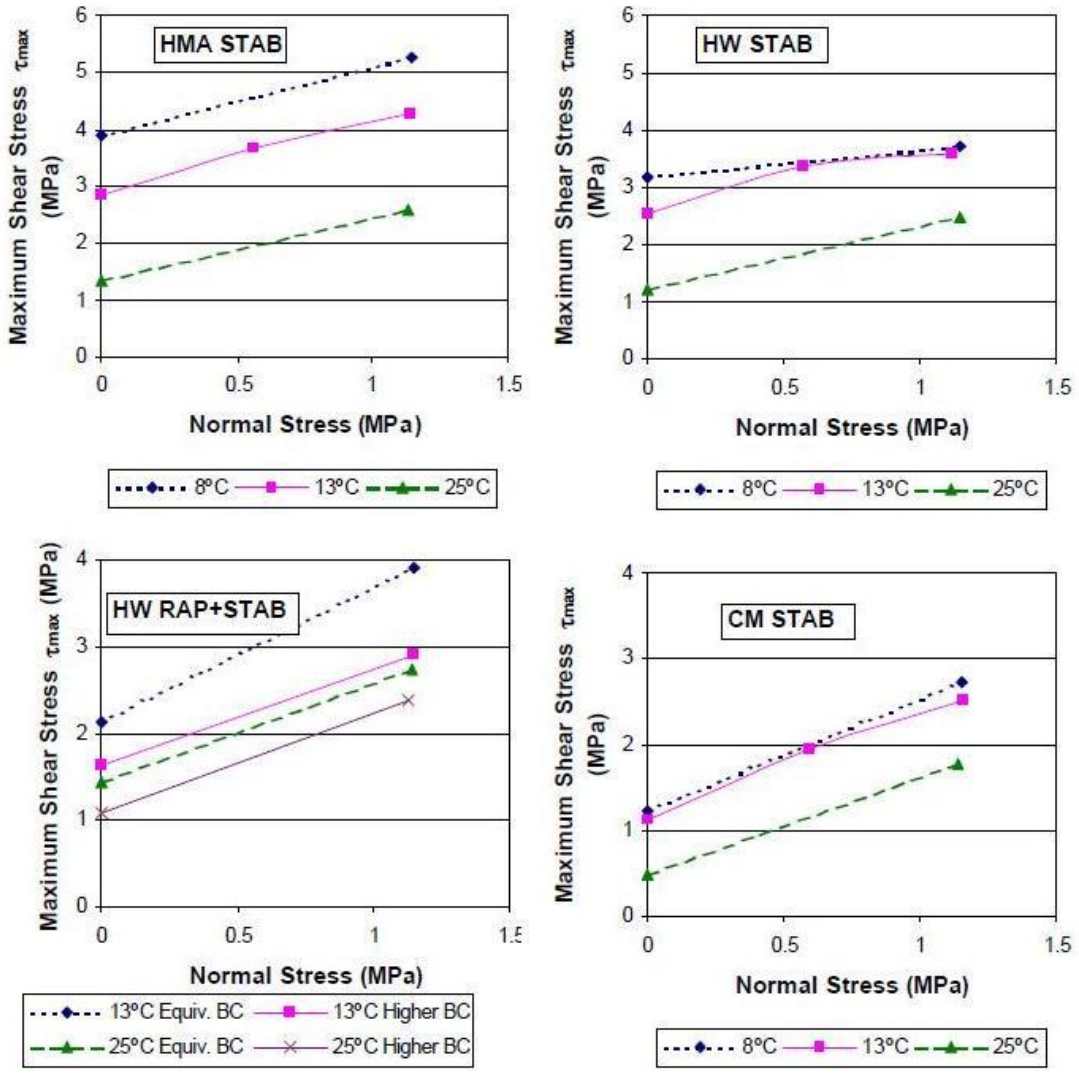

Figure 4.11: Shear failure envelopes of four equivalent asphaltic mixes (Jenkins, 2000)

The Shear strength in Figure 4.11, as like the compression strength in Figure 4.8, displays similar relations to test temperature variation. On the test temperature scale for monotonic loading, cracking becomes dominant at low temperatures (10°C) and rutting becomes dominant at high temperatures (40°C). The HWF characteristics lie between the BSM-foam and HMA and therefore would be less susceptible to both cases of distress over the full temperature range.

4.9.4 Mohr-Coulomb failure envelope

Jenkins (2000) found an acceptable correlation between shear and compression tests results, and combined failure envelopes were produced. This resulted in a reduction of the internal friction angle of the mixes in comparison to the results obtained from the Leutner shear test alone. The slight variation encountered could be a result of the different

displacement rates, geometry of the specimens and non-uniform shear stress distributions of the specimen in the Leutner test.

Figure 4.12 indicates the mix variations observed when producing Mohr-Coulomb failure envelopes by combining the shear and compression tests. At low test temperatures, very little variation is evident in the friction angle due to the binder's stiff state. Due to the high binder distribution, HMA exhibits the highest cohesion values. At higher test temperatures (25°C) the HWF failure envelope approaches the HMA failure envelope.

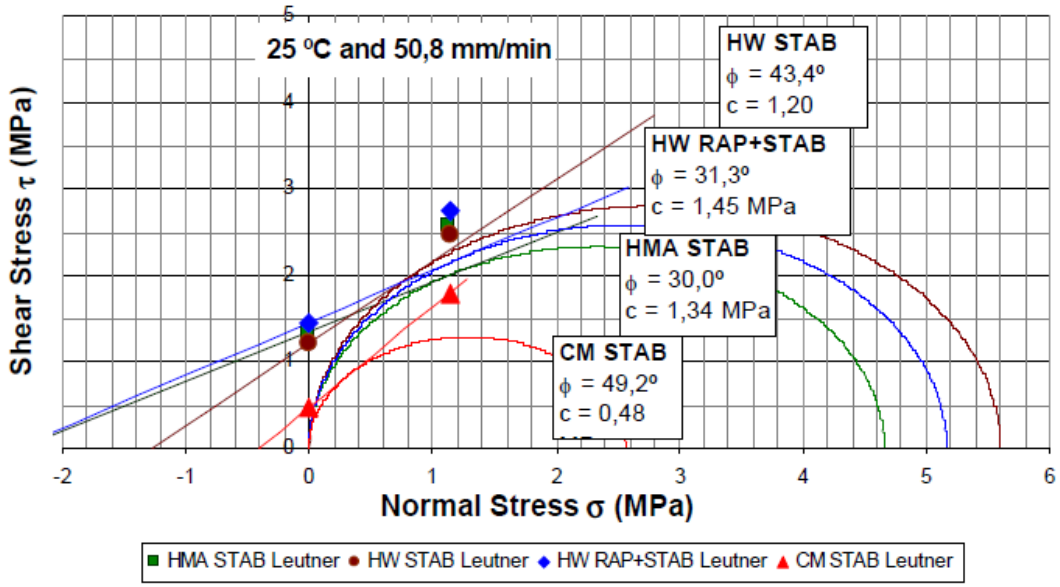

Figure 4.12: Failure envelopes for the combination of UCS and Leutner tests on various asphaltic mixes, (Jenkins, 2000).

4.9.5 Stiffness modulus and fatigue relationships

The visco-elastic nature of bituminous binder acts proportionately to loading rate and test temperature variations. The general trend is an increase in stiffness as the loading rate increases or temperature decreases. Monotonic variables consist of loading rate, test temperature and stress state. Vehicles, however, impose dynamic loads on pavement layers where the resultant displacements are substantially smaller than those encountered during monotonic tests. Dynamic loading simulates the effects of vehicle loads and requires aggregate interlock together with the binder's resilient modulus to resist permanent deformation.

Jenkins (2000) used the 4 Point Beam (4PB) apparatus to determine the dynamic properties of HWF mixes. The 4PB determines the flexural strength of specimens and was used to

generate master curves during fatigue analysis. Tests were conducted under displacement control conditions. The Master curves obtained are illustrated in Figure 4.13.

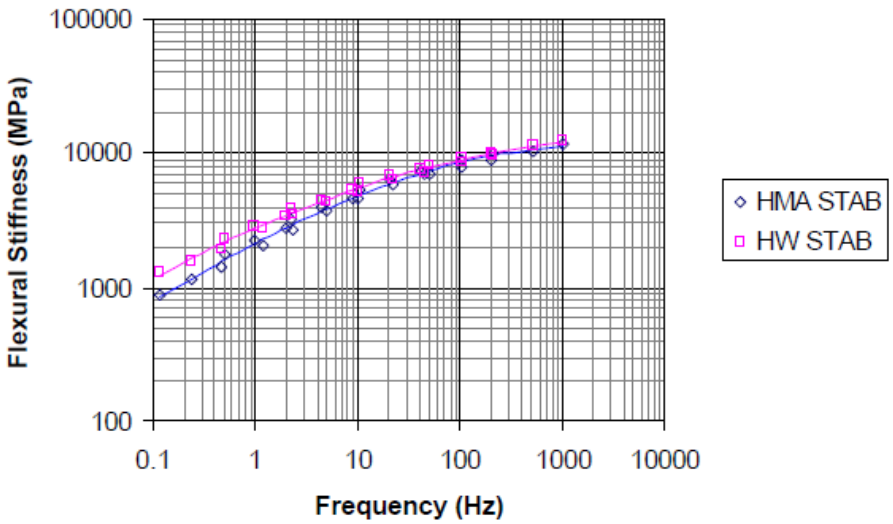

Figure 4.13: Mater curves of HMA and HWF mix, (Jenkins, 2000)

In relation to flexural stiffness obtained from generating master curves, the HWF STAB mixes, a Dutch type material similar to continuously graded crushed aggregate, illustrated a lower slope in relation to HMA STAB. This shift is similar to that of BSM-foam in relation to HMA as recorded in the research by Brosseaud et. al. (1997). The resulting higher stiffness of HWF at extended loading times or higher temperatures will therefore assist in the resistance to permanent deformation. It was suggested that this phenomenon was attributed to improved binder dispersion within the mineral aggregate and therefore the HWF tends more to HMA in this regard.

The production of WMA is undertaken in numerous ways, of which foamed bitumen, a free water system, is one method. This method is similar to that used by Jenkins (2000) to produce the HWF mix. Mbaraga (2011) investigated a free water system, namely Foam Tech, to produce WMA amongst other WMA technologies. The results indicated that the flexural stiffness of the free water system WMA was consistently lower than that of the control HMA mix for all test temperatures and frequencies investigated. The master curves for the study is presented in Figure 4.14. Both studies conducted the test at 20°C.

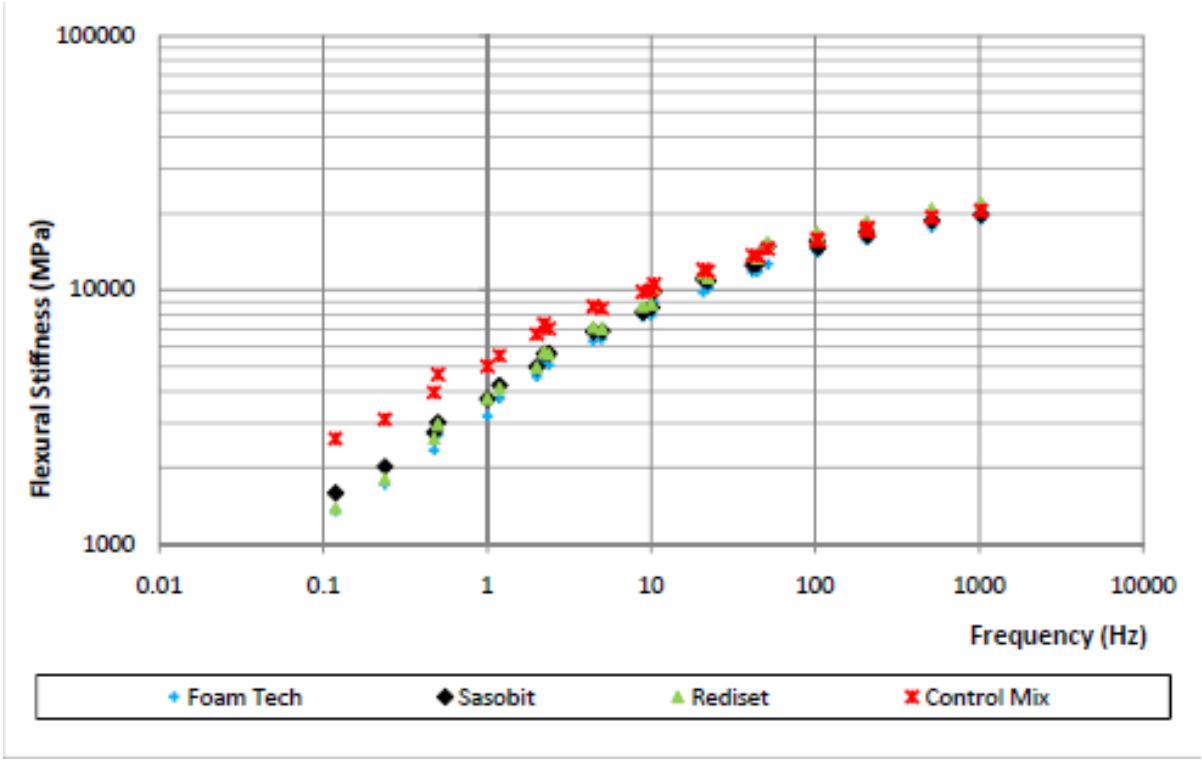

Figure 4.14: Master Curve for WMA and HMA at 20°C reference temperature (Mbaraga, 2011)

The findings of Mbaraga (2011) vary to that of Jenkins (2000) as illustrated in Figure 4.13. This variation is contrary to the expected norm considering that HWF is produced at a lower temperature. The HWF mix produced by Jenkins (2000) however used a slightly higher penetration grade binder with no addition of RA in relation to the 10% RA used for the WMA mix. The binder content for the WMA was marginally lower, and no indication was provided by Mbaraga (2011) on the half-life or expansion ratio of the foaming process.

The fatigue behaviour of HWF 4PB test results was determined using the Wohler model as part of the research conducted by Jenkins (2000). Failure was determined by the number of load repetitions to reduce the specimen's flexural stiffness to half its original value, according to Van Dijk (1975). The original flexural stiffness was determined using regression analysis. The fatigue characteristics of HWF and HMA are illustrated in Figure 4.15. The test concluded that the steeper HMA curve was marginally more sensitive to strain variation. However the close spread of the data points can be perceived to yield comparable fatigue behaviour in the absence of the regression lines.

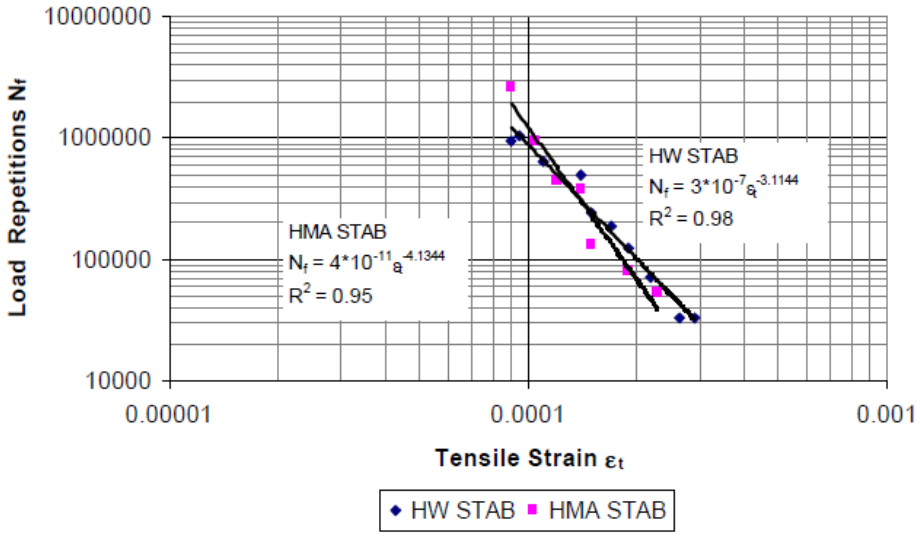

Figure 4.15: Fatigue characteristics of HWF and HMA from 4PB tests at 20°C and 10Hz. (Jenkins, 2000)

The field performance of HWF STAB in relation to HMA STAB was theoretically calculated by Jenkins (2000), based on a shift factor approach to relate laboratory and field results. The fatigue performance of the HWF STAB was determined to require 90% of the horizontal tensile strain of HMA STAB under field loading to yield an equivalent 10^6 standard axle repetitions to failure in similar conditions. This achievement is substantial considering the reduction in energy to produce the HWF mix in comparison to HMA.

Mbaraga (2011) assessed fatigue relations of the free water system WMA mix in relation to an HMA control mix of the same constituents. The WMA mix indicated a flatter curve, being less sensitive to overloading, as that of Jenkins (2000) for the HWF mix when compared to their respective HMA control mixes.

van de Ven et. al. (2007) studied the application of warm mix asphalt below 100°C under in-field manufacturing conditions. The flexural stiffness was evaluated using the 4PB test, conducted at 60 microstrain or constant strain and frequency of 8Hz. Results indicated that material stiffness for HWF STAB was similar to that of HMA STAB mixes using RA however the fatigue line was a little poorer than that of HMA STAB with RA. It was also noted that when comparing the HWF in-field fatigue results to that of the laboratory, the in-field mix appears to be more sensitive to overloading. The target binder content used during the study was 4.5%.

The initial phase angle to tensile strain relationship was conducted by Jenkins (2000) as depicted in Figure 4.16. The initial phase angle of a mix is defined as the phase angle measured after 100 load repetitions of the beam fatigue test. A decrease in the initial phase angle for HWF in relation to HMA was reported. A similar trend was reported by Brosseaud et. al. (1997) for BSM-foam. The phase angle provides insight to rutting potential of a mix as low phase angles indicate low viscous nature and hence higher elastic response. This is advantageous to the resistance of permanent deformation of the HWF material. The phase angles for HWF however does not exhibit the same magnitude of shift as for BSM-foam, but still remains nonlinear with respect to level of strain. The difference in phase angle decreases considerable at higher strain levels, but ultimately still remains lower than the phase angle of the HMA mix.

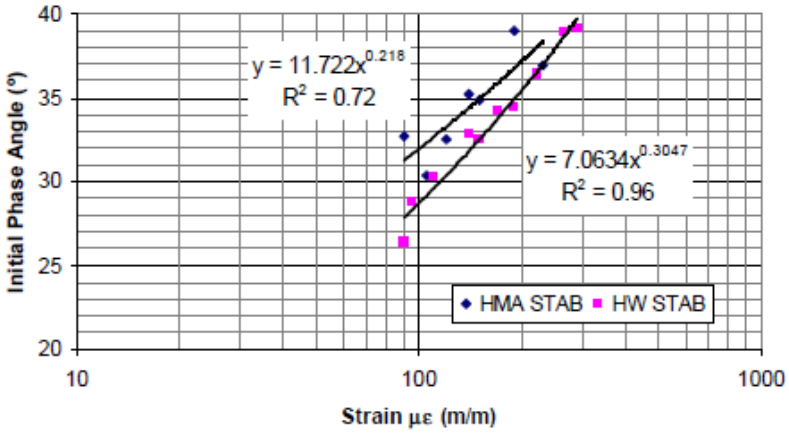

Figure 4.16: Relationship between Phase angle and strain for HWF and HMA, (Jenkins, 2000)

4.9.6 Mix repeatability

Jenkins (2000) initially suffered large variation in UCS results during HWF investigations. The repeatability of results was subsequently analyzed for HWF in relation to BSM-foam and HMA. The variables considered to influence the mixes were binder, moisture and temperature. The influences on the various mixes were defined as follows as:

- Hot-mix has one factor i.e. the binder with its variability,
- Cold mix has two factors i.e. the binder and moisture, and
- Half-warm mix has three factors i.e. the binder, moisture and aggregate temperature (a factor excluded from hot-mix, where the profound influence on particle coating is not evident).

The comparison attempt was simplified by considering each property variable as equally weighted in influence. Figure 4.17 illustrates the variability.

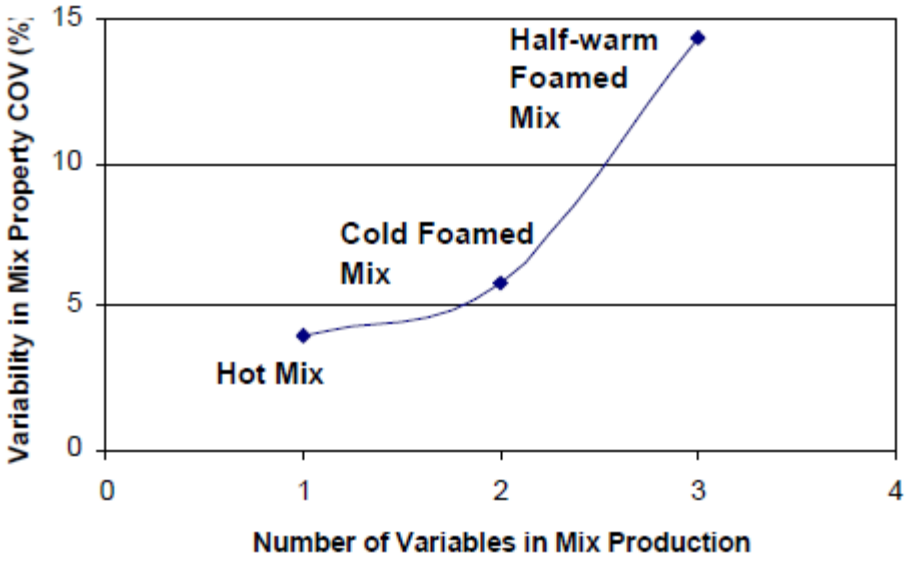

Figure 4.17: Influence of number of variables on mix inconsistency, (Jenkins, 2000)

Compaction and binder distribution are facilitated by the moisture content present in a mix, however, the loss of moisture occurs at elevated temperatures. Increasing temperature will increase the binder's dispersion and adhesion between particles and assist in the frequency and tensile strength of "spot-welds" during compaction. The reduction in binder viscosity at these elevated temperatures tends to also assist compaction, although the measure of constellation in light of the moisture loss is not explicitly known. It is understood that the potential to completely coat particles forfeits the rut resistance gained by the aggregate interlock of BSM-foam. It is suggested by Jenkins (2000) that further investigations into the constituents interaction is required to understand the process and reduce the variability of the mix characteristics.

CHAPTER 5: METHODOLOGY

5.1 Introduction

The use of microwave heating technology during this investigation is focused on the effectiveness of heating bituminous stabilized mixes volumetrically. This effectiveness was evaluated on energy efficiency and the engineering properties of samples produced. Energy efficiency is affected by many direct and indirect factors. Direct factors include the material properties of the samples whilst indirect factors include the achievable rate of HWF production. Limitations on the production rates depend on the ability to implement sufficiently large microwave heating equipment to portable in-plant BSM-foam machinery. Previous literature by Jenkins (2000) suggested that the heating of aggregates was not achievable by using conventional cold in-place recycling and in-plant cold mix techniques and therefore not much interest was afforded to research above ambient temperature stabilization. The use of heating equipment required adequate space to be made available. Furthermore, it should be noted that, the use of a microwave heating device to heat aggregates is not common within the pavement engineering industry.

This investigation can be divided into two sections, namely the Preliminary investigation and the Primary investigation. The Preliminary investigation consisted of focusing on intrinsic variables, such as moisture content and heating times, which could be optimised for producing adequate HWF mixes. The Primary investigation builds on further from the preliminary investigation, and investigated mix properties that best suit volumetric heating. The following is an outline of headings discussed:

- Equipment;
- Preliminary investigation; and
- Primary investigation.

Figure 4.1 in Section 4.2, indicates the spatial reference to bituminous mixtures produced at various temperatures as illustrated by Jenkins (2000). Considering the relation between aggregate coating and temperature, there exists a point on the temperature scale at which complete coating is achievable, depending on the material properties. This point divides bitumen stabilized mixes from asphalt mixes. This study primarily focuses on bitumen stabilized materials due to low binder contents used and aggregate gradation.

5.2 Equipment

This section discusses the various apparatus utilized during this investigation to produce HWF. The apparatus includes primarily the Microwave Unit, Conveyer Belt System, Bitumen Foam and Mixing plant, as well as Compaction equipment.

5.2.1 Microwave Unit

The microwave heating apparatus was sourced from the Chemical Engineering laboratory at the University of Stellenbosch. The device consisted of a high power electromagnetic microwave generator, model number GMP 60 KSM produced by SAIREM. The microwave generator was coupled to an aluminium wave-guide leading to a continuous flow conveyor type applicator. This applicator where the microwaves received the workload is flanked by 1.35m applicator tunnels on either end. The applicator and applicator tunnel were also manufactured using aluminium. The purpose of the applicator tunnels was to provide enough volume to dissipate the electromagnetic waves and prevent leakages during normal operation. The “free” electromagnetic waves would thus be absorbed by the material on the conveyor belt entering and leaving the applicator. It might not always be the case that the workload is able to absorb the microwaves. Therefore microwave measuring equipment was used to monitor any leakages.

The applicator tunnel is approximately 3 metres in length, with a cross sectional dimension of 90mm x 90mm. The Microwave unit was coupled to a three phase electrical power supply.

Technical data for the microwave generator is as follows:

Frequency:	2450 MHz +- 25 MHz
Output Power:	0.6kW - 6.0kW
Magnetron Type:	YJ1600, water cooled
Magnetron Power Supply:	7200 V (dc)
Max reflected power:	3.0kW

The power output ranges from 0.6kW to 6.0kW and can be adjusted as required. The cooling of the power supply as well as the magnetron, was accomplished using a water pump connected to a water reservoir. The unit was equipped with a timer to automatically disengage the heating process once the set time expired. Figure 5.1 below, illustrates the control unit for the microwave generator.

Figure 5.1: Control unit used with the microwave generator.

5.2.1.1 Microwave Intensities

Power to the microwave unit was supplied by a three phase electrical socket in the laboratory. The Preliminary investigation consisted of varying microwave incident power over the units range. This was to investigate the material reaction to various incident power intensities and their potential to rapidly heat mixtures.

During the Primary investigation only one power intensity setting was used (6kW), however, two differing time durations were utilised to produce varying heat temperature increases. This is later discussed as the High Power (HP or High) and Low Power (LP or Low) settings.

The unit displayed the user set power intensity, the actual forward power absorbed by the material in the applicator, as well as the reflected power lost during the heating process. The Reflective power was recorded during all Preliminary and Primary investigations. The reflective power is absorbed by the water cooling system circulating through the microwave and power supply unit. The water reservoir had a capacity of 200 litres which was sufficient to prevent overheating of the microwave unit or potential damage as a result of the reflective power. An electrical pump was used to maintain a continuous flow of water between the microwave unit, electrical power unit and water reservoir. The unit was able to monitor the water flow through the system and would systematically shut-off if the water flow rate dropped to below 4 litres per minute or if the maximum water temperature exceeded 30°C.

The microwave unit could set the maximum absorbed reflective power up to 3kW. Should this maximum set reflective power be reached, the unit would automatically reduce the forward power accordingly so that the set reflective power is not exceeded. Throughout the duration of this experimentation, the maximum reflective power was maintained at 3kW.

5.2.2 Continuous flow conveyor system

A continuous flow conveyor belt system was obtained, along with the microwave unit, from the Chemical Engineering department at the University of Stellenbosch. This system consisted of pulleys, a thin Kevlar reinforced Teflon coated conveyor belt and an electrical motor powered by an electrical invertor.

5.2.2.1 Invertor

A WEG, CFW-08 Variable Frequency Drive Invertor was used to drive the electrical motor for the conveyor belt. The invertor permitted the control for the speed and torque of the phase alternating current induction motor. A reducing gear was used between the electrical motor and the main pulley, to reduce the operating speed range of the pulleys. The invertor could be set to two control options namely; vector control and V/F (scalar) settings. The vector control mode was primarily used, as this allowed the motor performance to be optimised for torque and speed regulation. Figure 5.2 illustrates the electrical motor used during this investigation.

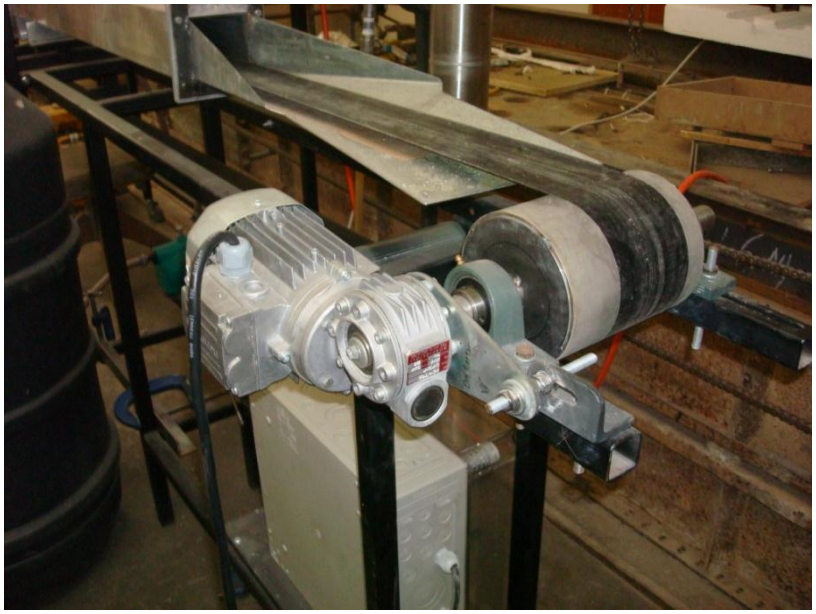

Figure 5.2: Electrical motor and gear attached to primary pulley.

5.2.2.2 Conveyor system - Alteration1

The sourced conveyor system forming part of the continuous flow microwave apparatus was designed and produced locally, by the Chemical / Mechanical Engineering faculties at University of Stellenbosch. Polytetrafluoroethylene (PTFE) coated Kevlar was used for the belt as this material had a low loss factor and provided a good strength to size ratio. This resulted in the utilization of a paper thin belt that would consume minimal space along the length of the applicator tunnels. The belt was driven by a main pulley on one end and on the other end a second primary pulley was used to regulate the tension along the belt. Additionally, there were two minor pulleys along the belt system to facilitate the belt movement.

Students at Chemical Engineering faculty previously used handmade cardboard containers to house their material being fed on the conveyor belt system. Cardboard is easily available and the containers are similarly easy to manufacture. The cardboard containers are known to be suitable for short durations or at maximum microwave intensities of up to 1.8kW. It was initially decided to construct cardboard containers and test its suitability to transport the aggregates utilized within current investigation.

During the trial run, using cardboard boxes, it was noted that the cardboard did not suit the current investigation and an alternative method was required. The reason being as follows; firstly the cardboard boxes absorbed the moisture from the wet aggregates and secondly, the cardboard boxes were scorched by the heated aggregates, see Figure 5.3. This reduced the re-usage of the cardboard boxes.

Figure 5.3: Scorched cardboard boxes observed after heating materials.

With the availability of the vertical feed vibratory hopper, as shown in Figure 5.4, conveyor belt Alternative 1 was conceived with the idea of implementing a continuous feed industrial style heating system. This would mimic a realistic, in-field process on a smaller scale.

Figure 5.4: Illustrates the vertical hopper used during this investigation

This alternative consisted of overlapping glass fibre reinforced PTFE sections attached to the conveyor belt. The sheet sections were approximately 250mm by 250mm in dimension. This provided the material to be encompassed on either side, as the material was fed through the applicator tunnel on the conveyor. Figure 5.5 below illustrates the overlapping glass fibre reinforced PTFE sheets on the Kevlar conveyor belt.

Figure 5.5: Illustration of the overlapping glass fibre reinforced PTFE sheets on the Kevlar conveyor belt as per Alteration 1.

The glass fibre reinforced PTFE material contains a low loss factor and is not significantly affected by microwave heating. The PTFE coated glass fibre square sheets were sufficiently strong for its purpose. These sheets do not have the same tensile strength as the Kevlar belt; however, they were not subjected to the same stresses and are significantly cheaper to source. The method to house the aggregate through the applicator tunnel maintains the conveyor belts flexibility, with the walls of the tunnel providing the support for the glass fibre sheets. The glass fibre sheets were sewn together in an overlapping formation on the conveyor belt as adhesive bonding for PTFE proved too costly. See Appendix B for information on the various belting materials used.

At the entrance of the conveyor applicator tunnel, metal guides were designed and manufactured to assist the square sheets into the applicator tunnel as they rolled off the pulley. The guide folds the sheets into a U-shape, as they entered the applicator tunnel. These guides further provided a steady platform for the vertical hopper to off load the aggregates on the conveyor belt. Figure 5.6 illustrates the metal guides manufactured.

Figure 5.6: Metal guides manufactured for Alternative 1 conveyor system.

The vertical hopper was able to accommodate approximately 70kg of material and could be refilled whilst in operation. The continuous feed conveyor system allowed for the mixed aggregate to be fed from the preloaded hopper on to the moving conveyor belt. The vertical hopper contained a variable setting, vibrating table, which permitted the regulation of the material quantity being fed. The speed of the vibratory table was set to and in accordance with the conveyor belt speed. The conveyor speed in turn was to be regulated so as to provide sufficient exposure time for heating as required. On the other end of the tunnel the material would exit either into a pugmill mixer or container depending on whether pre- or post-mixing method was utilized. The speed of the conveyor belt would be calculated using the material volume and its heating properties. Figure 5.7 illustrates the microwave unit and conveyor belt layout.

Figure 5.7: Microwave unit and conveyor belt layout

As previously discussed in Section 2.6.1, the acceptable limit for human exposure to microwave radiation should be maintained at below 10mW. The conveyor system did not have chokes to contain the free microwaves, in the event of leakages. A microwave measuring device was used during operation to ensure the microwave leakage was kept within the minimum range.

5.2.2.3 Drawbacks to Alternative 1

The execution of alternative 1 was marred by various drawbacks, these are summarised as follows:

- **Cardboard boxes:** The cardboard boxes would weaken after absorbing the aggregate moisture and once high temperature were achieved; the cardboard boxes were scorched, deeming them insufficient for re-use in the current study.
- **Hopper:** With implementation of the continuous feed system, it was immediately noticed that the vertical hopper experienced segregation of the particle sizes as the smaller particles would filter through faster between larger aggregate particles. With the addition of moisture, the segregation was reduced, however regular blockages then occurred as the material adhered to each other. This made it extremely difficult to align the speed of the hopper feed to supply sufficient material at the correct conveyor speed.
- **Conveyor belt:** Moisture loss during the heating process resulted in adhesion between the applicator tunnel's vertical wall and the PFTE sheets. These various forces on the square sheets along the conveyor tunnel and the varying orientation of

the aggregate resulted in the conveyor belt deviating from its centre line path, intermittently.

- **Tunnel Guides:** The tunnel guides experienced large resistance when trying to shape the material as it entered the applicator tunnel. This put added strain on the drive pulley.
- **Electrical Motor:** Due to all the friction and adhesion encountered, together with the initial increasing load of the material being fed, indicated that the motor was unable to supply sufficient torque. Intermittent slippages on the drive pulley were encountered.

5.2.2.4 Conveyor system – Alteration 2

During the preliminary testing using Alternative 1, thermal runaway was encountered whilst heating quartzite aggregate. This resulted in the melting of the Kevlar reinforced conveyor belt as illustrated in Figure 5.8 below. This required the use of Alternative 1's conveyor belt system to be reconsidered. The following factors were considered in determining a new variation to the conveyor belt system:

- **Cost and procurement of material:** The time delay and cost involved in procuring the new belt and square sheets.
- **Manufacturing Alternative 1 belt:** The stitching for alternative 1 required time and cost.
- **Drawbacks to Alternative 1:** As previously discussed in Section 5.2.2.3.

Figure 5.8: Scorched Kevlar reinforced conveyor belt after thermal runaway during testing.

The set back of having to dismantle the applicator tunnel, after the thermal runaway, provided an opportunity to address the drawbacks experienced during Alternative 1. The following items were altered at this point during the investigation:

- **Addition of PTFE strips to reduce friction:** The dismantling of the two 1.35m applicator tunnels after the thermal runaway, allowed for the friction resistance along the applicator tunnel to be addressed. The applicator tunnels were sent away to SMD (Sentrale Meganiese Dienste), at the University of Stellenbosch, for the addition of the PTFE strips along its inner base. The PTFE strips were 5mm thick and were deemed sufficiently thin so as not to create an increase in advent leakages of microwave radiation.
- **Increasing pulley diameter:** It was further noted within the initial trial that slippages at the drive pulley were encountered as the mass of the material along the conveyor belt increased. To solve this problem, it was decided to supply larger diameter primary pulleys, which effectively increased the surface contact between the pulley and the conveyor belt. The newly manufactured pulleys were covered by soft latex to increase its grip on the PTFE belt.
- **The manufacturing of polypropylene boxes:** These were similar in size as the cardboard boxes used in previous investigations. The factors for selecting material considered for the manufacturing of the boxes were based on the microwave invisibility (low loss factor), melting points, availability of adhesive products and cost. The other materials considered were; polycarbonate and HDPE. PTFE boxes cannot be manufactured due to a lack of bonding agents available. Order specific PTFE boxes are machined to shape out of PTFE slabs, making them significantly expensive. The loss factor for HDPE is low, but was not as low as with the other three materials. Table 5.1 lists the properties of polycarbonate and polypropylene considered during selection.
- **Conveyor belt guides:** Guides were made and attached close to the drive pulley which assisted in maintaining the conveyor belt on it centre line during operation.

Table 5.1: Material characteristics of Polycarbonate and Polypropylene sheets.

	Polypropylene	Polycarbonate
Cost (R/ sheet)	150 (2mm)	1040 (2mm)
Softening point (°C)	100	155
Density (g/cm3)	0.92	1.2
Bond type	polypropylene welds	Claritite glue
Tensile strength (MPa)	27	55 - 75

The use of the polypropylene boxes allowed for the reduction in material to be mixed and conditioned for each test run in relation to that of Alternative 1. Initially the material was wasted by providing leakage protection along the applicator tunnel at the commencement and end of the heating process. This was approximately 20kg of material that would have been wasted. With the polypropylene boxes; re-usable moist river sand was utilized at the beginning and end of each test run. The river sand has a high hygroscopic moisture value and therefore has the ability to hold large amounts of moisture. The only provision was therefore to ensure sufficient moisture was maintained in the river sand to absorb the free microwaves.

The Polypropylene boxes were made, with the cross sectional dimensions, to suit the applicator tunnel size. Sufficient tolerance was provided to prevent friction caused by the tunnel walls, but small enough to reduce leakages. The thickness of the polypropylene sheets was approximately 2mm. These boxes were produced by bending and welding it with polypropylene rods using a heat gun. The lengths of the boxes were based on the achievable length without sacrificing the rigidity when being handled and the length of the applicator (300mm). The manufactured polypropylene box dimensions were 500mm x 86mm x 70mm (LxBxH). A typical polypropylene box is illustrated in Figure 5.9. A total of 18 boxes were manufactured.

Figure 5.9: Typical polypropylene box as manufactured for Alternative 2

Repeat tests was administered to quantify any heating variations to be encountered using Alteration 2. The test results indicated no apparent variation. With the friction reduced, it was then discovered that the motor suffered speed variations as the belt was loaded. The inverter was subsequently reprogrammed to allow constant speed in its vector mode. This, however, did not solve the problem encountered. It was later discovered that at the low operating speed required, the electric motor could not generate enough torque. A larger step down gear ratio was required.

5.2.3 Foam & mixing plant

A Wirtgen WLB-10 foam plant and a Wirtgen WLM-30 mixing plant were used during the Primary investigation to produce a foam bitumen stabilized materials. The foam plant consisted of a heated bitumen tank and a pressurized water tank. The Bitumen temperature used throughout the primary investigation was maintained at approximately 160°C. The WLB-10 foam plant used could set the amount of bitumen foam sprayed as well as regulating the foam bitumen expansion ratio and half-life by varying the percentage of water added during foaming. These variables were evaluated and will be discussed under Section 5.4.3.

The WLM-30 is a dynamic twin shaft pugmill mixer. During in-field mixing the material is agitated and flung to a far greater extent that can be simulated under laboratory conditions. Jenkins (2000) determined that a pugmill mixer was superior to the Hobart mixer in producing bitumen stabilized materials. The paddles of the pugmill mixer allow the aggregate to be suspended in mid-air providing the foamed bitumen to be mixed homogeneously.

Unlike the Hobart mixer, the pugmill mixer does not segregate the finer particles from the course particles. The WLM-30 was used to mimic in-field mixing and was allowed to run for at least 30 seconds prior to adding foam bitumen to generate enough energy during the mixing process. The collapse of the foam bitumen occurs rapidly on contact with the aggregate in the mixer. The duration of the mixing with foam bitumen was approximately 30 seconds. An illustration of the Wirtgen WLB-10 foam plant and a Wirtgen WLM-30 mixing plant is provided in Figure 5.10.

Figure 5.10: Wirtgen WLB-10 foam plant and a Wirtgen WLM-30 mixing plant used for the production of BSM-foam and HWF mixes.

Throughout the primary investigation the mixing drum was heated to approximately 25°C to maintain the energy equilibrium for the production of HWF during the post-heating method. As for the pre-heating method, the mixing drum was heated to approximately 50°C. The difference in the mixing drum temperature was due to the material temperature at mixing. With post heating, the material temperature was at 25°C, whereas the pre-heating process the heated material was recorded at 50°C.

5.2.4 Compaction equipment

The laboratory compaction was achieved by means of a Bosch vibratory hammer with an additional surcharge weight of 20kg, see Figure 5.11. The compaction method used was based on those finding as formulated in Kelfkens (2008).

Figure 5.11: Vibratory hammer with 20kg surcharge weight as used for compaction.

The densities for mixers used in the Primary investigation were firstly evaluated using the Modified AASHTO compaction effort. The mixers were evaluated in this regard for both clean mixes and thereafter verified for stabilized mixes to determine Optimum Moisture Content (OMC) and Maximum Dry Densities (MDD). This formed the bases in determining the duration for compaction using the vibratory hammer.

The moulds used were 150mm in diameter. To prevent heat loss during compaction the moulds were heated to approximately 25°C for the cold mixes and approximately 35°C for the HWF mixes. The typical moulds used are illustrated in Figure 5.12.

Figure 5.12: Typical steel moulds used during compaction.

5.3 Preliminary investigation

This section will cover the Preliminary investigation of heating virgin aggregates at different moisture contents, microwave intensities and heating time durations to investigate maximum heating results. It was during this phase that the belt mechanism was changed from Alternative 1 to Alternative 2.

5.3.1 General Process

The Preliminary investigation process consisted of sourcing various aggregates from different quarries and stockpiled for use. Sufficient samples, per aggregate type, were air dried overnight. The hygroscopic MC was recorded and mixed with water to obtain the required moisture contents for testing.

All aggregates mixed to their prescribed moisture contents were bagged to prevent moisture loss and placed into a refrigerator room. This allowed for the material to be preconditioned at 10°C over a minimum period of 24 hours. This reduced the likelihood of samples benefitting from daily ambient temperature variation. The temperature of the sample batch would nonetheless increase during testing, as the material was exposed to ambient temperatures before microwave heating. Time taken to perform six tests at different exposure times and

intensities on a sample for the given moisture content took on average one hour. The bulk of the time was spent loading the conveyor belt and temperature readings taken with a probe type thermometer. The laboratory ambient temperature was not maintained via air-conditioning, however, no significant variation in daily temperatures was observed during the periods of the Preliminary investigation.

Each aggregate type was heated at various combinations of moisture content, microwave intensities and heating durations. The combinations of these variations are tabulated in Table 5.2.

Table 5.2: Combinations of variables exercised during the Preliminary investigation

Aggregate type	Rock classification	Moisture contents (%)	Microwave intensity (kW)	Time duration (sec)
Eucrite (G1)	Basic, Igneous	0, 3, 5, 7 %	0.6, 2 ,4, 6	30, 60, 90, 120
Granite (G2)	Acidic, Igneous	0, 3, 5, 7 %	0.6, 2 ,4, 6	30, 60, 90, 120
Hornfels (G2)	Metamorphic	0, 3, 5, 7 %	0.6, 2 ,4, 6	30, 60, 90, 120
Quartzite (G2)	Metamorphic	0, 3, 5, 7 %	0.6, 2 ,4, 6	30, 60, 90, 120
Reclaimed Asphalt	(Variable)	0, 3, 5, 7 %	0.6, 2 ,4, 6	30, 60, 90, 120

Heating results of the exposed aggregate during each trial run were recorded at twelve predetermined positions. These results were averaged to provide a final temperature increase for each trial. The predetermined positions were spaced in parallel, as three sets down the centreline at just below the surface as well as mid-depth. A graphical illustration is provided in Figure 5.13. In total, 12 readings were taken per 300mm length of samples heated. In addition, an infrared thermometer was used to measure the surface temperature at three locations, evenly spaced apart.

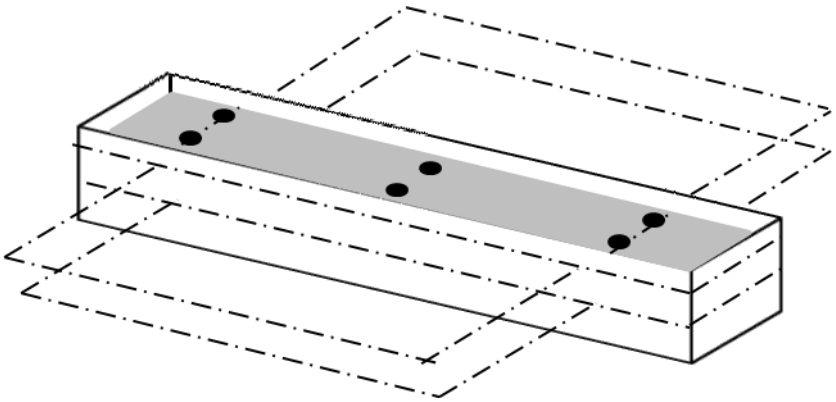

Figure 5.13: Relative positions for temperature measurements per polypropylene box

No information was previously noted by the author for loss factors of any bituminous binders. The theory to determine dielectric properties are complicated and time consuming, not to mention the availability of the correct equipment and expertise. Therefore it was decided to test the binder's ability to be heated by microwave as with the rest of the aggregates. Clean binder was tested at ambient temperature.

Properties such as microwave intensity along with the heating duration were varied with aggregate moisture contents during testing. This was to quantify the heating potential of the samples and the subsequent moisture losses encountered under variable heating conditions. The moisture losses would thereafter be used to evaluate usability of Equation 10, as discussed under Section 4.5.

The results of the Preliminary investigation are provided in Appendix C and summarized in the results section. The material with the best heating potential was to be selected for the primary investigation.

5.3.2 Material selection

Four aggregate types were obtained from four quarries within the Western Cape. All materials sourced, apart from the RA, were either G1/ G2 quality. This was due to the availability of aggregate types sourced. The difference between G1 and G2 materials is the occurrence of weathered rock allowable in the G2 specification. The weathered composition is noted to potentially accommodate more hygroscopic moisture to a lesser extent. This holds the potential for more moisture to be absorbed in light of the moisture's affinity for microwave irradiation during heating. Otherwise additional moisture would exist as free water and could be detrimental to the mix. The additional moisture absorption for G2 hornfels can however be deemed negligible as the percentage weathered rock content was minimal. No blending of aggregates took place during this phase.

5.3.2.1 Virgin aggregate

The production of BSM-foam is considered to be primarily mechanical unlike its BSM-emulsion counterpart. It is therefore not surprising that all rock types are suitable for BSM-foam production. The TG2 (2009) document does however recommend, through experience, that calcrete gravels should not be treated using foamed bitumen. According to Weinert (1980), South African natural road building materials can be grouped according to their mineral composition. The selection of the rock groups was based on the acid and basic rock. Quarries around the Western Cape were researched to determine rock type availability. The natural aggregates obtained are as summarized in Table 5.3.

Table 5.3: Origin and classification aggregates evaluated during Preliminary investigation

Rock Type	Location of source	Aggregate classification	Rock classification
Hornfels	Tygervalley	G2	High Silica Rock (Metamorphic)
Quartzite	Grabouw	G2	High Silica rock (Metamorphic)
Granite	Saldanha	G2	Acid Crystalline Rock (Igneous)
Eucrite	Worcester	G1	Basic crystalline rock (Igneous)

Acid and basic crystalline rocks are liable to decompose in an environment where the Weinert N-value is less than 5. They contain the most complex composition and pose more durability problems than any other class of rock.

Most common characteristic of basic crystalline rock is that they contain little quartz and decompose into montmorillonite, a highly expanding clay. Olivine is the first mineral to decompose. Acid Crystalline rocks on the other hand do not possess the montmorillonite formation stage during decomposition. The minerals in this group therefore decompose to kaolinite.

High Silica rocks form part of the disintegrating rock group. The main minerals present decompose very slowly in comparison to the decomposing rock class and leads to the clay

mineral, kaolinite. Kaolinite acts as a binder to the disintegrated rock and seldom causes problems, (Weinert, 1980).

Eucrite is not a common geological term and was summarized as follows, “Eucrite is a particular kind of gabbro (intrusive igneous rock). Gabbro is typically a coarse grained basic rock composed of basic plagioclase (labradorite to anorthite, ie high calcium and low sodium) and pyroxene (the monoclinic augite or orthorhombic crystals of hypersthene (in norite)). Olivine may or may not be present. Eucrite consists of bytownite/anorthite plagioclase (very high calcium (70-100%) and low sodium), one of the pyroxenes (either augite or hypersthene) and always with olivine. Essentially it is a high calcium olivine gabbro.” (Page-Green, 2011)

Materials classified as G1 or G2 are considered to be adequate for base course in most roads. The angularity of these crushed materials resulted in good compressive strength results when stabilized with foamed bitumen.

5.3.2.2 Reclaimed Asphalt (RA)

The use of RA in pavement engineering is driven by the need to conserve natural resources. The addition of RA into warm mix asphalt has been proven by many researchers to be beneficial to the final mix as the old residual bitumen blends with the new bitumen to produce a stiffer binder that is less susceptible to moisture. The heat input during HWF is maintained below 100°C and is, however, not sufficient to allow complete blending between the residual with the new binder.

The RA will therefore still be considered as “black rock” when blended with the virgin aggregate. The concept of darker colours having greater potential to absorb more light energy differs for microwaves where heat potential is based on loss factor characteristics. It is believed that the residual binder might hold more adsorbed moisture and therefore facilitate heating with microwave. It was therefore initially hypothesized that the inclusion of RA could increase the heating potential of the mixture.

The volumetric heating ability of microwaves are further considered to be beneficial to RA, as the coated surface only required heating when in contact with foamed bitumen during mixing. This would result in total energy saving during manufacturing of the stabilized materials. The energy dissipation into the rock aggregate is however to be considered and will be dealt with under Section 6.3.7.

The RA material sourced for the investigation was obtained from a local asphalt plant in Eerste River, Western Cape. The material obtained was sourced from the same stockpile as those previously used by both de Vos (2010) and Cloete (2010). During their investigation on the RA material, the recovered binder contents of 4% as evaluated by the in-house laboratory at the asphalt plant. The discrepancy of the higher penetration and the softening point values for the aged RA as opposed to the fresh RA residual binder is noted. This discrepancy could be a result of the asphalt plant workforce not storing their fresh and aged RA on the correct stockpile assigned and thus mixing the aged and fresh RA materials. The fresh RA and aged RA blend was subsequently used during this study.

Table 5.4: Residual binder characteristics of sourced Reclaimed Asphalt, (Cloete, 2010)

	Recovered binder (%)	Penetration @ 25°C (0.1mm)	Softening point (°C)
Fresh RA (100%)	4.5	35	58.3
Aged RA (100%)	3.3	40	67.1
50:50 RA blend (Aged : Fresh)	4	30	61

5.3.2.3 Bitumen

Literature investigation on microwave radiation on clean bitumen did not return successful results. Additional tests were then conducted on clean bitumen to observe the rate of temperature increase under microwave radiation. The presence of polar aromatics was considered to be beneficial; however, the stiff nature of the viscous material might be detrimental to heating mechanisms involved.

Fresh Bitumen canisters, 80/100 grade, was preheated to 110°C in a conventional oven to reduce the viscosity. The liquid bitumen was then poured into the lined polypropylene containers and left to cool to room temperature. The container with the bitumen was then placed in the applicator with the moist sand filled polypropylene boxes sealing the applicator tunnels. The bitumen was exposed to 6kW of microwave power intensity for 30 seconds. Figure 5.14 is an illustration of the fresh bitumen in a polypropylene box at room temperature.

Figure 5.14: Clean bitumen in polypropylene box for microwave testing

5.3.3 Moisture Content

It was previously mentioned in the Section 2.5.2.1 that the heating potential of materials improved when moisture contents were above the hygroscopic moisture value. Hygroscopic moisture content for aggregates are however low. The influence of the moisture content in cognisance of OMC for aggregates was to be investigated.

To determine the influence of the moisture content on the aggregates, the moisture contents were varied between 0%, 3%, 5% and 7%. It was evident that for the glassy granite aggregate, 7 % was over the OMC and the water would segregate to the bottom in a short space of time.

For the purpose of testing using the conveyor system Alternative 1, batches of 60kg were mixed with water using a mechanical mixer. Changing to the conveyor belt Alternative 2 method reduced the required material per test to 30kg.

Microwave times for heating the aggregate were varied from 30 seconds to 120 seconds. It was, however, seldom achievable to reach aggregate temperatures close to 100°C. In most cases, 120 seconds of exposure would result in near complete drying of the samples for the given volume in the applicator.

Microwave application is in many industrial processes key to rapid moisture removal. The use of high temperatures is known to increase moisture loss in any heating application or

instance. Jenkins (2000) determined a moisture loss formula with acceptable reliability during his investigation of HWF. The rapid and efficient evaporation encountered during the preliminary testing will therefore need monitoring during the primary investigation of heating aggregates.

5.3.4 Microwave versus Conventional oven

In the mining industry, rocks containing no substance of value is called gangue material and regarded as unwanted material. With no significant mineral value and inherent high crushing strength, the gangue material makes for a suitable road building material. Gangue material is not readily heated by electromagnetic radiation and therefore the moisture would play an important part in the heating potential. The cost to source aggregates has an additional influence to the selection of suitable material. It should be noted that rocks, from certain mine wastes, could contain traces of metal ore. These materials would increase costs of hauling as their densities are approximately 1.5 times other natural road building materials, (Weinert, 1980). Marginal soils with slight clay content or synthetic materials such as Zeolites could assist with moisture retention, although not considered during this study.

The key concept of heating the outer surface of the aggregate selectively making use of the moisture and/ or aged bitumen in mixes is the theoretical ideology for the for energy saving volumetric heating exercise. Should the aggregate surface of a sample be predominantly affected under the microwave radiation, rapid temperature drop off over time would be evident as opposed to material aggregate completely heated to the same maximum temperature. The thermodynamic properties of the materials involved plays a vital role in the rate at which the heat is diffused within the aggregate particles.

To investigate the advent differences between microwave heating and conventional heating, two samples were heated to a similar temperature and allowed to cool to room temperature. One sample of RA aggregate was placed in a conventional laboratory oven at 100°C to heat over night, whilst another moist RA sample was heated with the microwave. The samples for both heating modes were cooled congruently. Temperature readings were recorded intermittently in the centre of the samples. The results are presented under Section 6.2.

5.4 Primary investigation

This section on Primary investigation will cover the manufacturing of HWF mixtures using microwave technology. The results obtained during the Preliminary investigation provide a basic insight for selecting input variables during this section.

5.4.1 Background

The implementation of microwave heating devices in typical in-plant recyclers were considered to be fundamental whilst determining limitations. The laboratory process is therefore required to take recognition of in-field parameters such as production rates and physical dimensions.

There is a direct relation between the microwave frequency and penetration depth, as discussed in the Chapter 2. The availability of magnetrons with specific attributes such as operating frequency and the power intensity has a significant bearing on the initial setup phase and operation costs. Higher magnetron outputs are available only for the 900MHz frequency band when compared to the 2450MHz frequency band. The production rate is also linked to the heating rate. Thus, the volume throughput in turn depends on material depth to ensure penetration as well as the length of the proposed applicator unit. The length of travel for the aggregate is used to calculate the exposure time within the applicator for a given belt speed. This exposure time is essential to obtain the energy input and maximum heating capability of the system.

Current portable in-plant recyclers such as the Wirtgen KMA220 have a maximum production rate of 220 tons/hour. The KMA220 recycler, as shown in Figure 5.15, was used as a design instrument for implementation of portable HWF production units. The following factors were considered to influence applicability:

- Sizable location for microwave applicator placement;
- Conveyor belt size and length limitation for microwave applicator;
- microwave intensity to maintain production rates;
- Magnetron unit availability; and
- Power consumption.

Figure 5.15: KMA220 portable in-plant recycler

5.4.2 Aggregate selection

The results of the preliminary aggregate heating exercise did not indicate any superior heating attributes for the four virgin aggregates tested. It was therefore decided to use the hornfels aggregate for the Primary investigation based on its decomposition properties and its prevalence as a road building material within the Western Cape. The RA material showed improved heating potential under microwave radiation in relation to the virgin aggregates. RA material was therefore used in conjunction with the hornfels aggregate to form two blends.

The blending of RA to the virgin aggregate is considered to be two fold, for energy benefits to be realized. The concept of RA as a black stone could be beneficial in absorbing microwave energy more efficiently due to its potential to heat. RA usage is also inherently environmentally friendly as it promotes the use of recycled material. There was however, no certainty regarding the extent of the interaction between the fresh binder and the residual binder and this was to be determined by the temperatures achievable. If sufficient temperature increase exceeded the residual binders softening point, the interaction would result in a stiffer mix as evident with WMA technology.

Two blend variations were considered for testing, these are as follows:

- **80RA**: 80% Reclaimed Asphalt + 20% G2 Hornfels
- **20RA**: 20% Reclaimed Asphalt + 80% G2 Hornfels

High percentages of RA do not provide sufficient shear strength in relation to 100% crushed aggregate mixtures. The vast percentage differences between the two materials for the blends were used to determine the significance of the RA in the blend.

5.4.2.1 Grading

The grading of the hornfels and RA material were evaluated in accordance with the TG2 (2009) specifications and grading curves for BSM-foam production. The grading of the G2 hornfels material fell within the BSM-foam ideal grading envelope. The RA material lacked the required fine content passing the 0.425mm sieve and lower. Natural filler material (hornfels) was sourced from an asphalt plant and 4.5% was added to bring the grading to within the ideal envelope range.

The blend ratios initially decided on were 75% RA to 25% G2 and 75% G2 to 25% RA. The blend was later reassessed at the time to consider the potential benefit of the RA material to the mix for adequate heating. To further accommodate the 4.5% natural filler to the high percentage RA blend, the ratios were adjusted by 5% to maintain at least 75% RA to the 80 RA blend. The grading for the two blends, 80RA and 20RA, are provided below in Figure 5.16, respectively. Crushing the RA aggregate, to increase its fine content, was not undertaken as the crushed fine material would contain clean faces in any event.

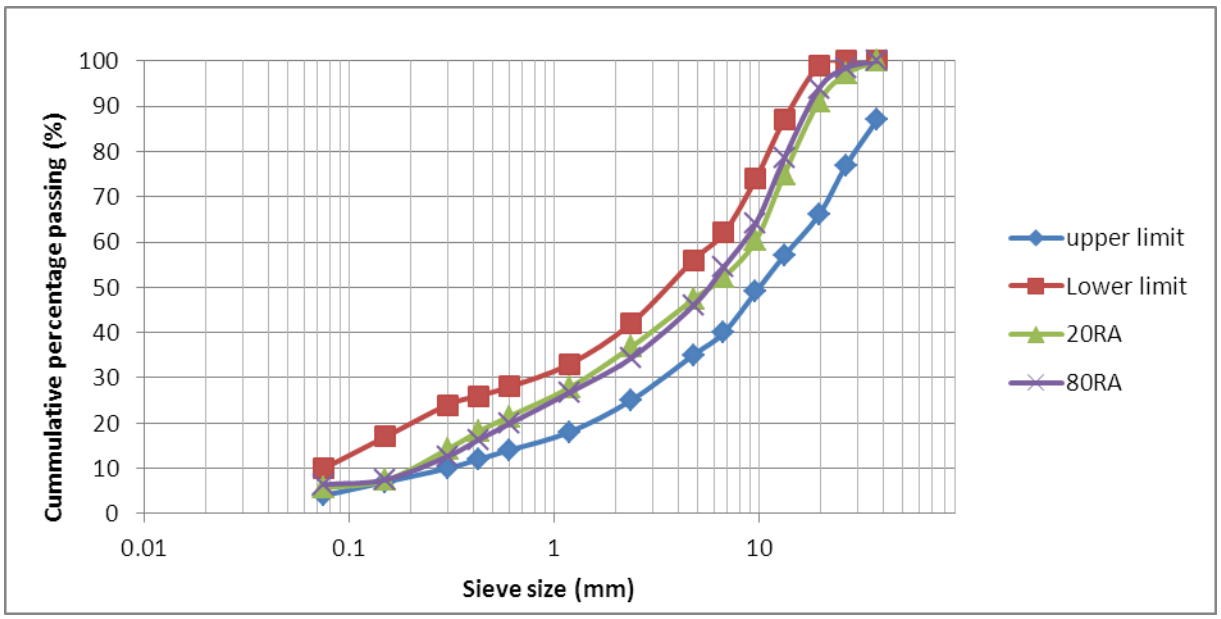

Figure 5.16: Grading curve for 80RA and 20RA aggregate blends

The 19mm stone sizes are considered to have an adverse effect on the voids content when compacting 150mm diameter samples. Materials retained on the 19mm sieve were substituted by weight using material retained on the 13,2mm sieve. To determine the

benefits of the microwave volumetric heating, no active filler was included in the blend as this could have distorted results to be evaluated.

5.4.2.2 Moisture Content

The two material blends were evaluated by means of the Modified AASHTO compaction method to determine their Optimum Moisture Content (OMC) and Maximum Dry Density (MDD). The mechanical compaction apparatus used in the laboratory is illustrated in Figure 5.17. The moulds used in the laboratory were 150mm diameter and 100mm in height.

Figure 5.17: Mechanical compaction apparatus to evaluate Modified AASHTO density

The results for the OMC and MDD were recorded and used initially to determine the compaction time required by the vibratory hammer, to achieve the same densities for BSM-foam. Subsequently, it was discovered that the addition of foamed bitumen and 5% variation in the blend fractions reduced the total MDD achievable. The new MDD was thereafter determined by means of the Modified AASHTO compaction method for the BSM-foam mixture at the previous OMC for both blends. These results were thereafter used as the optimum values. The MDD results aided in the quantifying the aggregate mass required per

sample to be produced. The results are tabulated below in Table 5.5, and graphically presented in Figure 5.18 and Figure 5.19.

Table 5.5: Maximum Dry Density and Optimum Moisture Content results for 80RA and 20RA blends

	MDD (kg/m^3)	OMC (%)
80RA Blend	2214	5.5
20RA Blend	2291	5.1

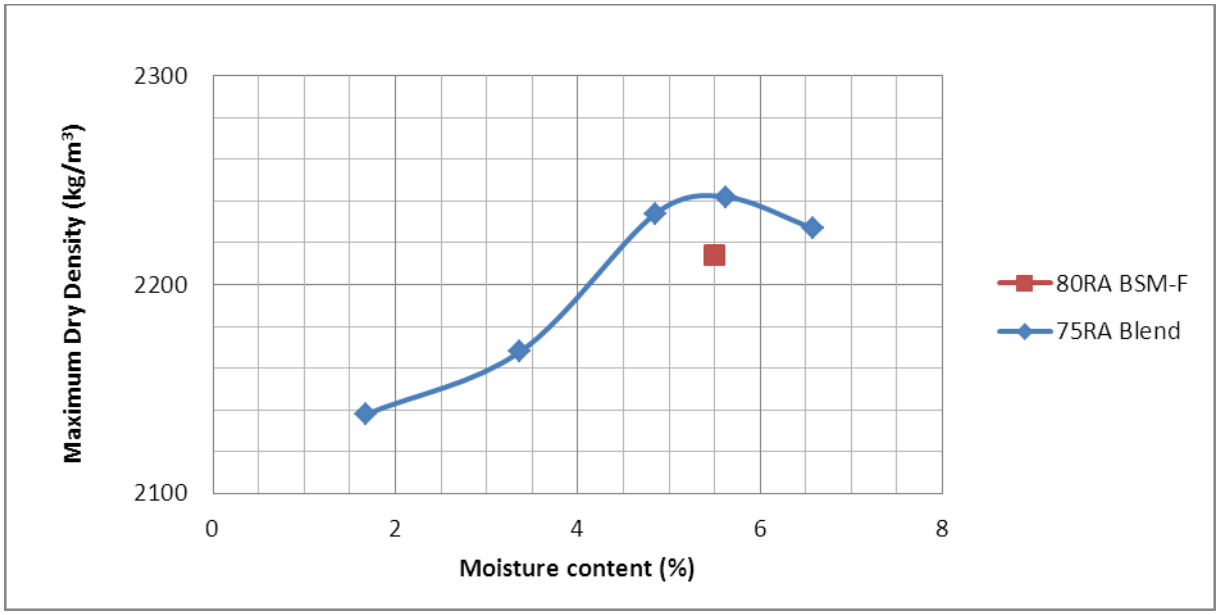

Figure 5.18: Maximum Dry Density (MDD) and Optimum Moisture Content (OMC) for 80RA blends

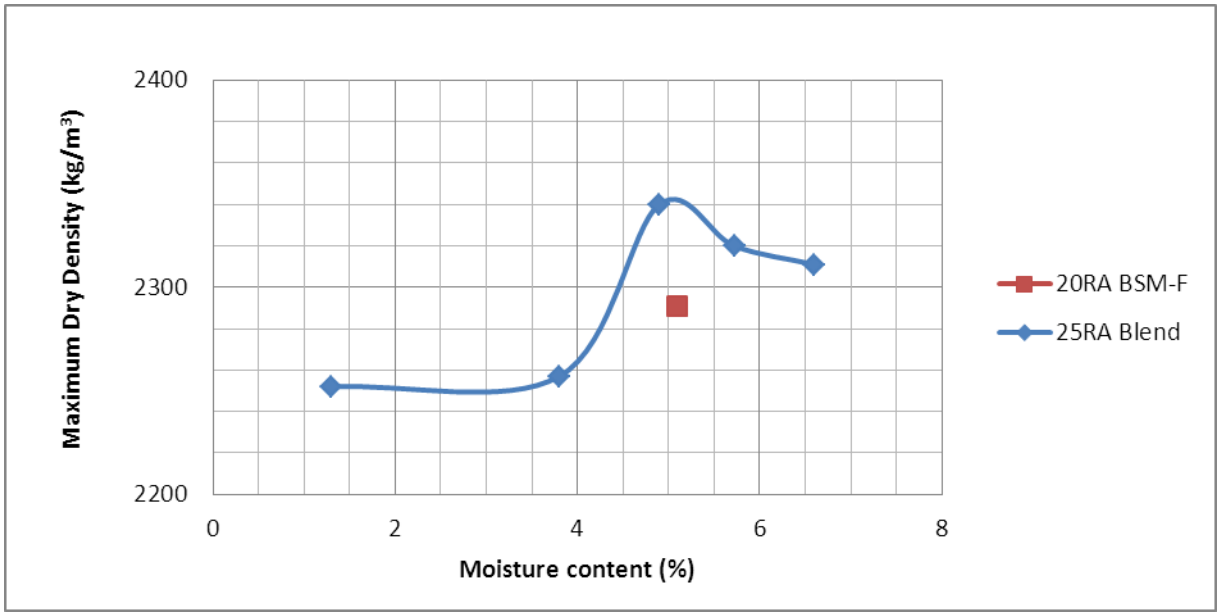

Figure 5.19: Maximum Dry Density (MDD) and Optimum Moisture Content (OMC) for 20RA blends

The fluff point MC is usually specified to promote maximum BSM-foam benefits during mixing. Fluff point MC is defined as the moisture content at which the maximum bulk volume of loose mineral aggregate is obtained. The fluff point of aggregates is usually in the vicinity of 80% of a material's OMC. Wirtgen (2010) suggests the use of fluff point MC during mixing and the addition of the remainder MC, to achieve the Optimum Compaction Moisture Content (OCMC) for compaction, to obtain the required final densities. Wirtgen (2010) further suggests that the OCMC normally approximates the OMC of the parent material. The TG2 (2009) suggests an upper limit of the parent materials OMC for the mixing moisture content of BSM-foam.

The focus to simulate an in-plant recycling process lead to the decision that the addition of water after mixing might impact on the heat gained by the microwave and reduces the efficacy between mixing to final sample compaction. Including an additional watering phase was also considered to reduce production rates. The general experimental aim was also to reduce all time consuming heat loss events during the process. It was therefore decided to provide sufficient moisture, so that by the compaction process, the materials were at its OMC.

Jenkins (2000) indicated that the elevated temperatures experienced during the production of HWF mixes results in considerable moisture losses before compaction. It was suggested that additional moisture was required to produce HWF mixes for the preheated aggregates.

The preliminary investigation results further indicate that material moisture contents of 5% benefited the microwave heating process the best. At 3% moisture contents, microwave leakages occurred whilst using the continuous flow microwave system. It was anticipated that exceeding the fluff point moisture content would result in less than optimum mixes, although still at an acceptable standard. Subsequent, BSM-foam mixes were continuously monitored after mixing to ensure adequate binder dispersion. Figure 5.20 provides and illustration of ITS and triaxial samples after testing, indicating the extent of binder distribution.

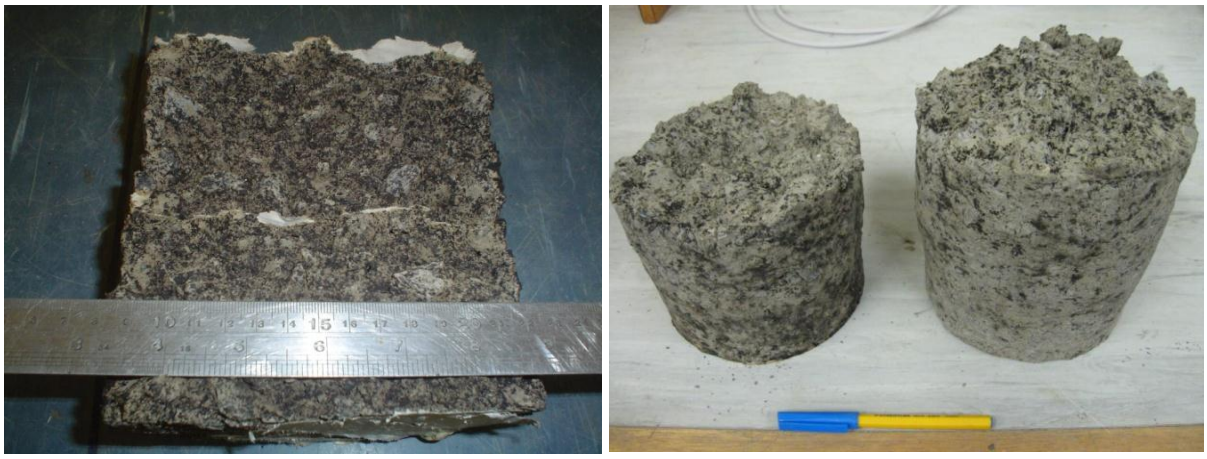

Figure 5.20: 80RA ITS sample heated after 12 seconds exposure (Left), and 20RA triaxial sample heated after 12 seconds exposure (Right)

The moisture loss relationship (Equation 10), Section 4.5, established during the research by Jenkins (2000) was evaluated and thereafter used during this study. The coefficient of correlation (R^2) for the equation is low considering its intentional simplification of significant variables (R^2= 0.60). This useful estimation provided relatively close values for moisture loss compensation required during the microwave heating process.

All mixing variables during this study fell within range of the limitations specified by Jenkins (2000) for the implementation of Equation 10, with the exception of the mixing time. The mixing time variation, however, did not reduce the efficacy of the equations, based on results during the preliminary investigation. The additional moisture used for the various heating intensities are provided in Table 5.6.

Table 5.6: Additional moisture contents to overcome evaporative moisture loss

	High Power (12 seconds)	Low Power (6 seconds)
80RA	0.7%	0.2%
20RA	0.7%	0.2%

5.4.3 Binder content

The binder used during the study was 80/100 grade bitumen received from CHEVRON. Binder contents for BSM-foam typically range from 1.7% to 2.5% as indicated in the TG2 (2009) document. Previous studies by Brennen et. al. (1983) using RA material suggested optimum stability values at binder content of 0.5% to 1%. To gain the most benefit from the heating of the material as well as the heating potential provided by the moisture captured by the binder as envisaged, 2% and 2.3% was used for the 80RA and 20RA blends, respectively. The difference in binder content is to accommodate the residual binder present in the RA. Previous research conducted at the University of Stellenbosch using aggregates from the same source indicates that the aforementioned binder quantities are suitable for the BSM-foam production.

The half-life and expansion ratio were investigated prior to the commencement of the BSM-foam production. These two variables are dependent on a large number of factors such as:

- Bitumen type;
- Bitumen temperature;
- Quantity of foamant water added;
- Presence of foamant or anti-foamants;
- Configuration of the foaming nozzle; and
- Container temperature in which the foamed bitumen is sprayed.

For the constant binder temperature of 160°C in the WLB-10 foam plant, the half-life and expansion ration was determined for various quantities of foamant water. The results of the half-life and expansion ratio are provided in Figure 5.21 below. The procedure to obtain to the optimum water foamant percentage was conducted as per Jenkins (2000) and Wirtgen (2010).

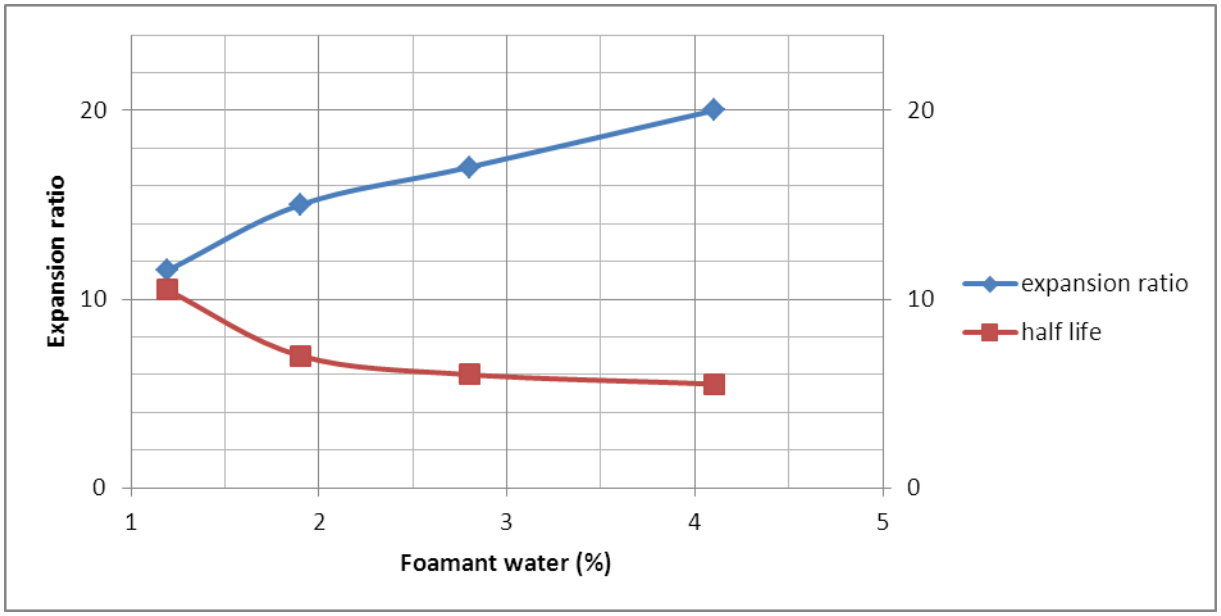

Figure 5.21: Half-life and expansion ratio evaluation of CHEVRON 80/100 grade bitumen.

From Figure 5.21, it can be observed that the foamant water percentage should be between 1% and 3%, based on the minimum recommended minimum expansion ratio and half-life of 8 and 6 respectively. It was therefore decided to use 2% foamant water.

5.4.4 Microwave heating

Microwave radiation has the potential to selectively heat certain components of the mix. The heating of materials to produce HWF mixes can be undertaken at two different instances. It can occur prior to mixing the moist aggregate with foamed bitumen or immediately after producing BSM-foam. The two methods are hypothesized to interact and benefit from each process in different ways.

Heating moist aggregates prior to mixing with foamed bitumen reduces the temperature difference between the hot foamed bitumen and aggregates. This allows for increase particle coating of the larger aggregate sizes, thereby increasing adhesion of the mix as previously recorded by Jenkins (2000). It is believed that the moisture and residual binder from the RA will facilitate the volumetric heating of the surface of the aggregate and promote energy saving whilst producing HWF mixes. For this process, moist aggregates are heated and immediately fed into the pre-heated mixer. The moisture content will be proportioned to ensure the final heated aggregate has sufficient moisture when placed into the mixer. All aggregate batches were individually mixed with the measured moisture content and stored at 25°C the evening prior to the HWF process. Figure 5.22 below illustrates the pre-heat process.

Figure 5.22: Process chart for microwave pre-heating procedure

Manufacturing BSM-foam and thereafter heating the mix (post-heating), focuses on using trapped moisture to facilitate bitumen bonds between aggregate. The addition of RA is believed to facilitate the heating process. Interaction between the residual binder and the fresh bitumen depends on the heating temperature achievable. For this process, aggregates are heated after producing BSM-foam. Sufficient moisture (OMC and moisture loss compensation) is mixed before the foamed bitumen mixing process. All aggregate batches were individually mixed with the measured moisture content and stored at 25°C the evening prior to the HWF process. Figure 5.23 below illustrates the post heat process.

Figure 5.23: Process chart for microwave post-heating procedure

Temperature increase is depended on production rate, given that only a limited longitudinal length is available for a microwave applicator in the recycling plant in practice. The laboratory trials consist of two temperature variations as well as a cold BSM-foam control mix for both aggregate blends. The temperature variations considered will therefore be depicted by the production rate and economic costs rather than optimisation of engineering properties. Using the heating rates recorded from the preliminary test results, the maximum achievable temperature per exposure duration was calculated.

5.4.5 Mixing

The Wirtgen WLB-10 foam plant and the WLM-30 mixing plant were used to produce the BSM-foam and HWF mixes. The WLM-30 was preheated prior to mixing the microwave heated materials to the temperatures as specified in Section 5.2.3. Caution was noted not to overload the mixer, as this would reduce the mixing speed of the paddles and therefore result in non-homogeneous mixes.

The conservation of heat during the experiment was considered vital. To reduce heat loss between the various processes, insulated containers were made and used to transport the material between heating and compaction equipment. The heated mixes were additionally weighed off depending on the sample to be made and sealed in plastic bags to prevent moisture loss in transit to the compaction equipment. Temperature readings were recorded after mixing and after heating.

5.4.6 Compaction

The Bosch vibratory hammer was used to achieve the required compaction densities for the various samples. The vibratory hammer weighed 10.1kg and an additional 20kg surcharge weight was attached to the hammer. This was done to decrease the compaction duration. The vibratory hammer frequency was set to its maximum of 31.5Hz. The vibratory hammer is specified to produce a total of 25J per cycle without the surcharge weight.

Compaction time during the production of samples was kept constant to maintain the same energy expenditure. Using the same compaction energy across all sample variations allowed for the evaluation of workability and MDD to be analysed.

The moulds used were split column moulds, 150mm in diameter and 300mm in height. The moulds were lubricated to prevent adhesion of the samples to the inside walls.

The ITS sample mass was weighed off, using the MDD results and compacted to a height of 75mm. Three ITS samples, of each mix variation, were produced for testing purposes due to the inherent repeatability shortfall of the ITS test. In certain instances three additional samples of a mix variation were produced for Tensile Strength Ratio (TSR) tests. These ITS samples were compacted as one uniform layer. The compaction duration was set at 25 seconds.

The ITS specimen height differs from those suggested value of 127mm as prescribed in the TG2 (2009). The variation in the specimen height is a result of the size if the test jig used for testing at the University of Stellenbosch. The variation in the specimen size in relation to normal practice is considered acceptable due the experimentation being a comparative study.

The triaxial samples were compacted to a height of 300mm, in five layers of 60mm each. The compaction duration of each layer was 15, 25, 25, 35, and 25 seconds. These compaction times differ slightly from those recommended by Kelfkens (2008). The variation

is a result of two factors namely; the moisture contents differed, and the Mod AASHTO compaction method was used for comparison to achieve 100% Mod AASHTO compaction. The compaction values were nonetheless based on the methodology specified by Kelfkens (2008) to achieve the 100% Mod AASHTO density. The material required was again calculated using the MDD results from the Mod AASHTO density relationship as presented in Section 5.4.2.2. Three samples were produced per aggregate type, to be tested at various confinement stresses, due to the materials stress dependent nature.

The use of moulds at ambient temperature during compaction could adversely affect density results due to heat loss around the walls of the mould. To reduce heat loss, the moulds were preheated to approximately 30 to 35°C for the heated samples.

5.4.7 Curing

The samples were to be cured under accelerated curing conditions at 40°C for one day unsealed and two days sealed as specified by the Wirtgen manual (2010). The accelerated curing process simulates 6 months in-field curing and deemed appropriate to simulate the realistic strength gain for BSM-foam. After curing, the samples were securely placed within a sealed plastic bag, and intact until testing. The oven cured samples were tested within two days after curing was completed. Efforts were made to ensure that the period between curing and testing remained constant in all cases. Moisture contents were tested for each sample after compaction.

The TSR test samples were submerged for 24 hours in a water bath at 25°C after accelerated curing. The TSR samples were tested immediately after being conditioned in the water bath.

5.4.8 Testing apparatus

The heating of the aggregate improves the coating of the aggregates. This improved coating is believed to be a result of the tensile strength and cohesion of a mix. The study by Jenkins (2000) indicated improved shear properties for HWF. The increased cohesion value indicates the ability of a mix to withstand higher stresses and thus reduced rutting. The Indirect Tensile Strength (ITS) tests were used for the evaluation of the tensile strength and the monotonic triaxial test was used to evaluate the shear properties of the mixes.

All specimens were conditioned to achieve a core temperature of 25°C before testing as this is believed to be the average representative temperature of a BSM base layer in Southern Africa (Moloto, 2010).

5.4.8.1 Indirect Tensile Strength (ITS) apparatus

The ITS tests were carried out using the Universal Test Machine (UTM-25) in the University's pavement engineering laboratory. The specimens were conditioned in the UTM-25 machine to achieve a core temperature of 25°C before testing.

The specimen dimensions are 150mm in diameter and 75mm in height. The specimen strength is evaluated under the displacement control condition. The tests consisted of loading the specimen along its diametrical axis at a rate of 50.8mm/minute until failure. The load versus displacement was recorded and evaluated to determine the maximum tensile strength. Figure 5.24 illustrates an ITS specimen to be tested in the UTM-25 apparatus.

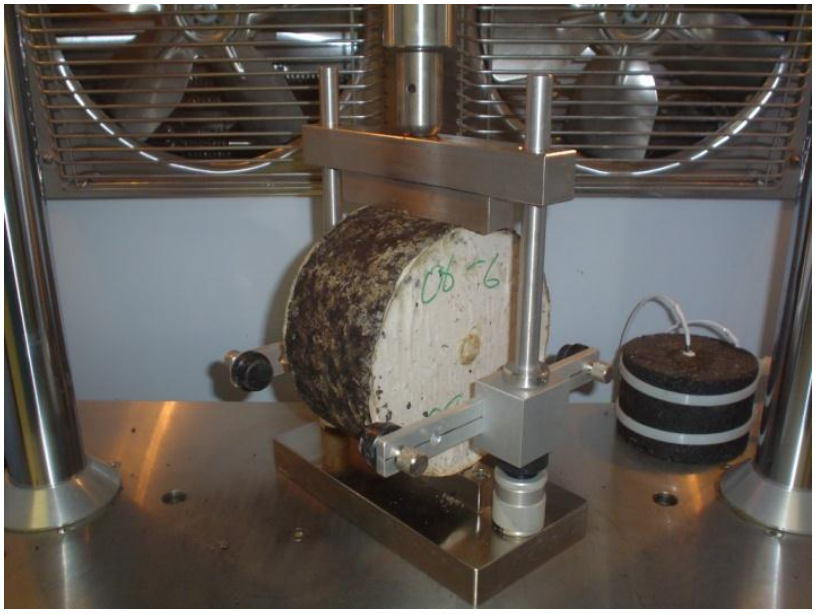

Figure 5.24: ITS specimen as tested in the UTM-25 apparatus at 25°C

The ITS test is commonly considered to lack repeatability. Further disadvantages of the ITS tests consists of unrealistic stress states during testing in relation to in-field and the high stresses at the supports, initiating local failure. The use of the ITS here, however, is sufficient to determine improvements in HWF mixes in opposed to BSM-foam.

5.4.8.2 Triaxial apparatus

The monotonic triaxial test was carried out using the Material Testing System (MTS-810) in the University's pavement engineering laboratory. The testing system is a closed loop servo-hydraulic testing system.

The specimen strength is evaluated under the displacement control condition. The tests consisted of loading the specimen at a rate of 6.3mm/minute (2,1% strain for 300mm high

specimen) until failure. The confinement pressures were set to 50, 100, 200kPa for the three tests performed. The load versus displacement was recorded and evaluated to determine the maximum deviator stress at failure.

The monotonic triaxial test was performed on the control BSM-foam mix and the HWF mix for 20RA blend specimens. Confinement pressures of 50, 100, 200kPa was used to determine cohesion values and internal friction angles as per Mohr-Coulomb failure criterion. The specimen dimensions were 150mm diameter and 300mm in length. The specimens were conditioned in ovens to achieve a core temperature of 25°C before testing. Figure 5.25 illustrates a triaxial specimen to be tested in the MTS-810 apparatus.

Figure 5.25: Triaxial specimen as tested in the MTS-810 apparatus at 25°C

CHAPTER 6: RESULTS

6.1 Introduction

A continuous flow microwave applicator has been used to heat various aggregates in the Laboratory. By analyzing the current laboratory findings in conjunction with theoretical heat and mass transfer calculations, the economic feasibility of up scaling the laboratory microwave heating concept to a full scale industrial production facility to produce HWF mix can be determined.

Various past researchers have identified that the use of warm aggregate in Foam Bitumen Stabilized Material (BSM-foam) improves its engineering properties. It is proposed that the increase in aggregate temperature reduces the foam bitumen's rate of energy loss or viscosity increase and therefore promotes improved particle coating, (Jenkins, 2000). This improved particle coating provides a more uniform increase in adhesion between particles which in turn improves the engineering properties. Heating aggregates can, however, be costly and time consuming. Essentially, heating the entire stone for foamed bitumen stabilization would be unnecessary, as it is only the outer skin of the aggregate that affects the dispersion capabilities of the foamed bitumen when exposed.

Microwave heating is a form of electrical volumetric heating, and has the application potential of heating arbitrary portions of a sample selectively depending on the variation in dielectric properties of the constituents. If the outer skin of the aggregate has a greater potential to absorb microwave power than inside the aggregate itself, then the use of microwave heating could be beneficial in selectively heating the outer skin making it a suitable energy application in creating better foamed mixes economically. The general aggregates used for road building don't absorb microwave energy easily.

This chapter consists of three subsections; the first subsection focuses on the Preliminary investigation and its obtained test results, whereas the second subsection discusses the Theoretical evaluation centred on the findings of the Preliminary investigation. This led the research study into the third section, Primary investigation, by providing probable prospects based on the obtained results and drawbacks in the Preliminary investigation.

6.2 Preliminary investigation

The main aim of the Preliminary investigation was to investigate the heating potential of the various aggregates sourced at differing moisture contents. In addition, the heating intensity

and exposure time were evaluated. This would enable inferences to be drawn about which combination of the above mentioned factors, (aggregate, moisture, intensity, and time), are best suited to produce half-warm aggregates suitable for HWF production.

Each sample was only tested once due to the time, size and nature of initially preparing samples on the Alternative 1 conveyer belt system. A sample size of 60kg was deemed necessary to perform the heating tests at varying intensities, (0.6kW, 2kW, 4kW, 6kW), for a given MC. The larger sample size is to ensure no leakages occur at the ends of the conveyor belt during testing. Using Alternative 2, dummy boxes containing river sand could be placed at the entrance and exit, allowing the centre boxes to be heated without leakage risks.

Good correlation was observed whilst heating when the material was continuously being fed in relation to holding the material in the applicator; provided each section of the material was exposed under the same time limit as with the stationary heating. The stationary heating technique displayed “hot spots” on certain instances, which is a result of the applicator and waveguide design, and the materials orientation. The average temperature increase, however, was constant in relation to the continuous feed method. During the Preliminary investigation, it was decided to use the stationary feed method due to similarity of the temperature increase of the two methods and additionally, it reduces the effort during the preparation of the samples. The values recorded for the results are averaged. Records of the heating results are presented in Appendix C.

Even though the microwave chamber is small (area: 300mm x 90mm and specimen, and specimen height of 50mm), temperature variations were observed over the heated sections. Up to 10˚C variations in temperature was found to be common, and in some instances 20˚C variations were recorded for samples heated in excess of 100°C.

6.2.1 Temperature versus exposure time

Figure 6.1 compares the heating potential of the various aggregates at increasing time durations with a microwave intensity of 0.6kW and a MC of 3%. RA however was tested under similar conditions with the exception of the microwave intensity set to 2kW. Moisture contents at 3% experienced excessive microwave leakages early during testing when heated at an intensity of 2kW. On assessing the materials after leakages were witnessed, it was apparent that the cause for the leakages was a result of excessive evaporation. Heating tests at an MC of 3% were subsequently tested at 0.6kW at which no microwave leakage

occurred. RA however is not affected in the same manner and was tested at 2kW with almost 60°C rise in temperature as indicated in Figure 6.1.

Dry aggregates were not tested due to excessive microwave leakage with the exception of RA. The RA material does respond consistently to the microwaves and could be tested without leakages at higher intensities and low moisture contents, but within limits.

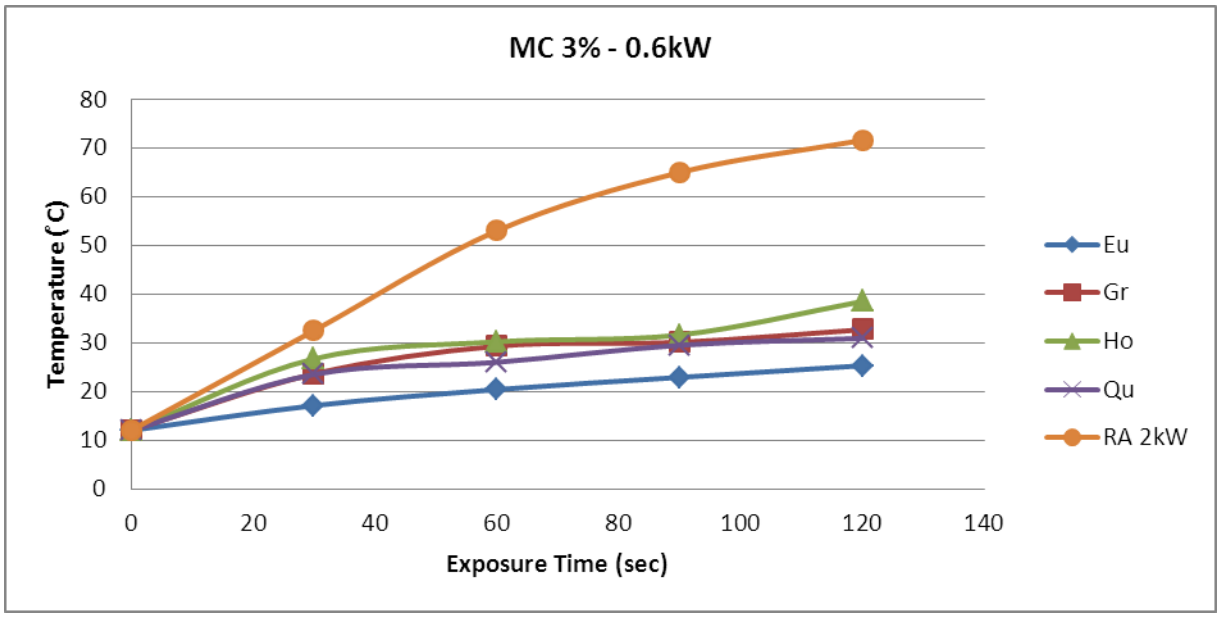

Figure 6.1: Combined results for aggregates heated at 0.6kW (RA – 2kW) and 3% moisture content

Figure 6.2and Figure 6.3 compare the heating potential of the various aggregates at increasing time durations with a microwave intensity of 2kW and a MC of 5% and 7% respectively. No large temperature variations were observed between testing with MC of 5% and 7%. The reason might be due to the excessive moisture (free water) that is more susceptible to microwave heating and therefore absorbs the majority of the energy without releasing heat. It would appear that exceeding a MC of 5% would not benefit the G1/ G2. The comparative temperature increase appears constant for all aggregates at 5% MC.

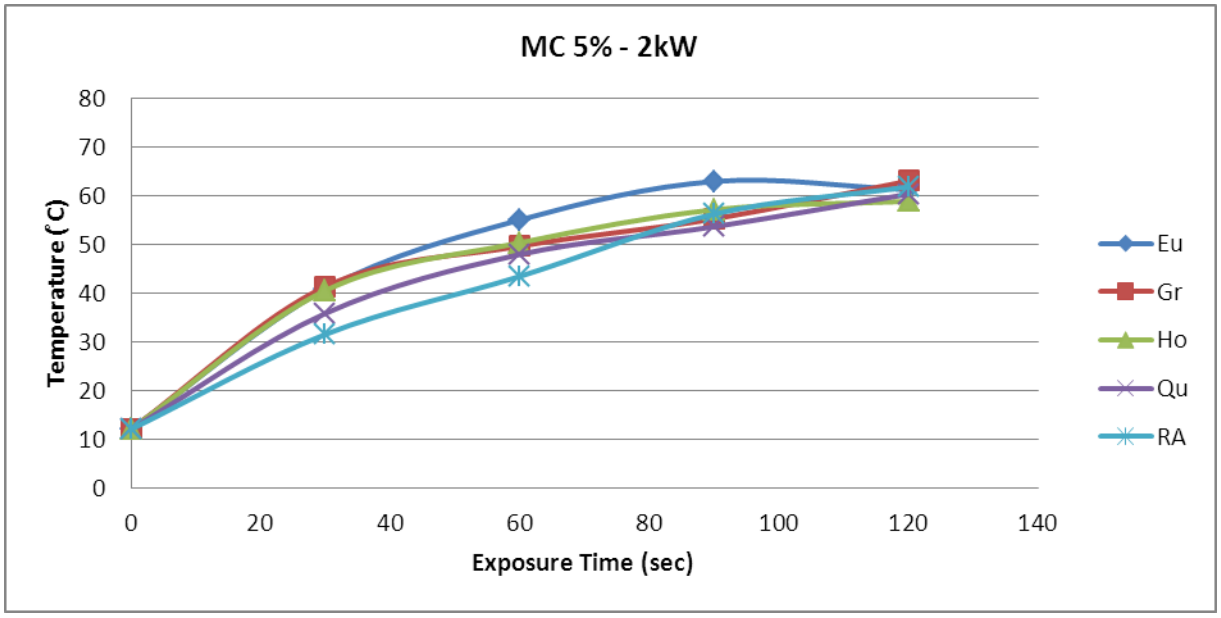

Figure 6.2: Combined results for aggregates heated at 2kW and 5% moisture content

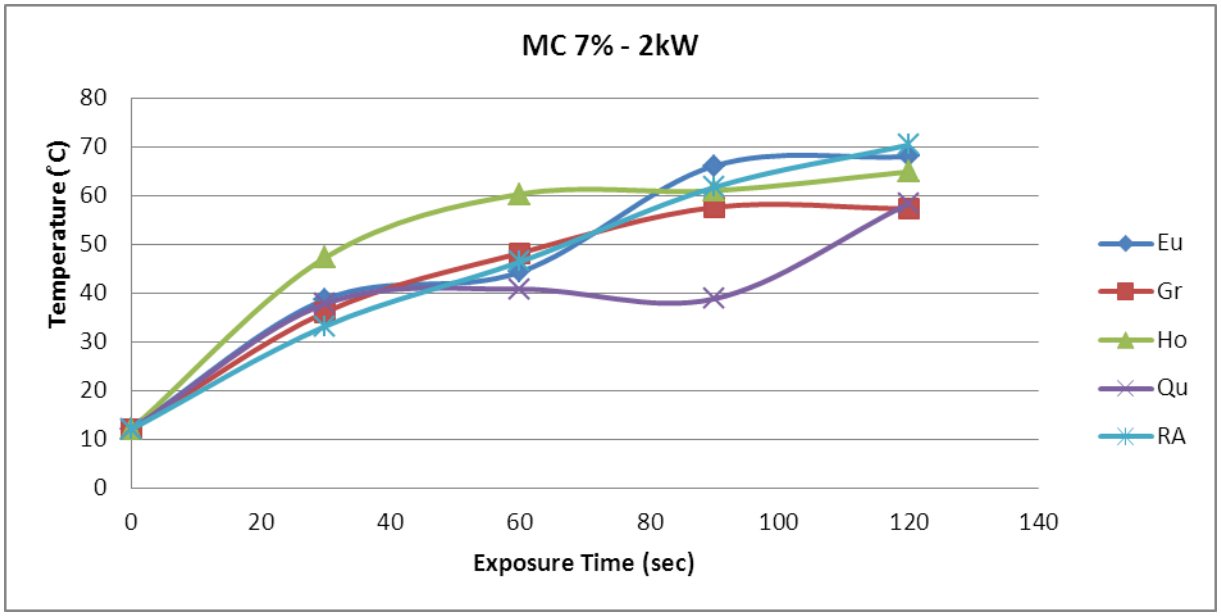

Figure 6.3: Combined results for aggregates heated at 2kW and 7% moisture content

The largest variation in temperature for aggregates with similar MC, time of exposure and intensity occurs at MC 7%. This could be a result of the aggregate homogeneity during testing and free water available dependent on the materials inherent OMC. Areas where more fine material congregates, would naturally contain more moisture. This would promote higher attainable temperature before the moisture would completely evaporate. The hornfels aggregate appears to have a high initial heating rate in comparison to the other aggregates.

Hornfels and eucrite (the darker aggregates) respond marginally better in temperature increase than the granite and quartzite (glassy aggregates). However the material colour has no direct relation to a samples loss factor.

6.2.2 Heating comparison per aggregate type:

Figure 6.4 to Figure 6.8 compare the heating potential per aggregate type at the various moisture contents. The rise in temperature increase with microwave exposure duration appears constant across all aggregates in general. The slow temperature gain for 3% MC for the various aggregates is a result of the lower microwave intensities (0.6kW) in relation to the 2kW used for the 5% and 7% MC's.

RA is not affected by low moisture content as can be observed in Figure 6.8, where it was heated at 0.6kW and 2kW with no additional moisture. The sudden rise in temperature for RA at 0% MC and 2kW power intensity is not known. It is however assumed that trapped moisture might be the reason for this sudden increase. This entrapped moisture might not receive the opportunity to evaporate and therefore heats the aggregates substantially after the free moisture evaporates.

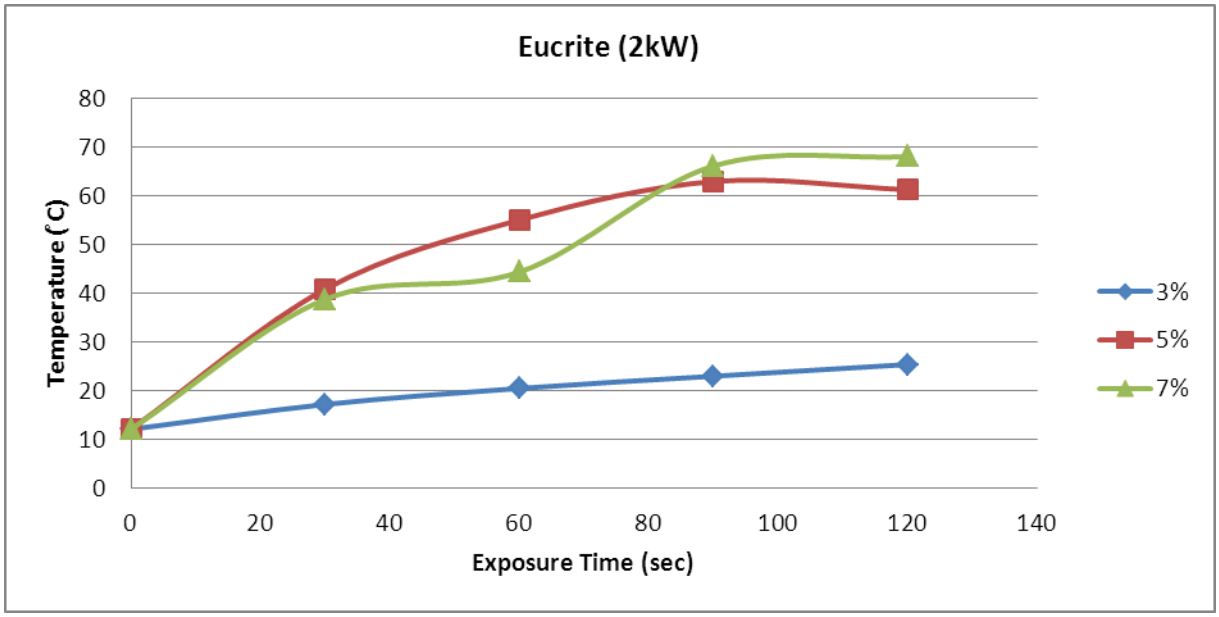

Figure 6.4: Eucrite (Eu) results for varying moisture contents heated at 2kW

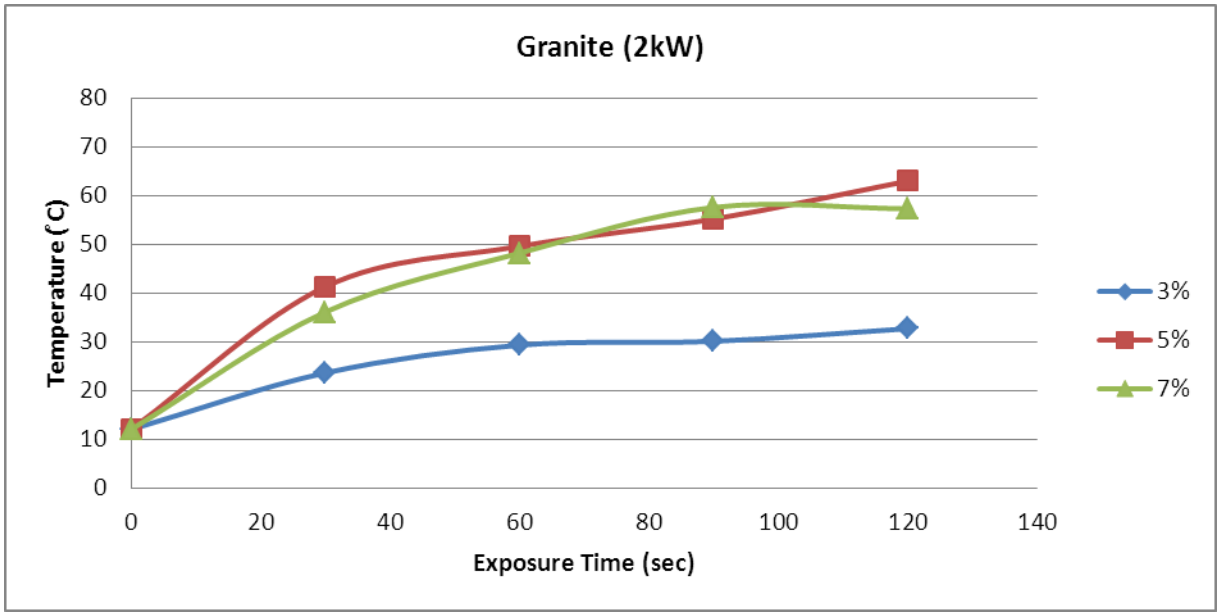

Figure 6.5: Granite (Gr) results for varying moisture contents heated at 2kW

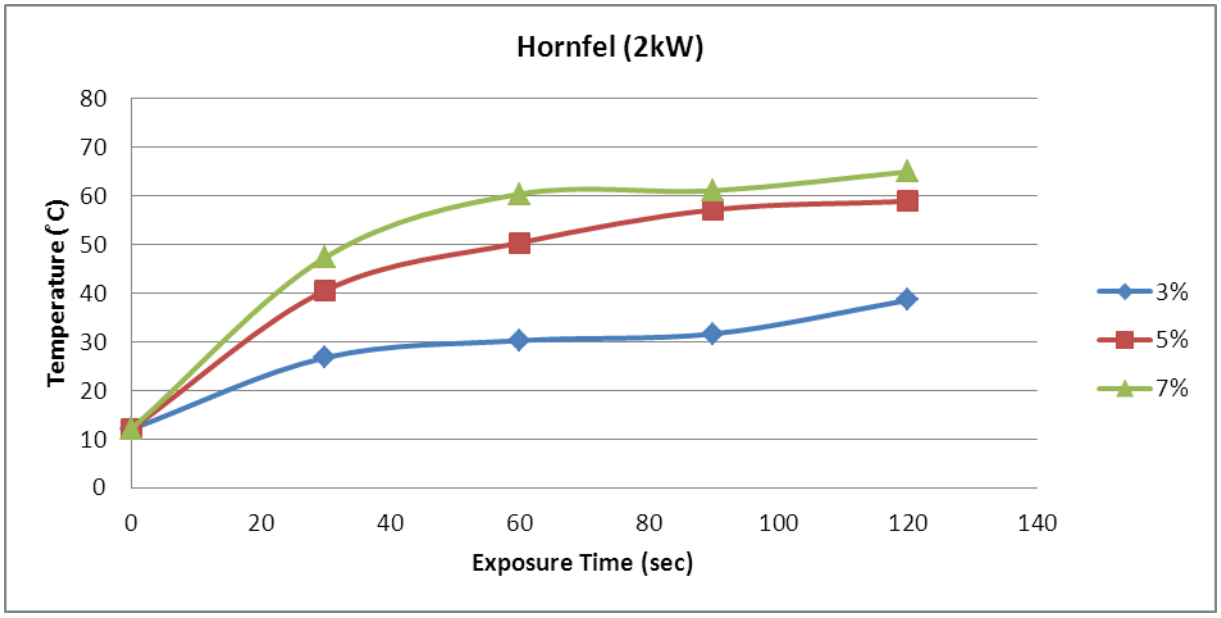

Figure 6.6: Hornfels (Ho) results for varying moisture contents heated at 2kW

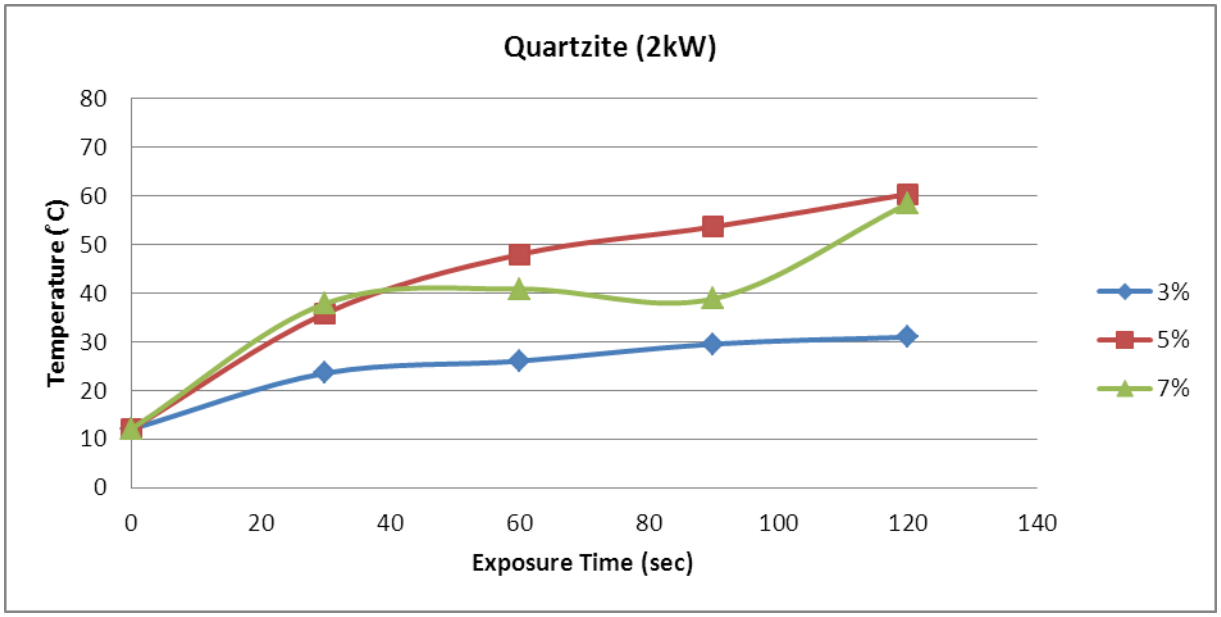

Figure 6.7: Quartzite (Qu) results for varying moisture contents heated at 2kW

Figure 6.4 to Figure 6.7 for virgin aggregates illustrate no significant variation when increasing the moisture content from 5% to 7%. Figure 6.8 illustrating RA illustrates only marginal increase when moisture content is increased from 5% to 7%.

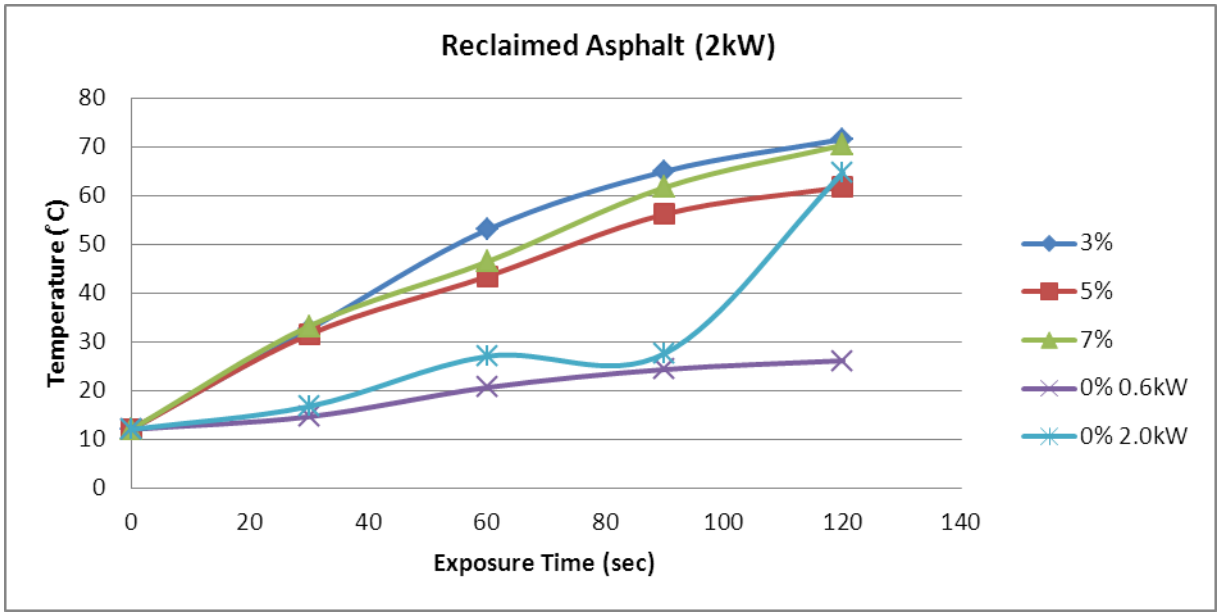

Figure 6.8: Reclaimed Asphalt (RA) results for varying moisture contents heated at 2kW

6.2.3 Sensitivity analysis

Figure 6.9 and Figure 6.10 compare the heating potential over the same time duration at various intensities per aggregate type. No information was recorded for RA at intensities at 6kW at 120 seconds, as the sudden temperature increase could damage the polypropylene boxes and the conveyor belt.

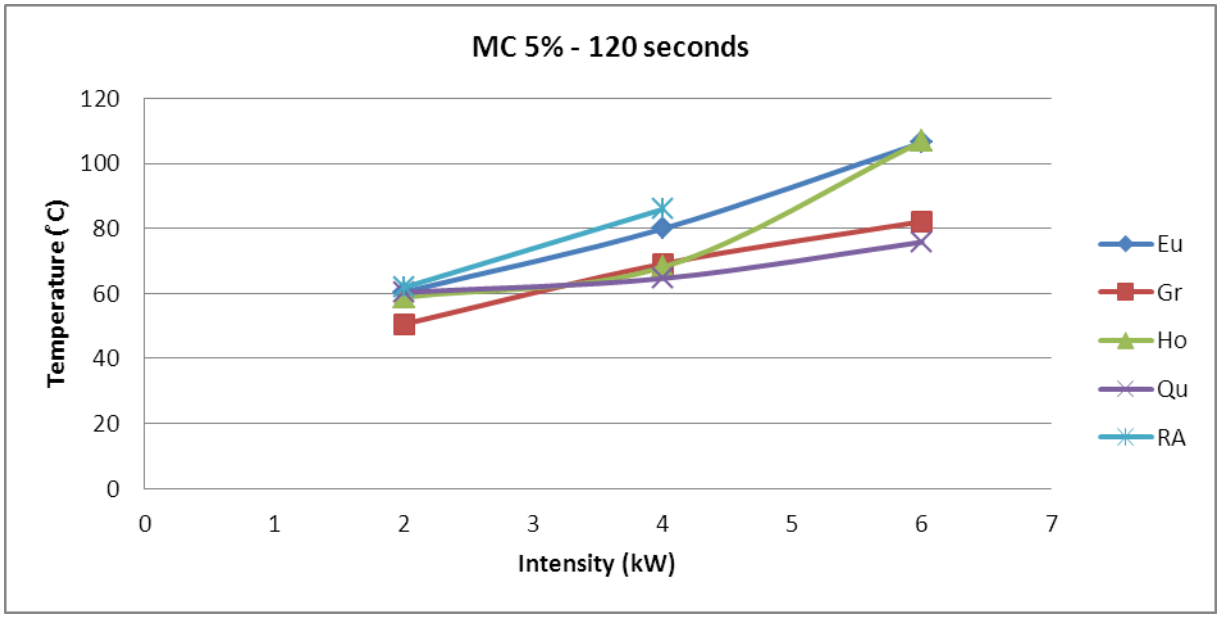

Figure 6.9: Heating comparison of aggregates with 5% moisture content for microwave intensities of 2, 4 and 6kW.

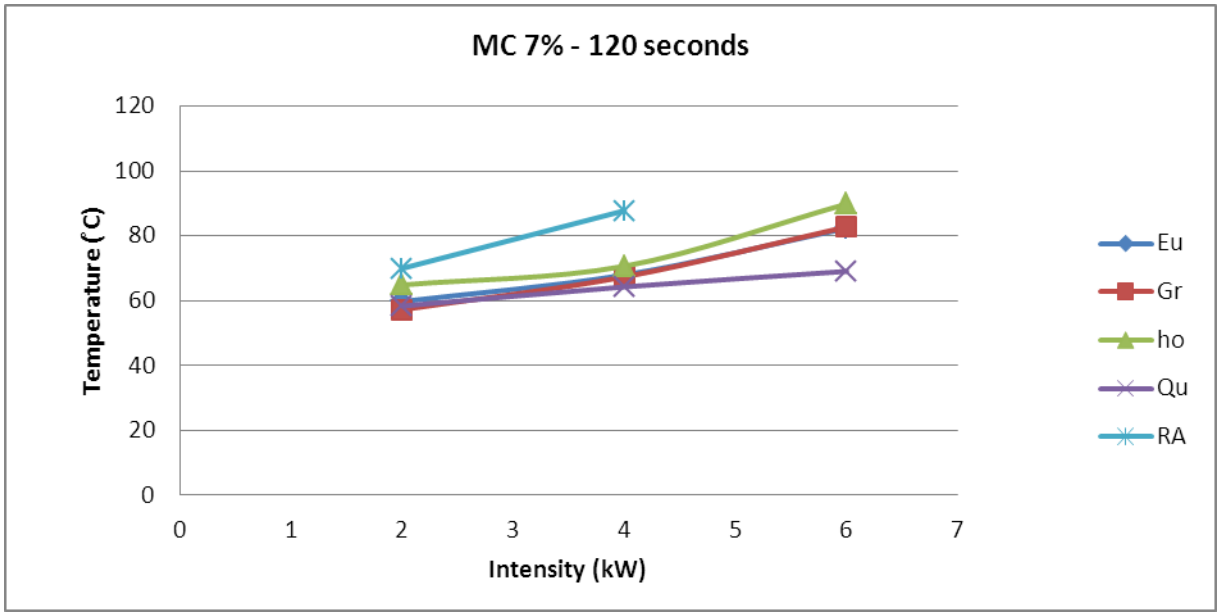

Figure 6.10: Heating comparison of aggregates with 7% moisture content for microwave intensities of 2, 4 and 6kW.

Figure 6.9 and Figure 6.10 illustrate the superiority of RA material over the virgin aggregates in its heating ability. It can also be noted that hornfels and eucrite achieve higher temperatures than granite and quartzite. Once again it can be observed that increasing the moisture content above 5% is not beneficial for maximum heating temperatures achieved.

6.2.4 Intensity versus time duration

Intensities were compared over similar time durations to observe its impact on the heating potential on RA at 5% and 7% MC. This is illustrated in Figure 6.11 and Figure 6.12, where the temperature increases were achievable by double the power intensities.

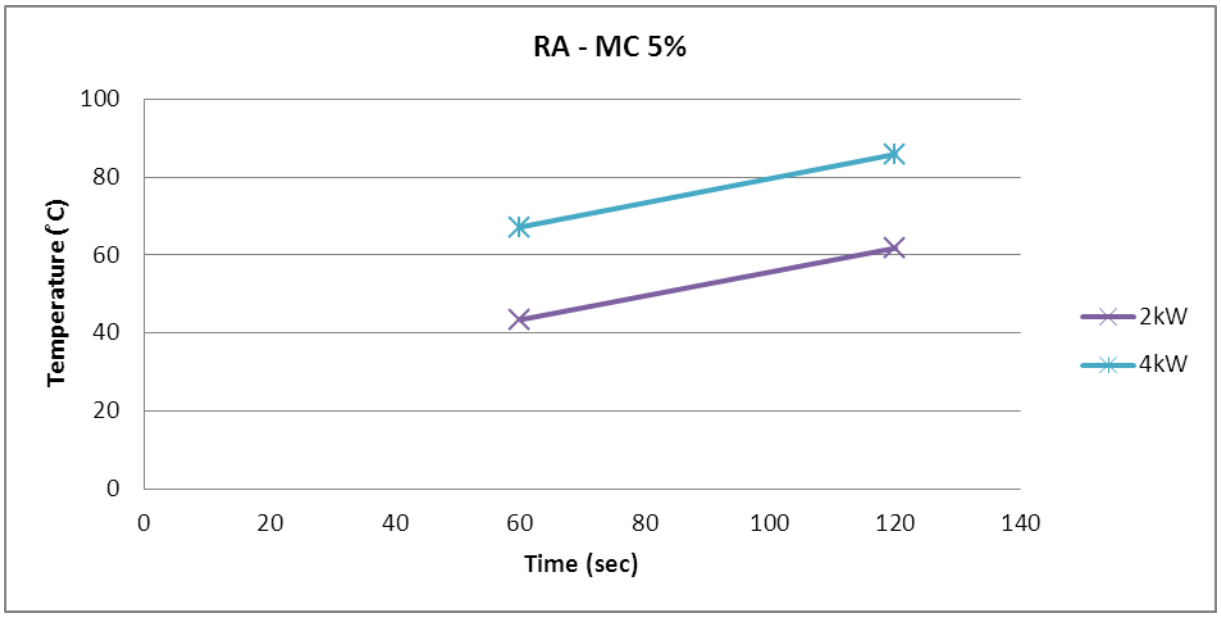

Figure 6.11: Heating comparison of RA with 5% moisture content for microwave intensities of 2 and 4kW

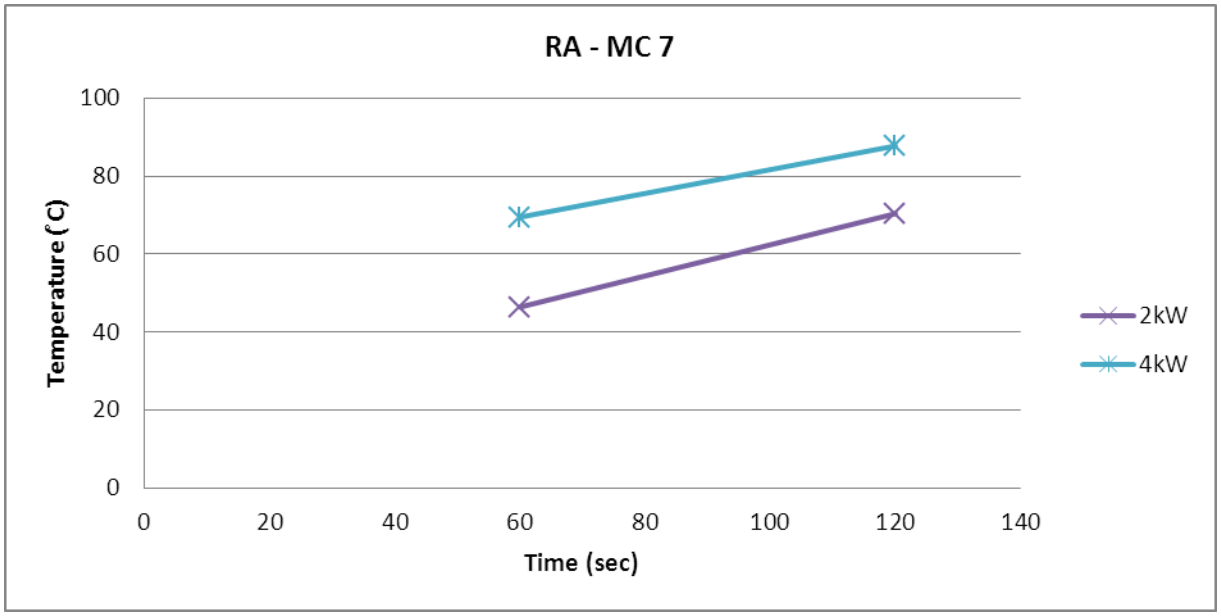

Figure 6.12: Heating comparison of RA with 7% moisture content for microwave intensities of 2 and 4kW.

It was observed that doubling the intensity and using the same time duration did not double the final heated temperature. Doubling the intensity and halving the exposure time does however heat material to a similar temperature.

6.2.5 Heating of Reclaimed Asphalt

RA illustrated similar heating characteristics to the virgin aggregates at moisture contents of 5% and 7%, however at lower moisture contents it heats up rapidly. The rapid heating rates were observed when RA was tested at low moisture contents as illustrated in Figure 6.8.

Figure 6.13 illustrates other additional heating curves for RA heated at low moisture contents. It is apparent that the RA does indeed absorb the microwave energy more efficiently than virgin aggregate samples, even though the moisture contents are low. RA is therefore better suited for microwave heating and will be used in the feasibility calculations.
The reflective power recorded during heating of the materials illustrated in Figure 6.13 was significantly high. The effective forward power (the difference in the set forward power and the reflected power) was recorded to be in the region of 2 to 4kW.

To evaluate the reason for RA's improved heating potential in relation to the other aggregates, heating tests were performed on pure bitumen. In this way it could be determined what the influence of the bitumen was when no moisture is present. The results obtained were not as expected. The temperature increase recorded was minimal.

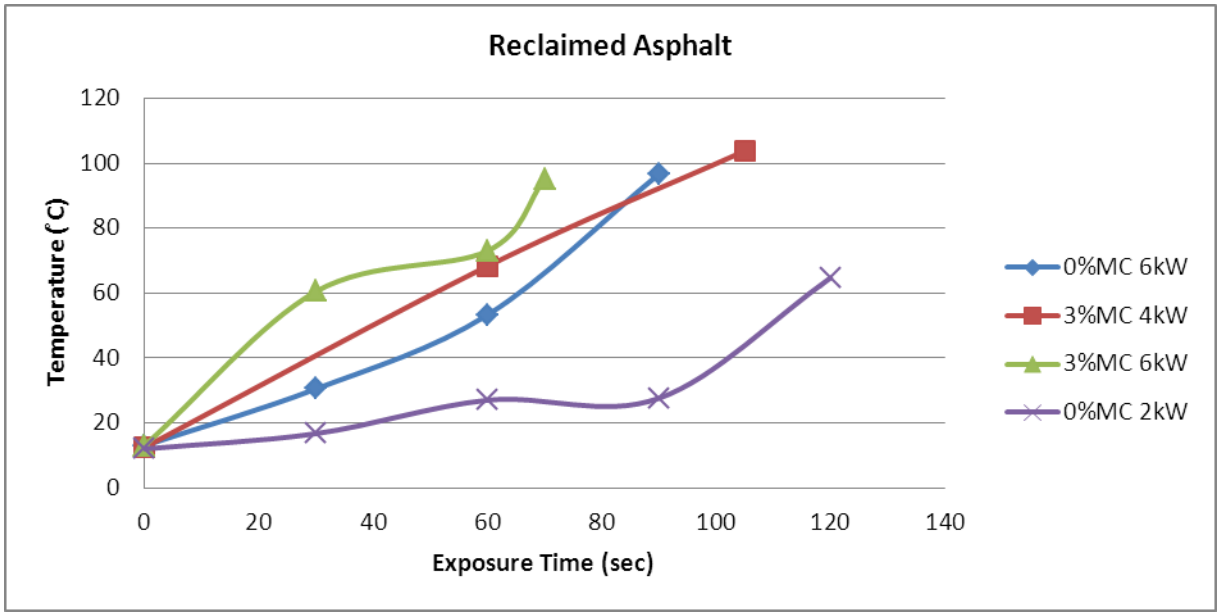

Figure 6.13: Heating results of RA at low moisture contents

6.2.6 Heat dissipation

To evaluate the effectiveness of the microwave heated sample, heat dissipation rates for the microwave heated sample as well as oven heated sample were compared. The RA sample used for the oven test was left in the oven overnight whereas the microwave heated sample was heated for 60 seconds at 6kW power intensity using the 2450MHz unit. It was initially thought that due to the volumetric heating assumption, the dissipation curve for the microwave heated RA would drop off faster as there would be a delay in the heat absorption into the aggregate before equilibrium was reached, provided the heat transfer occurred at a slow enough rate. Figure 6.14 shows that this is not the case and that all the energy had already been absorbed into the aggregate of the RA material immediately after heating. This indicated that not only are the surfaces of the aggregates heated by the microwave after 60 seconds, but the entire stone. This is attributed to the convection of the heat from the moisture on the outer aggregate skin to aggregate stone and not the aggregate loss factor properties.

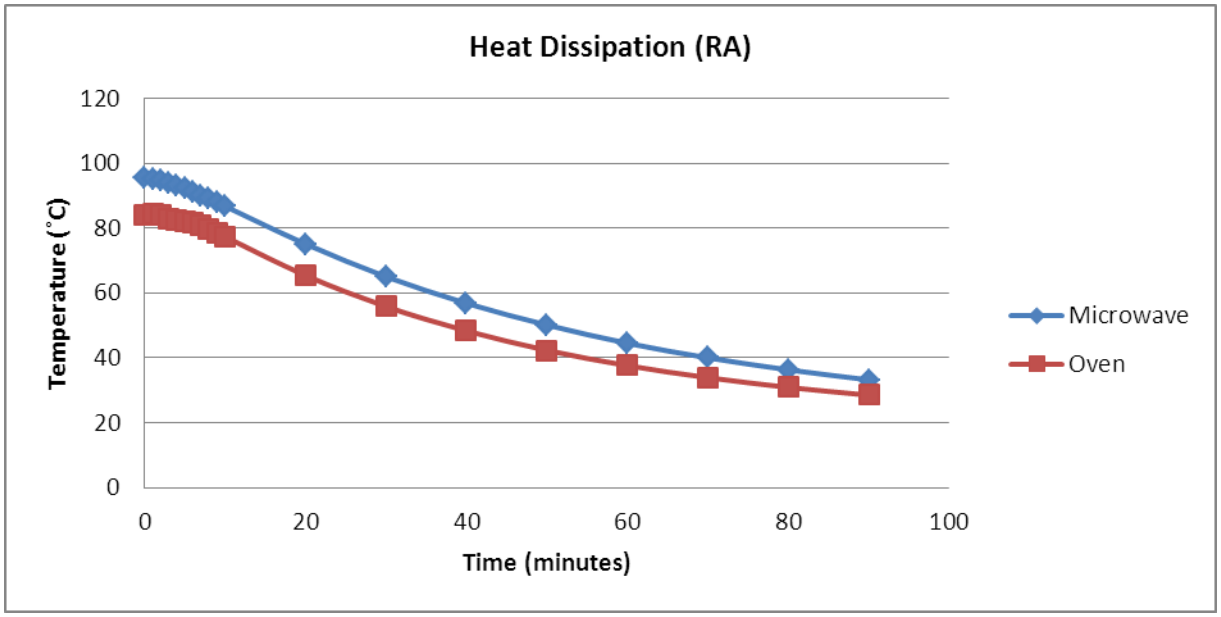

Figure 6.14: Heat dissipation of microwave versus oven heated RA samples.

Realizing that all the microwave input energy was absorbed into the stone after one minute, attention was focused in determining how much energy was used to heat the sample and how quick the energy dissipated into the mix. Factors influencing the rate of heat dissipation are the transfer heat coefficient and the specific heat capacity of the materials in a mix.

6.3 Theoretical evaluation

The concept of preheating the moist aggregates before mixing with bitumen foam is believed to improve the surface energy and improve coating. Post heating after mixing the foamed bitumen on the other hand is considered to be beneficial for microwave heating in that it is hypothesised that the foamed bitumen might further entrap moisture in the mix and improve the heating potential.

6.3.1 Energy requirements

For an ideal volumetric heating system, the rate in rise of temperature in a dry and constant workload is related to the power dissipation in the workload, mass of the workload and the workloads specific heat capacity. This can be illustrated by Equations 11 and 12 for any heating process, irrespective of the nature of the power source.

Batch process (Fixed mass)

$$P = M \frac{dT}{dt} s_p \qquad \text{(Equation 11)}$$

Continuous flow process (Fixed Temperature rise)

$$P = \frac{dM}{dt}\, T\, s_p \qquad \text{(Equation 12)}$$

Where,

P, is the total power (watts) dissipated into the workload

M, material mass (kg)

T, Temperature (°C)

s_p, specific heat capacity of the material

The specific heat capacity (s_p) for various individual materials is readily available. For a mixture however, a weighted average can be used to estimate its specific heat capacity. Although the equations are for dry workloads, they may be adapted by including the latent energy required for evaporation of liquids. The latent heat for the evaporation of water at 100˚C is approximately 2247kJ/kg. The specific heat for the various materials and their combined averages are as follows:

	Virgin Aggregate	0.8 kJ/(kg.K)	
	Bitumen	2.1 kJ/(kg.K)	
	Water	4.1 kJ/(kg.K)	
	Bitumen & Water (50:50)	3.29 kJ/(kg.K)	*(weighted average)*
	RA (5% Water & 5% Bitumen)	1.034 kJ/(kg.K)	*(weighted average)*

6.3.2 Full-scale considerations

The design recycling unit considered for fitting a microwave generator would be a typical Wirtgen KMA220 in-plant mixer. This unit has a production potential of up to 220 ton/hr. The basic heat transfer equation for a continuous flow process as given previously, can be used to evaluate the basic workload heating requirement for a given flow rate on the KMA220.

In assuming that virgin aggregate encapsulated by the bitumen and water in RA is totally invisible to microwaves, the energy required to heat the outer skin of the RA particles only can be calculate for the sample's bulk mass.

With a specific heat of 3,29 kJ/(kg.K) and using a material flow rate of 2,8 kg/s (0,1 x 27,72 kg/s (100ton/h)) and a temperature rise of 30 ˚C, it is evaluated that a total minimum energy of 277 kW or 277kJ/s has to be absorbed to heat the bitumen-water phases. This is illustrated in Figure 6.15. This energy does not take into account any latent energy requirement should water evaporation occur.

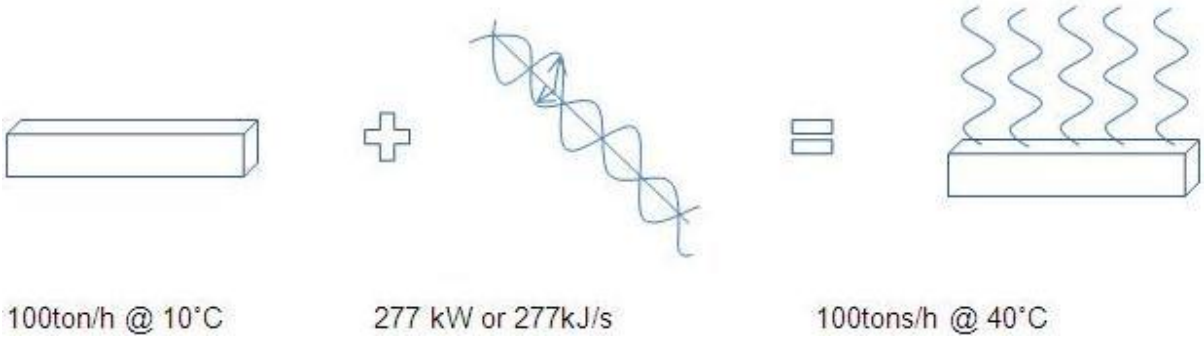

Figure 6.15: Basic energy requirements to selectively heat bitumen & water phases at 100ton/h flow rate (evaporation ignored)

6.3.3 Industrial microwave generators

Microwave power units are mainly available at various intensities in two frequency ranges, namely 2450MHz, and 915MHz. The higher intensities are predominantly available for the 915MHz frequency band with intensities of up to 200kW. It is therefore evident that one microwave power unit cannot heat the material sufficiently, but could manage if the material flow rate was reduced by 200kW/277kW, i.e. reduced to 72 tons/h. The potential of adding multiple application units to operate simultaneously is possible, but the energy to power these units will be limiting.

The microwave energy absorption into a workload is dependent on numerous material properties. These properties will affect the energy efficiency for a given workload. Provision should also be made for reflective power that is essentially energy lost during the process as well as energy absorbed by the latent heat requirement.

6.3.4 Laboratory assessment

During the preliminary testing, a 65˚C rise in temperature of was observed after 60 seconds at 6kW power intensity on a stationary RA sample with a moisture content of 5%. The laboratory microwave applicator size can house a sample with a maximum cross section of 90mm x 90mm with the applicator length being 300mm. The wet sample used however was 50mm in height and using a loose packing density of 1300kg/m^3, the sample mass at a given instance in the applicator is approximately 1,7 kg. The initial sample temperature being 10 ˚C heated to a 75 ˚C final average temperature.

It was recorded that an average reflective power of 1.5kW was observed during heating. This means that only 4.5kW was effectively used to heat the entire sample. The reflective power loss is attributed to the air and sample interface and the geometry of the microwave applicator. The average energy input was therefore 270kJ.

The amount of drying experienced during the 60 seconds was recorded to be 4.18% by mass with the initial moisture at 6.35%. Taking the latent heat requirement into consideration, the theoretical energy consumption concurs closely with the energy input.

6.3.5 Full-scale application

In microwave power applications, the energy output recorded can be linearly scaled when comparing the ratio energy intensities applied. The KMA 220 conveyor belt system dimensions were considered during this volumetric scaling. Consider a 1,7kg sample heated at 6kW experiencing a temperature raise of 30˚C after 30seconds. This equates to 0,057 kg/second moving along the conveyor with a microwave intensity of 6kW and the temperature being raised by 30˚C. Noting that microwave power units of maximum 200kW are readily available, a ratio for the volumetric output will therefore be 200kW/6kW. The final processing rate at full scale is now 1,9kg/s or rather 6.8 tons/hour.

This production rate seems to be much less than previously calculated 72 ton/hour using the energy requirement equation. Factors such as reflective power, latent heat and loss due to of heat dissipation into the aggregate are responsible for this discrepancy. The 6.8 ton/hour value would be a realistic assessment, because reflective power, latent heat loss through evaporation and heat dissipation are a reality in full-scale production. Recorded rates of reflective power are included, but these are dependent on the design of the applicator and will vary.

6.3.6 Heat dissipation

The evaluation in effectiveness of the microwave heated sample previously illustrated that that complete heat dissipation occurred within the 60 seconds of microwave irradiation. The rapid heat transfer of microwave energy required attention in determining how much energy was used to heat the sample and how quick does the energy dissipate into the mix.

To consider the energy implications of heating the bulk of the material, the general specific heat of the entire RA sample (water + bitumen + aggregate) with 5% bitumen and 5% moisture content by mass equates to 1.034 kJ/(kg.K). Using a material flow rate of 27.72 kg/s (100ton/h) and a temperature increase of 30 ˚C, a total energy consumption of almost 1MW is estimated. If the rate of heat dissipation is indeed rapid, then the assumption of only heating the outer skin of the aggregate is not possible.

6.3.7 Heat transfer mechanism

The specific heat of the RA (water + bitumen + aggregate) was averaged to be 1.034 kJ/(kg.K). As previously observed during testing, the power required to heat the 1.7 kg sample at 1.1˚C/sec (65˚C/60sec) is 4.5kW.

With aggregates having a significantly lower loss factor than the water and bitumen, the heat absorbed by only the aggregate could be assumed to be negligible. The power is therefore only absorbed by the water and bitumen film around the aggregate. Using the specific heat value to 3.29kJ/(kg.K) for the water and bitumen combination (10% by mass), latent heat energy is ignored and Equation (12) is used to obtain a heating rate of 3.57˚C/second. Although heating the sample may not be linear in reality, this assumption is used as a rough indication. The oven and microwave heat dissipation comparison indicates that although the bitumen/water rises at a rapid rate, the energy is however dissipated into the aggregate over the 60 second period. The focus is now on estimating the rate at which heat is absorbed into the aggregate.

The proposed sample being heated contains a grading curve of a high quality graded crushed stone (G2) type material and contains various stone sizes. To calculate the heat transfer into the aggregate, an average stone size was selected. With half the stone sizes by weight being below the 4.75mm sieve, the 4.75mm size was chosen as the average. Equation 13 is based on the basic heat transfer concept for unsteady flow and is defined as:

$$\begin{pmatrix} Increase\ of\ the\ internal \\ energy\ of\ the\ solid\ over \\ the\ time\ interval\ dt \end{pmatrix} = \begin{pmatrix} heat\ flow\ into\ the\ solid \\ through\ the\ outer\ surfaces \\ over\ the\ time\ interval\ dt \end{pmatrix}$$

$$\rho\ V\ s_p\ dT = Q(t)\ dt \qquad \text{(Equation 13)}$$

Where,

ρ, material density

V, material volume

T(t), material temperature

Q(t), total rate of heat flow in the body

ρV is equal to the total mass of the body and indicates that mass is directly proportional to heating rate. Smaller sized aggregates would heat up faster to the desired temperature, thereafter radiating the access heat to the larger aggregates.

The approximate analytical solution for heat transfer to the centre of the sphere is defined by Equation 14,

$$\frac{T_0 - T_\infty}{T_i - T_\infty} = A_1 e^{-\lambda_1^2 \tau} \qquad \text{(Equation 14)}$$

for $\tau > 0{,}2$ where,

T_0, temperature of the sphere after a given time

T_∞, temperature outside, surrounding the sphere

T_i, initial temperature of the sphere

A_1 and λ_1 are both functions of the Biot number (dimensionless heat coefficient, hL/k)and can be obtained with Heisler charts

τ is a dimensionless time value (Fourier number) equal to $\alpha t/L^2$ of the body

An exact number for the heat transfer coefficient for water varies considerably, 500 – 15000 W/(m^2.K). A conservative value of 500 W/(m^2.K) was adopted for the transfer calculation as choosing a low value would under estimate the rate of heat transfer. This is very conservative. The bitumen film was considered negligible as even though it would have a very low heat transfer coefficient value, its film size is negligibly thin.

Hence for Equation 14 above, considering the first instance (the first second - 1second) of microwave application, $T_i = 10^{\circ}C$, $T_\infty = 10 + 3.57 = 13.57$ and $T_0 = 10 + 1{,}1 = 11.1$. For a 4,74mm sphere, τ = 0.3, therefore the heat transfer can be calculated to be close to complete within 2 seconds. As time progresses, the external temperature continues to rise and therefore increases the temperature gradient between the centre and surface of the sphere. This gradient will cause an increase in the heat absorption rate until a possible equilibrium is reached.

It can therefore be seen that at no point will the RA particles have a higher external temperature compared to its internal temperature for long enough before being exposed to the foamed bitumen.

6.4 Primary investigation

The primary investigation uses the “preliminary heating” and the “theoretical investigation” as a starting point for the target temperature during the HWF mix production preparation of the various test samples.

To heat the BSM-foam samples to by 30 ˚C and maintain a production rate of 6.8ton/hour at full scale (see theoretical investigation, section 6.3.5), the feed through the laboratory conveyor applicator would require an exposure time of almost 30 seconds whilst using an intensity of 6kW. By reducing the exposure time to 12 seconds, the production rate can be increased to 25ton/hour although at a reduced temperature increase.

During the preliminary investigation, it was noted that doubling the exposure time did not necessarily double the final heating temperature of the aggregate. In fact the final temperature was significantly less than double. The reciprocal would mean that halving the exposure time, would not suggest a large reduction in the final heating temperature. It was therefore decided to produce an additional HWF mix at half the exposure time, 6 seconds. This relates to an in-field production rate of 50ton/hour.

The rapid heat transfer of the energy between the moisture and the aggregates directed the focus of the HWF production to the post-heating method. This entails heating the BSM-foam cold mix prior to compaction. It was anticipated that even though the exposure time is significantly reduced, sufficient energy from the volumetric heating system would ensure the moisture would be heated in the vicinity of the bitumen’s softening point, a sufficiently low viscosity to promote cohesion. An additional method of pre-heating the aggregate blend before mixing with foamed bitumen was also be evaluated. Aggregates were fed

continuously through the conveyor system to ensure uniform temperature increase during heating.

Figure 6.16 provides a summary of the test sample preparation and mix variables. A total of 27 ITS samples were manufactured for testing of which 9 were conditioned in a water bath for TSR tests. 3 ITS samples were prepared per mix to observe consistency due to the tests lack of repeatability. The ITS results recorded were averaged.

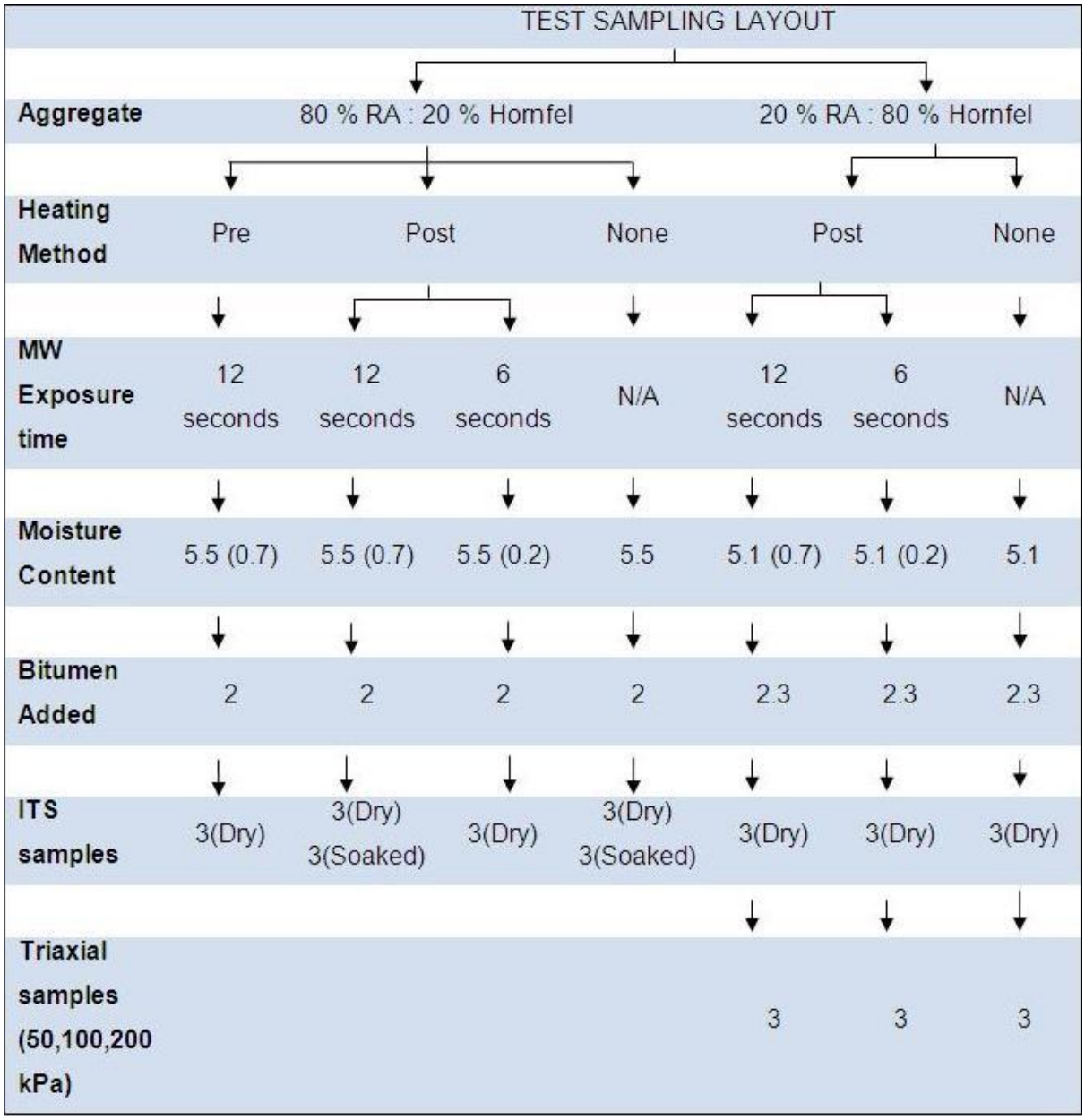

Figure 6.16: Primary test layout

It was initially postulated that the 80RA blend was going to outperform the 20RA blend. The ITS results indicated differently as will be illustrated later in this Chapter. Triaxial samples

that were initially to be produced for the 80RA blend, was cancelled and triaxial samples for the 20RA control and post heating mix were incorporated. Records of the heating results during the Primary investigation are presented in Appendix D.

6.4.1 ITS results

6.4.1.1 Heating of sample blends

The recorded temperature increases and compaction temperatures are presented in Figure 6.17 for the two aggregate blends over the range of heating methods. The mix type, as displayed on the horizontal axis, depicts the BSM-foam control mix (Control) at which no heating was undertaken; the short duration exposure (6 seconds) post-heating method (Low); the long duration exposure (12 seconds) post-heating method (High); and the long duration exposure (12 seconds) pre-heating method (Pre-heat).

The use of the lower exposure times of 6 and 12 seconds indicated improved temperature gains than those during the Preliminary investigation during extended heating. Temperature gains of 12°C and 25°C was recorded for the two lower exposure times respectively. These equate to a temperature rise of approximately 2°C/second. This value lies between those recorded during the Preliminary investigation (1.1°C/second) and those theoretically calculated for the heating of the water and binder phases only (3.6°C/second). This could be a result of numerous reasons. Two plausible reasons could be that lower moisture loss through evaporation occurs whilst heating at shorter durations and that the added binder could encapsulate some moisture, therefore benefiting from the selective heating mechanism.

The two upper most curves in Figure 6.17 indicate the steady rise in temperature for the control mix and two heating durations. This contradicts the previous assumption that halving the heating time duration would still result in a temperature increase of more than half. This discrepancy between results from the preliminary investigation and those of the primary investigation suggests that there are many more factors to be taken into consideration in determining final temperatures when using microwave heating. The final heating temperature is also 5°C less than what was calculated in Section 6.3.2. This could be due to the handling and time delay while waiting for the entire batch to be fed through the microwave applicator.

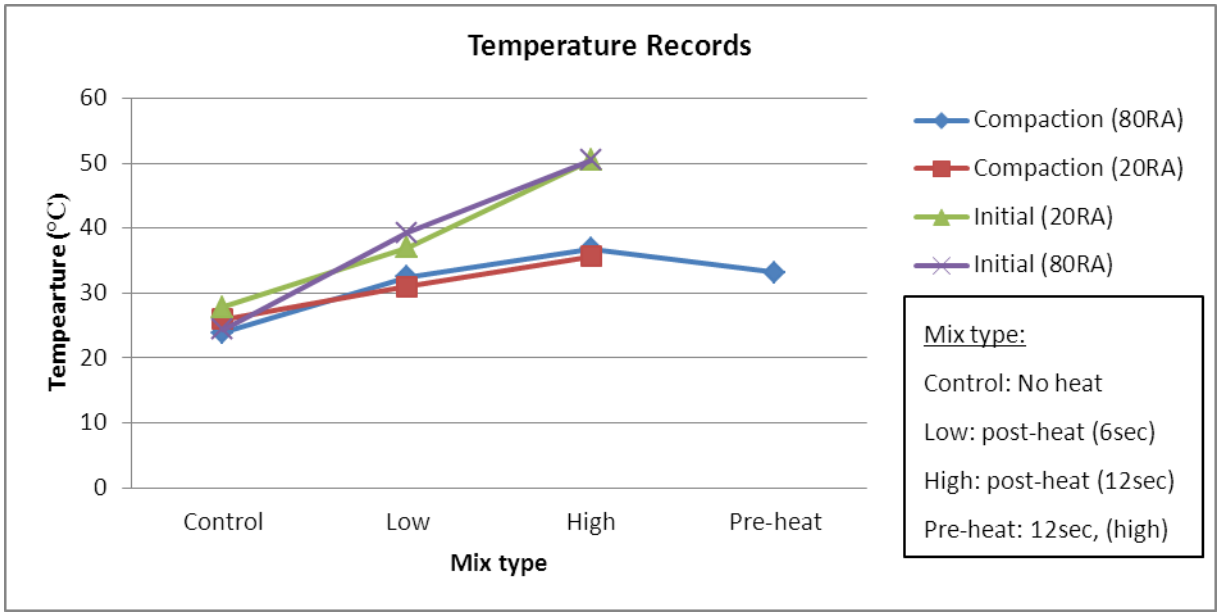

Figure 6.17: ITS heating results and temperatures at compaction for 80RA and 20RA blends.

There is a considerable drop in temperature between heating to the time of compaction (15°C for the highest heating temperature achieved). Numerous precautions were put in place such as using insulated container and maintaining a steady temperature for the mixer and moulds during mixing and compacting respectively, to mitigate temperature loss. Considering the temperature losses, these measures were however not adequate. The maximum time between, when the aggregate was initially heated, to when the last of 3 samples per batch was compacted extends to 12 minutes. Laboratory conditions and apparatus procedures does not allow for this time delay to be reduced. It was further realised that during the time delay between heating and compaction, heat transfer still continued to reach equilibrium, considering the initial volumetric heating encountered primarily by the water surrounding the bitumen and aggregate. This highlights, again, the temperature differential between centre and surface of the aggregate, which underlines the importance of the continuity of the mixing process to optimise benefits from higher surface temperatures.

The thermodynamics are such that small delays (experienced within the laboratory in relation to full scale production) could have significant implications on the mix performance as a result of heat loss. Up-scaling of this technology has been shown in the past (van de Ven *et. al*, 2007) to not follow linear trends, as critical mass effects play a role. The experiences documented by van de Ven et. al. (2007) would suggest that up-scaling would benefit the production material's heat retention; with possible reduction in critical moisture content for optimum performance of the HWF material.

The maximum temperature for the pre-heated mix was not recorded. It was observed after heating, that steam was escaping from the aggregate as the material was excited by the microwave. There was however great pressure to get the heated aggregate into the WLB-10 mixer and thereafter to the compaction equipment in the least amount of time, which resulted in the temperature reading to be overlooked. The lower recorded final compaction temperature of the preheated aggregate in relation to the post heated mixes could also be a result of additional time required for mixing.

6.4.1.2 ITS test results

The ITS test results are summarized in Figure 6.18 below for the two aggregate blends over the range of heating methods. The aggregate mix containing the high RA content did not gain any improvement for the various temperature increases. This might be due to the temperature increase not exceeding that of the residual RA's softening point of 61°C throughout the mix.

The aggregate blend containing 80% crushed aggregate and slightly more binder (0.3%) experienced an increase in tensile strength of over 100%. The increase is further not affected by the slight reduction in temperature when the exposure time was halved. No samples were produced for the pre-heating method with 80% crushed aggregate blend.

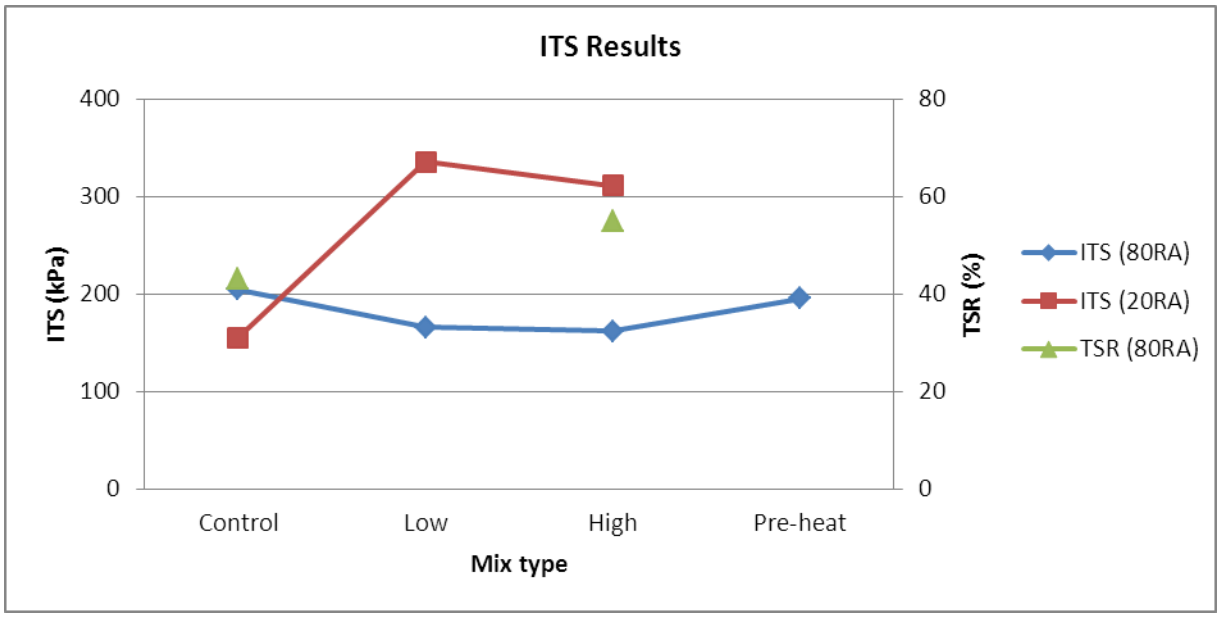

Figure 6.18: ITS results of BSM-foam and HWF for both 80RA and 20RA blends

The TSR results were conducted for the 80RA blend. The TSR result for the HWF mix is higher by 27%. TSR increase is however misleading, as the ITS strength results for both the

HWF and BSM-foam were similar and the cause of the increase is a result of the low dry strength for the HWF mix.

The TG2 (2009) indicate that the 150mm ITS samples require a tensile strength of 175kPa to be classified as BSM1. The microwave heated 20RA samples exceed this value two fold. The control mixes and 80RA heated samples marginally fall short of this minimum criteria. It should be noted that the sample height used during this study was limited to 75mm as explained in Section 5.4.6, and the standard height is normally taken as 127mm when evaluating the BSM-foam tensile strength during the Level 2 mix design.

6.4.1.3 Compaction results

The compaction test results are summarized in Figure 6.19 below for the two aggregate blends over the range of heating methods. The maximum dry density investigation of the blends indicate the less coarse nature of the 20RA blend results in a lower material density than the 80RA blend under the same compaction effort. The 80RA blend however did not increase its density much after microwave heating.

The 20RA blend appears to gradually increase its compaction density as the compaction temperature increases. This is not uncommon for bituminous materials, and generally results in an improvement in engineering properties.

In light of the gradual increase in compaction density for the 20RA blend at the shorter heating duration, the drop in compaction density of the 80RA blend might be from the aggregate packing arrangement during compaction.

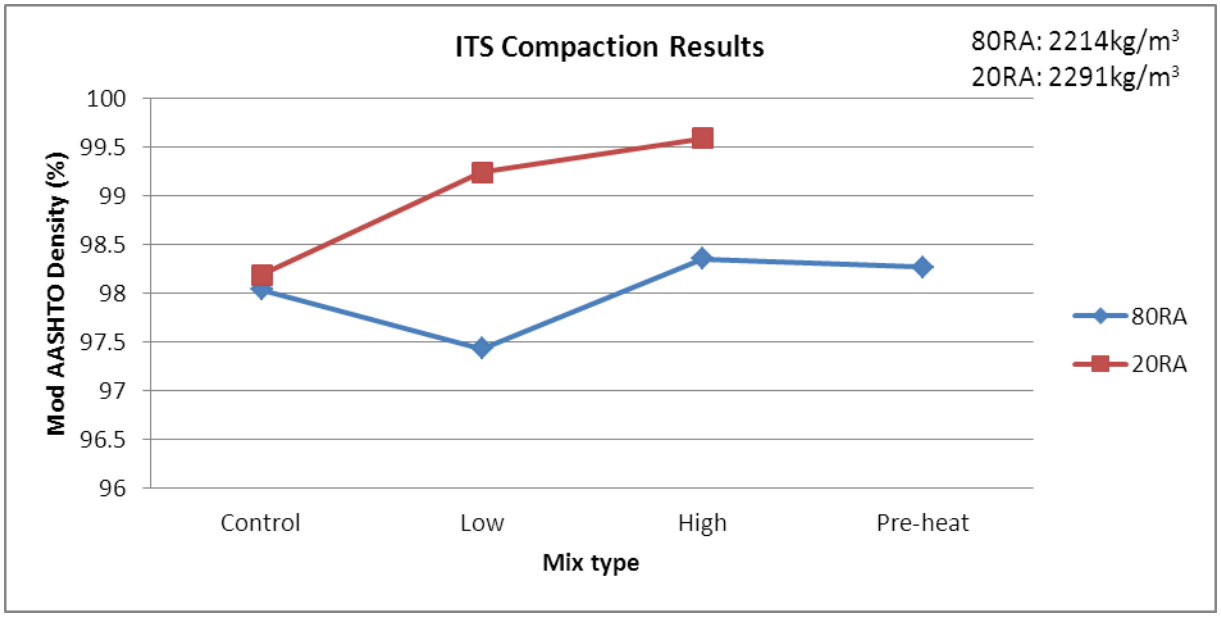

Figure 6.19: Compaction results of BSM-foam and HWF ITS specimens using 80RA and 20RA blends

6.4.1.4 Sample moisture contents

The MC results for the samples during compaction and after accelerated curing are summarized in Figure 6.20. The two upper most curves are the compaction moisture contents. These are close to those determined during the dry density and OMC analysis. The two lower curves are the recorded moisture contents after the accelerated curing. It is evident that the moisture contents for the microwave heated 20RA blends after curing are less than half that of the 80RA blend.

The moisture variation could be due to a combination of factors. The 20RA blend might benefit from the increased temperature of the samples after compaction and during curing which results in higher moisture loss for the heated samples. In the 80RA blend, however, the RA might contain trapped moisture and not benefit from the volumetric heating to release this moisture. A reduction in moisture after compaction and during service life of a bituminous stabilized material is beneficial. The accelerated curing method is designed to achieve an equilibrium moisture content of 50% of the virgin aggregate OMC. The control mixes indicate that the resultant moisture content were well below the equilibrium moisture content. Plotting the MC versus ITS strength on a log scale indicates an exponential relationship as indicated in Figure 6.21.

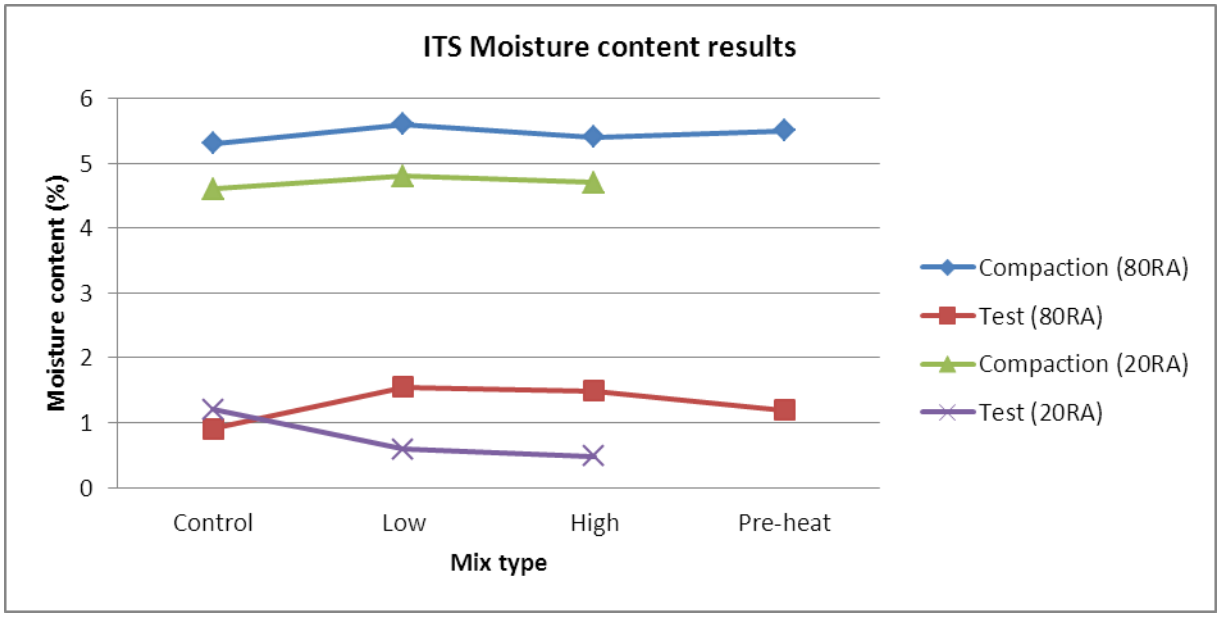

Figure 6.20: MC results for the ITS specimens during compaction and after accelerated curing

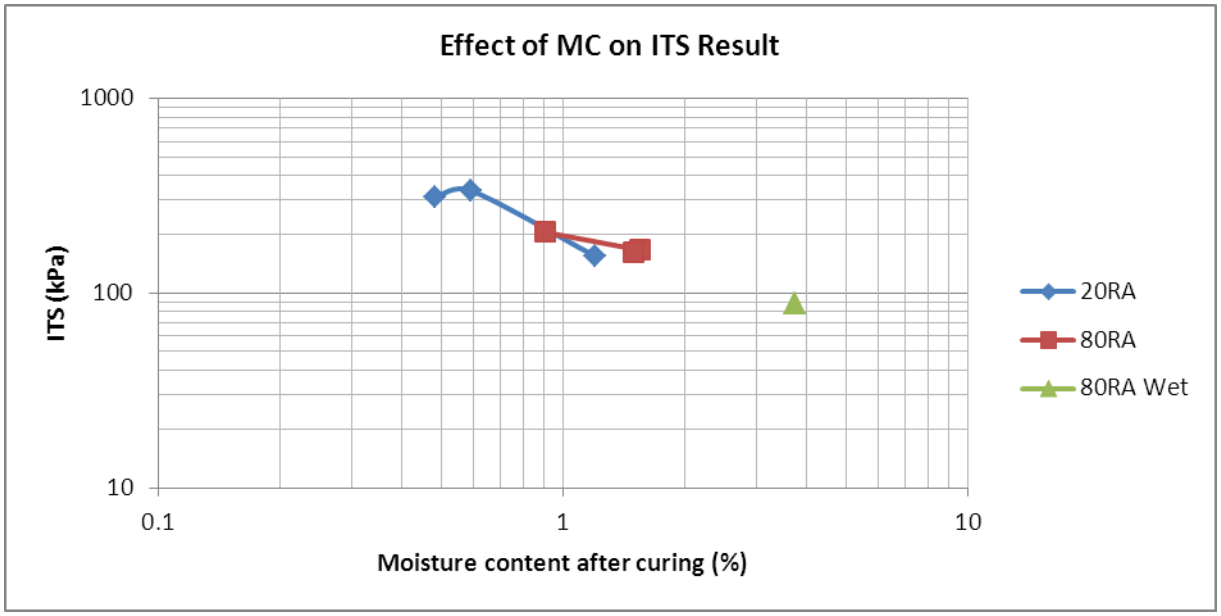

Figure 6.21: Relationship between ITS strength and moisture content

6.4.2 Triaxial results

It was initially envisaged that the 80RA samples would respond best to the microwave heating to produce HWF mixes. The ITS results however indicated that the 20RA samples performed better. Triaxial test samples were therefore produced, using the 20RA blend. One sample was manufactured per batch due to the size of the WLB-10 mixer and the time required to compact the triaxial samples in 5 layers.

A few triaxial test samples for the 80RA were produced though the testing of these samples were not successful. The samples failed prematurely and fine stress cracks were witnessed. It appeared that the samples were brittle.

6.4.2.1 Compaction versus temperature

The triaxial compaction density results in relation to temperature are illustrated in Figure 6.22. The temperature reduction between the heating the mix to compaction shows a similar trend as observed with the ITS samples. The vibratory hammer's cold top plate and base also reduces the samples temperature during compaction of the recommended 5 layers per sample.

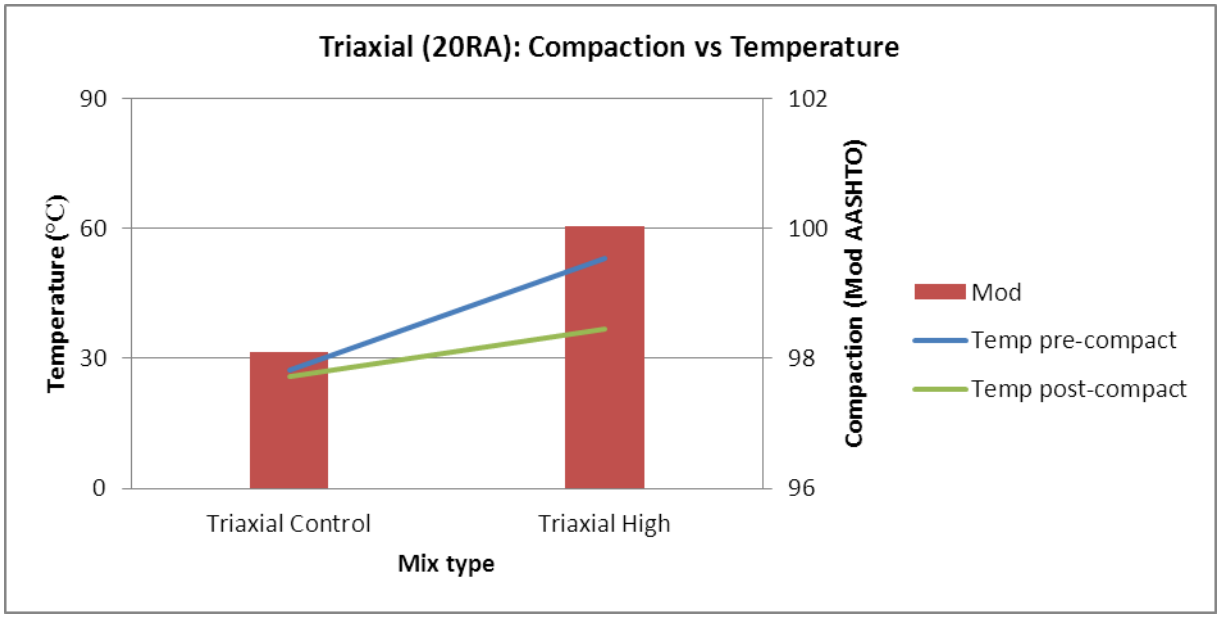

Figure 6.22: Triaxial compaction density results in relation to heating and compaction temperature

The increased temperature of the HWF mix resulted in the triaxial densities of 100% to be achieved. It was noted during compaction that even though the same MC was successfully used as for the HWF mix ITS samples, excess pore water seeped out at the bottom of the steel moulds during the compaction of the 5 layer for the triaxial samples.

6.4.2.2 Moisture content

The moisture content results in relation to time of compaction and time of testing are illustrated in Figure 6.23. The MC at the time of compaction is in the region of the OMC for the BSM-foam control mix and approximately 0.6% lower for the HWF mix. This indicates that even a reduction in MC of 0.6% still generated excess pore water as mention in Section 6.4.2.1.

The MC for the HWF mix in relation to BSM-foam at the time of testing displays the same trend as that encountered during the ITS tests. This meant that the moisture content for the HWF is less than half that of the control mix after the accelerated curing.

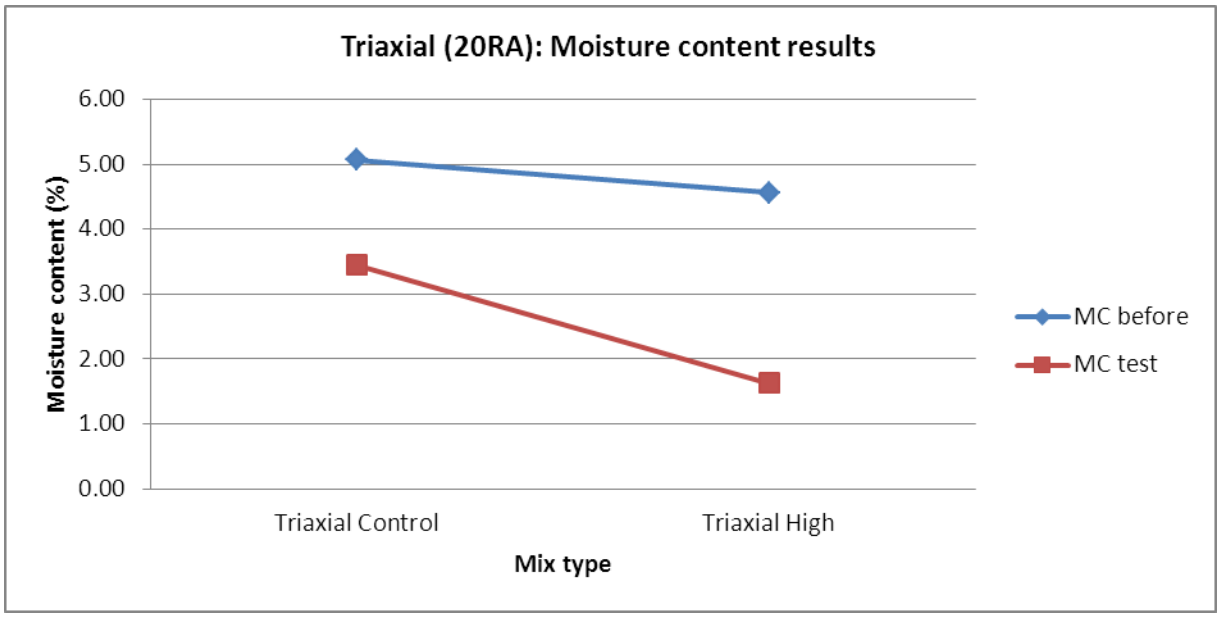

Figure 6.23: Moisture content results as recorded at time of compaction and after testing

The reduced MC for the HWF 20RA blend in relation to the BSM-foam control mix after the accelerated curing would benefit early in situ material strength gain of a compacted layer. This concept is illustrated in Figure 6.24, whereby the critical compaction temperature for the possibility of accelerated moisture reduction is set to 35°C as recorded during compaction in this study. The rapid moisture reduction could similarly reduce the time required for strength gain, before opening to traffic and thus indirectly reduce road user costs.

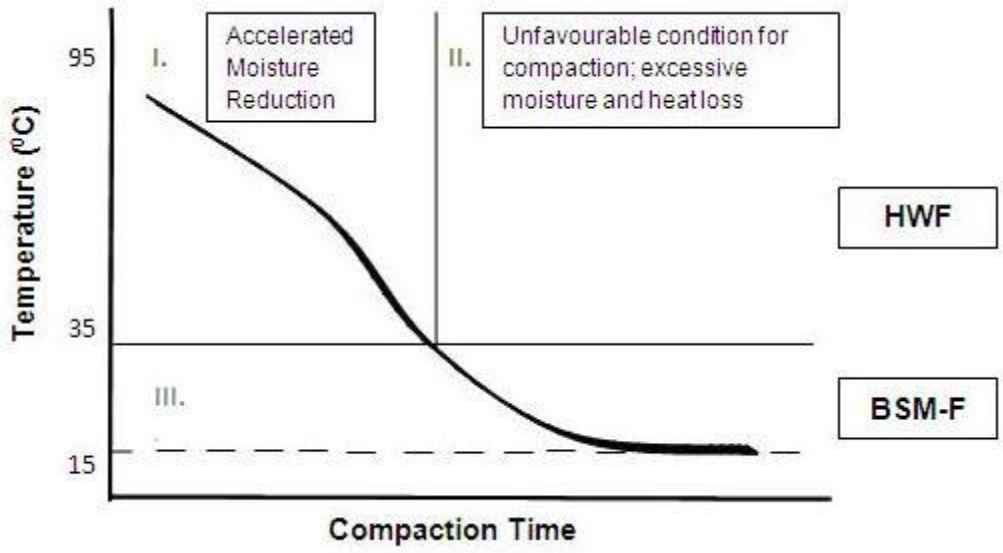

Figure 6.24: Schematic representation of minimum temperature and maximum duration before compaction to perceive best results for HWF based on moisture contents

6.4.2.3 Triaxial test results

The Mohr-Coulomb shear stress curves for monotonic triaxial test results are summarized in Figure 6.25 and Figure 6.26 for the HWF and control mixes. Figure 6.27 provides a comparative indication of the differences in shear properties between the BSM-foam control mix and the HWF mix. The monotonic triaxial curves for the various confinement stresses are presented in Appendix D.

There is approximately 15% increase in the cohesion of the HWF over that of the BSM-foam control mix with the friction angle marginally increasing. These results for the HWF mix is unexpected and not as Jenkins (2000) had obtained. The HWF production principal taken by Jenkins (2000) was to pre-heat the aggregate. During this study, post-heating was considered more viable using microwaves based on the heat transfer rates and energy requirements. As previously indicated, microwave heating technology become feasible when its selective heating ability is exercised.

Jenkins (2000) recorded a significant raise in cohesion and a reduction in the friction angle when tested at 25°C. The variation in the results of this study was a result of the compaction temperature which is 60°C less than that of Jenkins (2000). This low compaction temperature is a result of low initial rise in mix temperature before compaction and the heat

loss between heating and compaction. Jenkins (2000) also used 2.5% more binder during the manufacturing of his HWF mixes.

The added moisture required for the HWF mixes would have had a marginal effect on the binder's dispersion when the post-heating method is used. The method of particle coating also differs between pre- and post-heating. With pre-heating as exercised by Jenkins (2000), the reduced energy gradient between the hot foamed bitumen and warm aggregates improves particle coating. With post-heating, the initial particle coating, as achieved during mixing, is anticipated to also increase. This would occur through selectively heating the moisture which in turn softens the binder to promote particle coating. The selective heating of the moisture further promotes evaporation which aids particle coating.

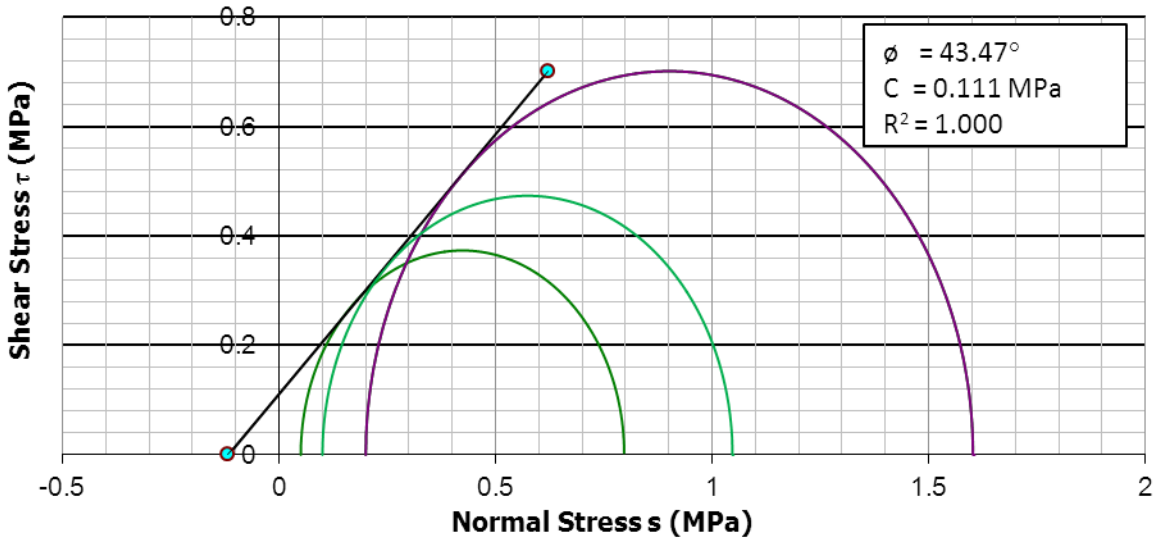

Figure 6.25: Mohr-Coulomb shear stress curves for 20RA control mix

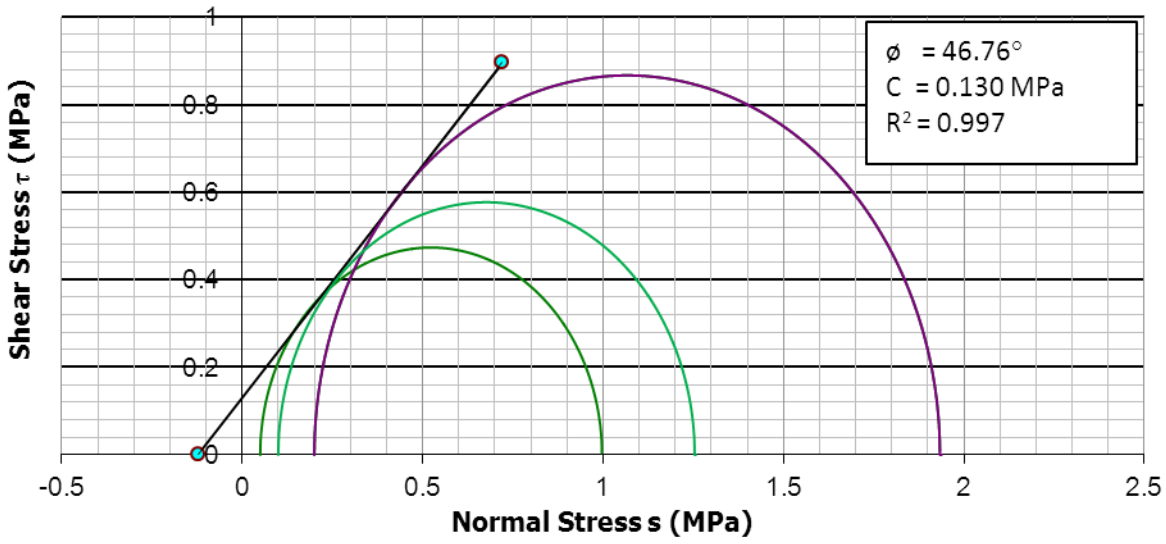

Figure 6.26: Mohr-Coulomb shear stress curves for 20RA HWF mix

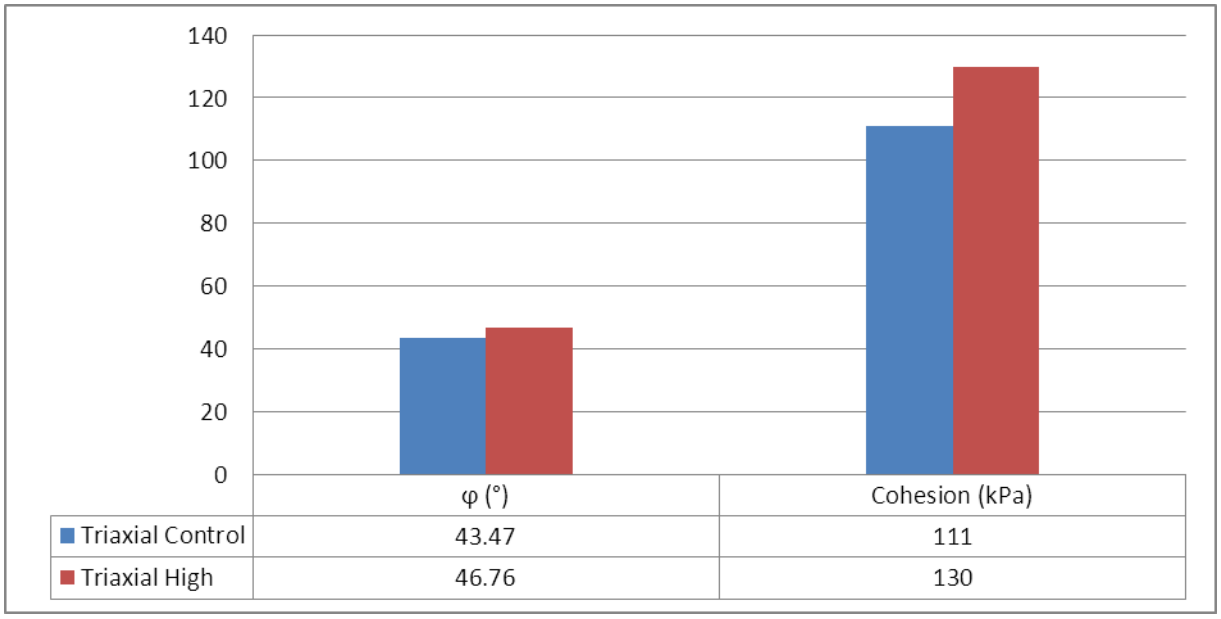

Figure 6.27: Cohesion and Angle of internal friction results for the BSM-foam control and HWF mix

CHAPTER 7: PAVEMENT ANALYSIS

7.1 Introduction

The previous chapter discussed the shear properties obtained using the monotonic triaxial for the HWF and BSM mixes. This chapter aims to evaluate and compare these properties by analysing the stress and strain conditions that are to be experienced under normal loading.

The stress and strain state of a pavement layer is usually calculated by means of a linear or non-linear elastic multilayer program. Elastic multilayer programs, however, have certain limitations in predicting the stress and strain accurately. These limitations can be overcome by using more complex programs that make use of finite element methods. The use of complex modelling techniques is, however, is outside the scope of this study.

A materials dynamic property is essential in predicting performance under loading in a pavement structure. The testing of dynamic properties of the HWF material is outside the scope of this investigation and these material properties were therefore sourced from various other academic papers where the materials tested were similar by definition. It is noted that slight variation of factors such as binder type, binder content and aggregate gradation, affect the bituminous stabilised materials performance.

Estimation of a pavement layers performance for a given material, is evaluated by means of fatigue models based on stress and strains such as the Wohler model or transfer functions. Various fatigue models do exist for HMA and BSM-foam, however, HWF is a relatively new concept and therefore no model is currently available. HWFs broad range of the classification of ranges from completely coated mixes to effectively stabilised mixes, depending on the mixing temperature, aggregate grading and bitumen properties to name a few, which further decreases the probability of finding a similarly suited model for HWF.

In light of the limited availability of HWF fatigue models, the deviator stress ratio curves for BSM-foam will ultimately be used to evaluate and compare the BSM-foam and HWF materials. The estimation of HWF critical deviator stress ratio, the boundary at which accelerated deformation occurs, will be estimated by super imposing a HMA critical limit for accelerated deformation on to that of the BSM-foam's deviator stress ratio curves.

The critical points of interests for discussion when analysing the stresses and strains in the pavement structure for structural capacity are as follows:

- Horizontal tensile strain at the bottom of the asphalt layer
- Principal stresses in the BSM layer
- Horizontal strains in bottom of the BSM layer
- Vertical strain in the top of the subgrade.

7.2 Critical stress limits

Jenkins (2000) and Ebels (2008) produced templates for permanent deformation modelling of BSM-foam for various aggregates and binder contents. These templates indicated critical limits based on deviator stress ratios using dynamic triaxial tests. The maximum critical stress ratio limit was calculated by Jenkins (2000) to be 55% for BSM-foam material with less than 4% binder and no active filler. It is further noted that the pavement industry has conservatively adopted a critical stress ratio of 45%. The results were graphically illustrated on a permanent axial strain versus load repetitions chart as illustrated in Figure 7.1. The critical stress ratio limit as determined by Jenkins (2000) is defined by material dependent variables and the materials deviator stress. The material properties define the fatigue behaviour between permanent strain and load repetitions.

Franken (1974) evaluated HMA by means of the dynamic triaxial test to define a critical ratio at which the material would fail exponentially. The investigation was not based on the deviator stress ratio, although the material properties were graphically illustrated using the permanent axial strain in relation to the time duration for load repetitions.

To estimate the critical ratio for HWF, the critical limit discovered by Franken (1974) was graphically superimposed on the findings of Jenkins (2000) as illustrated in Figure 7.1 below. Although the two materials are significantly different in nature and asphalt thickness design is usually based on a fatigue criterion not a stress ratio, the critical limit lies in close proximity between 1000 and 10000 repetitions. Thereafter, the limit for HMA exceeds that of the BSM-foam material. It is noted that the HMA curve used is material characteristic dependent as evident from Franken's research and not based on deviator stress ratios. It is however important to note that the HMA curve recorded by Franken used a deviator stress of 250kPa, frequency of 30 Hz and tested at 30°C. With the exception of the test frequency, these conditions are in excess of those used by Jenkins (2000) for BSM-foam, who recorded a deviator stress of 100kPa, frequency of 2Hz and a test temperature of 25°C. The flattening out of the BSM-foam curve could also be a result of aggregate interlock as opposed to the

bituminous nature of HMA. Based on Figure 7.1, it is therefore assumed that critical stress ratio for HWF could lie in the vicinity of the BSM-foam critical stress limit of 55%.

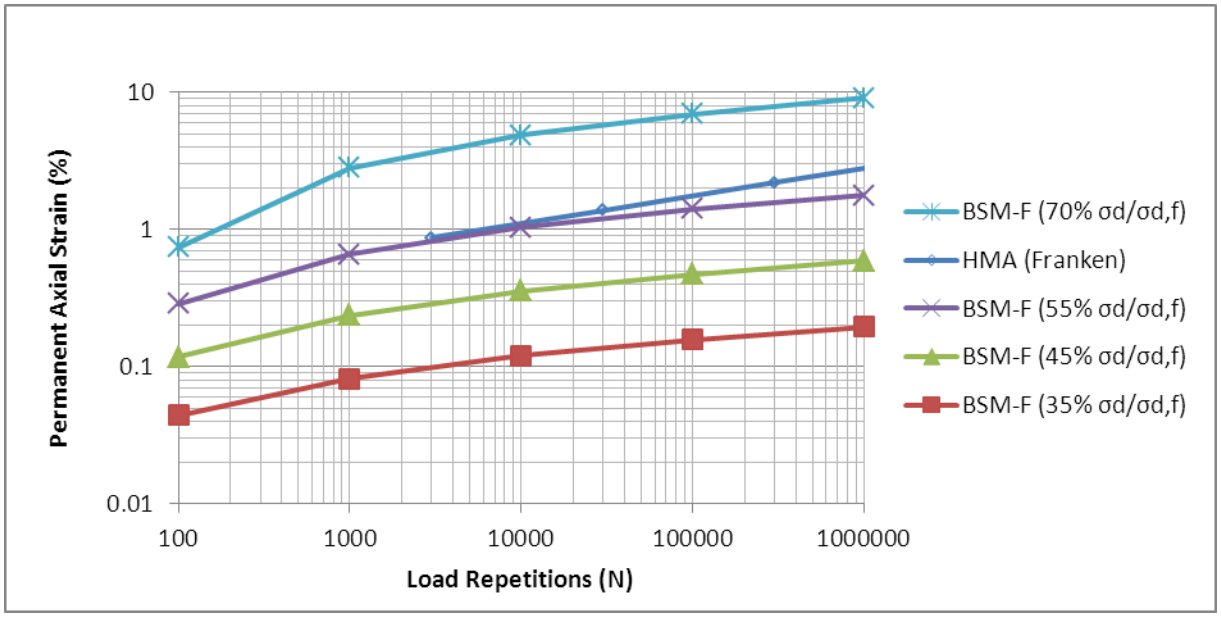

Figure 7.1: Permanent axial strain versus load repetitions for BSM-foam (Jenkins, 2000); and for HMA (Franken, 1974).

7.3 Pavement model

The computer program BISAR 3.0 (Shell, 1998), a multilayer linear elastic program used to evaluate the pavement stress and strain under loading in this study. To increase the accuracy of the base layer stiffness, the layer has been divided into 4 sub-layers to simulate the nonlinear M_r function. Ebels (2008) determined that subdividing layers in excess of 4 parts did not increase the accuracy of the nonlinear elastic model. An iterative approach was adopted to determine the correct stiffness of each sub-layer, given the resultant stress determined by the program. The defaults sign convention for BISAR is "-" for compression and "+" for tension. The calculation of the bulk stress, however, requires this sign convention to be reversed.

The pavement model analysed, consists of 40mm asphalt wearing course in good condition. The stiffness of 4000 MPa is taken from the suggested values for asphalt layers by Freeme as tabulated in the South African Mechanistic Design Method (SAMDM, Theyse et. al., 1996). The base layer consists of either BSM-foam or HWF and is 200mm in thickness. This is a typical layer thickness for in-situ recycled layer. The layers below the base has been modelled as on subgrade layer for simplicity. Two stiffness values will be used for the

supporting layer to evaluate the effect of stiff subgrades on the stresses generated in the base layer for the HWF material.

The stress inducing load consists of a 45kN super single tyre with a pressure of 700kPa. The loading point is modelled as a uniform circular load with a radius of 143mm as indicated in Figure 7.2. The 45kN load is used to simulate the current South African axle limit of 9 ton.

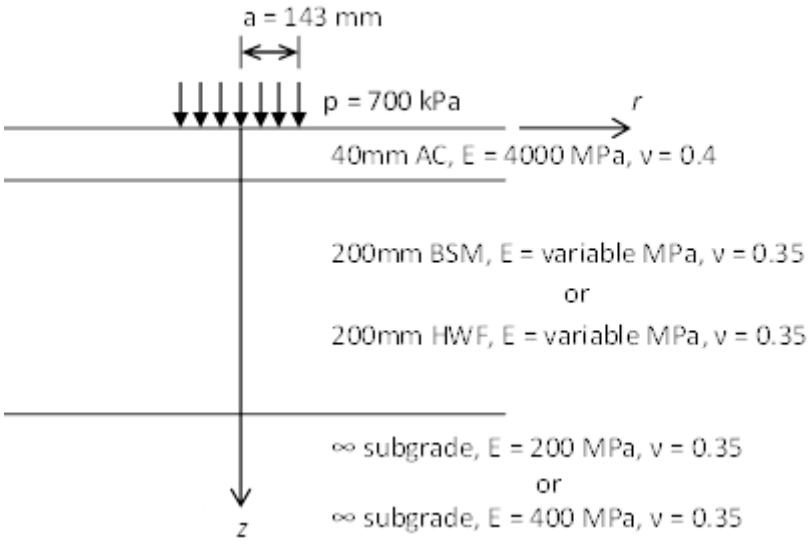

Figure 7.2: Illustration of pavement model analysed

The two variations for subgrade stiffness together with the BSM-foam and HWF layers will resulting in a total of 4 pavement structure variations to be analysed.

7.3.1 Resilient Modulus (M_r)

This stiffness for BSM-foam varies depending on its principal stresses. This non-linear variation is similar to that of granular material and is expressed in means of the materials resilient modulus, or M_r-θ model. This model can thereafter be used to calculate the non-linear stiffness using the principal stresses simulated in a layer at the time of loading. The model is a relatively simple relationship and is not entirely accurate. Many other more complex relationships have been developed, however, for the M_r-θ model, it is assumed sufficient for this hypothetical analysis.

The stress dependant nature of HWF is unknown and the investigation is outside the scope of this study. The M_r-θ model of BSM-foam in comparison has been investigated by numerous researchers. In the attempt to gather material parameters for HWF material, the dissertations of Jenkins (2000) and Ebels (2008) were referenced. Ebels (2008) investigated the correlation between beam stiffness during 4 Point Beam (4PB) tests and the M_r from

dynamic triaxial tests. Although the two test mechanisms are different, i.e. compression versus bending, it was found that their stiffness were comparable when evaluated at the same temperature and frequency. Jenkins (2000) had developed a master curve for HWF "Stab mix". The "Stab mix" is an asphalt concrete which was prepared at Half-Warm temperature. Using this master curve together with the bending stiffness and M_r as determined by Ebels (2008), a M_r curve was generated for HWF as illustrated in Figure 7.3. The HWF M_r–θ curve is essentially shifted by a factor determined from the BSM-foam and HWF bending stiffness at a frequency of 2Hz and at 25°C test temperature. The M_r-θ model for the BSM-foam was obtained from Ebels (2008) for a 75% crushed limestone and 25% RA mix containing 3.6% foamed bitumen and no active filler.

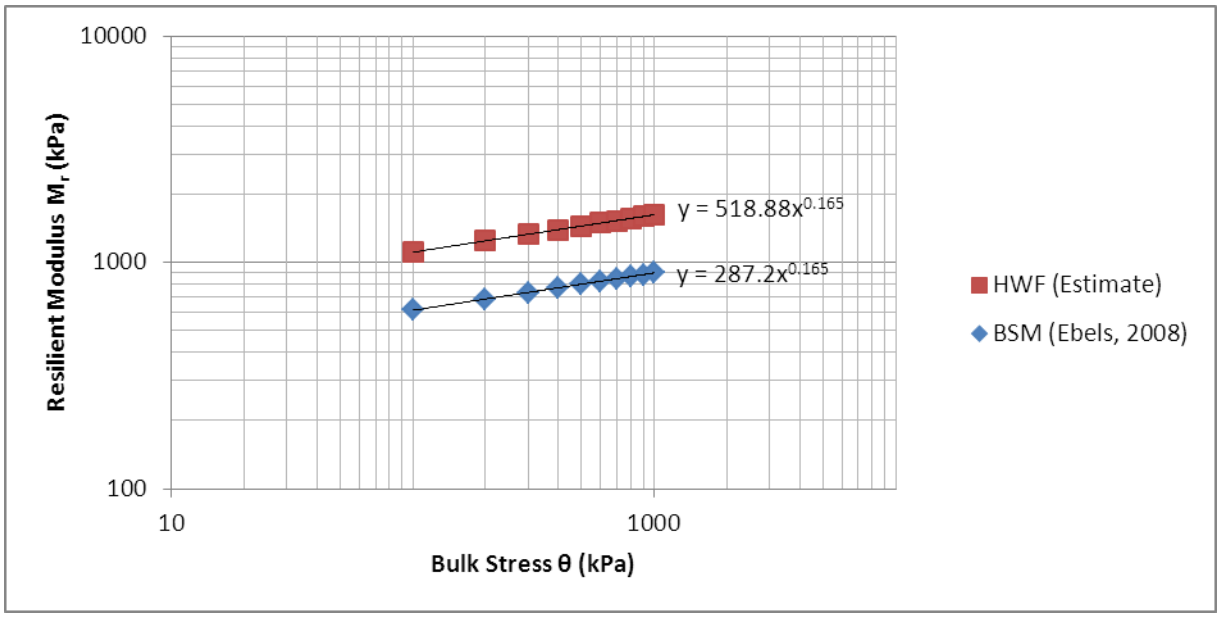

Figure 7.3: M_r–θ curves for BSM-foam and HWF, adapted from Ebels (2008)

The above assumed M_r-θ model for HWF might not be entirely correct due to the improved binder interaction with the aggregate as opposed to the standard BSM-foam. The improved binder distribution could result in a mix that is less dependent on stress resulting in a flatter curve than depicted above. The material constants, k_1 and k_2 for the M_r-θ models are provided in Table 7.1.

Table 7.1: Material constants k_1 and k_2 for the M_r-θ models used

	k_1	k_2
HWF (Estimate)	518.88	0.165
BSM-foam (Ebels, 2008)	287.2	0.165

7.3.2 Stresses and Strains

The use of the 4 sub layers for the base results in a nonlinear distribution of the material stiffness over its depth. A comparison of the various stiffness moduli over the base are provided in Figure 7.4.

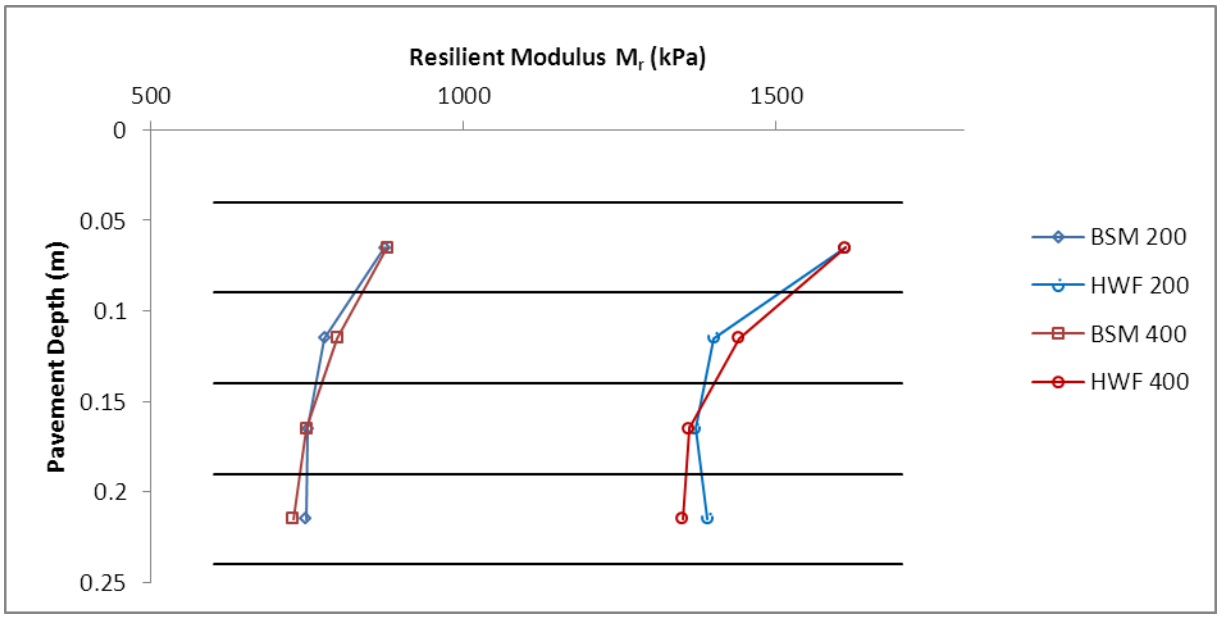

Figure 7.4: Comparative curves of M_r at mid-depth of the base sub-layers for BSM-foam and HWF

During the iteration whilst determining the M_r for the relevant principal stresses, it was observed that tension develops in the lower sub layers of the base for all the models simulated. This is normal for all elastic multilayer programs when the supporting layer stiffness is much lower than its upper layer. The stiff base layer generates tension and compression with its neutral axis dependent of the material stiffness and cross sectional area in similar nature to that of a rectangular beam.

The M_r-θ model was initially developed for granular materials which do not have any significant tensile strength due to its unbound state. To overcome this shortfall, the shifting of the principal stresses as suggested by the SAMDM (Theyse et. al., 1996) was adopted. This method sets the minor tensile principal stress (σ_3) to zero and by maintaining the deviator stress shifts the major principal stress (σ_1) further into compression. The shifting of the principal stresses is generally accepted as incorrect; however, Theyse suggests it provides for meaningful pavement designs in relation to proven practice of unbound granular layers.
The generation of negative bulk stresses (tension) for stiff pavement layers is unavoidable and this results in unrealistic complex numbers when the k_2 coefficient of the M_r-θ model is

less than unity. Figure 7.5 illustrates the shifting of the principal stresses for BSM-foam and HWF on the 200MPa subgrade stiffness.

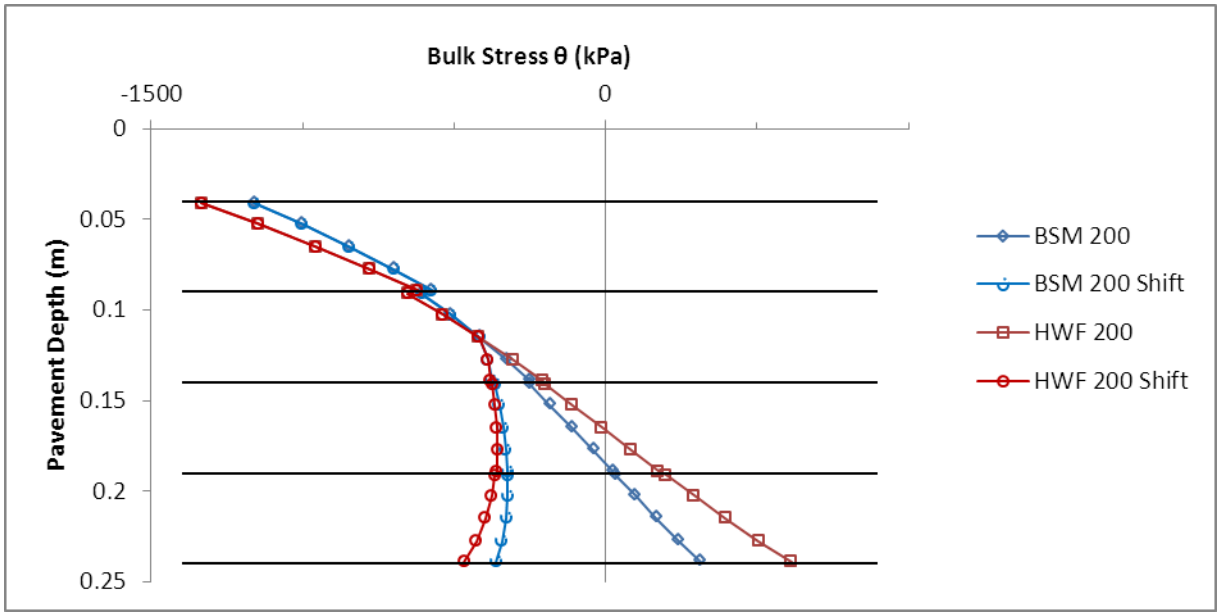

Figure 7.5: Effect on Bulk stress when shifting the principal stress to eliminate tension (negative) minor stress instances

The stresses and strains developed using the elastic multilayer program is illustrated in Figure 7.6 and Figure 7.7. The tensile stresses and strain are denoted as positive, whilst the compressive stresses and strains are negative. Evident from Figure 7.6 and Figure 7.7 is the step wise nature of the horizontal stress curves and vertical strain curves as a result of the nonlinear model simulation.

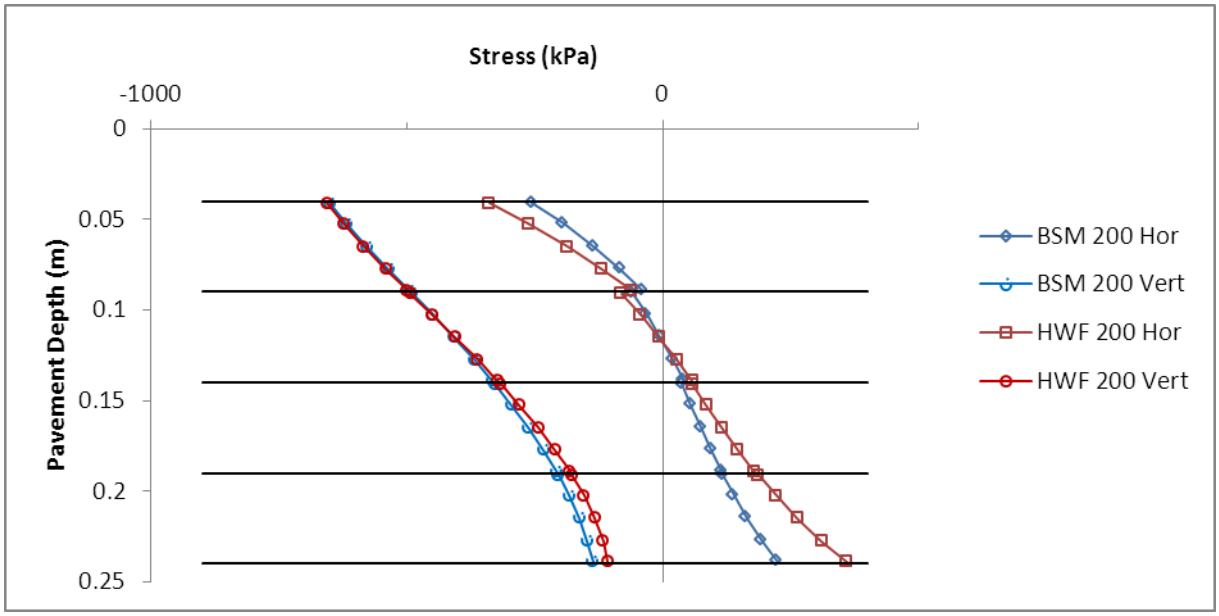

Figure 7.6: Comparison of vertical and horizontal stress for the BSM-foam and HWF base layers supported by the subgrade of 200kPa stiffness

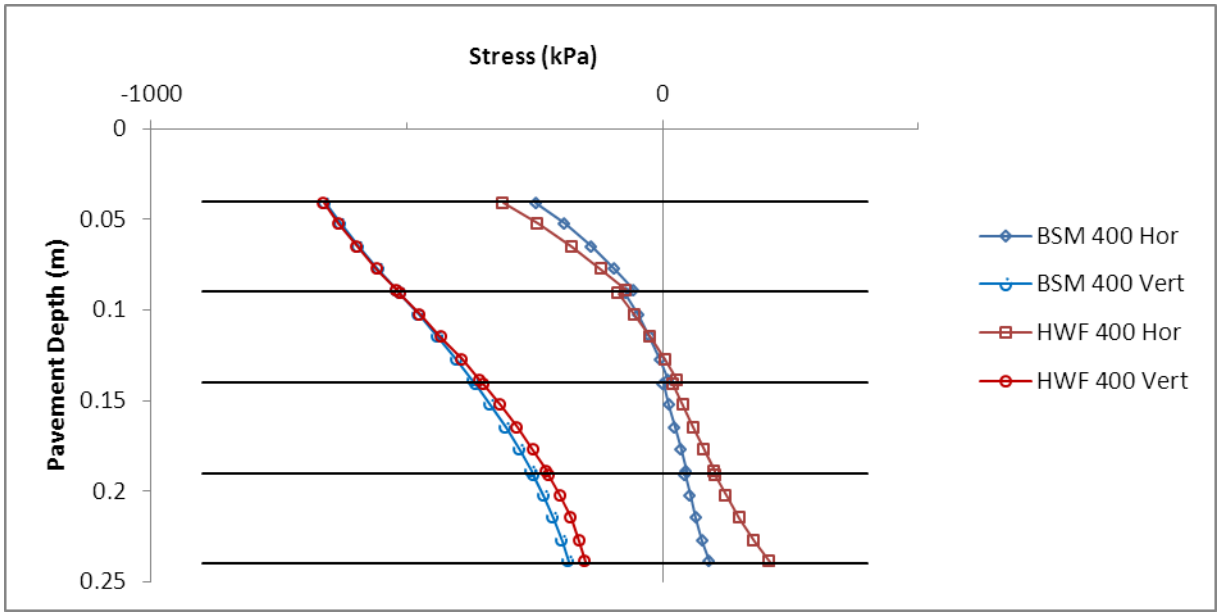

Figure 7.7: Comparison of vertical and horizontal stress for the BSM-foam and HWF base layers supported by the subgrade of 400kPa stiffness

The stiffer HWF layer generates more horizontal stress than that of the BSM layer in relation to vertical stress. This effect facilitates the protection of the subgrade by its increased load spreading ability. Increasing the subgrade stiffness does reduce the tensile stress by providing improved support for the bituminous stabilised layers. It is worth noting low vertical stress of the HWF layer on the 200 kPa subgrade in relation to its horizontal stress. The horizontal stress is almost double that of the vertical stress.

The vertical strain illustrated in Figure 7.8 and Figure 7.9 between BSM-foam and HWF indicates the significance of the stiffer HWF material over the BSM-foam, irrespective of the stiffer subgrade. The horizontal tensile strain is at the bottom of the base is however reduced when the subgrade stiffness is increased. This benefit is reflected more for the BSM-foam layer than the stiff HWF layer.

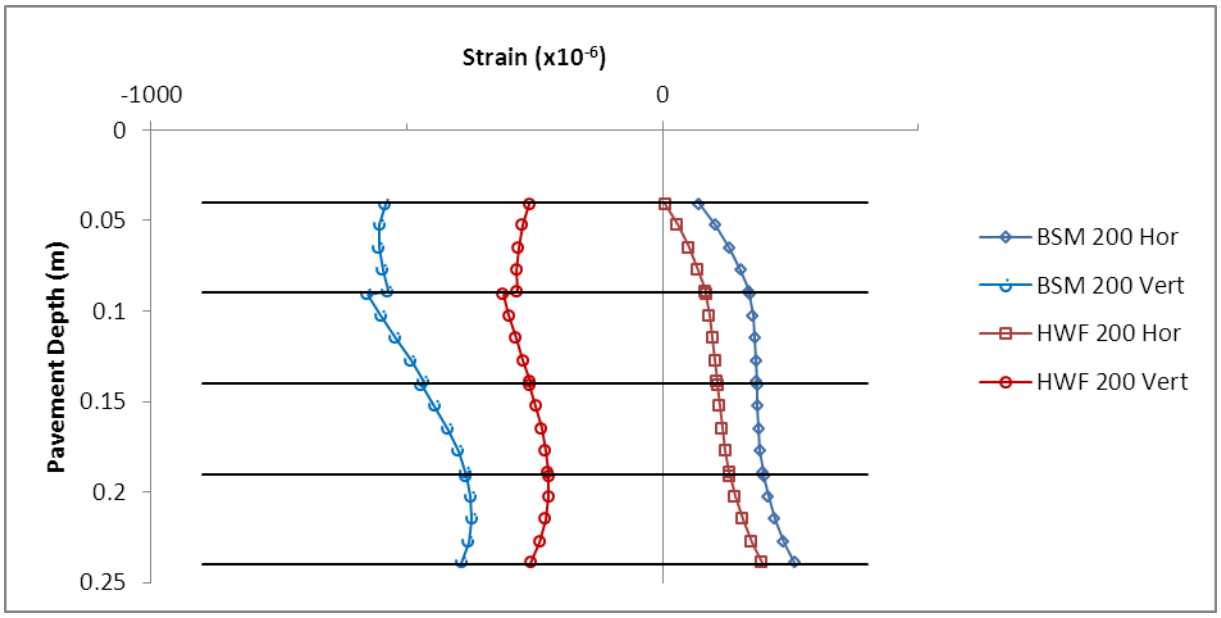

Figure 7.8: Comparison of vertical and horizontal strains for the BSM-foam and HWF base layers supported by the subgrade of 200kPa stiffness

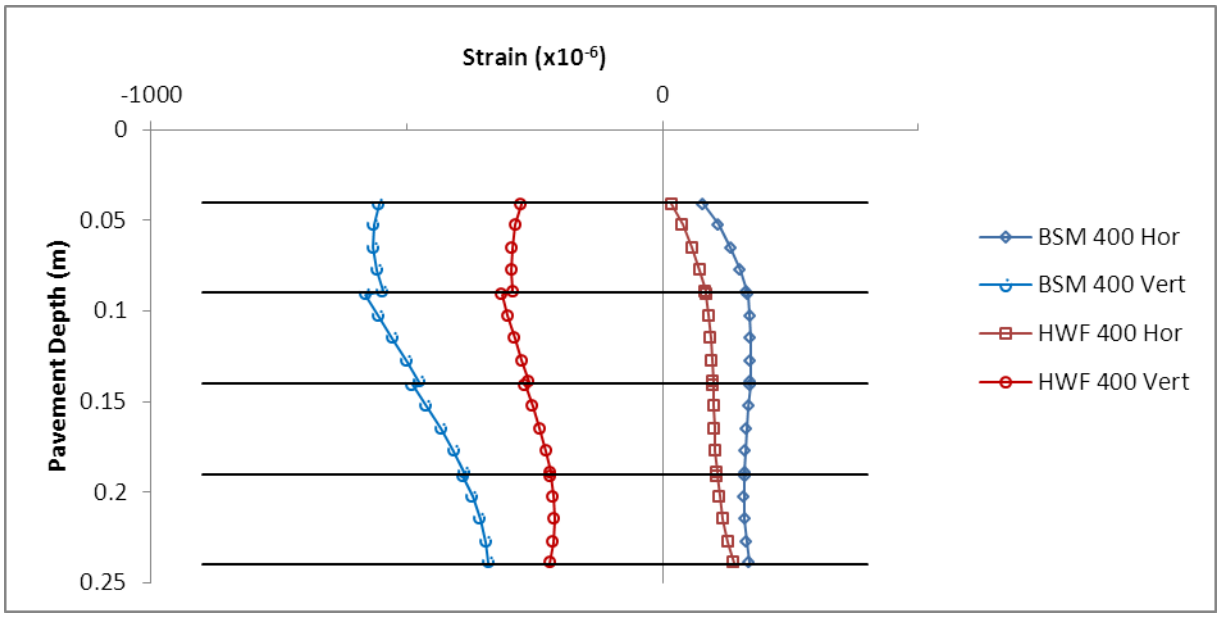

Figure 7.9: Comparison of vertical and horizontal strains for the BSM-foam and HWF base layers supported by the subgrade of 400kPa stiffness

7.3.3 Deviator Stress ratio

The deviator stress ratio was calculated at different points along the depth of the base using the stress distribution obtained from the elastic multilayer program and the results for the monotonic triaxial test as presented in Section 6.4.2.3. The deviator stresses are illustrated graphically in Figure 7.10 and Figure 7.11. It is to be noted that the cohesion and friction angle determined in this study differs significantly from that of the “Stab mix” produced by Jenkins (2000). Considering further that the M_r-θ model used for the pavement response simulation is based on the “Stab mix”, and to evaluate the layers stresses under load in relation to the stresses at failure obtained by means of the monotonic triaxial test in Section 6.4.2.3 is not entirely correct. The deviator stress ratio is however used here to simply evaluate the difference in monotonic triaxial test results between the BSM-foam control mix and the HWF mix. The deviator stress is determined using Equation 17 for the given minor principal stress in the layer.

$$\sigma_{1,f} = \frac{(1+\sin\varphi)\sigma_3+2C\cos\varphi}{1-\sin\varphi} \qquad \text{(Equation 17)}$$

Where,

$\sigma_{1,f}$ is the principal stress at failure

σ_3 is the minor principal stress

C is the material cohesion

φ is the shear failure angle

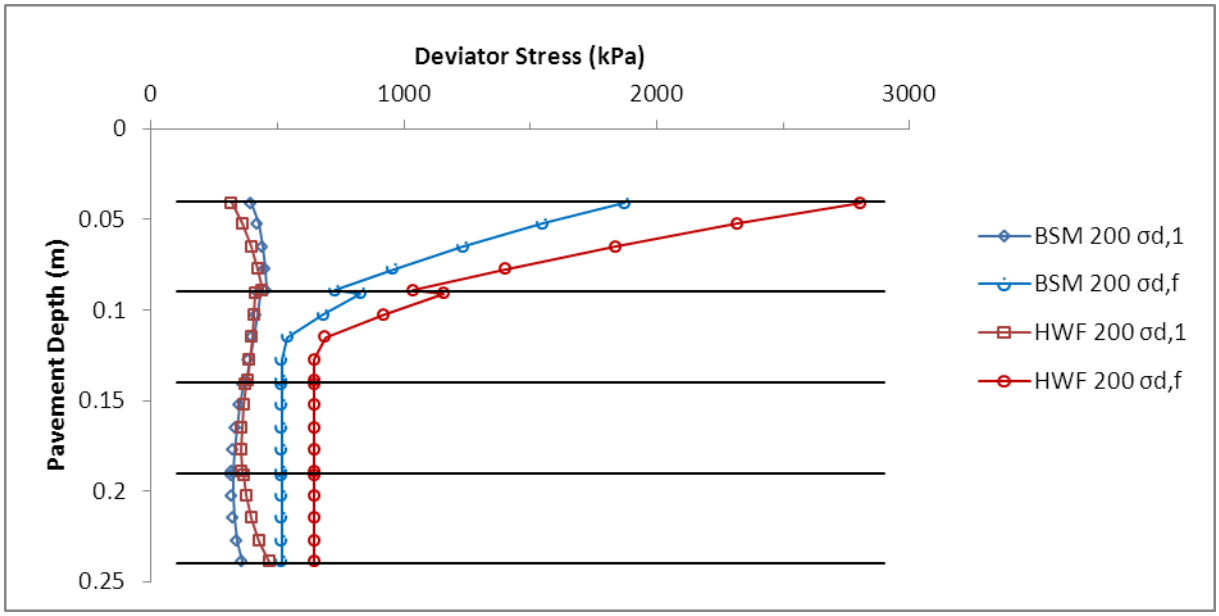

Figure 7.10: Comparison of deviator stress and deviator stress at failure for the BSM-foam and HWF base layers supported by the subgrade of 200kPa stiffness

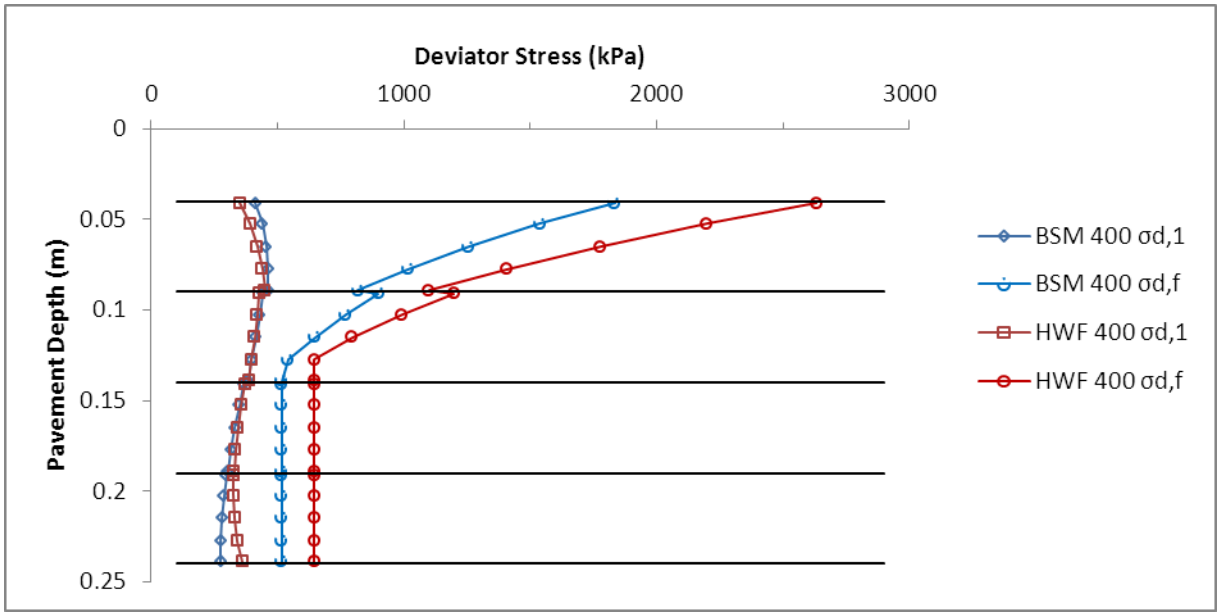

Figure 7.11: Comparison of deviator stress and deviator stress at failure for the BSM-foam and HWF base layers supported by the subgrade of 400kPa stiffness

The deviator stress under loading ($\sigma_{d,1}$) for the BSM-foam in relation to the HWF differ largely at the top sub-layer and the two lowest sub-layers. The stress recorded in the top sub-layer is lower for the HWF material. It is typical for this deviator stress to reduce gradually in a balanced pavement. The deviator stress for the HWF in the lower sub-layer increases once again along the layer depth due to the stiffness variation of the base and subgrade support.

The deviator stresses at failure ($\sigma_{d,f}$) for the BSM-foam and the HWF differ throughout the entire depth of the base layer. This is largely due to the improved cohesion and friction angle recorded for the HWF material in relation to the BSM-foam control material.

The deviator stresses under loading ($\sigma_{d,1}$) for both the BSM-foam and the HWF, ranges between approximately 350kPa and 450kPa along the depth of the base layer. The variation in stress as a result of the subgrade support is marginally small. The deviator stress values are therefore much lower than the 250kPa and 100kPa deviator stresses used in the laboratory by Franken (1974) and Jenkins (2000) respectively. The stresses under loading in the pavement simulation would therefore result in generally high deviator stress ratios.

Increasing the support stiffness does not impact the deviator stress ($\sigma_{d,f}$) by much; however, it reduces it at the bottom of the base layer significantly. The reason for the reduction in $\sigma_{d,1}$ here is a result of the reduction in the minor principal stress and subsequent reduction in the shift of the principal stresses to eliminate tensile forces. The depth at which the $\sigma_{d,f}$ reaches its constant value has shifted marginally lower when the support stiffness is increased.

Figure 7.12 illustrates the deviator stress ratio of the various pavement layer combinations. Here the peak deviator stress ratio for the base layer on the stiffer subgrade undergoes a shift in depth at sub-layer 2. This indicates a reduction in tensile stress and subsequent lowering of the neutral axis.

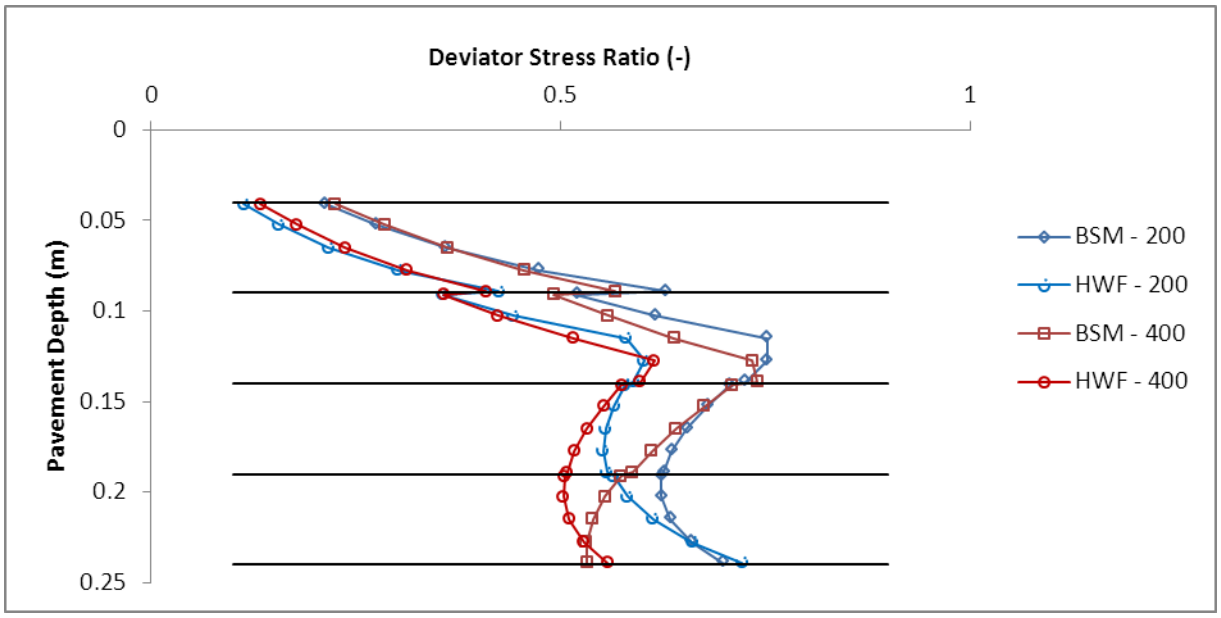

Figure 7.12: Comparison of deviator stress ratios for the BSM-foam and HWF base layers supported by the subgrade of 200kPa and 400kPa stiffness

The maximum deviator stress ratio for the HWF layer in relation to the BSM-foam layer at the centre of the base is reduced by approximately the same magnitude, 16 to 20%, for both subgrade stiffness values. This difference in deviator stress ratio would equate to a significant permanent strain reduction exceeding 300% for a given 1 million load repetitions as illustrated in Figure 7.13. It can also be deduced that for a 3% strain to develop, the variation in load repetitions differs by 0.9 million. This reduction is primarily due to the improved cohesion and stress angle of the HWF mix compared to the BSM-foam control mix.

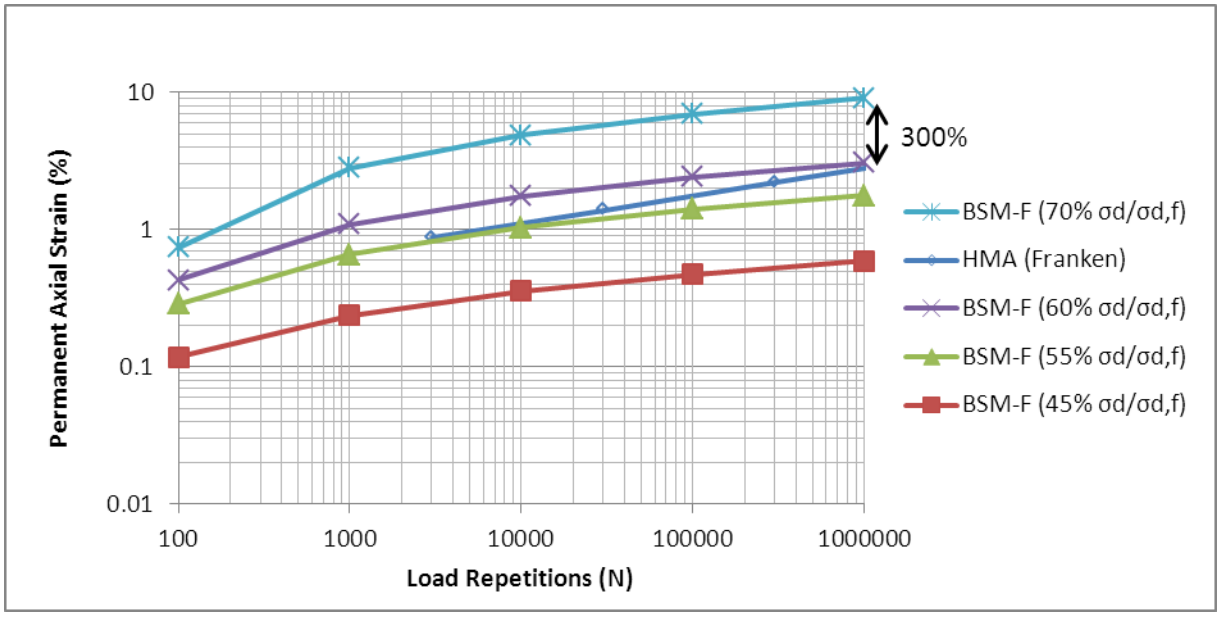

Figure 7.13: Permanent axial strain versus load repetitions graphs as determined by (Jenkins, 2000), to illustrate permanent strain benefits for HWF

Lower down the base layer, the deviator stress ratio increases significantly again when the HWF base layer is used. This sharp increase results from the combination of two factors. The stiffer HWF layer provides more support on a weaker subgrade and the shifting of the principal stresses to reduce the tension to zero. As previously discussed, the shifting of the principal stresses is not theoretically true, and even more so for the HWF material that can resist tensile stresses. The deviator stress ratio for the fourth sub-layer is therefore a gross overestimation of unrealistic vertical stresses and does not account for the horizontal tensile stress which is approximately double that of the compressive vertical stress. It should be noted that ITS results reported in Section 6.4.1.2, indicated a 100% tensile stress gain for HWF over the BSM-foam control mix. The tensile stress recorded was in excess of 300 kPa which is larger than that determined in the layer elastic simulation, however, it not

significantly greater. Placing the HWF layer on a stiffer stabilized subbase would reduce the high strains at the bottom of the layer.

Common BSM-foam stabilised layers contain up to 1% cement to increase the materials strength. The BSM-foam and HWF materials analysed here does not contain any active filler. This in combination with the high deviator stresses experienced has resulted in the high deviator stress ratios analysed under a standard axle load that would exceed the deviator stress ratio limit of 55%, falling into the accelerated permanent deformation phase. Microwave irradiation of cementitious materials indicates earlier strength gains than that in relation water cured specimens due to the presence of fewer microcracks, (Makul et. al., 2010).

7.3.4 Horizontal strain in asphalt

The horizontal strains generated in the asphalt surfacing layer using the elastic multilayer program are presented in Figure 7.14. The benefit of using the stiffer HWF layer results in a reduction of the strain by approximately 60 microstrain in relation to BSM-foam at the bottom of the asphalt surfacing. There is not much variation when the subgrade stiffness increases to 400kPa. The tensile strain for the HWF can be seen to be almost zero in both instances. Using the SAMDM (Theyse et. al., 1996) to evaluate the benefit of these low strains, results in an unrealistically high load application to failure for both HWF and BSM-foam. The reduction by 60 microstrain for the HWF layer results in an unrealistically high load application increase due to the exponential nature of the transfer function. The benefit of using the stiffer HWF layer remains apparent and would extend the life of the asphalt layer significantly.

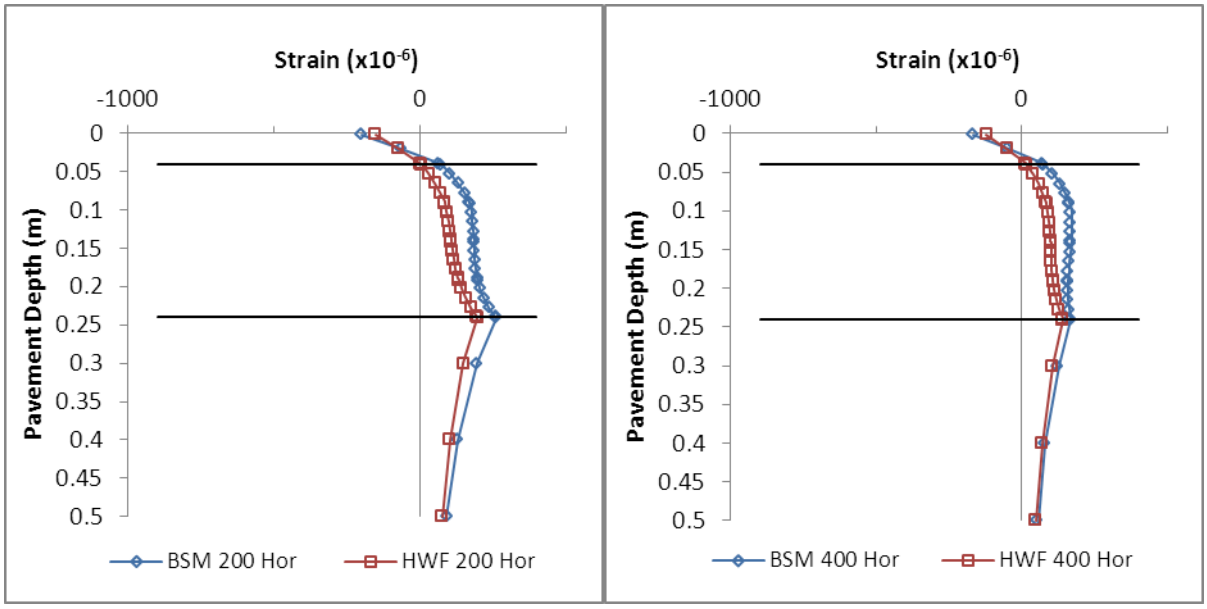

Figure 7.14: Comparison of the horizontal strain experienced in the pavement structure for the 200kPa and 400kPa subgrade stiffness.

7.3.5 Vertical strain in subgrade

The vertical strains generated in the subgrade using the elastic multilayer program are presented in Figure 7.15. Visually it is apparent that the subgrade stiffness has a significant impact on the vertical strain at the top of the subgrade. The benefit of using the stiffer HWF layer for both subgrade stiffness variations results in a reduction of the strain by almost 20% in relation to that recorded using the BSM-foam layer.

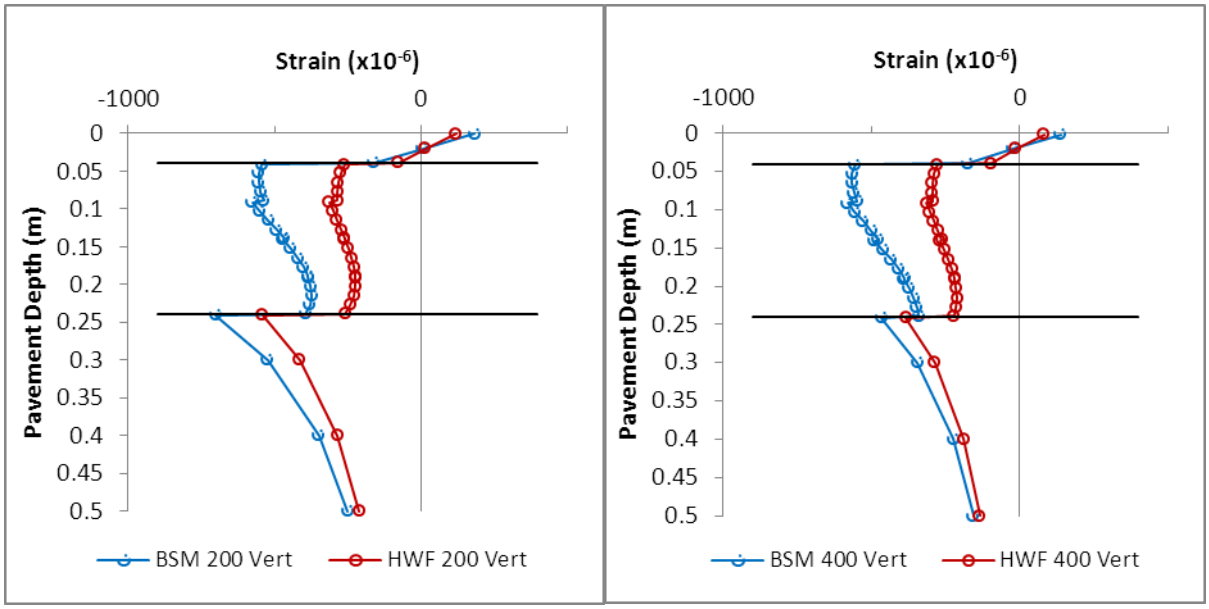

Figure 7.15: Comparison of the vertical strain experienced in the pavement structure for the 200kPa and 400kPa subgrade stiffness.

7.4 Conclusion

The use of material parameters from various papers has been used here to evaluate the performance of the HWF material in relation to BSM-foam to a certain extent. These parameters were however carefully selected by ensuring the original materials' static failure parameters were similar to those obtained in this study. On this basis, it is assumed that the results calculated here are not unrealistic with the exception for the high tensile stress generated for the HWF base on the weaker subgrade. The results for the ITS tests have shown a 100% increase in tensile strength for the HWF material over the flexible BSM-foam control material, thus suggesting added resistance to strain under fatigue.

Table 7.2 provides a summary of the stress and strains at the critical positions in the four pavement structures for the various layers. The principal stresses for the BSM-foam and HWF base layer are recorded at ¼ depth from the top, mid-depth and ¾ depth from the top. It is noticeable that the stiffer HWF layer reduces the horizontal tensile strain at the bottom of the asphalt significantly. There is further a remarkable reduction in the base layer's horizontal strain at the bottom and the vertical strain at the top of subgrade. These all promote a reduction in rutting.

Table 7.2: Stress and strain comparison for the four pavement structures modelled

Subgrade stiffness:	200kPa		400kPa	
Base layer type:	BSM-foam	HWF	BSM-foam	HWF
ε_h - bottom asphalt (10^{-6})	62	-0.2	72	13
σ_1/σ_3 @ z= 90mm (kPa)	-489 / -58	-513 / -72	-493 / -80	-513 / -86
σ_1/σ_3 @ z= 140mm (kPa)	-327 / 38	-366 / 1	-316 / 58	-350 / 21
σ_1/σ_3 @ z= 190mm (kPa)	-204 / 118	-253 / 44	-177 / 188	-223 / 104
ε_h - bottom base (10^{-6})	259	195	170	140
ε_v - top subgrade (10^{-6})	-700	-540	-466	-383

The use of the HWF material for the base layer as opposed to BSM-foam suggests improved performance for the base considering the stress states in the middle and upper parts of the layer. The stresses in the lower part of the base, as calculated for the stiff HWF layer, are an overestimation and mathematically incorrect due to the shifting of principal stresses method. With such a shift, the deviator stress remains constant but the deviator stress ratio decreases. For a linear elastic multilayer program that shows the materials to be in tension,

there is currently no other standard method of evaluating the performance of a semi-continuously bound layer using the deviator stress ratio.

The use of a HWF layer with its improved stiffness also facilitates the protection of the subgrade or lower layers by its improved load spreading ability. The asphalt wearing course also experiences a reduction in strain due to the HWF base layer's assistance in load distribution.

CHAPTER 8: CONCLUSIONS AND RECOMMENDATIONS

8.1 Introduction

The evaluation of the production suitability of microwave heated HWF stabilized mixes was systematically exercised. The study progressed from its preliminary investigation of various moist aggregates to the evaluation of two selected HWF blends. A pavement analysis simulation was additionally undertaken to evaluate the material findings of this study in conjunction with those of Jenkins (2000).

The summary of the findings are provided here to discuss the factors affecting the suitability of the microwave heating method to develop the HWF stabilized mix.

8.2 Conclusions

The use of a scaled microwave heating conveyor system to heat BSM-foam for the production of HWF materials was successfully implemented. Areas of interest for the volumetric heating process include the reflective power which equates to energy loss and the potential of thermal runaway at which high concentrations of heat occurs. Adequate design to optimize heating is therefore a necessity.

The binder contents used in the study is relative low, 2% - 2.3%, in relation to HMA and the HWF evaluated by Jenkins (2000) and van de Ven (2007), which generally exceeds 3.5%. The low binder content would therefore classify the HWF mix created here as a stabilized mix.

Microwaves have an initial high capital cost, which should be considered in relation to the benefit of its heating rate and potential for volumetric heating. The use of microwave technology to heat large volumes of material completely would thus make the technology uneconomical. The energy consumption to heat large volumes of material is significant. The use of microwave energy to focus on heating the moisture adjacent to the bitumen binder would maintain the energy consumption at acceptably manageable levels. This would therefore indicate that post-heating BSM-foam i.e. heating immediately after mixing as a BSM-foam, would benefit most as the heat dissipation occurs rapidly into the aggregates after being processed.

The heating potential of the various aggregates at specific moisture contents was fairly similar with the exception of the RA aggregates. The RA yielded a similar increase in

temperature at half the exposure time as the other aggregates during the preliminary investigation although the 80RA blend did not experience the same effect during the primary investigation. This could be due to the short heating time. It is considered that the RA may contain trapped moisture which assists rapid heating.

It was also noted that increasing the MC above 5% did not benefit the moist aggregates heating potential. The aggregates at 5% MC were able to reach in excess of 100°C with a heating duration of 120 seconds. It would appear that once MC of 5% was exceeded, there would be "free water" that would be excited and evaporate before energy transfer to the aggregates occurred, resulting in energy loss from the system. There appears to be a threshold at which sufficient MC is present to promote rapid heating. Above this value, the excess MC absorbs most of the energy and evaporates.

The application of microwave post-heating in cold BSM-foam processing can be evaluated up until the energy requirement ceiling of 200kW, as discussed previously. The temperature increase of the aggregate is therefore not as important as considering the energy input in comparison in engineering property improvements of the cold BSM-foam. That is to say that, if adequate energy can be added to improve the bitumen-aggregate adhesion selectively, then significant temperature increases are not necessary.

The achievable production rate of HWF at full-scale was determined using calculations based on the available free length and volume of the conveyor belt of typical foam in-plant recycling machinery. The production rate is affected by the microwave generator frequency and power, required temperature increase, material flow rate and material volume. The feasible production rates calculated were in the order of 25 to 50 tons per hour depending on the temperature increase, approximately 25°C to 12°C respectively. This was based on the theoretical calculations and extrapolation of laboratory measurements.

The slight increase in temperature was adequate to promote improved compaction for both blends. There was, however, unavoidable time loss between the heating process and compaction which resulted in significant decrease in compaction temperature.

The average maximum temperature achieved during the primary investigation was lower than the residual binders softening point which could be the reason that the 80RA blend had low ITS results in relation to the 20RA blend.

The strength gain for the HWF 20RA blend was consistently twice that of the control mix. This improved adhesion tends to indicate better bonds between aggregate and binder. The cohesion and friction angle for triaxial results illustrated marginal increases.

The MC for the HWF 20RA blend after the accelerated curing was significantly lower than that of the control mix. This would benefit the early in-situ material strength gain process as a result of the improved moisture reduction in relation to that of BSM-foam as illustrated in Figure 6.24.

The limited shear strength gain for the HWF mix in the triaxial test, relative to BSM-foam, could be the result of localised heat loss over the time duration required to compact the sample in 5 layers. The HWF mix also presented pore water leakage at the base plate during the compaction of the final layer. Test results indicated that the MC was lower than the OMC of its BSM-foam control. The pore water thus reduces ability to achieve a higher density.

The pavement analysis indicated that the deviator stress at failure, calculated using the cohesion and friction angle at the given stress state for the HWF layer, resulted in up to 20% improvement for the deviator stress ratio in comparison to the BSM-foam layer.

The stiffer HWF layer facilitates the protection of the subgrade and reduces the strain experienced in the bottom of the asphalt layer.

8.3 Recommendations

Potential still exists to post-heat cold BSM-foam samples using microwaves where the moisture would still be trapped within the sample. This could still improve the bituminous bonds onto the aggregates. In such a process, the microwaves would be used most effectively. In order to achieve this, consideration should be given to the recommendations provided below.

The RA aggregate appeared to heat rapidly in certain instances. This phenomenon should be investigated further to determine its benefit. The optimum RA content should thereafter be investigated to find the best compromise between accelerated heating and strength gain potential for a mix. The determination of the required MC for RA to achieve optimum heating results similarly requires more investigation.

One of the ways to improve heat transfer is to add an additional material with a good loss factor. If an economical additive with a better loss factor than water as well as a lower specific heat value could be sourced, it could increase the heating rate and reduce the moisture evaporation. The ceramic industry currently uses heating additives such as silicon carbide, although still to be investigated to ascertain if these will be economical for pavement heating applications. Other materials currently utilized in the asphalt industry that might assist rapid heating are natural rubber or zeolites. Ore rich aggregates such as magnetite from mining waste could be included to a mix to increase heating rates. It should be noted that with better microwave absorption properties come a reduction in penetration depth, though keeping the additives volume to a low percentage, would not reduce the penetration depth significantly.

There further exists the possibility of marginally increasing aggregate temperatures before mixing using cheaper fossil fuels to improve particle coating during mixing. Microwave heating can thereafter be implemented as post-heating to further assist the binder aggregate interaction. The combination of microwave heating with conventional heating is used in many industries and is considered more energy efficient and economical than when using the two heating methods individually.

Binders with higher concentrations of asphaltenes (polar molecules) could assist the heating potential using microwave irradiation. Increased asphaltene content affects the binder rheology. Investigation into the use of high asphaltene binders requires attention with focus on the rheological characteristics in relation to the foaming process and final mix characteristics.

An increase in fines content with a comparative increase in binder content can be explored to exploit the volumetric heating of microwave irradiation. The smaller sized fines would hold more moisture and the increased volume of the mastic could see significant improvement in its adhesion to the larger aggregates after heating. The correct moisture contents of mixes could further be investigated, so as to find the optimum amount to promote binder dispersion at mixing and maximize heating benefits when post-heating.

Further investigation into the rapid moisture reduction of microwave heated HWF mixes is required. The reduction in moisture content would expedite the curing process and ultimately the life of the HWF pavement layer in comparison to BSM-foam.

The 100% increase in the ITS tensile strength should be further investigated to evaluate its significance. The tensile strength gain should be reviewed in light of either improved binder distribution or moisture loss.

Research by Jenkins (2000) on HWF mixes was extended to full-scale production in the Netherlands from 2003 to 2011. The full-scale application has highlighted improvements to the laboratory results due to scale effects and critical mass considerations. Full-scale post-mixing trials with microwave post-heating of BSM-foam should be considered provided the volumetric heating potential of microwaves is exploited.

CHAPTER 9: REFERENCES

Abel F. and Hines C., 1978. **Base Stabilization with Foamed Asphalt**. Colorado Department of Highways, Denver, Interim Report. Pp 17

Acott S.M. and Myburgh P.A., 1982. **Design and Performance Study of Sand Bases Treated with Foamed Asphalt.** *Transportation Research Record 898.* Pp 290-296

Akeroyd F.M.L. and Hicks B.J., 1988. **Foamed Bitumen Road Recycling.** *Highways,* January. London. Pp 42-45

Akeroyd F.M.L., 1989. **Advances in Foamed Bitumen Technology.** *5th Conference on Asphalt Pavements for Southern Africa.* Swaziland. Pp VII-1 to VII-4

Asphalt Academy, 2009**. TG 2: The Design and Use of Foamed Bitumen Treated Materials**. Pretoria, South Africa.

Atwater J.E. and Wheeler R.R.J., 2004. **Microwave Permittivity and Dielectric Relaxation of a High Surface Area Activated Carbon**. *Applied Physics A - Materials science and processing,* 79**,** 125-129.

Bissada A.F., 1987. **Structural Response of Foamed-Asphalt-Sand Mixtures in Hot Environments**. *Transportation Research Record 1115*. Pp 134-149

Bowering R.H., 1970. **Upgrading Marginal Road Building Materials with Foamed Asphalt**. *Highway Enigineering in Australia*. Mobil Oil of Australia, Melbourne South.

Bowering R.H. and Martin C.L., 1976. **Foamed Bitumen Production and Application of Mixtures Evaluation and Performance of Pavements.** Proceedings, *Association of Asphalt Paving Technologists Volume 45.* New Orleans, Louisiana. Pp 453-477

Brennen M., Tia M., Altschaefl A. and Wood L.E., 1983. **Laboratory Investigation of the Use of Foamed Bitumen for Recycled Bituminous Pavements**. *Transportation Research Record 911*. Pp 80-87

Brosseaud Y., Gramsammer J-C., Kerzreho J-P., Goacolou H. and Le Bourlot F., 1997. **Expérimentation (premiére partie) de la Grave-Mousse ® sur le manége de fatigue**. *RGRA No 752 (Revue Géneralé des Routes et des Aerodromes)*, Juin. Pp 61 – 70

Buschkühl G., Gapski J. and Gründel R., 1990. **Bituminöse Tragschichten aus Müllverbrennungssasche und Schaumbitumen**. Diplomarbeit, Fachbereich Bauingenieurswesen, Fachhochschule Hamburg. Germany.

Castedo Humberto Franco L. and Wood L.E., 1982. **Stabilization with Foamed Asphalt of Aggregates Commonly used in Low-Volume Roads**. *Transportation Research Record 898*. Pp 297-302

Castedo H., Beaudoin C., Wood L. and Altachaeffl A., 1984. **Durability Characteristic of Foamed Asphalt Mixtures.**

Clark D.E., Folz D.C., Oda S.J., and Silberglitt R., 1995. **Microwaves: Theory and Application in Materials Processing III.** *Ceramic Transactions Vol. 59, The American Ceramic Society*. Westerville, Ohio.

Clark D.E., Folz D.C. and West J.K., 2000. **Processing Materials with Microwave Energy**. *Materials Science and Engineering,* 287**,** 153-158.

Cloete R.C., 2010. **Performance of Recycled Asphalt (100%) Stabilized with Foamed Bitumen or Emulsion.** *Undergraduate Skripsie,* published at the University of Stellenbosch, South Africa.

Collings D. and Jenkins KJ. 2011. **The Long-Term Behaviour of Bitumen Stabilised Materials (BSM's)**. *Proceedings of the 10th Conference on Asphalt Pavements for Southern Africa*, KwaZulu Natal, South Africa.

Csanyi L.H., 1957. **Foamed Asphalt in Bituminous Paving Mixes**. *Highway Research Board Bulletin Volume 10 No. 160*. Pp 108-122

Csanyi L.H., 1959. **Foamed Asphalt**. *American Road Builders Association (ARBA) Technical Bulletin, Volume 240.* Pp 3-14

Csanyi L.H., 1960. **Bituminous Mixes Prepared with Foamed Asphalt**. *Iowa Engineering Experiment Station Bulletin No 189*, Iowa State University.

CSIR Transportek, 1998. **Foamed Asphalt, Mix Design**. Website http:\\foamasph.csir.co.za:81/chap4.htm

de Vos S., 2010. **Performance of Aged Recycled Asphalt (RAP) Stabilized with Foam Bitumen or Emulsion.** *Undergraduate Skripsie,* published at the University of Stellenbosch, South Africa.

Ebels L.J., 2008. **Characterisation of Materials Properties and Rehabilitation of Cold Bituminous Mixture for Road Pavements**. *PhD dissertation*, published at the University of Stellenbosch, South Africa.

Eggers C., Holzhausen M. and Bartels J., 1990. **Bituminöse Tragschichten aus Müllverbrennungssasche und Schaumbitumen under besonderer Berücksichtigung von unterschiedlichen Tensiden**. Diplomarbeit, Fachbereich Bauingenieurswesen, Fachhochschule Hamburg. Germany.

Engelbrecht J.C., Roberts F.L. and Kennedy T.W., 1985. **Cold Recycled Mixtures, with emphasis on the Curing of Foamed Specimens – A Laboratory Study**. *AnnualTransportation Convention, S350 Volume T1*. Pretoria, South Africa.

Grant E.H., 1981. **Biological Effects of Microwaves and Radio Waves.** *IEEPROC, Vol. 128, Pt. A, No.9.*

Hagos E.T., 2008. **The Effect of Ageing on Binder Properties of Porous Asphalt Concrete**. *PhD dissertation published at the Technical University of Delft*. Netherlands.

Jenkins K.J., 2000. **Mix design Considerations for Cold and Half-warm Bituminous Mixes with Emphasis on Foamed Bitumen**. *PhD dissertation University of Stellenbosch*, South Africa

Jenkins K.J., van de Ven M.F.C., Ebels L.J. and Bredenhann S.J., 1999. **Possibilities for Cold Mix Bituminous Paving Blocks**. *Conference on Asphalt Pavements for Southern Africa, CAPSA 1999*. Victoria Falls, Zimbabwe.

Kelfkens R.W.C., 2008. **Vibratory Hammer Compaction of Bitumen Stabilised Materials**. *MSc.Thesis*. University of Stellenbosch. South Africa.

Knacke K., and Hesselmann., 1991. **Thermochemical Properties of Inorganic Compounds,** *Springer-Verlag***.**

Kobusheshe J., 2010. **Microwave Enhanced Processing of Ores.** *PhD dissertation University of Nottingham, UK.*

Lancaster J., McArthur L. and Warwick R., 1994. **VICROADS Experience with Fosmed Bitumen Stabilisation**. *Proceedings 17th ARRB Conference Part 3*. Australia. Pp 193-211

Lee D.Y., 1981. **Treating Marginal Aggregates and Soils with Foamed Asphalt**. *Association of Asphalt Paving Technologists Volume 50*. Pp 211-250

Little D.N., Button J.W. and Epps J.A., 1983. **Structural Properties of Laboratory Mixtures Containing Foamed Asphalt and Marginal Aggregates**. *Transportation Research Record 911*. Pp 104-113

Maccarrone S., 1994. **Cold Asphalt as an Alternative to Hotmix**. *9th AAPA International Asphalt Conference. Australia*. Pp 19-24

Maccarrone S., Holleran G., Leonard D.J. and Hey S., 1994. **Pavement Recycling using Foamed Bitumen**. *Proceedings 17th ARRb Conference Part 3*. Australia. Pp 349-365

Mbaraga A.N., 2011. **Master Curve and Fatigue Testing of Warm Mix Asphalt**. *Masters dissertation*, published at the University of Stellenbosch, South Africa.

Meredith R., 1998. **Engineers' Handbook of Industrial Microwave Heating**. *The Institution of Electrical Engineers,* London.

Metaxas A.C. and Meredith R. J., 1983. **Industrial Microwave Heating**. *The Institution of Electrical Engineers,* London.

Mutyala S., Fairbridge C., Paré J.R.J., Bélanger J.M.R., Ng S., and Hawkins R., 2010. **Microwave Applications to oil sands and petroleum: A Review.** *Fuel Processing Technology.* Pp 127 – 135

Mukal N., Rattanadecho P., Chatveera B., and Agrawal D.K., 2010. Microwave-assisted Heating of Cementitious Material: Relative Dieletric Properties, Mechanical Property, and Experimental and Numerical Heat Transfer Characteristics. *International Communication in Heat and Mass Transfer.* Elsevier.

National Treasury, (2010). **Reducing Greenhouse Gas Emissions: The Carbon Tax Option.** *Department : National Treasury.* Republic of South Africa.

Osepchuk J.M., 1984. **A History of Microwave Heating Applications.** *IEEE Transactions on Microwave Theory and Techniques,* Vol. MTT-32, No.9*.*

Page-Green P., 2011. **Email Correspondence.** *2nd November.*

Puesherner Microwaves, 1999. **Physical Basics of Microwave (Online).** *Available at* Http://www.Pueschner.com/engl/basics/basics.html

Randomthink, 2012. *Available at* Http://www.randomthink.net/blog/physics

Roberts F.L., Engelbrecht J.C. and KennedyT.W, 1984. **Evaluation of Recycled Mixtures using Foamed Bitumen**. *Transportation Research Record 968*. Pp 78-85

Ruckel P.J., Acott S. M. and Bowering R. H., 1983. **Foamed-Asphalt Paving Mixtures: Preparation of Design Mixes and Treatment of Test Specimens**. *Transportation Research* Record 911. Pp 88-95

Sakr H.A. and Manke P.G., 1985. **Innovations in Oklahoma Foamix Design Procedures**. *Transprtation Research Record 1034*. Pp 26-34

Saleh M.F., 2004. **New Zealand Experience with Foamed Bitumen Stabilisation**. *Annual TRB Meeting*, Washington USA.

Semmelink C.J., 1991. **The Effect of Material Properties on the Compactibility of some Untreated Road Building Materials**. PhD Dissertation, University of Pretoria. South Africa.

Shackel B., Makiuchi K. and Derbyshire J.R., 1974. **The Response of Foamed Bitumen Stabilised Soil to Repeated Triaxial Loading**. *7th ARRB Conference. Volume 7 Part7*.

Australia. Pp 74-89

Shell Bitumen, 2003. **Shell Bitumen Handbook**. Shell Bitumen UK.

Sutton W.H., 1989. **Microwave Processing of Ceramic Materials**. *American Ceramic Society Bulletin,* 68**,** 376-386.

Techcommentry, 1987. **Dielectric Heating: RA and Microwave.** *EPRI Centre for Materials Fabrication. Vol. 4, No.1.*

Twagira M.E., 2006. **Characterisation of Fatigue Performance of Selected Cold Bituminous Mixes.** *M.Sc. Thesis University of Stellenbosch*, South Africa.

Twagira M.E., 2010. **The Influence of Durability Properties on Performance of Bitumen Stabilised Materials.** *PhD dissertation*, published at the University of Stellenbosch, South Africa.

Van Wijk A. and Wood L.E., 1983. **Use of Foamed Asphalt in Recycling of an Asphalt Pavement**. *Transportation Research Record 911*. Pp96-103

Van de Ven M.F.C., Jenkins K.F., Voskuilen J.L.M., and Van den Beemt R., 2007. **Development of (half-) warm Foamed Bitumen Mixes: State of the Art.** *International Journal of Pavement Engineering,* Volume 8, No. 2, Pp 163-175.

Von Hippel A., 1954. **Dielectric Materials and Applications**. *Technology press of M.I.T., Wiley and Sons,* New York.

Voskuilen J.L.M., Mangnus S., Van de Ven M.F.C., van Wieringen J.B.M. and Bolk H.J.N. A., 2004. **Experiences with half-warm Foamed Bitumen Treatment Process in the Netherlands**. *Proceedings of the 8th Conference on Asphalt Pavements for Southern Africa*, Sun City, South Africa.

Walkiewicz J.W., Kazonich G., and McGill S.L., 1988. **Microwave Heating Characteristics of Selected Minerals and Compounds.** *Mineral and Metallurgical Processing,* 5**,** 39-42.

Weinert H.H., 1980. **The Natural Road Construction Materials of Southern Africa**. *Academia*. Cape Town. South Africa.

Wikipedia, 2012. *Available at* Http://en.wikipedia.org/wiki/energy_density

Wirtgen GmbH., 2010. **Cold Recycling Manual**, 2nd edition published by *Wirtgen GmbH, Windhagen*, Germany.

APPENDIX A:

BSM-foam CLASSIFICATION (TG2, 2009)

Test or Indicator	Material[1]	Design Equivalent Material Class			Not suitable for treatment	CF
		DE-BSM1	DE-BSM2	DE-BSM3		
Soaked CBR (%)	CS (98%)	>80	25 to 80	10 to 25	<10	0.4
	NG (95%)		>25	10 to 25	<10	
P0.075 (%) (Bitumen emulsion)	CS	4 to 15			>15	0.35
	NG		5 to 25	25 to 40	>40	
	GS		5 to 20	15 to 30	>30	
	SSSC			0 to 20	>20	
P0.075 (%) (Foamed bitumen)	CS	2 to 15			>15	
	NG		11 to 25	23 to 40	>40	
	GS		0 to 20	13 to 30	>30	
	SSSC			0 to 20	>20	
Relative density	All	>0.98	0.95 to 0.98	0.93 to 0.95	<0.93	0.1
DCP Pen (mm/blow)	All	<3.7	3.7 to 9.1	9.1 to 19.0	<19.0	0.1
FWD Backcalculated Stiffness (MPa)	All	>300	150 to 300	70 to 150	<70	0.1
Plasticity Index	CS	<10	>10			0.25
	NG	<6	6 to 12	>12		
	GS		>11	11 to 15	<15	
	SSSC			<15	>14	
Relative moisture (%)	CS	<90	>90			0.1
	NG	<70	70 to 100	<80		
	GS		>100	80 to 100	<100	
	SSSC			>100	>100	
Grading modulus	NG	2.0 to 3.0	1.2 to 2.7	0.15 to 1.2	<0.15	0.2
	GS		1.2 to 2.5	0.75 to 2.7	<0.75	
Cohesion (kPa)	All	>250	100 to 250	50 to 100	<50	0.45
Friction Angle (^{0})	All	>40	30 to 40	<30		0.4
Tangent Modulus (MPa)	All	>150	50 to 150	<50		0.1
ITS $_{dry/equil}$ (kPa)	100 mm[2]	>225	175 to 225	125 to 175	<125	0.1
	150 mm	>175	135 to 175	95 to 135	<95	0.15
ITS $_{wet}$ (kPa)	100 mm	>100	75 to 100	50 to 75	<50	0.1
UCS (kPa)	All	1200 to 3500	700 to 1200	450 to 700	<450	0.1
Retained Cohesion (%)	All	>75	60 to 75	50 to 60	<50	0.45
Rating	All	0.5 to 1.5	1.5 to 2.5	2.5 to 3.5	3.5 to 4.5	N/A

Notes:

1. CS = crushed stone; NG = natural gravel; GS = Gravel soil; SSSC = sand, silty sand, silt, clay; 98%,95%, 93%, 90% are Mod.AASHTO densities.
2. Diameter of specimen.

APPENDIX B:
MICROWAVE MATERIAL DETAILS

CHEMSTIK® CF203 (Tygaflor 308A/03T)

CHEMFAB® CF203 is a highly competitive PTFE coated glass cloth. It provides good release properties over a wide range of applications.

Applications:

CHEMFAB® CF203 is typically used as a non-stik surface in applications where regular replacement is the norm.

Typical Properties	Unit	Value	Test Method
Base PTFE fabric weight:	g/mm²	130	FTMS 191A-5041
Base Thickness:	mm	0.070	FTMS 191A-5030
Adhesive Thickness:	mm	0.045	FTMS 191A-5030
180° Peel Adhesion Strength:	N/cm	5.3	ASTM D330-83
Tensile Strength:	N/cm	180 x 140	FTMS 191A-5102
Adhesive Type:	-	Silicone	-
Temperature Resistance:	°C	-73 TO +260	-
Standard Widths:	mm	1000	-

*Formerly **CF 700-3**. Tygaflor 308A.*

QUADRANT

Quadrant Chemplast Pty Ltd

Engineering Plastics for Heat & Corrosive Applications

52 Kraft Road, P.O. Box 8049 Elandsfontein Germiston Gauteng South Africa 1406
H/O Tel: (0)11 828 0950, H/O Fax: (0)11 828 0336 Reg. No: 1972/002265/07
Durban Branch Tel: (0)31 579 2377, Cape Town Branch Tel: (0)21 555 4596
E-mail: marketing@chemplast.co.za Web: www.quadrantchemplast.co.za

CHEMFAB® TCK105 AS (350G Kevlar)

TCK105 AS is a PTFE coated Kevlar® fabric with antistatic properties. It has extremely high tensile strength relative to thickness.

Applications:

TCK105 AS is typically used in conveyor belt applications and is particularly suitable as an edge reinforcement material. Kevlar® is recommended for use in moist and/or steam environments.

Typical Properties	Unit	Value	Test Method
Weight:	g/mm²	220	FTMS 191A-5041
Thickness:	mm	0.125	FTMS 191A-5030
Tensile Strength:	N/cm	260 x 290	FTMS 191A-5102
Trap Tear Strength:	N	35 x 38	FTMS 191A-5136
Surface Resistivity:	Ω /square	<1 x 10^6	ASTM D257-78
PTFE Content:	%	74	-
Temperature Resistance:	°C	-73 TO +220	-
Standard Widths:	mm	1250	-

QUADRANT

Quadrant Chemplast Pty Ltd

Engineering Plastics for Heat & Corrosive Applications

52 Kraft Road, P.O. Box 8049 Elandsfontein Germiston Gauteng South Africa 1406
H/O Tel: (0)11 828 0950, H/O Fax: (0)11 828 0336 Reg. No: 1972/002265/07
Durban Branch Tel: (0)31 579 2377, Cape Town Branch Tel: (0)21 555 4596
E-mail: marketing@chemplast.co.za Web: www.quadrantchemplast.co.za

PRODUCT DATA SHEET

Polypropylene PP

Trade Names
Polystone

Product Description
Polystone PP a polyolefin which is much stiffer and harder with high heat resistance and excellent chemical resistance at elevated temperatures. Used extensively in the chemical process industry.

Key Features and Benefits:
- Mechanical Strength - a hard, stiff
- readily workable material.
- Impact resistance - robust and tough
- Moisture resistance - excellent food
- and chemical applications
- Weldable - suitable for fabrication.

Plastics Applications
- Pipe flanges
- Tanks - Chemical Storage
- Electroplating Barrels
- Fume Cupboards

Physical Properties

Specific Gravity Units g/cm^3	0.92
Minimum / Maximum Service Temperature in Air Unit °C	-10/100
Tensile Strength Yield Units MPa	27
Impact Resistance Units DIN 53505 Notched Impact Strength KJ/m^2	49,1
Hardness Units Shore D	72
Co-efficient of Thermal Expansion Units mm/(mmxK) x 10^{-5}	200
Dielectric Strength Units KV/mm	50
Surface Resistivity Units Ohms	1x10^{16}

Delivery Program
(beige, grey)

Sheet		**PPS(N/G)* (N-natural, G-grey)**
	Thickness:	1 - 80 mm
	Sizes:	2000 x 1000 mm
	Thickness:	3 - 25 mm
	Sizes:	3000 x 1500 mm
	Thickness:	6 - 30 mm
	Sizes:	4000 x 2000 mm
Rod		**PPR(N/G)* (N-natural/G-grey)**
	Outside Dia.:	8 - 300 mm

Colour code used by Maizey's for identification:
"Pastel Green" – Local
"Brilliant Green" – Import
"Metallic Green" – Import pressed

NB – Fleece Backed PP Sheets

A 3mm fabric backed sheet which can be bonded with an adhesive to metal substrates
Only available in 3000 x 1500mm

APPENDIX C:

PRELIMINARY INVESTIGATION HEATING RESULTS

Material: G1 Eucrite
Moisture content: 3%

Time Duration (s)	Initial Temp (˚C)	Final Temp (˚C)	Forward Power (kW)	Reflective Power (kW)
30	12.4	17.1	0.6	0.39 - 0.37
60	12.2	20.4	0.6	0.34 - 0.32
90	12.2	22.9	0.6	0.29 - 0.29
120	10.8	25.3	0.6	0.29 - 0.29

Material: G1 Eucrite
Moisture content: 5 %

Time Duration (s)	Initial Temp (˚C)	Final Ave Temp (˚C)	Forward Power (kW)	Reflective Power (kW)
30	15	40.8	2	0.04 - 0.04
60	14	55	2	0.51 - 0.23
90	14	62.9	2	0.04 - 0.16
120	14	61.2	2	0.03 - 0.00
90	19	55	2	0.47 - 0.30
120	16	60.4	2	0.50 - 0.74
120	18	79.9	4	0.55 - 0.41
120	19	106.4	6	0.45 - 0.52

Material: G1 Eucrite
Moisture content: 7 %

Time Duration (s)	Initial Temp	Final Temp	Forward Power	Reflective Power
30	16.8	38.7	2	0.31 - 0.31
60	16.8	44.3	2	0.4 - 0.55
90	16.8	66.1	2	0.38 - 0.1
120	16.8	68	2	0.2 - 0.1
90	17.2	68.6	2	0.12 - 0.05
120	17.2	59.8	2	0.02 - 0.14
120	17.2	68	4	0.55 - 0.78
120	17.2	82.4	6	0.5 - 0.7

Material: G2 Granite
Moisture content: 3%

Time Duration (s)	Initial Temp (˚C)	Final Temp (˚C)	Forward Power (kW)	Reflective Power (kW)
30	17	23.6	0.6	0.22 - 0.22
60	15.4	29.3	0.6	0.00 - 0.00
90	15.4	30.1	0.6	0.16 - 0.14
120	16.2	32.7	0.6	0.1 - 0.1
120	16.2	32.7	0.6	0.1 - 0.1
120	17	60	2	0.0 - 0.32
120	13.8	81	4	0.41 - 0.63

Material: G2 Granite
Moisture content: 5 %

Time Duration (s)	Initial Temp (˚C)	Final Ave Temp (˚C)	Forward Power (kW)	Reflective Power (kW)
30	14	41.3	2	0.00 - 0.00
60	14	49.6	2	0.00 - 0.06
90	14	55.2	2	0.07 - 0.24
120	14	63	2	0.12 - 0.00
120	15.2	50.5	2	0.17 - 0.2
120	16	69.1	4	0.26 - 1.37
120	12	82.1	6	1.0 - 0.6
60	14	49.6	2	0.00 - 0.06
60	14	73.7	4	0.40 - 0.48

Material: G2 Granite
Moisture content: 7 %

Time Duration (s)	Initial Temp	Final Temp	Forward Power	Reflective Power
30	17.5	36.1	2	0.33 - 0.25
60	16.8	48.2	2	0.7 - 0.81
90	16.2	57.6	2	0.0 - 0.14
120	15.8	57.3	2	0.15 - 0.11
120	15.8	57.3	2	0.15 - 0.11
120	15.2	67.4	4	0.33 - 0.46
120	13.6	82.8	6	1.9 - 0.24

Material: G2 Hornfels
Moisture content: 3%

Time Duration (s)	Initial Temp	Final Temp	Forward Power	Reflective Power
30	21.6	26.7	0.6	0.53 - 0.5
60	20.4	30.2	0.6	0.43 - 0.41
90	15.4	31.6	0.6	0.45 - 0.41
120	13.2	38.5	0.6	0.53 - 0.45
120	13.2	38.5	0.6	0.53 - 0.45
120	14.8	59.5	2	1.05 - 0.5
120	13.6	97.7	4	1.7 - 0.5

Material: G2 Hornfels
Moisture content: 5 %

Time Duration (s)	Initial Temp	Final Temp	Forward Power	Reflective Power
30	24.2	40.5	2	1.1 - 1.2
60	22.8	50.3	2	0.8 - 0.8
90	17.6	57.1	2	0.65 - 1.00
120	16.6	58.8	2	0.6 - 1.00
120	16.6	58.8	2	0.6 - 1.00
120	14	68.1	4	1.7 - 1.8
120	13.6	106.8	6	2.5 - 1.6

Material: G2 Hornfels
Moisture content: 7 %

Time Duration (s)	Initial Temp	Final Temp	Forward Power	Reflective Power
30	25.4	47.3	2	0.5 - 0.52
60	20.6	60.3	2	0.03 - 0.02
90	19.2	61	2	0.25 - 0.45
120	16.2	64.9	2	0.08 - 0.3
120	16.2	64.9	2	0.08 - 0.3
120	14.6	70.7	4	0.14 - 2.18
120	13.8	89.9	6	1.66 - 1.58

Material: G2 Quartzite
Moisture content: 3%

Time Duration (s)	Initial Temp (˚C)	Final Temp (˚C)	Forward Power (kW)	Reflective Power (kW)
30	17.6	23.5	0.6	0.02 - 0.02
60	17	26	0.6	0.02 - 0.02
90	17	29.5	0.6	0.02 - 0.02
120	15.2	30.9	0.6	0.0 - 0.0

Material: G2 Quartzite
Moisture content: 5 %

Time Duration (s)	Initial Temp (˚C)	Final Ave Temp (˚C)	Forward Power (kW)	Reflective Power (kW)
30	15.6	35.8	2	0.72 - 0.79
60	14.8	47.9	2	0.27 - 0.2
90	15.4	53.6	2	0.06 - 0.45
120	12.8	60.3	2	0.56 - 0.55
120	12	64.6	4	0.85 - 1.1
120	12	75.8	6	1.15 - 1.85

Material: G2 Quartzite
Moisture content: 7 %

Time Duration (s)	Initial Temp	Final Temp	Forward Power	Reflective Power
30	16.8	37.8	2	0.5 - 0.7
60	16.4	40.8	2	0.6 - 0.8
90	15.6	38.8	2	0.5 - 0.5
120	14.4	58.4	2	0.22 - 0.24
90	17.9	60.6	2	0.67 - 0.15
120	14.4	58.4	2	0.22 - 0.24
120	12.4	64.3	4	1.09 - 0.84
120	12.4	69.1	6	1.64 - 1.95

Material: RA
Moisture content: 0%

Time Duration (s)	Initial Temp (˚C)	Final Temp (˚C)	Forward Power (kW)	Reflective Power (kW)
30	11.7	14.6	0.6	0.45 - 0.42
60	11.7	20.6	0.6	0.06 - 0.06
90	12.4	24.3	0.6	0.31 - 0.29
120	13.2	26.1	0.6	0.35 - 0.38
120	13.2	26.1	0.6	0.35 - 0.38
120	13.8	30.4	1	0.51 - 0.49
120	14.8	64.7	2	0.96 - 0.98

Material: RA
Moisture content: 0%

Time Duration (s)	Initial Temp (˚C)	Final Temp (˚C)	Forward Power (kW)	Reflective Power (kW)
30	10.8	16.7	2	1.1 - 1.1
60	10.8	27	2	0.96 - 0.8
90	11.6	27.6	2	1.1 - 1.0
120	14.8	64.7	2	0.96 - 0.98
60	12.8	49.5	4	1.63 - 1.38
30	12.8	30.5	6 (5.0 kW)	2.91 - 2.91
60	13	53.3	6 (5.0 kW)	2.91 - 2.91
90	13.4	96.7	(5.0 kW) - 6	2.91 - 2.5
60	10.8	27	2	0.96 - 0.8
60	12.8	49.5	4	1.63 - 1.38
60	13	53.3	6	2.91 - 2.91

Material: RA
Moisture content: 3%

Time Duration (s)	Initial Temp (˚C)	Final Temp (˚C)	Forward Power (kW)	Reflective Power (kW)
30	10.8	32.5	2	0.62 - 0.61
60	11.6	53	2	0.75 - 0.55
90	11.6	65	2	0.84 - 0.64
120	12.8	71.6	2	0.64 - 0.37
120	12.8	71.6	2	0.64 - 0.37
60	10.8	68.3	4	1.5 - 1.0
105	13.8	103.8	4	1.3 - 1.0
30	12.2	60.5	6	1.6 - 1.1
60	12.8	73	6	1.5 - 3.0
70	13.8	95.2	6	2.0 - 2.0
60	11.6	53	2	0.75 - 0.55
60	10.8	68.3	4	1.5 - 1.0
60	12.8	73	6	1.5 - 3.0

Material: RA
Moisture content: 5 %

Time Duration (s)	Initial Temp (˚C)	Final Ave Temp (˚C)	Forward Power (kW)	Reflective Power (kW)
30	9.8	31.5	2	0.47 - 0.45
60	9.8	43.4	2	0.66 - 0.65
90	10.6	56.2	2	0.5 - 0.15
120	10.8	61.8	2	0.61 - 0.41
30	11.4	63	6	1.3 - 0.15
60	9.8	43.4	2	0.66 - 0.65
60	12.2	67.2	4	0.68 - 0.42
60	11.4	76.2	6	1.55 - 1.15
90	11.2	83.5	6	0.5 - 0.8
120	14	85.9	4	1.4 - 0.2

Material: RA

Moisture content: 7 %

Time Duration (s)	Initial Temp (˚C)	Final Ave Temp (˚C)	Forward Power (kW)	Reflective Power (kW)
30	10.2	33.2	2	0.45 - 0.6
60	10.2	46.4	2	0.48 - 0.75
90	10.6	61.7	2	0.48 - 0.44
120	11	70.4	2	0.32 - 0.62
60	10.2	46.4	2	0.48 - 0.75
60	10.8	69.5	4	0.45 - 0.7
60	11.8	78.8	6	2.0 - 0.36
30	11.6	65.3	6	1.0 - 1.0
120	12.2	87.8	4	0.23 - 1.0
90	11.4	76.9	6	1.31 - 1.75

APPENDIX D:

PRIMARY INVESTIGATION RESULTS

ITS Results

Mix: 20RA
MDD: 2291 kg/m3 @ 5.1% MC

Group	Sample	Load (kN)	ITS (kPa)	Temp Comp	TSR (%)	MC (%)	% Compaction	MC Final (%)	MW Incident Power (kW)	Max Temperature (°C)
ITS Control	04-2	2.6	147.13	25.4		4.6	98.3	1.32		
ITS Control	04-3	2.9	161.95	26.2			97.1	1.05		27.8
ITS Control	04-4	2.3	131.91	26.4			99.0	1.50		
ITS Control	04-5	3.2	178.70	25.8			98.3	0.94		
ITS Low	07-10	6.1	345.19	31.4		4.8	99.0	0.59		
ITS Low	07-11	5.4	305.58	31.8			99.3	0.62	4.93	37
ITS Low	07-12	6.3	356.51	29.8			99.4	0.56		
ITS High	07-7	5.3	299.92	33.8		4.7	99.1	0.68		
ITS High	07-8	5.5	311.24	37.4			99.7	0.26	5.54	50.4
ITS High	07-9	5.7	322.55	35.8			100.0	0.51		

ITS Results

Mix: 80RA

MDD: 2214 kg/m3 @ 5.5% MC

Group	Sample	Load (kN)	ITS (kPa)	Temp Comp	TSR (%)	MC (%)	% Compaction	MC Final (%)	MW Incident power (kW)	Max Temperature (°C)
ITS Control wet	07-1	1.4	77.17	23.2	43.07	5.1	97.6	3.81		
ITS Control wet	07-2	1.6	88.19	23.4			97.7	3.72		24.4
ITS Control wet	07-3	1.8	99.21	23.4			97.5	3.69		
ITS Control	07-4	3.4	189.87	23.8		5.3	97.3	0.85		
ITS Control	07-5	3.7	209.38	23.8			98.3	1.01		
ITS Control	07-6	3.8	215.04	24			98.5	0.86		
ITS High wet	08-1	1.5	83.77	37.4	54.92	5	100.0	3.41		
ITS High wet	08-2	1.6	89.35	35			100.3	3.48	5.07	
ITS High wet	08-3	1.7	93.70	34.6			100.2	3.28		
ITS High	08-4	2.7	150.78	36.2		5.4	98.2	1.39		
ITS High	08-5	3.2	178.70	37.4			98.5	1.44	5.33	50.4
ITS High	08-6	2.8	156.36	36.8			98.4	1.64		
ITS Low	08-7	2.8	156.36	34.2		5.6	97.3	1.44		
ITS Low	08-8	3.2	178.70	31.8			97.6	1.62	5.13	39.3
ITS Low	08-9	2.9	161.95	31.4			97.4	1.58		
ITS High Pre	09-1	3.8	212.21	32.8		5.5	98.5	1.07		
ITS High Pre	09-2	3.5	195.45	33.4			98.2	1.30	5.16	
ITS High Pre	09-3	3.2	178.70	33.4			98.1	1.19		

Triaxial Results

Mix: 20RA
MDD: 2291 kg/m3 @ 5.1% MC

Group	Sample	σ_3 (kPa)	Load (kN)	σ(1,f) kPa	Maximum mixing Temp (°C)	Compaction Temp (°C)	mix MC (%)	MC final (%)	Compaction Density (%)	MW incident power (kW)
High	10-1	50	16.58	989.48	47	36	5.0	2.0	100.1	5
High	10-2	100	20.27	1248.29	58	37	4.6	1.7	99.6	4.78
High	10-3	200	30.5	1927.19	54	37	4.1	1.2	100.4	4.28
Control	10-4	50	13.11	793.11	27.4	26	4.9	3.2	98	N/A
Control	10-5	100	16.57	1038.91	27.4	25.8	4.9	3.4	98.7	N/A
Control	10-6	200	24.48	1586.52	27.2	25.4	5.3	3.7	97.6	N/A

Monotonic triaxial curves (20RA)